TP 5456E

REDESIGN OF THE M.V. ARCTIC BOW
- DESIGN AND MODEL TESTING -

November 1984

For:
Transportation Development Centre
Montreal, Quebec

By

D.N. Baker
Melville Shipping Ltd.
Esso Plaza, East Tower
Suite 1900
425 First Street S.W.
Calgary, Alberta
T2P 3L8

PROJECT TEAM

The project team for Melville Shipping Ltd. was composed of:

Mr. R.A. Dick

Mr. D.N. Baker

Dr. B. Dixit

Dr. H.C. Cheung

Mr. T. Anderson

ACKNOWLEDGEMENT

The authors gratefully acknowledge the advice and assistance of Mr. M. Luce, of Canarctic Shipping and the personnel of the AVMRI, in particular Mr. D. Molyneux and Dr. M. Williams.

DISCLAIMER

The contents of this report reflect the view of the Contractor and not necessarily the official views or policies of the Transportation Development Centre.

REPORT DOCUMENTATION FORM

1. Transport Canada Report No.	2. TDC Project No.	3. Recipient's Catalogue No.
TP 5456E	4871	

4. Title and Subtitle	5. Report Date
Redesign of the M.V. Arctic Bow: Design and Model Testing	May 1984
	6. Performing Organization Report No.

7. Author(s)	8. Transport Canada File No.
D. Baker	D1460-166-32

9. Performing Organization Name and Address	10. DSS File No.
Melville Shipping Ltd. Esso Plaza, East Tower, Suite 1900 425 First Street S.W. Calgary, Alberta T2P 3L8	10SD.T8200-2-2555
	11. DSS or Transport Canada Contract No.
	OSD82-00137

12. Sponsoring Agency Name and Address	13. Type of Report and Period Covered
Transportation Development Centre (TDC) 1000 Sherbrooke Street West Suite 2421 Montreal, Quebec H3A 2R3	Final; Jan. 83 - May 84
	14. Sponsoring Agency Code
	TDC 4871

15. Supplementary Notes	16. TDC Project Officer
	R.S. Nishizaki

17. Abstract

The report describes the development and subsequent testing in ice and open water of a model of the existing icebreaking cargo vessel M.V. Arctic, along with two modified bows.

Development of the new bows included a brief overview of existing predictor equations and an analysis of bow form geometry to arrive at five alternative bow forms. Two of these bow forms, together with the existing bow, were subsequently model tested.

Open water testing was conducted at the National Research Council (NRC), Arctic Vessel and Marine Research Institute (AVMRI) in Ottawa. The ice testing was completed at the Arctec Canada Ltd. ice tank in Ottawa. The models were tested in level ice, broken ice and in a simulated rubble field. The results of the test program were analyzed and showed a marked improvement of one new design over the existing ship. This improvement was also reflected in a transit analysis.

18. Key Words	19. Distribution Statement
Bow design, Icebreaking vessel, Ice class ship, M.V. Arctic, Model testing	Limited number of copies available from the Transportation Development Centre

20. Security Classification (of this report)	21. Security Classification (of this page)	22. No. of Pages	23. Price
Unclassified	Unclassified		nil

TDC CDT 79.005

FORMULE DE DOCUMENTATION POUR RAPPORT

1. N° du rapport Transports Canada	2. N° de l'étude — CDT	3. N° de catalogue du destinataire
TP 5456E	4871	

4. Titre et sous-titre	5. Date du rapport
Redesign of the M.V. Arctic Bow:Design and Model Testing	mai 1984
	6. N° du rapport de l'organisme executant

7. Auteur(s)	8. N° de dossier Transports Canada
D. Baker	D1460-166-32

9. Nom et adresse de l'organisme executant	10. N° de dossier — ASC
Melville Shipping Ltée Esso Plaza, Tour est, suite 1900 425 First Street S.W. Calgary (Alberta) T2P 3L8	10SD.T8200-2-2555
	11. N° de contrat — ASC ou Transports Canada OSD82-00137

12. Nom et adresse de l'organisme parrain	13. Genre de rapport et periode visee
Centre de développement des transports (CDT) 1000 ouest, rue Sherbrooke Suite 2421 Montréal (Québec) H3A 2R3	Final; jan. 83 - mai 84
	14. Code de l'organisme parrain CDT 4871

15. Remarques additionnelles	16. Agent de projet — CDT
	R.S. Nishizaki

17. Résumé

Ce rapport relate les travaux de mise au point ainsi que les essais en eau libre et dans les glaces d'une maquette du cargo brise-glace Arctic dont la proue originale a été remplacée tour à tour par deux proues modifiées.

Dans la partie consacrée aux travaux de mise au point, le rapport passe rapidement en revue les modèles mathématiques de comportement existants et récapitule les travaux de géométrie analytique ayant débouché sur cinq formes de proue différentes, dont deux ont été par la suite testées en bassin de carènes.

Les essais en eau libre ont eu lieu aux installations de l'Institut de dynamique marine du CNRC à Ottawa. Quant aux essais en eau chargée de glaces, ils ont été réalisés au bassin de la firme Arctec Canada Ltée, également à Ottawa, en eau couverte tour à tour d'une couche de glace uniforme, de glaces brisées et enfin d'un champ de glaces brisées resoudées ensemble par le gel.

L'analyse des résultats obtenus a montré que l'une des deux nouvelles proues était nettement supérieure à la proue actuelle de l'Arctic. Cette supériorité ayant été confirmée à la lumière d'une analyse des périples habituels de l'Arctic.

18. Mots-clés	19. Diffusion
Etude d'une proue, brise-glace, navire de côte arctique, Arctic, essais sur maquette	Disponibilité d'exemplaires en nombre limité au Centre de développement des transports

20. Classification de sécurité (de ce rapport)	21. Classification de sécurité (de cette page)	22. Nombre de pages	23. Prix
non-classifié	non-classifiée		aucun

CDT TDC 79-005

TABLE OF CONTENTS

		PAGE
1.0	INTRODUCTION	1.1
2.0	ENVIRONMENTAL ANALYSIS	
	2.1 General	2.1
	2.2 Open Water	2.1
	2.3 Ice Covered Waters - Canadian Arctic	2.1
	2.3.1 Snow Cover	2.6
	2.3.2 First-Year, Ice Cover, Thickness and Strength	2.6
	2.3.3 Old Ice	2.10
	2.3.4 Ridging	2.10
	2.4 Ice Covered Waters - Baltic Sea	2.11
	2.5 Summary	2.11
3.0	DEVELOPMENT OF MODIFIED BOWS	
	3.1 General	3.1
	3.2 The Development of a Predictor Equation	3.1
	3.3 Development of New Bow Forms	3.20
	3.3.1 Design	3.26
	3.3.2 Prediction of Performance	3.28
4.0	MODEL TESTS	
	4.1 Open Water Tests	
	4.1.1 General	4.1
	4.1.2 Test Program	4.1
	4.2 Ice Tests	
	4.2.1 General	4.4
	4.2.2 Test Procedure	4.7
	4.2.3 Test Data Analysis	4.12
	4.2.4 Additional Analysis	4.12
	4.2.5 Conclusions of Ice Testing	4.18
5.0	ANALYSIS OF RESULTS	
	5.1 General	5.1
	5.2 Level Ice	5.1
	5.3 Broken Channel	5.9
	5.4 Rubble Field	5.14

TABLE OF CONTENTS

	PAGE
6.0 BENEFIT ANALYSIS	
6.1 General	6.1
6.2 Transit Analysis	6.1
7.0 CONCLUSIONS AND RECOMMENDATIONS	
7.1 Conclusions	
7.1.1 Environmental Analysis	7.1
7.1.2 Bow Design	7.1
7.1.3 Model Testing	7.2
7.1.4 Transit Analysis	7.3
7.2 Recommendations	7.3

APPENDICES

Appendix 1. Summary of Canadian Arctic Environmental Criteria

Appendix 2. Lines Plans and Body Plans of the M.V. ARCTIC and Modified Bow Forms

Appendix 3. Notes on Ice Model Tests

Appendix 4. Summary of Ice Conditions and Transit Times for Voyage From Europe to Nanisivik

LIST OF FIGURES

		PAGE
Figure 2.1	Average Sea Spectra - North Atlantic	2.2
Figure 2.2	Arctic Waters Pollution Prevention Act - Shipping Safety Zones	2.4
Figure 2.3	Mean Snow Depth on June 30 at 12:00 GMT - Based on the Period 1955-1972	2.7
Figure 2.4	Mean Snow Depth on December 31 at 12:00 GMT- Based on the Period 1955-1972	2.8
Figure 3.1	Definition of Angles Representing Bow Geometry	3.6
Figure 3.2	Comparison of Various Level Ice Prediction Equations	3.8
Figure 3.3	Level Ice Prediction - Existing M.V. ARCTIC	3.11
Figure 3.4	Resistance Components in Level Ice Prediction Existing M.V. ARCTIC	3.12
Figure 3.5	Ice Strength Variation Level Ice Prediction - Existing M.V. ARCTIC	3.14
Figure 3.6	Breaking Resistance as Percentage of Total Resistance at Creeping Speed vs Beam	3.17
Figure 3.7	Hull Form Coefficient Variation Level Ice Prediction Existing M.V. ARCTIC	3.19
Figure 3.8	Length Variation Level Ice Prediction - Existing M.V. ARCTIC	3.21
Figure 3.9	Forward Block Coefficient Variation Level Ice Prediction - Existing M.V. ARCTIC	3.22
Figure 3.10	Flare and Waterline Angles for a Selection of Icebreaker Designs	3.24
Figure 3.11	Flare and Waterline Angles for the Existing and Modified Bows of the M.V. ARCTIC	3.27
Figure 3.12	Level Ice Resistance for the M.V. ARCTIC and the 5 Modified Bow Forms	3.30
Figure 4.1	Open Water Test of M.V. ARCTIC Propeller at 22.5 Deg. Propeller Pitch	4.3
Figure 4.2	Full-Scale Resistance Prediction of M.V. ARCTIC and Two Modified Bow Forms	4.5
Figure 4.3	Full-Scale Power Prediction of M.V. ARCTIC and Two Modified Bow Forms	4.6
Figure 4.4	Diagramatic of ACL Tank Basin Divider	4.9
Figure 4.5	Hull Form Coefficient Representation of the Relative Performance of the Three Bows	4.16
Figure 4.6	Mathematical Prediction	4.17
Figure 4.7	ACL Final Prediction for Models A, B and C	4.19
Figure 4.8	ACL Broken Channel Predictor and Full Scale Broken Channel Data	4.20
Figure 5.1	Full-Scale Resistance Data and ACL Model Scale Prediction for the Existing M.V. ARCTIC	5.2
Figure 5.2	MSL Prediction Based on Full-Scale Data and ACL Prediction for the Existing M.V. ARCTIC	5.3
Figure 5.3	MSL Prediction and ACL Prediction for Bow B	5.5
Figure 5.4	MSL Prediction and ACL Prediction for Bow C	5.6
Figure 5.5	Effect of Surface Roughness on the Coefficient of Friction Between Ice and Steel	5.7

LIST OF FIGURES (continued)

		PAGE
Figure 5.6	Resistance Correction for Full-Scale Prediction Of Resistance for Bows C and B	5.10
Figure 5.7	MSL Predictor Equation for Model A	5.11
Figure 5.8	MSL Final Prediction for Bow B	5.12
Figure 5.9	MWSL Final Prediction for Bow C	5.13
Figure 5.10	ACL Predictor for Broken Channel and Full-Scale Data for the Existing M.V. ARCTIC	5.15
Figure 6.1	Transit Days vs Mid-Month for the Existing and Modified M.V. ARCTIC and Data from 1982 Season	6.3

LIST OF TABLES

		PAGE
Table 2.1	Period of Navigation for the Shipping Safety Control Zones	2.5
Table 3.1	M.V. ARCTIC - Principal Particulars	3.2
Table 3.2	Primary Characteristics Affecting Level Ice Resistance	3.4
Table 3.3	Ice Resistance Predictor Equation Forms	3.7
Table 3.4	Breaking Component as Percentage of Total Resistance at Different Ice Strengths from the Melville Predictor Equation	3.15
Table 3.5	Resistance Distribution in Model and Full-Scale of Three Different Icebreakers (After Vance, 1975)	3.16
Table 3.6	Principal Particulars of the Modified Bows	3.29
Table 3.7	Comparison of Existing and Modified Icebreaking Bows	3.31
Table 4.1	Propeller 68 and Duct Design Particulars	4.2
Table 4.2	ACL Test Schedule	4.8
Table 4.3	Resistance Test Data (Reproduced from ACL Report)	4.10
Table 4.4	Self-Propulsion Test Data (Reproduced from ACL Report)	4.11
Table 4.5	Predictor Equations From Model Scale Tests Conducted at ACL	4.13
Table 4.6	Rubble Field Test Data	4.14
Table 4.7	Geometry Friction Coefficients	4.15
Table 6.1	Transit Days	6.4

LIST OF NOMENCLATURE

R	=	Total Resistance
R_I	=	Inertial Resistance
R	=	Breaking Resistance
R_V	=	Velocity Resistance
R_O	=	Open Water Resistance
B	=	Ship Beam
h	=	Ice Thickness
L	=	Ship Length
C_{bf}	=	Forebody Block Coefficient
σ_f	=	Flexural Strength
g	=	Gravitational Constant
v	=	Ship's Speed
μ_1, μ_2,	=	A.C.L. Hull Form Coefficient
μ_{12}	=	$\mu_1 + 1.17\ \mu_2$
T_p	=	Propeller Thrust
E	=	Young's Modulus
ρ	=	Mass Density
γ	=	Stem Angle
α	=	Waterline Entrance Angle
β	=	Flare Angle at Waterline
T	=	Ship Draught

1.0 INTRODUCTION

The continuing commercial development of the resources in the Canadian Arctic has resulted in a similar development in the technology of the hardware to bring the raw materials to markets in the south. Part of this development involves research into the ice capability of commercial ships operating in ice infested waters.

The M.V. ARCTIC is a 28,000 DWT bulk carrier which, during the summer and fall months, carries lead and zinc concentrates between mine sites in the Northwest Territories and Europe. The mine sites are the Polaris mine on Little Cornwallis Island and the Nanisivik mine on the northwest corner of Baffin Island. The ARCTIC is classed as an Arctic Class 2 ship in accordance with the Canadian Arctic Shipping Pollution Prevention Regulations, and is fitted with an icebreaking bow.

Over the past few years the M.V. ARCTIC has been tested in both level ice, broken channels and ridges. The results of these tests, together with operational experience, highlighted a number of areas which could be improved to enhance the vessel's capability. One of these areas was the bow form.

Clearly, if the design of the M.V. ARCTIC bow could be modified to improve its ice transiting capability, then a number of advantages may be forthcoming.

- The improvement in ice transiting capability may allow an extended operating season.

- The improvement may allow alternative trade routes to be considered.

- The investigation may assist ship designers with vessels of the future.

However, these operational benefits will depend on obtaining comparative, or better, open water performance together with significant improvements of the icebreaking performance. In addition, any redesigned bow would have to be suitable for retrofitting onto the existing vessel.

As a result of these considerations and the request of Canarctic Shipping Company Limited, the Transportation Development Centre (TDC) contracted Melville Shipping Ltd. (Melville) to redesign the ARCTIC's bow and complete a benefit analysis that would determine the new bow's effectiveness.

The development of the new bow form was completed in a number of steps.

a) Environmental analysis;
   - An environmental analysis to define the open water and ice conditions likely to be encountered.

b) Development of hull form criteria and alternative bow forms;
   - A brief review of current technical papers and predictor equations was undertaken in order to develop a tool to measure the relative performances of the modified bow forms.

     Only semi-empirical formulations were considered both because of the complexity of analytical formulations and the need to consider only the relative improvement in ice breaking performance.

   - Using an existing predictor equation, modified to reflect the actual performance of the M.V. ARCTIC, and an analysis of bow geometry, five alternative bow forms were developed.

c) Model testing;
   - Open water and ice tank tests were conducted on a model of the existing ARCTIC and the two most promising designs. Open water tests were conducted at the National Research Centre (NRC) Arctic Vessel and Marine Research Institute (AVMRI) in Ottawa, and ice tests were conducted at Arctec Canada Ltd. (ACL), also in Ottawa.

d) Benefit Analysis;
   - An overview of the operational benefit of the best alternative bow forms was conducted to compare the effectiveness of each bow during the Arctic seaons.

Following completion of the model tests, the model test data was analysed and together with full-scale data available for the existing M.V. ARCTIC, full-scale predictions are made for the new bows tested.

This report is limited to the work undertaken by Melville Shipping Ltd. (Melville) to test the model at AVMRI and ACL. However, following this testing in Canada the model of the existing M.V. ARCTIC and one of the modified bow forms was tested in the ice tanks of the Hamburgische Schiffbau - Versuchsaustalt, GMBH (HSVA) in Germany and the Wartsila Arctic Research Centre (WARC) in Finland. Details of this subsequent work can be found in Ref. 1.1.

2.0 ENVIRONMENTAL ANALYSIS

2.1 General

In order to redesign the bow of the M.V. ARCTIC, it is necessary to define the environmental conditions through which the vessel will be required to operate. These environmental conditions can be divided into two sections:

- open water
- ice infested waters

The majority of the vessel's time is currently spent in open water. This occurs in coastal waters, inland waterways, lakes and deep sea. In terms of operational criteria, the worst open water area through which the vessel is expected to operate is the North Atlantic. The vessel's operation in ice infested waters may occur both in northern Europe during the early part of the year, and the Canadian Arctic during the latter months of the year.

The ice parameters discussed in this section are taken largely from the report entitled "The M.V. ARCTIC - Northern Routing Environment" (Ref. 2.1). This report may be referred to, together with the other noted references, if any additional or detailed information is required.

Rarely, if ever, are conditions in the Arctic similar from one year to another. Therefore the ice data presented in this report represents the mid-month, median or typical conditions that may be encountered. The data presented does not take account of extremes and/or local, regional or annual variations either in particular environmental parameters, or in how various combinations of these parameters influence the environment as a whole.

2.2 Open Water

The design criteria to be taken into consideration with regard to the open water operation are both the size and period of the waves likely to be encountered. The maximum significant wave height recorded in the North Atlantic is 45 feet (13.7 m), recorded four times in 13 years (Ref. 2.2). Figure 2.1 shows the significant wave height versus percentage occurrence.

It can be seen that the predominant wave heights will be in the order of 3 to 4 m. These will be associated with average wave periods of 7 to 9 seconds.

2.3 Ice Covered Waters - Canadian Arctic

The M.V. ARCTIC is designed and built in accordance with the Canadian Arctic Shipping Pollution Prevention Act and its associated regulations, (CASPPR), to comply with an Arctic Class 2 notation.

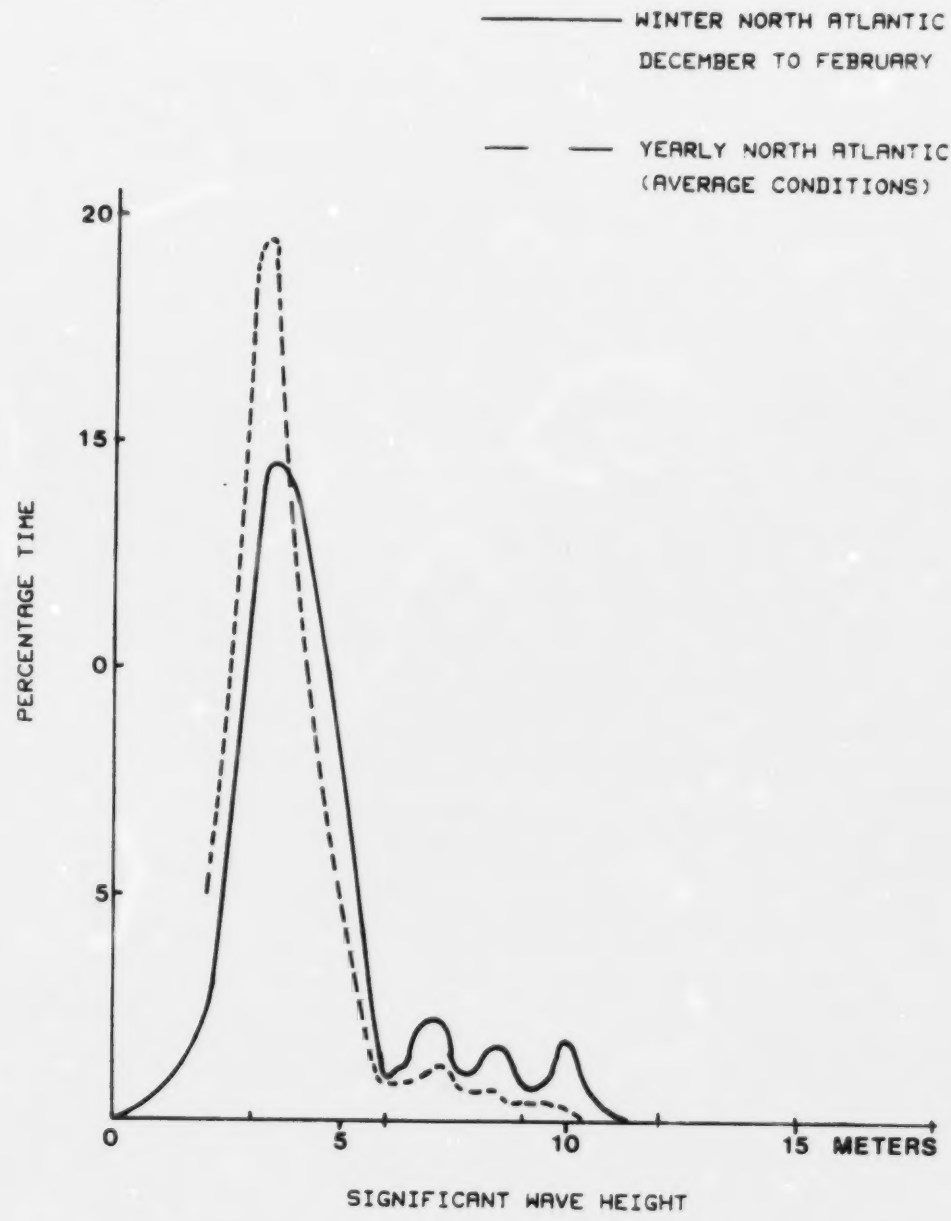

AVERAGE SEA SPECTRA-NORTH ATLANTIC

FIGURE 2.1

The CASPPR put forward regulations which outline the hull integrity, machinery installation, and outfit of Arctic type and class ships. The CASPPR also define Canadian Arctic zones and the times during which Arctic class ships may navigate in them. Except for the requirement that the hull form should "break" and "clear" ice "effectively", there is no requirement for a special type of hull form.

Depending on the time of year, the M.V. ARCTIC may pass through all or part of 4 safety control zones as defined by the CASPPR. The safety control zones are shown in Figure 2.2 and the times during which Arctic class vessels may navigate in them are shown in Table 2.1.

With specific reference to the M.V. ARCTIC voyages to the Polaris and Nanisivik mines, these safety control zones and permissible entry dates are:

Zone 6 - Western Barrow Strait and McDougall Sound
- August 15 to November 20

Zone 13 - Northwestern Baffin Bay, Lancaster Sound and Admiralty Inlet
- June 25 to November 15

Zone 9 - Northwest Davis Strait and western Baffin Bay
- August 1 to December 20

Zone 10 - Mid-western Davis Strait
- July 25 to December 20

It can be seen that the CASPPR permits the M.V. ARCTIC to call on the Nanisivik mine between June 25 and November 15, and the Polaris mine between August 15 and November 20. This section of the report studies the environmental conditions the M.V. ARCTIC may meet on route through:

- Davis Strait: Cape Farewell to Disko Island (60° - 70°N)
- Baffin Bay; Disko Island to the entrance of Lancaster Sound (70° - 76°N)
- Lancaster Sound (94°W - 80°W)
- Admiralty Inlet (Nanisivik mine)
- Barrow Strait and McDougall Sound (Polaris mine)

Six ice parameters will be discussed in this section with reference to the Canadian Arctic:

- snow cover
- first-year ice
  - . cover
  - . thickness
  - . strength
- old ice
- ridging

In addition, a brief review is made of ice conditions in the Baltic.

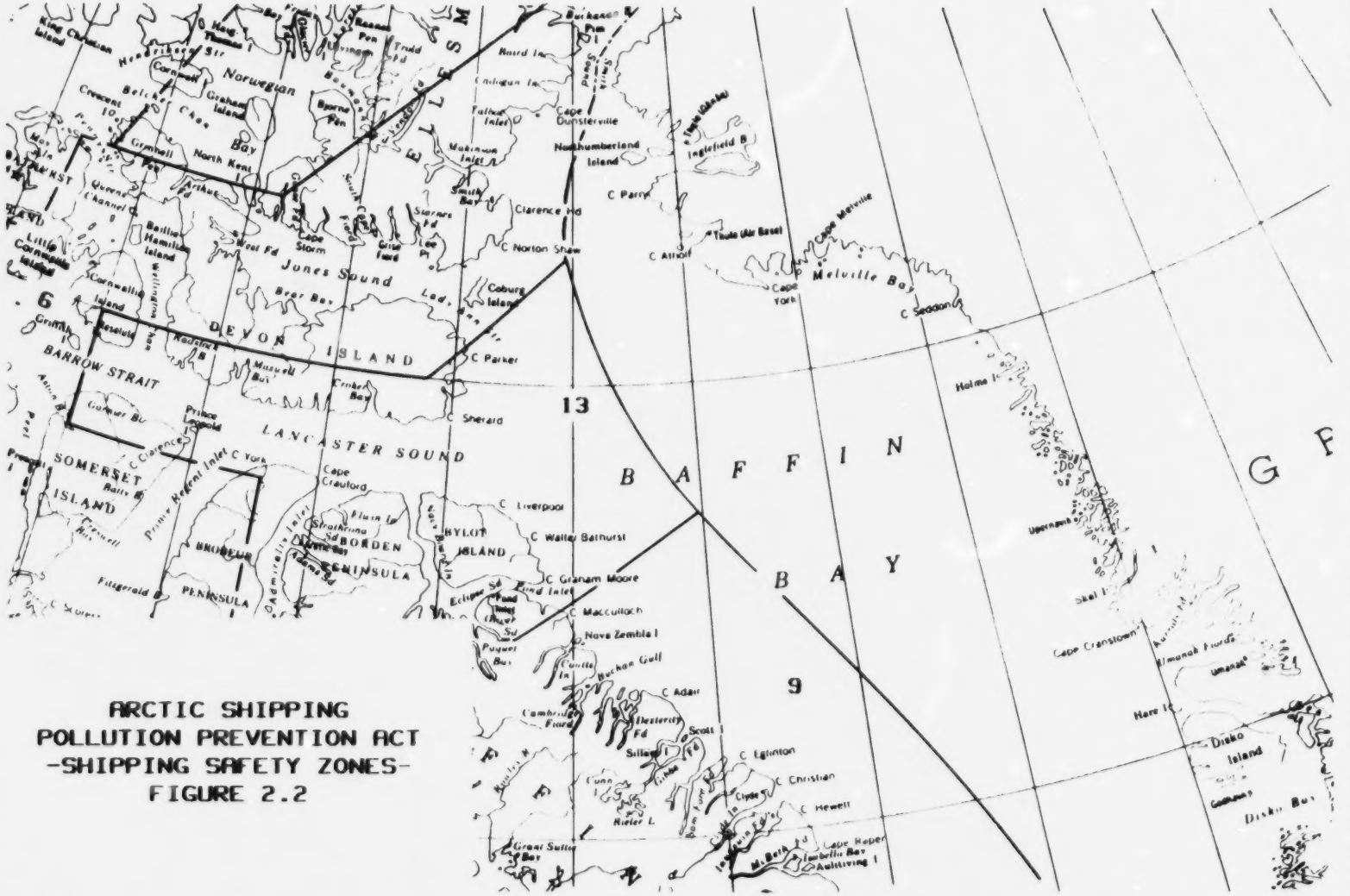

ARCTIC SHIPPING
POLLUTION PREVENTION ACT
-SHIPPING SAFETY ZONES-
FIGURE 2.2

Column I Category	Column II Zone 1	Column III Zone 2	Column IV Zone 3	Column V Zone 4	Column VI Zone 5	Column VII Zone 6	Column VIII Zone 7	Column IX Zone 8	Column X Zone 9	Column XI Zone 10	Column XII Zone 11	Column XIII Zone 12	Column XIV Zone 13	Column XV Zone 14	Column XVI Zone 15	Column XVII Zone 16
Arctic Class 10 1.	All Year	All Year	All Year	All Year	All Year	All Year	All Year	All Year	All Year	All Year	All Year	All Year	All Year	All Year	All Year	All Year
Arctic Class 8 2.	Jul. 1 to Oct. 15	All Year	All Year	All Year	All Year	All Year	All Year	All Year	All Year	All Year	All Year	All Year	All Year	All Year	All Year	All Year
Arctic Class 7 3.	Aug. 1 to Sept. 30	Aug. 1 to Nov. 30	Jul. 1 to Dec. 31	Jul. 1 to Dec. 15	Jul. 1 to Dec. 15	All Year	All Year	All Year	All Year	All Year	All Year	All Year	All Year	All Year	All Year	All Year
Arctic Class 6 4.	Aug. 15 to Sept. 15	Aug. 1 to Oct. 31	Jul. 15 to Nov. 30	Jul. 15 to Nov. 30	Aug. 1 to Oct. 15	Jul. 15 to Feb. 28	Jul. 1 to Mar. 31	Jul. 1 to Mar. 31	All Year	All Year	Jul. 1 to Mar. 31	All Year	All Year	All Year	All Year	All Year
Arctic Class 4 5	Aug. 15 to Sept. 15	Aug. 15 to Oct. 15	Jul. 15 to Oct. 31	Jul. 15 to Nov. 15	Aug. 15 to Sept. 30	Jul. 20 to Dec. 31	Jul. 15 to Jan. 15	Jul. 15 to Jan. 15	Jul. 10 to Mar. 31	Jul. 10 to Feb. 28	Jul. 5 to Jan. 15	June 1 to Jan. 31	June 1 to Feb. 15	June 15 to Feb. 15	June 15 to Mar. 15	June 1 to Feb. 15
Arctic Class 3 6.	Aug. 20 to Sept. 15	Aug. 20 to Sept. 30	Jul. 25 to Oct. 15	Jul. 20 to Nov. 5	Aug. 20 to Sept. 25	Aug. 1 to Nov. 30	Jul. 20 to Dec. 15	Jul. 20 to Dec. 31	Jul. 20 to Jan. 20	Jul. 15 to Jan. 25	Jul. 5 to Dec. 15	June 10 to Dec. 31	June 10 to Dec. 31	June 20 to Jan. 10	June 20 to Jan. 31	June 5 to Jan. 10
Arctic Class 2 7.	No Entry	No Entry	Aug. 15 to Sept. 30	Aug. 1 to Oct. 31	No Entry	Aug. 15 to Nov. 20	Aug. 1 to Nov. 20	Aug. 1 to Nov. 30	Aug. 1 to Dec. 20	Jul. 25 to Dec. 20	Jul. 10 to Nov. 20	June 15 to Dec. 5	June 25 to Nov. 15	June 25 to Dec. 10	June 25 to Dec. 20	June 10 to Dec. 10
Arctic Class 1A 8.	No Entry	No Entry	Aug. 20 to Sept. 15	Aug. 20 to Sept. 30	No Entry	Aug. 25 to Oct. 31	Aug. 10 to Nov. 5	Aug. 10 to Nov. 20	Aug. 10 to Dec. 10	Aug. 1 to Dec. 10	Jul. 15 to Nov. 10	Jul. 1 to Nov. 10	Jul. 15 to Oct. 31	Jul. 1 to Nov. 30	Jul. 1 to Dec. 10	June 20 to Nov. 30
Arctic Class 1 9.	No Entry	No Entry	No Entry	No Entry	No Entry	Aug. 25 to Sept. 30	Aug. 10 to Oct. 15	Aug. 10 to Oct. 31	Aug. 10 to Oct. 31	Aug. 1 to Oct. 31	Jul. 15 to Oct. 20	Jul. 1 to Oct. 31	Jul. 15 to Oct. 15	Jul. 1 to Nov. 30	Jul. 1 to Nov. 30	June 20 to Nov. 15
Type A 10	No Entry	No Entry	Aug. 20 to Sept. 10	Aug. 20 to Sept. 20	No Entry	Aug. 15 to Oct. 15	Aug. 1 to Oct. 25	Aug. 1 to Nov. 10	Aug. 1 to Nov. 20	Jul. 25 to Nov. 20	Jul. 10 to Oct. 31	June 15 to Nov. 10	June 25 to Oct. 22	June 25 to Nov. 30	June 25 to Dec. 5	June 20 to Nov. 20
Type B 11.	No Entry	No Entry	Aug. 20 to Sept. 5	Aug. 20 to Sept. 15	No Entry	Aug. 25 to Sept. 30	Aug. 10 to Oct. 15	Aug. 10 to Oct. 31	Aug. 10 to Oct. 31	Aug. 1 to Oct. 31	Jul. 15 to Oct. 30	Jul. 1 to Oct. 25	Jul. 15 to Oct. 15	Jul. 1 to Nov. 30	Jul. 1 to Nov. 30	June 20 to Nov. 10
Type C 12.	No Entry	No Entry	No Entry	No Entry	No Entry	Aug. 25 to Sept. 25	Aug. 10 to Oct. 10	Aug. 10 to Oct. 25	Aug. 10 to Oct. 25	Aug. 1 to Oct. 25	Jul. 15 to Oct. 15	Jul. 1 to Oct. 25	Jul. 15 to Oct. 10	Jul. 1 to Nov. 25	Jul. 1 to Nov. 25	June 25 to Nov. 10
Type D 13	No Entry	No Entry	No Entry	No Entry	No Entry	No Entry	Aug. 10 to Oct. 5	Aug. 15 to Oct. 20	Aug. 15 to Oct. 20	Aug. 5 to Oct. 20	Jul. 15 to Oct. 10	Jul. 1 to Oct. 20	Jul. 30 to Sept. 30	Jul. 10 to Nov. 10	Jul. 5 to Nov. 10	Jul. 1 to Oct. 31
Type E 14	No Entry	No Entry	No Entry	No Entry	No Entry	No Entry	Aug. 10 to Sept. 30	Aug. 20 to Oct. 20	Aug. 20 to Oct. 15	Aug. 10 to Oct. 20	Jul. 15 to Sept. 30	Jul. 1 to Oct. 20	Aug. 15 to Sept. 20	Jul. 20 to Oct. 31	Jul. 20 to Nov. 5	Jul. 1 to Oct. 31*

TABLE 2.1
PERIOD OF NAVIGATION FOR THE SHIPPING SAFETY CONTROL ZONES

2.3.1 Snow Cover

Snow cover is routinely only recorded at a limited number of coastal stations in the Arctic. As a result, there is not a large data base of snow cover recordings. For the purposes of this report however, a number of observations can be made:

- There is in general, low precipitation among the Canadian Arctic Islands. The region is classified as a polar desert.
- October has the highest mean value for snowfall, and the highest mean number of measurable snowfall days.
- 50% of the snow falls before early December.

Specific precipitation values can be referred to in Ref. 2.1.

Figures 2.3 and 2.4 show the mean snow depth at the end of June and end of December respectively. These figures show that the maximum snow depths which are likely to be encountered are between 5 and 10 cm in June and less than 30 cm in December.

It can be concluded that the precipitation of snow is very small. As a result, the effect of snow on bow design will be ignored.

2.3.2 First Year Ice; Cover, Thickness and Strength

In Davis Strait, the ice cover will be concentrated on the western side of the strait due to the influence of the cold Canadian or Baffin Island current. As a result, the M.V. ARCTIC's route passes up the eastern side of the strait where the warm west Greenland current promotes thinner, weaker ice.

In Baffin Bay, during May, the first-year ice will be in a range from 1.3 to 1.6 m thick. Mean confined compressive strengths of the ice will be in the 10 to 15 MPa range, and mean flexural strengths in the 450 to 500 kPa range. By June the level ice thickness will have reduced to 0.7 to 1 m and the mean confined compressive strength is expected to be about 6 MPa with a mean flexural strength of about 350 kPa. The level ice continues to decay into July by which time large areas of open water will be present.

Ice will begin to form again in western areas of the Bay close to shore during October. By November, Baffin Bay will be largely covered with moving pack ice. The new ice will be approximately 0.2 to 0.4 m thick. During December, the ice will be about 0.75 m thick with an estimated mean flexural strength of 300 to 400 kPa and a mean confined compressive strength of 12.5 to 15 MPa.

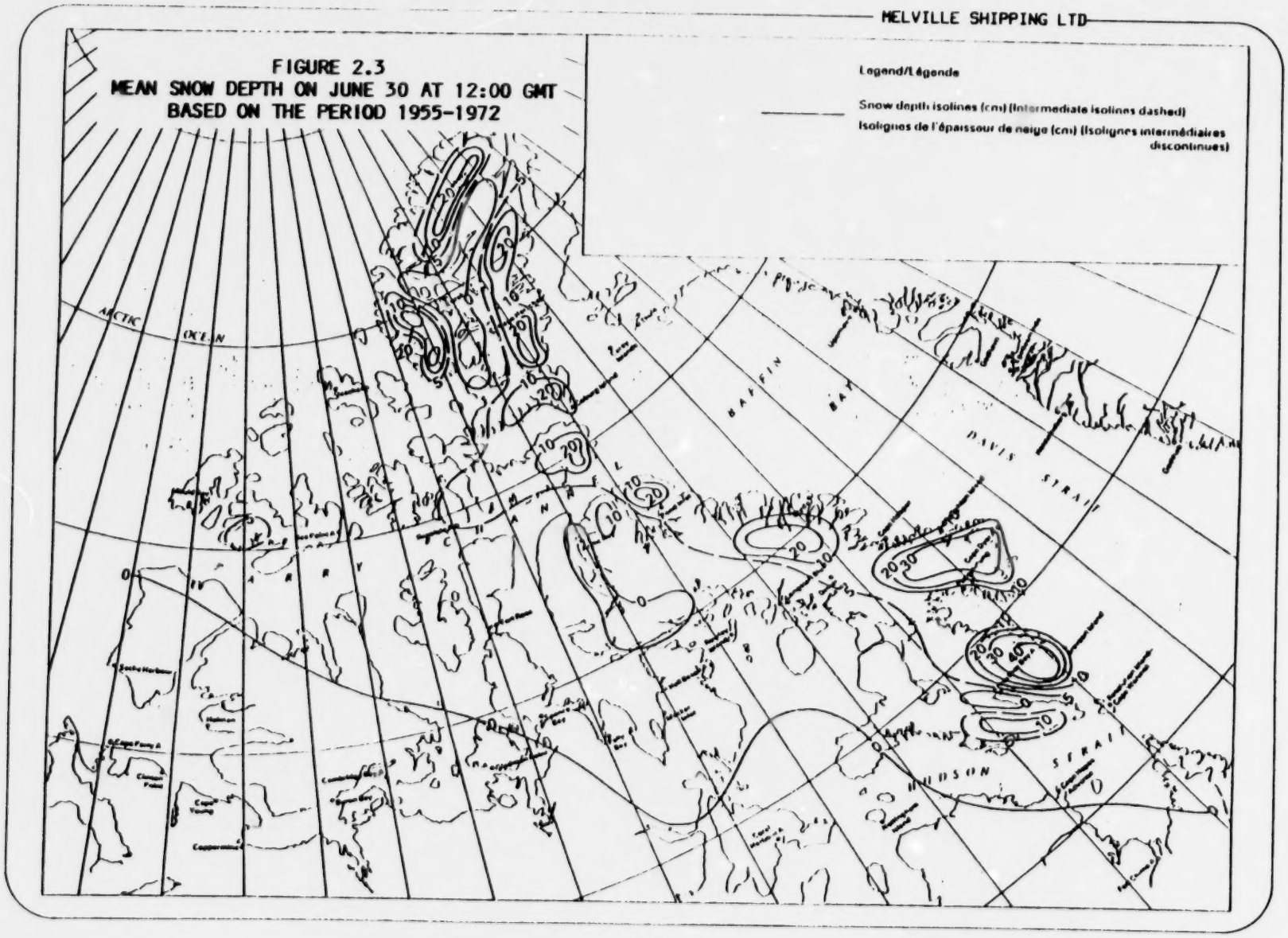
MELVILLE SHIPPING LTD
FIGURE 2.3
MEAN SNOW DEPTH ON JUNE 30 AT 12:00 GMT
BASED ON THE PERIOD 1955-1972
Legend/Légende
Snow depth isolines (cm) (Intermediate isolines dashed)
Isolignes de l'épaisseur de neige (cm) (Isolignes intermédiaires discontinues)
ARCTIC OCEAN
BAFFIN BAY
DAVIS STRAIT
HUDSON STRAIT

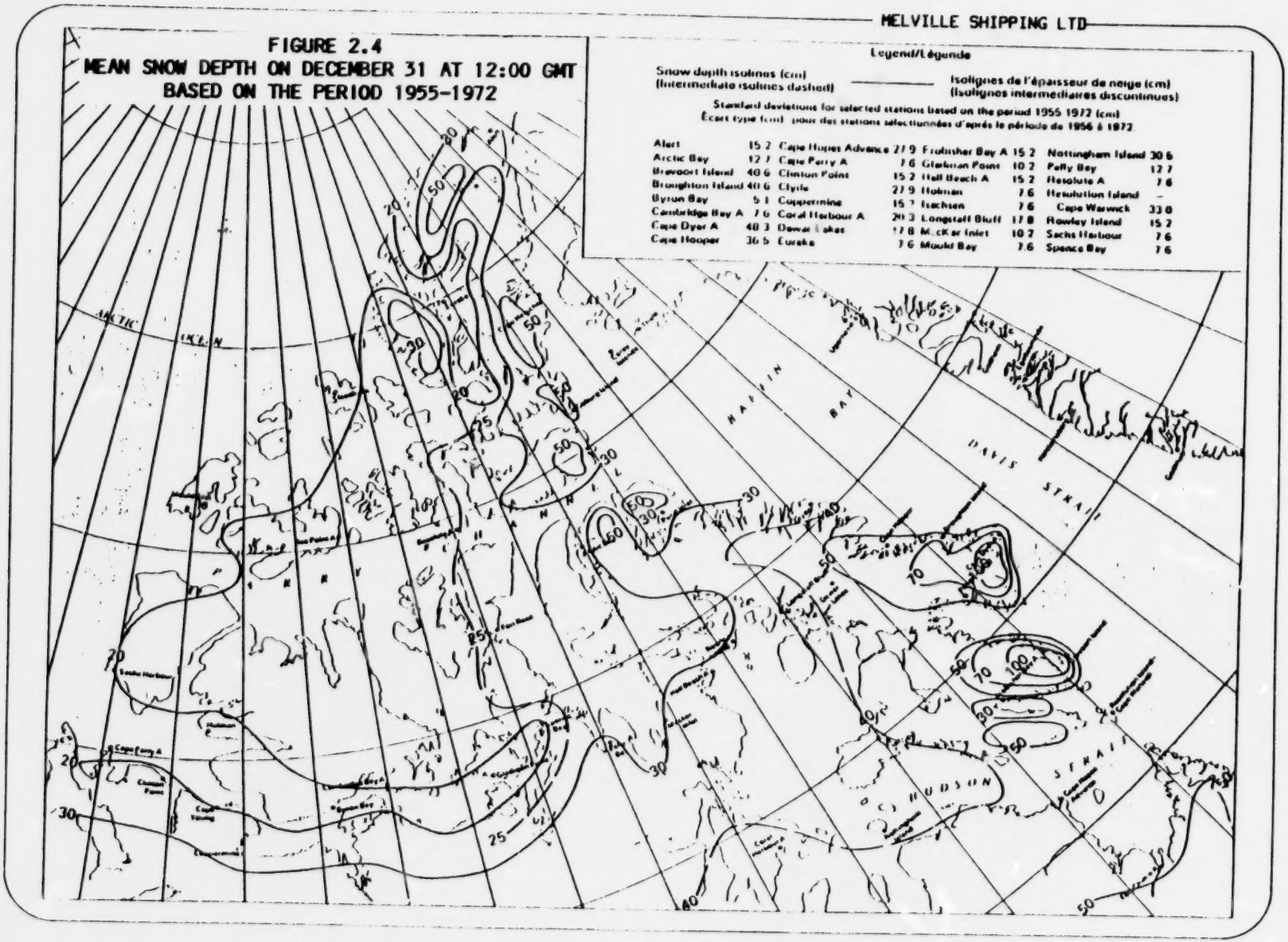
FIGURE 2.4
MEAN SNOW DEPTH ON DECEMBER 31 AT 12:00 GMT
BASED ON THE PERIOD 1955-1972
Legend/Légende
Snow depth isolines (cm)
(Intermediate isolines dashed)
Isolignes de l'épaisseur de neige (cm)
(Isolignes intermédiaires discontinues)
Standard deviations for selected stations based on the period 1955-1972 (cm)
Ecart type (cm) pour des stations sélectionnées d'après la période de 1956 à 1972
Alert 15.2
Arctic Bay 12.7
Brevoort Island 40.6
Broughton Island 40.6
Byron Bay 5.1
Cambridge Bay A 7.6
Cape Dyer A 48.3
Cape Hooper 36.6
Cape Hopes Advance 27.9
Cape Perry A 7.6
Clinton Point 15.2
Clyde 27.9
Coppermine 15.7
Coral Harbour A 20.3
Dewar Lakes 17.8
Eureka 7.6
Frobisher Bay A 15.2
Glenlion Point 10.2
Hall Beach A 15.2
Holman 7.6
Inuvik 7.6
Longstaff Bluff 17.8
McKar Inlet 10.2
Mould Bay 7.6
Nottingham Island 30.6
Pelly Bay 12.7
Resolute A 7.6
Resolution Island -
Cape Warwick 33.0
Rowley Island 15.2
Sachs Harbour 7.6
Spence Bay 7.6
ARCTIC
CIRCLE
BAFFIN
BAY
DAVIS
STRAIT
HUDSON
STRAIT

Lancaster Sound, during May, will be entirely covered with ice. In the western section of Lancaster Sound the ice cover will be consolidated and land fast. The eastern edge of this consolidated ice forms an ice edge which runs in a north/south concave arc near Prince Leopold Island. East of this edge, the ice cover will be very close pack, approximately 1.8 to 2.0 m thick with a mean confined compressive strength of 17.5 to 20 MPa and flexural strengths calculated to be about 500 kPa. By mid-June much of the route will be in open water. Any remaining ice will be in very open pack and may be about 0.75 m thick.

Ice will begin to form again in the southern part of Lancaster Sound during October and by November, this first-year ice will form an unconsolidated moving pack. The ice will be about 0.5 m thick with a flexural strength of 300 to 400 kPa. The mean confined compressive strength of the ice will be about 18 MPa. Level ice in December in Lancaster Sound will be moving pack with fast ice in the coastal areas. At this time, level ice thicknesses will be about 0.8 to 0.9 m with a mean flexural strength of about 450 to 550 kPa and a mean confined compressive strength of about 15 MPa.

Admiralty Inlet in May will be covered with consolidated level ice 1.75 to 2.0 m thick. The mean flexural strengths will be about 500 kPa and the mean confined compressive strength will be in the 17.5 to 20 MPa. In mid-June the thickness of the ice is expected to remain unchanged although the mean flexural and confined compressive strengths are expected to have dropped to 450 kPa and 13 MPa respectively.

The mean date of fracture for Admiralty Inlet is 25 July. The floes will be decaying and the thicknesses are expected to be 1.0 m to 1.25 m. It should be noted that the melting of the ice cover occurs in the grain boundaries and not only in the air/ice or ice/water interface. Consequently, the ice cover will not grow significantly thinner before disappearing, but will grow significantly weaker.

Ice will begin to form in Admiralty Inlet again during October and by November the Inlet will be covered with fast ice about 0.3 m thick with flexural strength in the 400 kPa range and with a mean confined compressive strength of 5 to 10 MPa.

In Barrow Strait the ice cover will be very close pack about 1.5 to 1.75 m thick with a mean confined compressive strength of 15 MPa and a mean flexural strength of 300 to 400 kPa. The ice is expected to fracture by August and the ice cover will be in a state of decay with thicknesses of 1.0 to 1.25 m with low flexural and compressive strengths.

The median date for the reappearance of ice in Barrow Strait and McDougall Sound is September 24th. The ice will be mobile with very low strengths. By November the ice cover in Barrow Strait will be moving pack with thicknesses in the 0.5 to 0.6 m range and a mean flexural strength of 400 kPa and a mean confined compressive strength of 10 MPa. McDougall Sound will be covered in fast ice cover, fairly smooth and about 0.6 m thick.

In December, the mean ice thickness in Barrow Strait and McDougall Sound will be about 0.9 m thick with a mean confined compressive strength of 15 to 17.5 MPa and a mean flexural strength of about 550 kPa.

2.3.3 Old Ice

Old ice is defined as ice which has survived at least one summer melt. Multi-year ice is ice that has survived at least two summer melts. The two categories are usually very difficult to identify from each other so, for the purpose of this report, they have been considered together.

Old ice is usually thicker than any surrounding first-year ice by virtue of having survived at least one summer melt and because in general it will have its origin in colder temperature regions. The old ice will also be generally stronger than the surrounding ice due to its low brine content resulting from brine drainage which occurs during the summer season.

In Baffin Bay, the median amount of old ice will only be a trace in the last week of June. Quantities rise in July as two tenths from mid-July until mid-August before dropping to zero over most of the area through September and October.

Clearing of the summer ice cover permits old ice to move from the reservoirs in the Sverdrup basin, western Viscount Melville Sound and elsewhere into eastern Parry Channel and Baffin Bay. In September, when the open water extent is generally the greatest, old ice is most mobile. Influx of old ice from Nares Strait and Smith Sound produces an increase in the concentration across the entrance to Lancaster Sound in the autumn. In late October and November the median amount of old ice in this area is 2 tenths.

2.3.4 Ridging

Ridging is defined as a wall of broken ice forced up by pressure. These may form for a number of reasons; land fast ice being in contact with a mobile pack, or large ice floes moving in pack ice.

Ridging will be present in the northwestern area of Baffin Bay as the general anticlockwise motion of the pack as well as possible onshore winds, pushes the moving pack onto the land fast ice. Ridging will be the most severe at the entrance to Lancaster Sound with ridging frequency in the order of 5 to 7 ridges per km. The mean sail height of these ridges will be about 1.1 m and the depth of consolidation will be about 40% more than the adjacent ice.

Very little ridging occurs in Admiralty Inlet or McDougall Sound. Ridging in Barrow Strait is highly varied as a consequence of the geometry and location of islands in the channel. Ridging frequency data shows a variation from 1.29 to 5.62 per km. The mean ridge height is reported to be from 0.83 to 1.05 m.

2.4 Ice Covered Waters - Baltic Sea

The maximum ice extent that may be expected in the Baltic is during March. Average dates for the first formation of ice in this area are late October for the northern end of the Gulf of Bothnia, and mid-December for the Gulf of Finland. The mean level ice thickness is 0.6 to 0.75 m in the northern part of the Gulf of Bothnia and 0.3 to 0.45 m in the southern part of the Gulf of Bothnia and the Gulf of Finland. The maximum absolute ice thicknesses are estimated to be about 2.1 m close to the shore and 0.9 to 1.2 m further offshore in the northern part of the Gulf of Bothnia.

Apart from very close to the coast or in shallow area, "pressured ice" can reach heights of 0.3 to 0.9 m above sea level, with a total thickness of about 1.8 to 2.7 m. These maximum thicknesses occur during February to mid-March. The ridging frequency in the Baltic is quite high mainly because of the shallowness and restricted nature of the Gulf of Bothnia and the thinness of ice.

2.5 Summary

The maximum ice thicknesses and strengths that will be encountered by the M.V. ARCTIC on the voyages to Nanisivik and Polaris will be in Admiralty Inlet during May. Ice thicknesses here will be 1.75 to 2.0 m thick and 500 kPa. As a result these figures are used in the subsequent sections as design targets for the capability of the modified bow form. The ice conditions in the Canadian Arctic, described above, have been summarized in tabular form and are presented in Appendix 1.

3.0 DEVELOPMENT OF MODIFIED BOWS

3.1 General

A great part of the M.V. ARCTIC's time is spent in open water. A smaller part of her time is spent in continuous icebreaking and an even shorter time in a non-continuous ramming mode.

The three primary modes of operation can be said to be:

- open water
- continuous icebreaking
- non-continuous icebreaking

The open water characteristics are discussed later in the report. The continuous icebreaking mode is the condition where the propeller thrust is sufficient to overcome the icebreaking resistance. Non-continuous icebreaking, is the condition where propeller thrust alone is not sufficient to break the ice. In this case, the vessel backs away from the ice edge, then, by moving forward again impacts the ice edge with some forward velocity. In this case, the force used to break the ice is partly due to the thrust from the propeller but is predominantly from conversion of the vessel's kinetic energy.

Recently, a great deal of research and testing has been conducted to predict the effect of hull form on icebreaking resistance. The mechanism of ice breaking, although not thoroughly understood, is now much clearer. Some of this research has involved the M.V. ARCTIC. Table 3.1 gives the vessel's main dimensions and form coefficients.

This section of the report investigates the form of resistance predictor equations, develops new bow forms and discusses how the new forms may perform.

3.2 The Development of a Predictor Equation

Of the two icebreaking modes discussed above, continuous icebreaking lends itself more to analysis than non-continuous. Since it is also the condition that the vessel will predominantly be operating in, the continuous mode should be considered of primary importance. The non-continuous or ice ramming mode, is more directly a function of ship mass, although the bow form does have some effect on the vessel's ramming ability.

With reference to the continuous mode, the evaluation of icebreaking resistance can be based on three approaches (Ref. 3.1, 3.2):

- Theoretical
- Semi-empirical
- Empirical

CLASS	- Lloyd's Register of Shipping 100A1 - L.M.C. "Ice Class 1A Super" Arctic Shipping Pollution Prevention Regulations for Class 2 Vessel
LENGTH OA	- 209.55 m
LENGTH BP	- 196.59 m
BREADTH MLD	- 22.86 m
DEPTH MLD	- 15.24 m
DRAUGHT Max.	- 10.97 m
DISPLACEMENT	- 38,249.04 (salt water)
BLOCK COEF. C_B	- 0.756
* FORWARD BLOCK COEF. C_{Bf}	- 0.515
MIDSHIP SECTION COEF.	- 0.991
LENGTH OF PARALLEL MID-BODY	- 42.6 m
PROPULSION	- MAN 14V-52/55A 14,770 BHP @ 450 RPM CP Propeller, 5.27 m DIA, 4 blades Fixed NSMB 19A Nozzle

* The forward block coefficient used here is defined as the block coefficient forward of the parallel mid body at the load waterline.

TABLE 3.1
M.V. ARCTIC - PRINCIPAL PARTICULARS

Early researchers had little full-scale ship data and developed theoretical and mathematical expressions for resistance. Runeberg, Kari, Simonson and Vinogradov are the most influential of these researchers (Ref. 3.3).

Authors such as Milano (Ref. 3.4) are developing theoretical solutions for the effect of bow form and ice characteristics on ship resistance in ice. Other authors, such as Enkvist (Ref. 3.2) and Kashteljan (Ref. 3.1), have developed semi-empirical methods which involve coefficients derived from model test programs and full-scale data. Purely empirical evaluation has been disregarded as a useful tool since it can only be applied to a vessel type which has passed through its trials and cannot be considered as applying to a range of parametrically different hull forms.

There are then two useful approaches to icebreaking prediction; semi-empirical and theoretical.

Due to the complexity of the theoretical approach to ice resistance prediction and its early stage of development, it was decided to develop a semi-empirical formulation which could be used as a design tool to redesign the M.V. ARCTIC's bow.

It has been shown by a number of authors (Ref. 3.1, 3.2) that in the form of a semi-empirical equation, the total icebreaking resistance can be divided into a number of components.

These can be represented by the equation:

$$R_T = R_1 + R_2 + R_3 + R_4$$

R_T = Total ice resistance

R_1 = Resistance associated with breaking ice

R_2 = Resistance associated with turning and submerging the ice

R_3 = Resistance associated with velocity including inertial forces

R_4 = Open water resistance

Each of these components can be represented by variables or groups of variables associated with that particular component. The variables which affect ice resistance are shown in Table 3.2. These variables may be represented in one, or all of the ice resistance components.

In order to develop a useful design tool the significance of each of these ship and ice variables on the total resistance of the vessel must be considered. These components can then be combined in a predictor equation to allow correlation with full-scale and model scale tests.

THE ICE		THE SHIP	
Ice Thickness	(h)	Stem Angle	(γ)
Ice Strength	(σ_f)	Waterline Entrance Angle	(α)
Ice Modulus of Elasticity	(E)	Flare Angle at Waterline	(β)
Mass Density	(ρ)	Beam	(B)
		Draught	(T)
		Length	(L)
		Displacement	(Δ)
		Fore Body Block Coefficient	(C_{bf})
		Ship Speed	(V)
		Friction Coefficient	(f)

TABLE 3.2
PRIMARY CHARACTERISTICS AFFECTING LEVEL ICE RESISTANCE

The ice variables which are thought to be most significant are strength and thickness. The ship variables which are thought to be most significant are stem angle, waterline entrance and flare angles, beam, length, forebody block, speed and friction. These parameters are discussed in some detail later in this section as they effect the developed predictor equation. The waterline and flare angles as used in this report are defined in Figure 3.1.

The remaining characteristics which are listed in Table 3.2 are discussed below:

- Modulus of Elasticity of Ice (E)

This parameter only affects the icebreaking component of resistance. In terms of model testing, which will be discussed later, it represents the most difficult scaling parameter.

- Mass Density (ρ)

The mass density component will enter into both the turning and submerging resistance component and the resistance associated with velocity.

- Displacement (Δ)

The displacement will be associated with the vessel's ability to ram. High displacement will result in a larger kinetic energy. The effect of this higher displacement will be to increase the ice crushing/bending forces.

- Draught (T)

The draught of the vessel is not always included in predictor equations as a variable. However, the draught will, to some degree, determine the depth to which the broken ice is submerged, (Ref. 3.2). Breaking and velocity components would appear to be independent of draught.

A number of predictor equations have been developed by various authors over the last few years and some of these are shown in Table 3.3.

Three of these equations have been selected, together with a purely analytical approach developed by Milano (Ref. 3.4), and are shown in Figure 3.2 for a "Wind Class" icebreaker. The predictor equations have been plotted for 0.61 m (2 feet) level snow-free ice, and with the exception of the Milano formulation, use a flexural strength of 500 kPa. The Milano formulation, following the author's use of ice strength, is set at 167 psi (1151 kPa). It may be argued that this figure is too high if it represents purely ice flexural strength. However, since this is the ice strength recommended by the author for use in the formulation, it is reproduced here. It is believed that a subsequent paper by Milano (Ref. 3.5) uses a lower strength value but the modified computer program is unavailable for comparison.

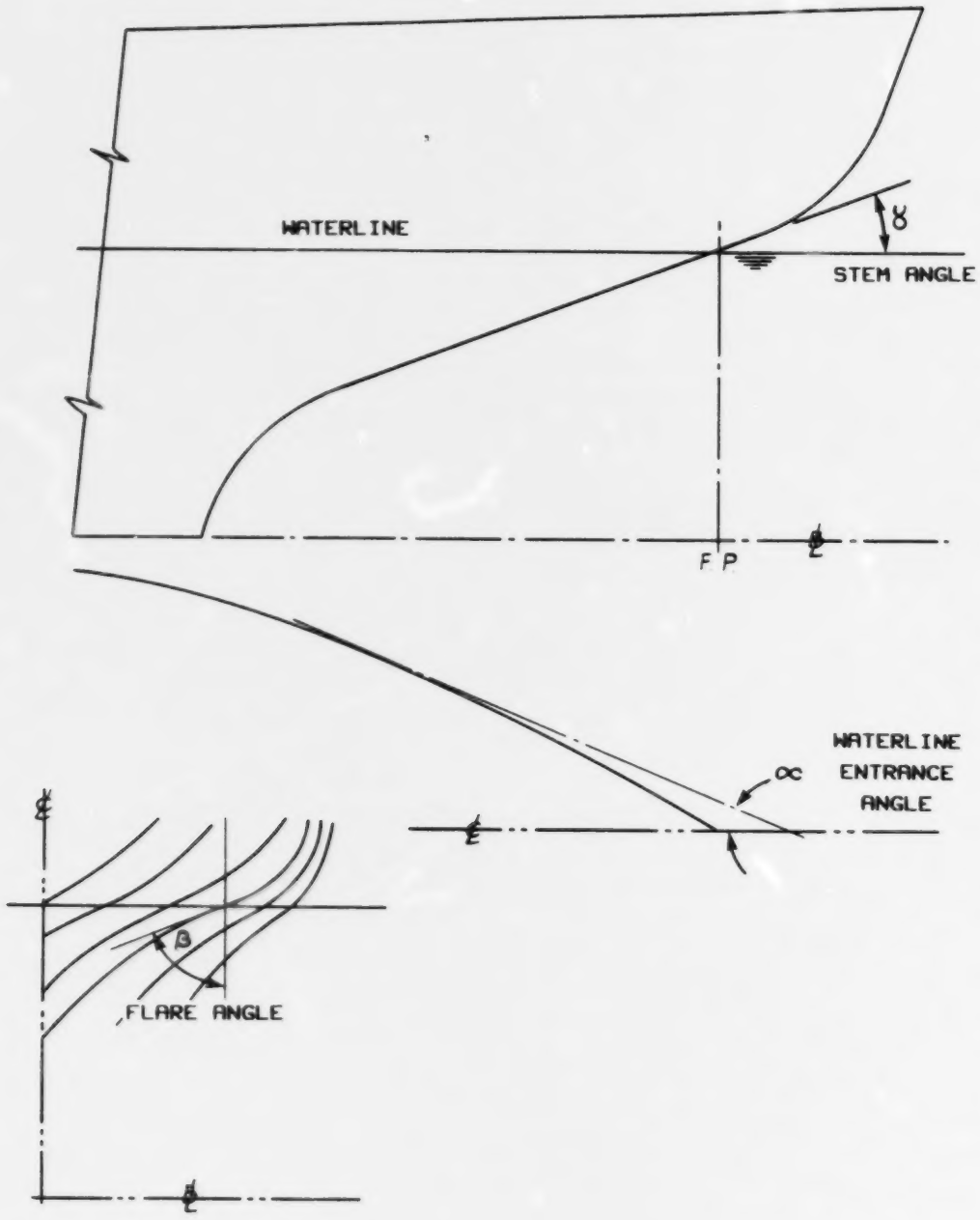

DEFINITION OF ANGLES
REPRESENTING BOW
GEOMETRY
FIGURE 3.1

AUTHOR	BREAKING		INERTIAL		VELOCITY
POZNYAK 1981	$C_0\ h^2\sigma_f$	+	$C_1\ \rho gBh$	+	$C_2\ \rho hB^2v$
EDWARDS, NAWWAR 1978	$C_0\ Bh\sigma_f$	+	$C_1\ Bh^2$	+	$C_2\ Bhv$
EDWARDS, ET AL 1976	$C_0\ Bh\sigma_f$	+	$C_1\ \rho gBh^2$	+	$C_2\ \rho gBh^{1.5}g^{0.5}v$
KASHTELJAN 1973	$C_0\ Bh\mu_0\sigma_f$	+	$C_1\ \gamma_2 Bh^2\mu_0$	+	$C_2\ B^n hv\ \frac{1}{\eta_2}$
WARTSILA 1973	$C_0\ Bh\sigma_f$	+	$C_1\ \rho gBhT$	+	$C_2\ \rho Bhv^2$
EDWARDS, ET AL 1972	-	+	$C_1\ \rho gBh^2$	+	$C_2\ (\frac{v^2}{gh} + \frac{v}{\sqrt{gh}})$
ENKVIST 1972	$C_0\ Bh\ \frac{\sigma_f}{E}\ \sigma_f$	+	$C_1\ \rho gBh$	+	$C_2\ Bhv^2$
LEWIS, EDWARDS 1970	$C_0\ h^2\sigma_f$	+	$C_1\ \rho gBh^2$	+	$C_2\ \rho Bhv^2$

TABLE 3.3
ICE RESISTANCE PREDICTOR EQUATION FORMS

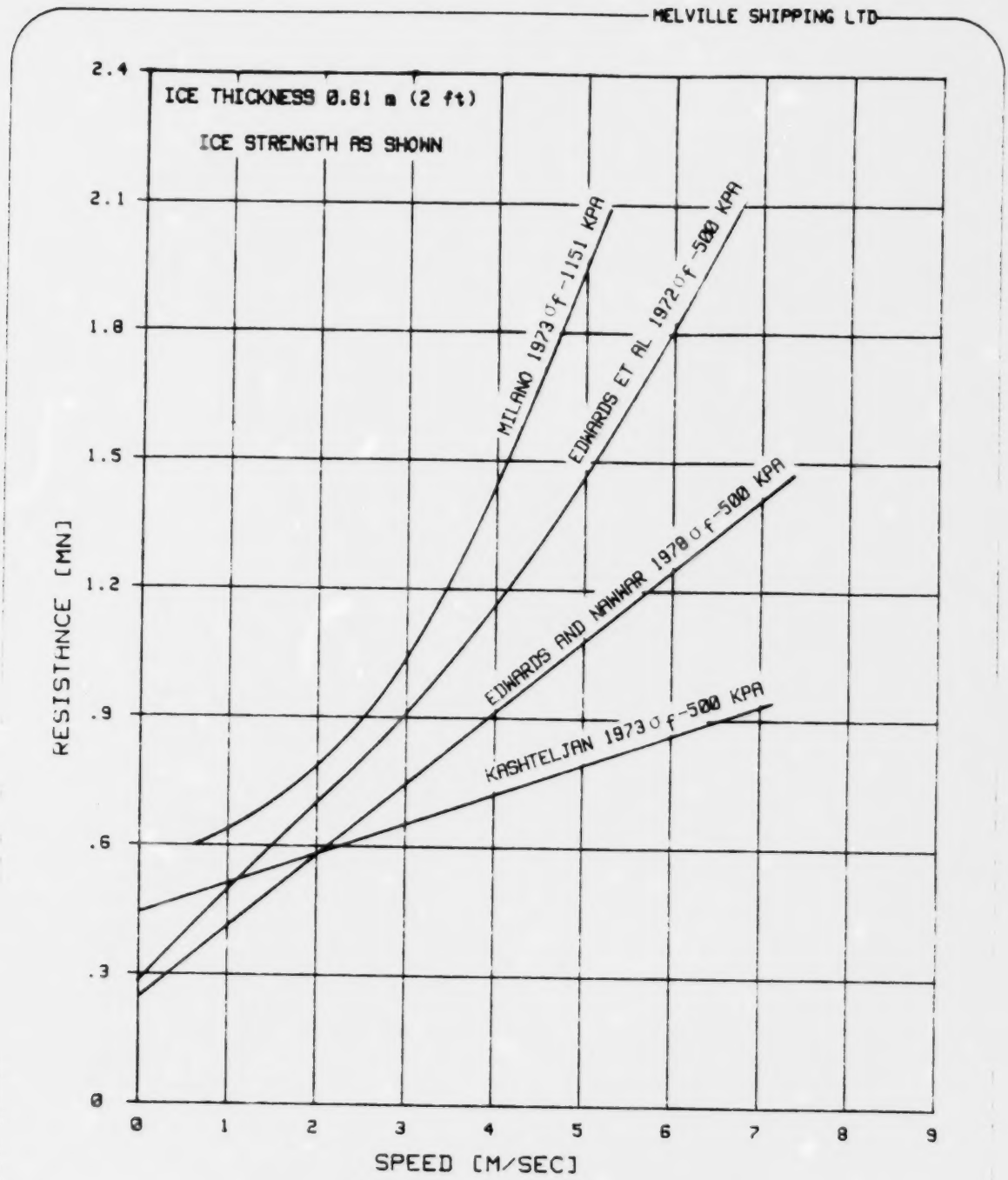

COMPARISON OF VARIOUS
LEVEL ICE PREDICTION EQUATIONS

FIGURE 3.2

During 1977/78, ARCTEC CANADA LIMITED completed a report for the Transportation Development R&D Centre (Ref. 3.11), which compiled all the readily available data on existing and proposed icebreaking designs.

Using a regression analysis technique the following predictor equation was generated:

$$\frac{R}{\gamma_i B h^2} = 0.727\ \mu_{12}^{\cdot 965}\ (L/B)^{1.036}\ (\tan\gamma_0)^{\cdot 332}\ (\cos\beta_5)^{-0.678} +$$

$$0.363\ C_{bf}^{\ 2.92}\ (\tan\gamma_0)^{-0.841}\ (\cos\beta_5)^{14.54}\ \frac{\sigma_f}{\gamma_i h}\ .\ \frac{V}{\sqrt{gh}}$$

See nomenclature for definition of symbols (pg. xii).

Following an analysis of this equation a number of observations can be made:

- The equation contains form coefficients, a friction coefficient and the primary vessel dimension ratios and coefficients.

- Due to the treatment of friction in μ_{12} the distribution of friction force acts against the buttock sections; as a result the friction component reduces to zero at the point of zero waterline angle. Crushing and breaking does occur at and near the fore body shoulders and will undoubtedly result in some friction value.

- The total icebreaking resistance is comprised of an inertial component and a combined strength and velocity component. This does not allow for a separate analysis of strength and velocity.

- The exponent of ($\tan\gamma$) in the second component results in higher resistance forces at lower flare angles. This appears to be contrary to reality.

In light of the number of vessels used to develop this equation, and the involvement of Transportation Development Centre in its formulation it was decided to use this equation as a base for the Melville design equation. The non-applicable variables were removed and coefficients modified to;

- Force the predictor equation to correctly predict the available full-scale data on the M.V. ARCTIC (Ref 3.6).

- Obtain reasonable correlation between the relative importance of each of the variables in the predictor equation to the known relative importance of these variables in either full or model scale.

The resulting equation is:

$$R_T = R_I + R_v + R_{\sigma_f} + R_o$$

$$R_I = 0.202\ u_{12}{}^{0.965}(L/B)^{1.036}h^{1.5}\ g\ B$$

$$R_v = 150\ C_{hf}{}^{2.92}\ v\ B\ h^{1.436}/\sqrt{g}$$

$$R_\sigma = 0.332\ \sigma^{0.75}\ B\ h$$

$$R_o = 3.342\ v^{2.5}$$

Although the form of this equation is different from that generated for the existing M.V. ARCTIC in Ref. 3.6, which represents the full-scale data the predicted full-scale values are the same. This is shown in Figure 3.3.

Figure 3.4 shows how the four components of resistance are represented for 0.8 m thick level ice. To further investigate the effect of individual parameters, each may be varied in the equation to highlight their significance. This has been done for 6 parameters.

- Ice thickness
- Ice flexural strength
- Bow form
- Beam
- Length
- Forward block coefficient

These parameters have been independently changed in the equation and the resulting resistance plotted. It is understood that with an actual bow it may be unrealistic to change one variable without necessarily changing a related variable. However for the sake of this analysis it was felt appropriate to do so.

a) Ice Thickness
It can be shown that ice thickness is one of the most important single parameters which affects the total ice resistance. Ice thickness will enter into all three of the resistance components. The thicker the ice, the more energy it will take to break the ice cover. The thickness will also determine the size of the ice block broken off. The thickness of the ice will therefore be associated with the inertial and velocity components of ice resistance.

b) Ice Strength
The significance of ice strength in the total ice resistance is not fully agreed upon. Poznyak (Ref. 3.7) for example, has represented the icebreaking component which most authors believe is directly proportional to ice flexural strength as a significant percentage of the total icebreaking resistance. Johansson (Ref. 3.8), has taken the opposite approach and has dropped the subgroup based on ice strength because of the belief that its influence on full-scale resistance is negligible compared with other components.

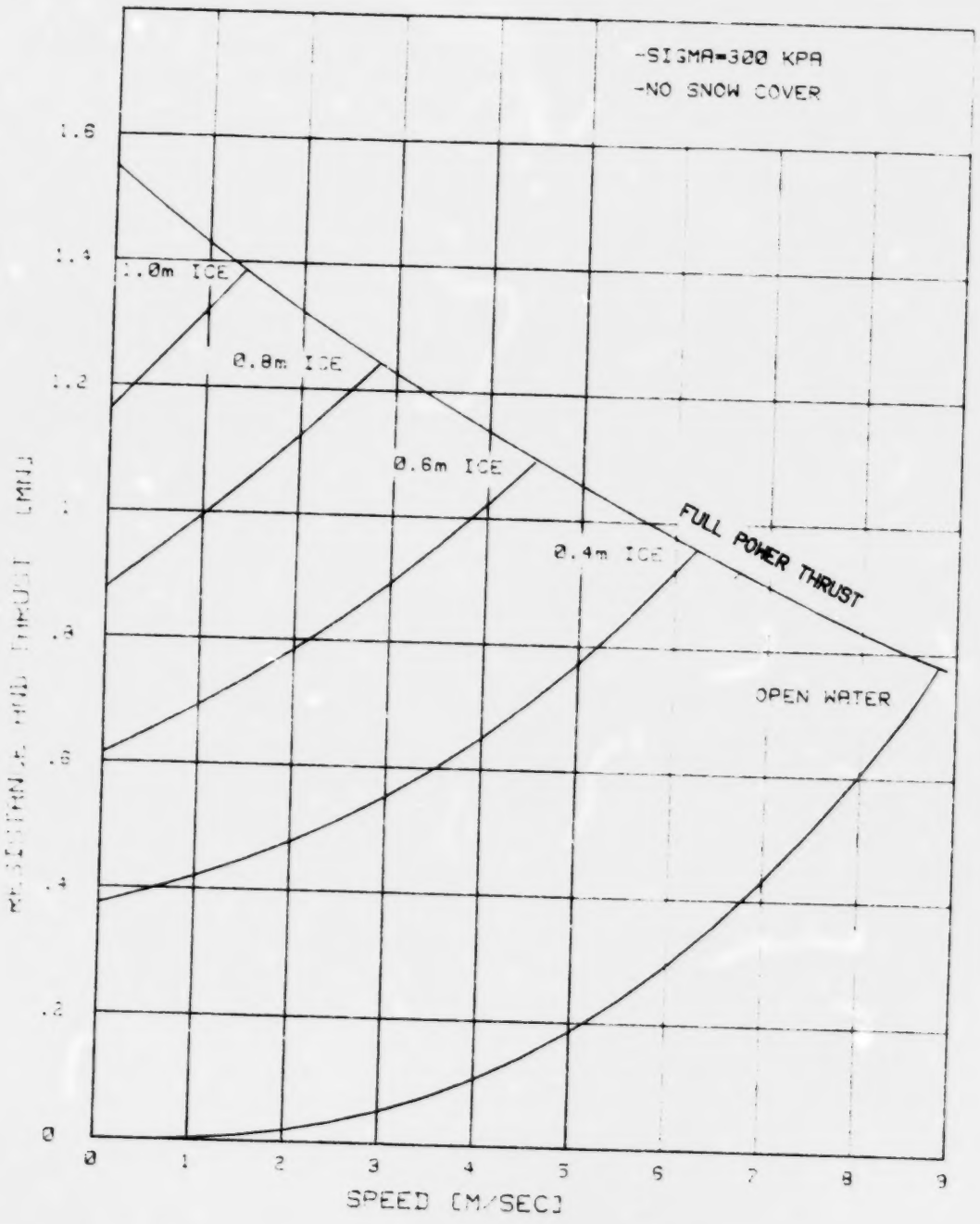

LEVEL ICE PREDICTION
EXISTING M.V. ARCTIC

FIGURE 3.3

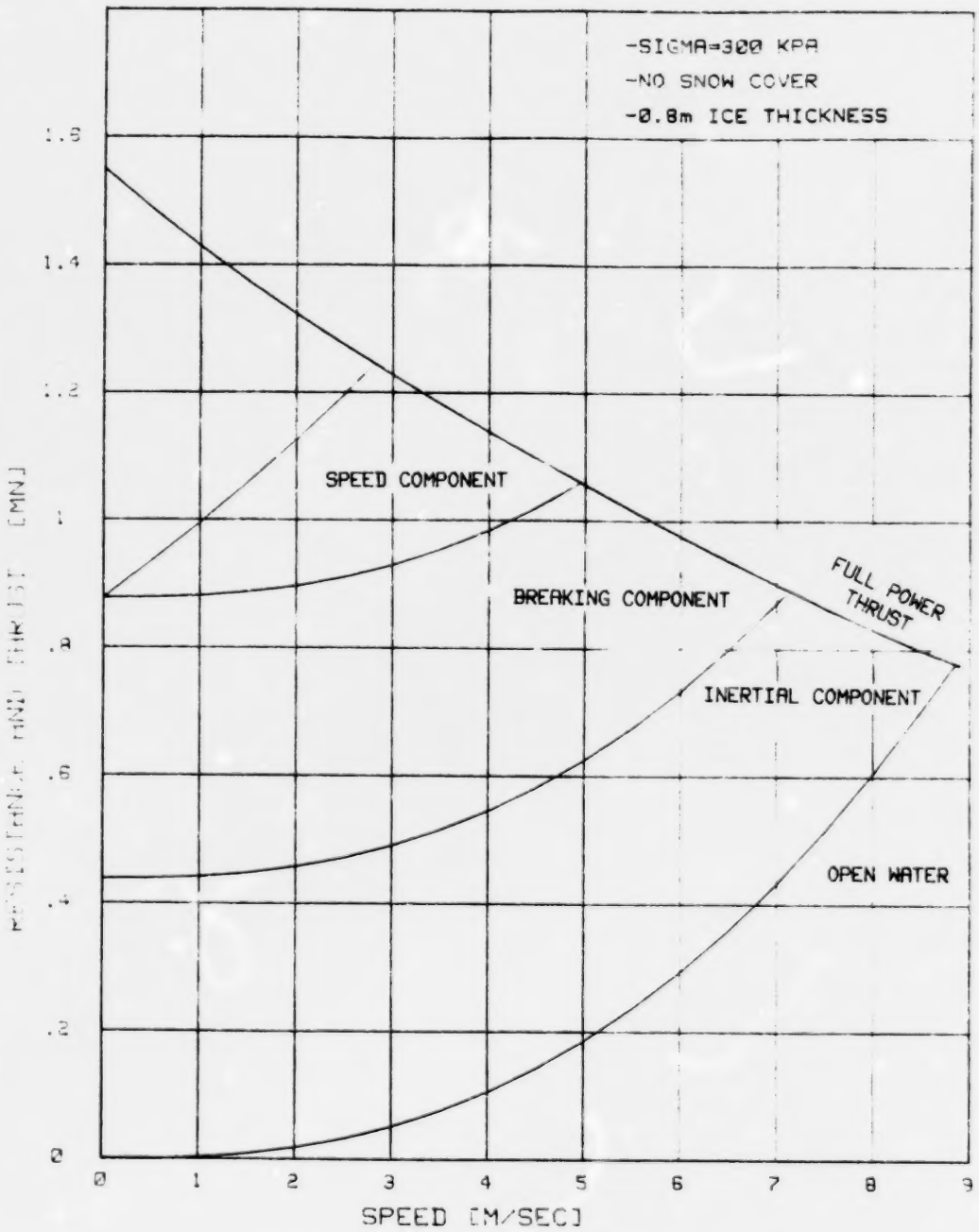

RESISTANCE COMPONENTS IN
LEVEL ICE PREDICTION
EXISTING M.V. ARCTIC

FIGURE 3.4

Figure 3.5 shows the predicted performance of the M.V. ARCTIC travelling through 0.4 and 0.8 m thick ice of 300, 400, 500 and 600 kPa flexural strength as predicted by the Melville equation. Table 3.4 gives a tabulated presentation of the percentage change of the total icebreaking resistance due to the change in flexural strength.

Table 3.5 has been reproduced from Vance, (Ref. 3.9) and shows how the individual components of resistance contribute to the total resistance during model and full-scale tests. It can be seen from this table how the proportional influence of the breaking component is higher in full-scale tests than in model scale tests. This has been partially confirmed by Enkvist in a recent paper (Ref. 3.10). Full-scale and model scale testing was conducted to indicate the relative size of the breaking and submerging components of resistance. The basic conclusions of this work were:

- The breaking component of resistance varies between 40 and 80% of total resistance at low speeds.
- The breaking component depends on the ship's beam.
- The breaking component is insensitive to ice thickness.

The strength dependency of the Melville equation can be compared to the Enkvist results (Ref. 3.10). This is done in Figure 3.6 and it can be seen that the Melville equation strength dependency is within the bounds of the data presented by Enkvist.

Although by comparing both of these references (Ref. 3.9 and 3.10) to the Melville equation, it would appear that the equation represents the strength component reasonably well, there still exists too much uncertainty with regard to this component and it is the focus of continual research.

c) Bow Form

The definition of bow form includes the three bow form parameters, stem angle (γ), waterline entrance angle (α) and waterline frame flare angle (β), defined earlier in this section.

Data collected for Melville Shipping Ltd. during model tests with an Arctic LNG tanker indicate that a reduction in stem angle results in a significant reduction in resistance. This however, should be viewed in association with the forward body block coefficient. A reduction in stem angle will generally result in a reduction in forward block coefficient, which may have the stronger influence. However, it would appear that a value for stem angle of approximately 15° to 20° should be used. This will result in both low block coefficients and high flare angles.

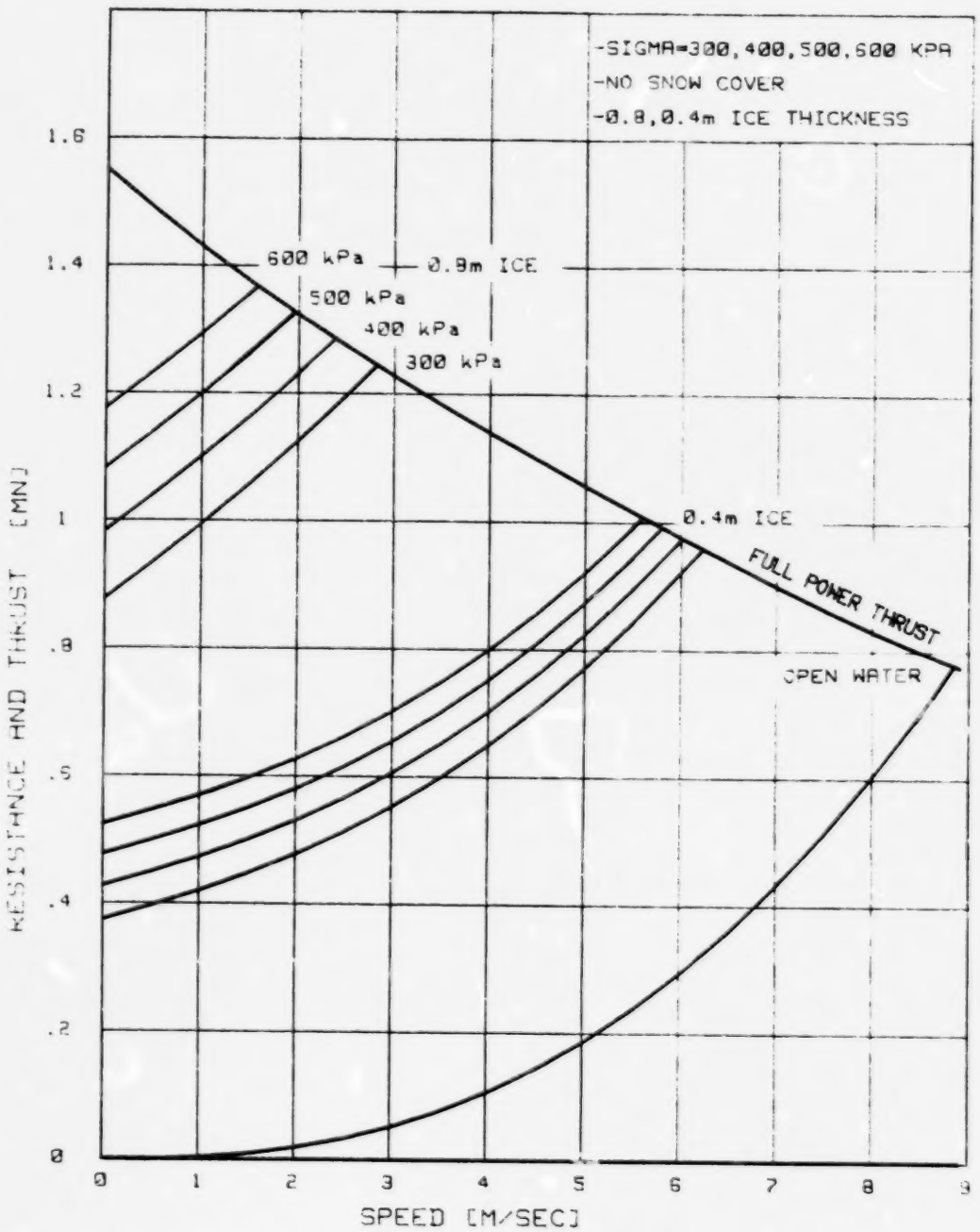

ICE STRENGTH VARIATION
LEVEL ICE PREDICTION
EXISTING M.V. ARCTIC

FIGURE 3.5

SPEED (M/SEC)	PERCENTAGE BREAKING COMPONENT (300 KPA)	PERCENTAGE BREAKING COMPONENT (400 KPA)	PERCENTAGE BREAKING COMPONENT (500 KPA)	PERCENTAGE BREAKING COMPONENT (600 KPA)
0	54	59	63	66
2	42	47	51	55
4	32	37	41	44
6	24	28	32	35
8	18	21	24	27.0

N.B. Ice Thickness = 0.6 m

TABLE 3.4
BREAKING COMPONENT AS PERCENTAGE OF TOTAL RESISTANCE AT DIFFERENT ICE STRENGTHS FROM THE MELVILLE PREDICTOR EQUATION

VELOCITY	RESISTANCE PORTION	MACKINAW MOD. %	MACKINAW FS %	MOSKVA MOD. %	MOSKVA FS %	FINNCARRIER MOD. %	FINNCARRIER FS %
1 Ft/sec (0.305 m/sec)	Fracture	43	71	6	68	32	53
	Gravity	57	29	94	32	68	47
	Inertia	00	00	00	00	00	00
7 Ft/sec (2.13 m/sec)	Fracture	34	44	5	57	24	43
	Gravity	46	23	77	27	53	39
	Inertia	20	22	18	16	23	18
21 Ft/sec (6.4 m/sec)	Fracture	13	20	2	25	8	17
	Gravity	18	9	31	12	19	16
	Inertia	69	71	67	63	73	67

N.B. Ice Thickness = 0.61 m
Ice Flexural Strength = 718 kPa

TABLE 3.5
RESISTANCE DISTRIBUTION IN MODEL AND FULL-SCALE OF THREE DIFFERENT ICEBREAKERS (AFTER VANCE, 1975)

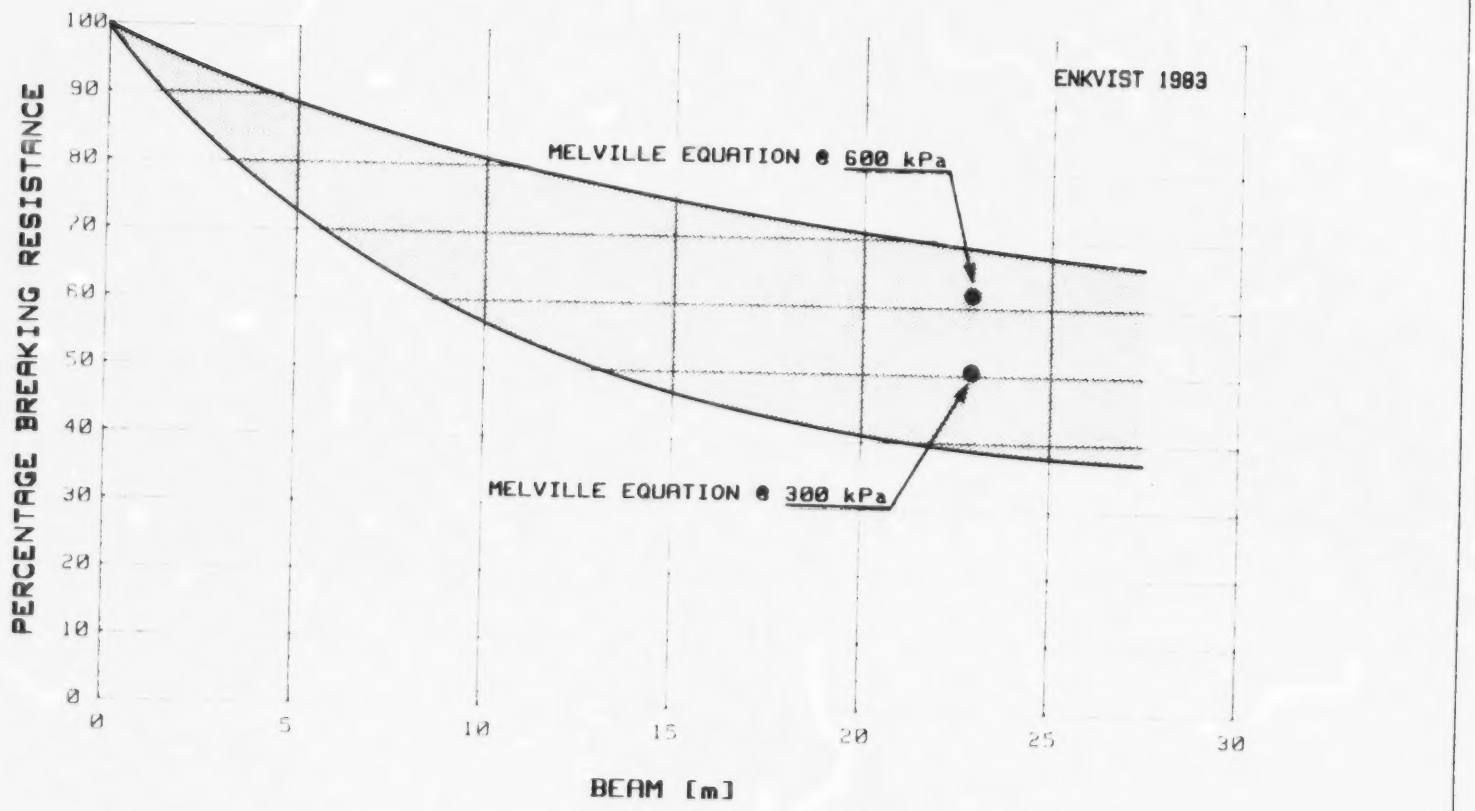

BREAKING RESISTANCE AS PERCENTAGE OF TOTAL RESISTANCE AT CREEPING SPEED VS. BEAM

FIGURE 3.6

The waterline entrance angles can be associated with ice clearing and the inertial components of icebreaking. However, it should also be considered together with the waterline flare angles. Larger flare angles should be correctly associated with waterline angles to ensure that sufficient downward force is exerted by the vessel to cause ice failure in bending rather than crushing.

The hull form coefficient used in the Melville equation was developed by Arctec Canada Ltd. (ACL) (Ref. 3.11). In the report, ACL define the coefficient and its development. The coefficient is a function of:

- Friction
- Waterline entrance angles
- Waterline flare angles

The coefficient is closely related to the Shimanski and Kashteljan coefficients widely used in icebreaker design.

Friction is one of the more important parameters of icebreaking and can have an effect on all three components of resistance. However, the degree to which friction does affect each parameter is not fully understood. Enkvist, for example (Ref. 3.2), believes that the coefficient is responsible for 50% to 70% of the total resistance and manifests itself in the breaking, submerging and velocity components.

The use of friction in the ACL hull form coefficient is perhaps a little questionable since the assumed distribution of the frictional force results in zero friction at the shoulders and the friction also acts only horizontally. However, it is recognized as an improvement from the Shimanski and Kashteljan coefficients in its treatment of friction, and as such it is used in the Melville equation. Figure 3.7 shows the effect of varying the hull form predictor in the Melville equation. It can be seen that varying the coefficient by 0.5 significantly varies the prediction. In the case of the M.V. ARCTIC, a change in hull form coefficient of 0.5 represents a change in friction factor of about 0.13.

Other work, reported by Vance (Ref. 3.12) in an analysis of a model test program conducted by Melville Shipping Ltd., indicates that changing the coefficient of friction by 0.1 results in a change of resistance of approximately 30% at a thickness of 1 m, and is insensitive to velocity. At 1 m, the Melville equation will be affected 13% by a 0.1 change in friction coefficient. This is thought to be too low.

d) Beam

The variation of ice resistance with beam is not relevant in this analysis because of the original design constraint which dictated

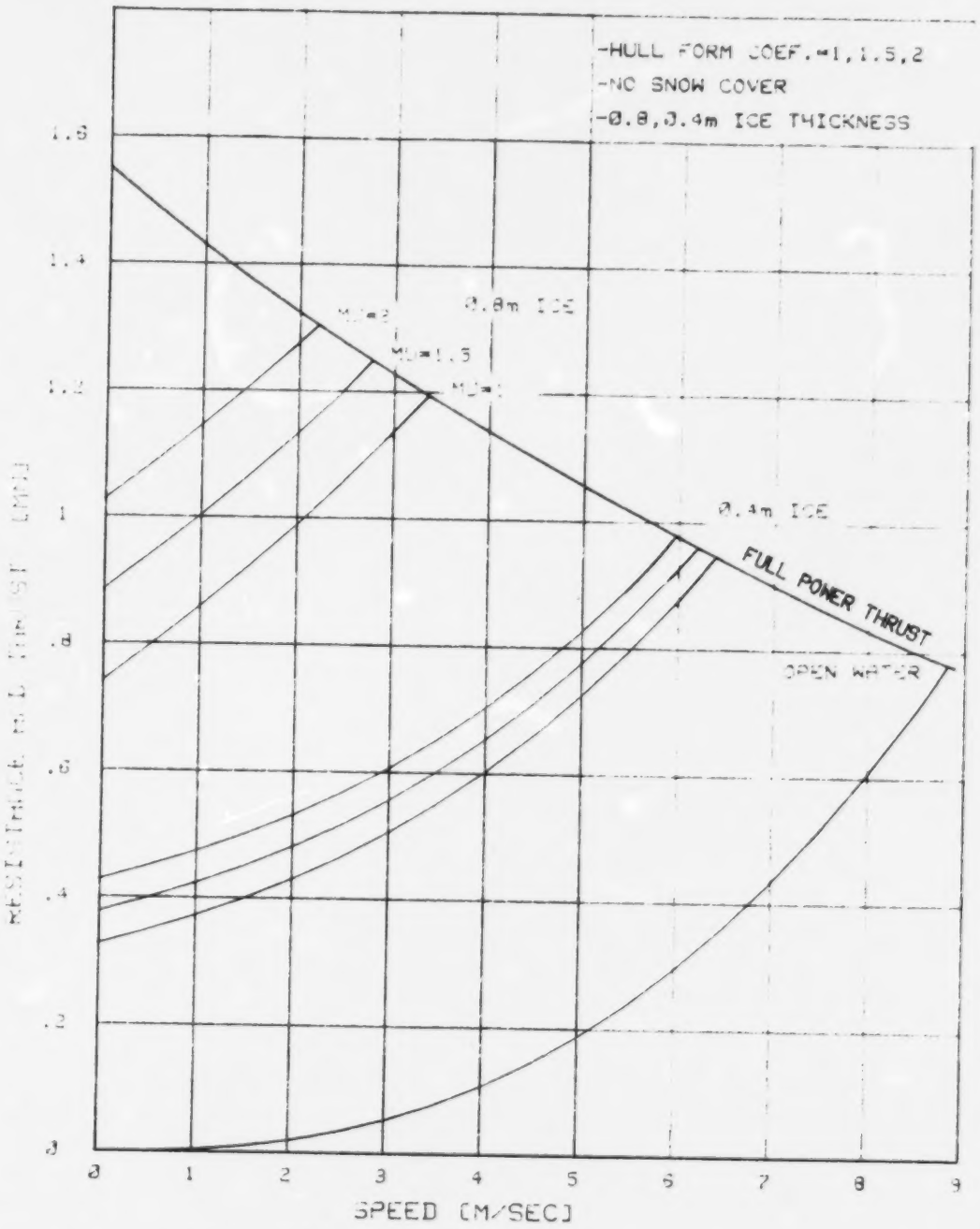

HULL FORM COEFICIENT VARIATION
LEVEL ICE PREDICTION
EXISTING M.V. ARCTIC

FIGURE 3.7

that the beam should not change. It is included in the equation as a constant. From a brief analysis of the Melville equation is does not respond well to beam variation.

e) Length
The vessel's length will be more or less significant depending on the bow form. If the broken channel is wider than the vessel beam, so that the surrounding ice field is not in contact with the vessel's side, it will be less important than if there is contact or if broken ice floes are allowed to surface between the ship's hull and the ice sheet.

Figure 3.8 presents the Melville equation length variation from 160 to 240 m. A reduction in length of 20% results in a reduction in resistance of approximately 7.6% and a length increase of 20% results in an increase in resistance of 7.62%. Work conducted by Johansson (Ref. 3.13), generally confirms this dependency. Unfortunately, the Johansson results were not conclusive, and since there is no other reported length variation series available for comparison the dependency on length is still a little vague. However, since this range of length increase for the new bow is relatively small; a maximum of 8%, it was decided not to modify the predictor any further.

f) Figure 3.9 shows the effect of varying the forward block coefficient in the Melville predictor equation. There has been very little work done on the effect of the forward block coefficient on resistance, largely because it is highly dependent on the waterline and flare angles. Work completed for Melville Shipping Ltd. (Ref. 3.12) indicates that lower forebody block coefficients are advantageous but that it is very difficult to analyze the discrete effect of the forward block without the associated change in stem angle, waterline angles and flare angles.

The discussion above has considered the response of the Melville predictor equation to changes in the primary ice breaking variables. The value of the analysis has been to qualify the use of the predictor equation as a design tool for the development of the new bow forms. Clearly however, the use of this predictor is limited to the M.V. ARCTIC, much in the same way as most semi-empirical formulations are limited to predicting values similar to the data set upon which they are based.

3.3 Development of New Bow Forms

The predictor equation and form parameters discussed in Section 3.2 allow the designer to be cognizant of the importance of the major design parameters.

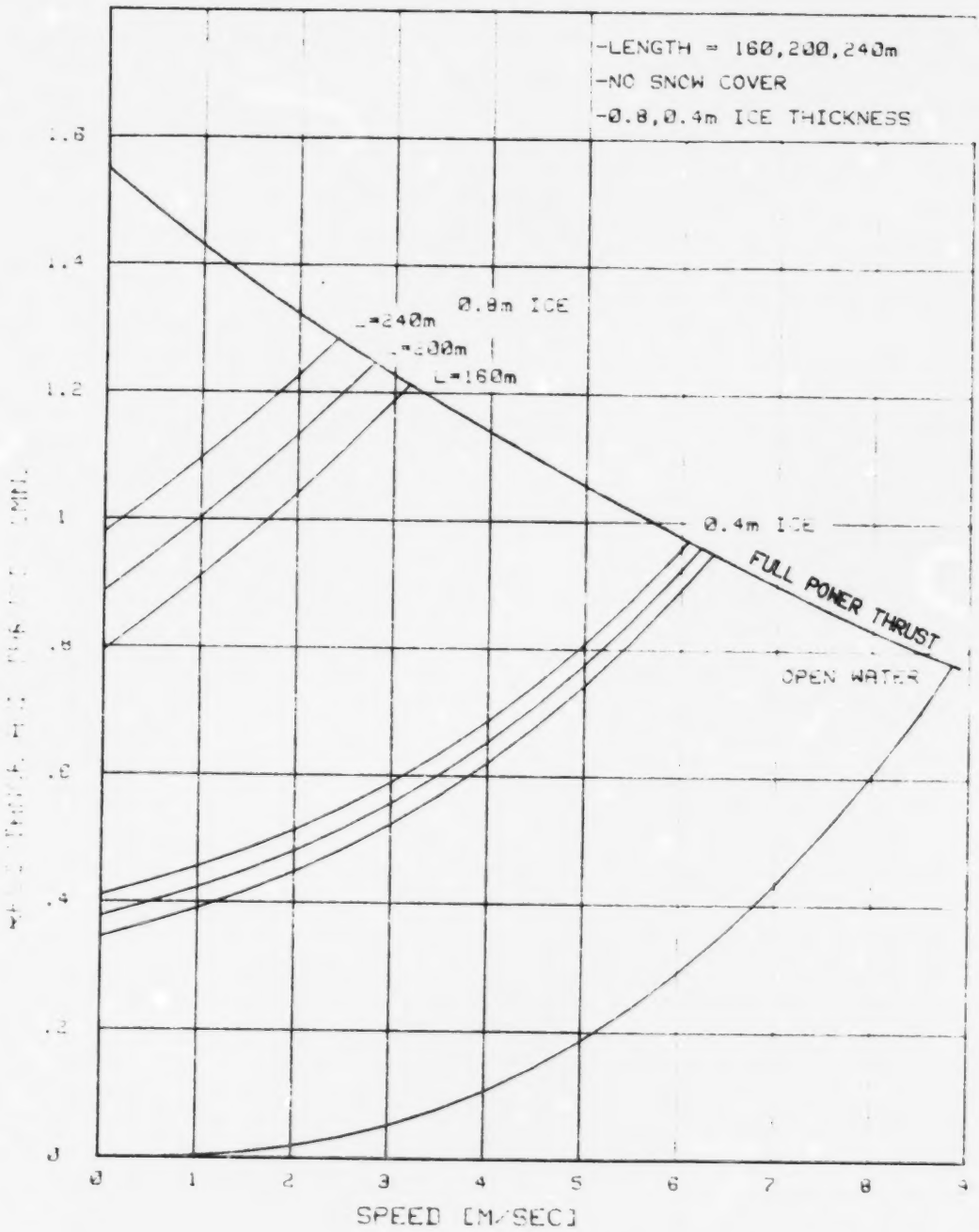

LENGTH VARIATION
LEVEL ICE PREDICTION
EXISTING M.V. ARCTIC

FIGURE 3.8

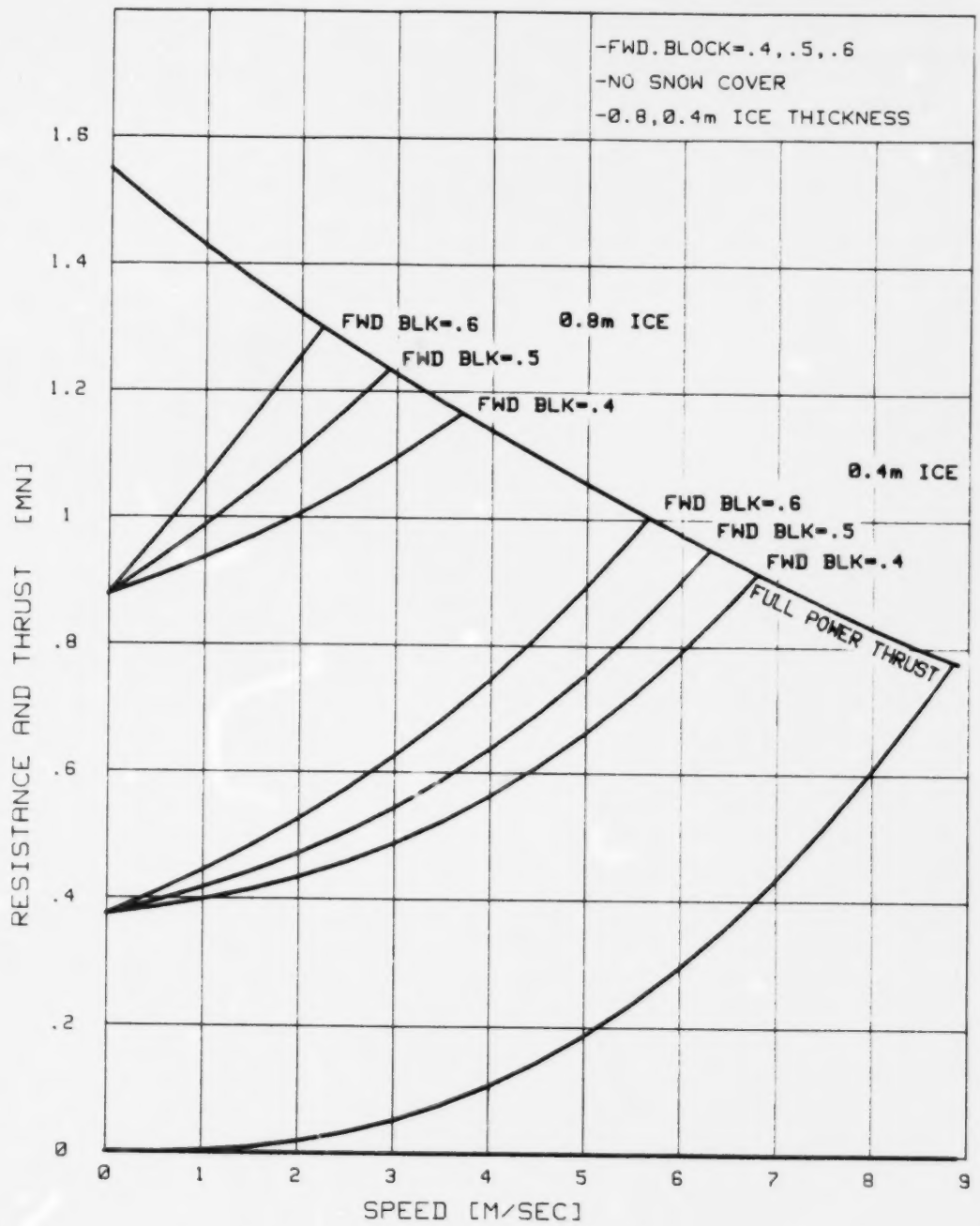

FWD. BLOCK COEF. VARIATION
LEVEL ICE PREDICTION
EXISTING M.V. ARCTIC

FIGURE 3.9

The ACL hull form coefficients discussed in Section 3.2, depend on the absolute value of the waterline and flare angles. The waterline entrance, waterline flare and stem angles are defined earlier in Figure 3.1. Since the calculation of these coefficients involve an integration of the angles, the coefficients alone do not recognize the relationship between the two angles at discrete positions on the bow. Figure 3.10 present the waterline and flare angles for a number of vessels plotted against a non dimensional forebody length. The six vessels considered in these figures are the:

- M.V. ARCTIC
- U.S.C.G. POLAR STAR
- C.C.G.S. NORMAN MCLEOD ROGERS
- 'R' CLASS ICEBREAKER
- HANSEN
- LOUIS S. ST. LAURENT

The POLAR STAR is a United States Coast Guard vessel built in 1973 and was the first of the "Polar Class" icebreakers. The vessel's principal dimensions are:

Length overall	121.6m
Breadth moulded	25.5m
Draught	8.5m
Displacement	10,886 tonnes
Shaft Horsepower	60,000 SHP Gas Turbines
	18,000 SHP Diesel Electric
Number of Propellers	3
Stem Angle	28°
Parallel mid-body flare	12.5°

The C.C.G.S. NORMAN MCLEOD ROGERS was built in 1969. This vessel was the first icebreaker to be installed with a diesel electric propulsion system augmented by gas turbines.

The vessel's principle dimensions are:

Length overall	90m
Breadth	19m
Draught	6.2m
Displacement	5,959 tonnes
Shaft horsepower	13,200
Number of propellers	2
Stem angle	62.1°
Parallel mid-body flare	0°

The 'R' Class icebreaker was developed following construction of the NORMAN MCLEOD ROGERS to improve the icebreaking capability of a vessel of the same size and power. The principal dimensions are:

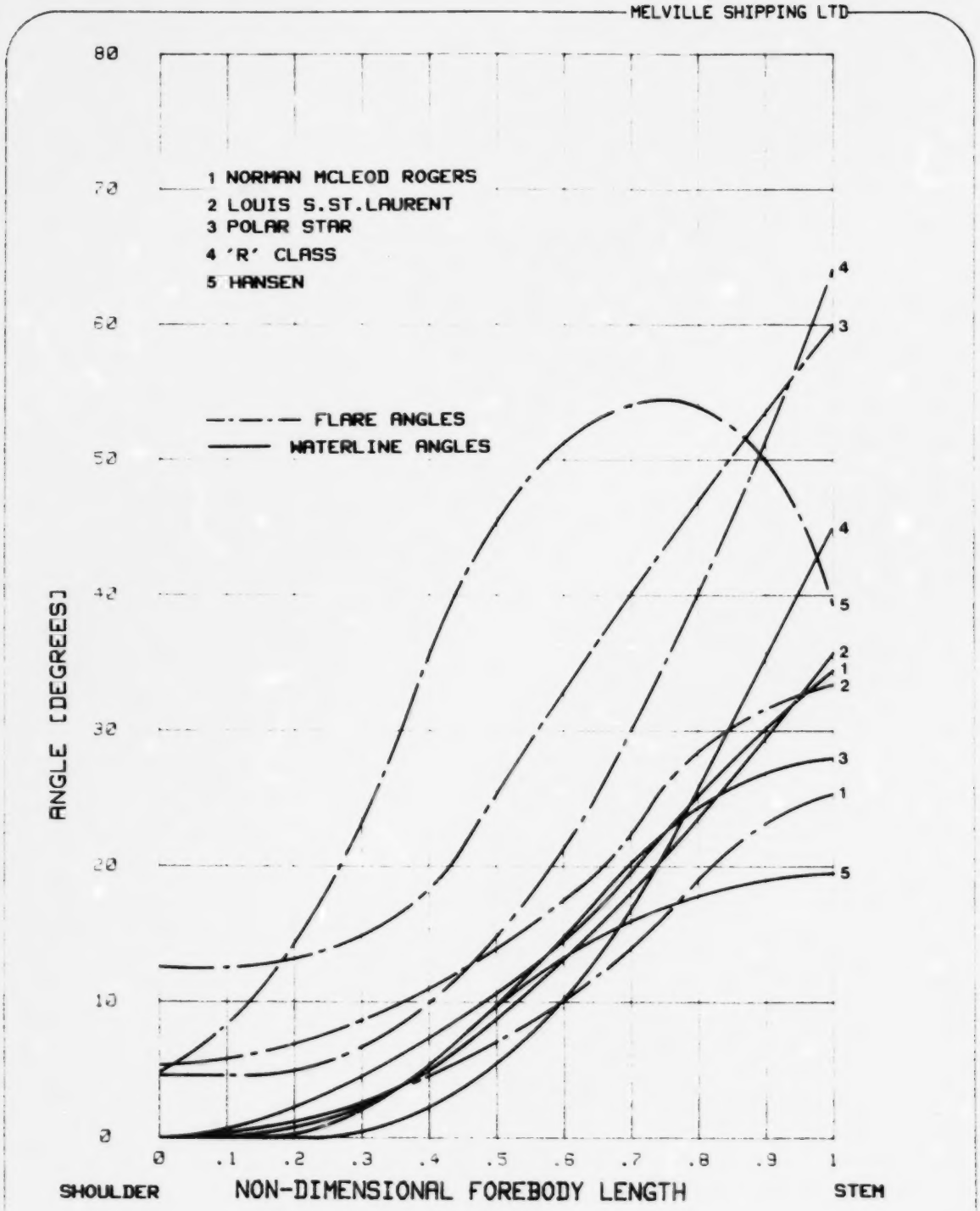

FLARE AND WATERLINE ANGLES
FOR A SELECTION OF ICEBREAKER
DESIGNS
FIGURE 3.10

Length	96m
Breadth	19.2m
Draught	6m
Stem angle	18°
Parallel mid-body flare	4.5°

The HANSEN form is a design proposed for the Northumberland Strait ferry. Proposed dimensions are:

Length overall	152m
Breadth	25.7m
Draught	6.3m
Displacement	14,784 tonnes
Stem Angle	20°
Parallel mid-body flare	5.7°

The C.C.G.S. LOUIS S. ST. LAURENT, Canada's most powerful icebreaker, was built in 1969.

The vessel's principal dimensions are:

Length overall	111.7m
Breadth	24.4m
Draught	9m
Displacement	13,513 tonnes
Shaft Horsepower	24,000
Number of propellers	3
Stem angle	32°
Parallel mid-body flare	6.5°

To break ice effectively, it is necessary to have a sufficiently large downward force developed by the bow on the ice. This is the basic assumption for the development of the Kashteljan icebreaking coefficient (μ). However, it is not sufficient to have high flare angles if ice crushing is taking place further along the bow. An example of this is the M.V. ARCTIC. From Figure 3.10 it can be seen that the bow flare angles are almost linear with forebody length. The waterline angles are similarly uniform with a distinguishable 'shoulder' over the sections 0.3 to 0.7. Relatively high waterline angles exist well aft, while at the same time, the flare angles are reducing rapidly. As a result, the bow will break ice quite effectively with the forward part of the bow where flare angles are in the 30 to 55° range. However, further aft, whilst the waterline angles are still high there is a rapid drop in the flare angles, as a result it can be expected that significant crushing will occur at the shoulders of the vessel around stations 0 to .4. The POLAR STAR, also shown on Figure 3.10, has been designed with a parallel mid-body flare of 12.5° and as a result can maintain higher flare angles over the range of waterline angles.

Figure 3.10 shows the 'R' CLASS ICEBREAKER and the NORMAN MCLEOD ROGERS. It can be seen that the waterline and flare angles of the NORMAN MCLEOD ROGERS are much lower than the 'R' CLASS. The 'R' CLASS ICEBREAKER

was developed from the NORMAN MCLEOD ROGERS to have the same overall size and displacement but by improving the bow design, achieve a better icebreaking performance. Model tests were carried out in 1973 on the new 'R' CLASS ICEBREAKER, together with the NORMAN MCLEOD ROGERS (Ref. 3.8). It was observed during these tests, that the resistance of the 'R' CLASS ICEBREAKER was as much as 30% lower than the NORMAN MCLEOD ROGERS. It can be seen from Figure 3.10 that this was achieved by designing for high flare angles associated with a much lower stem angle of 18°.

Figure 3.10 also shows the HANSEN, which is a design for the Northumberland Strait ferry, and the LOUIS S. ST. LAURENT. It can be seen that the HANSEN design has achieved high flare angles down to a parallel mid-body flare of 5.7°. In addition to this, the waterline angles associated with the high flare angles are high so that further aft when the flare angles reduce to the 10 to 30° range, the waterline angles are very low and do not exceed 5°.

3.3.1 Design

From an analysis of the above diagrams and the icebreaking mechanism, it is clear that the optimum bow will have large flare angles associated with high changes in waterline angle so that, in the case of the M.V. ARCTIC, as the flare reduces to zero as it approaches parallel mid-body, there are no large waterline angles which may result in ice crushing and not icebreaking. A series of bows have been designed which progressively modify the distribution of waterline and flare angles over the forebody. Figure 3.11 shows the flare and waterline angles for this progression of bow designs, from Bow 2 to 6.

Bow 2 is based on the existing ARCTIC bow with the exception that the waterline angles in the forward bow have been reduced. In addition to this, the stem angle was reduced to 25° thus reducing the block coefficient forward of midships from 0.8 to 0.754. The flare angles were left unchanged. By reducing the waterline angles in this way it was hoped to increase the ice clearing ability of the vessel without changing the icebreaking performance.

Bow 3 was developed from Bow 2 by retaining the lower waterline angles of Bow 2 and increasing the flare angles. The stem angle of the bow was also reduced to 15°, further reducing the block coefficient.

In view of the earlier discussion concerning the need to maintain lower waterline angles near the aft area of the bow, where flare angles are lower, Bow 4 was developed by maintaining the higher flare angles of Bow 3 and further reducing the waterline angles. In this way, it was possible to achieve high flare angles over the area of high waterline angles. Bow 5 was a further development of the flare angles from Bow 4. The HANSEN Bow form, discussed earlier in this section, achieved an increase in flare angle from the stem, associated with low waterline angles. This concept was developed in the flare angles of Bow 5. Maximum flare angles of about 65° are achieved and these, combined with the lower waterline angles near the aft end of the bow, and a stem angle of 20°, should reduce the likelihood of crushing at the shoulder.

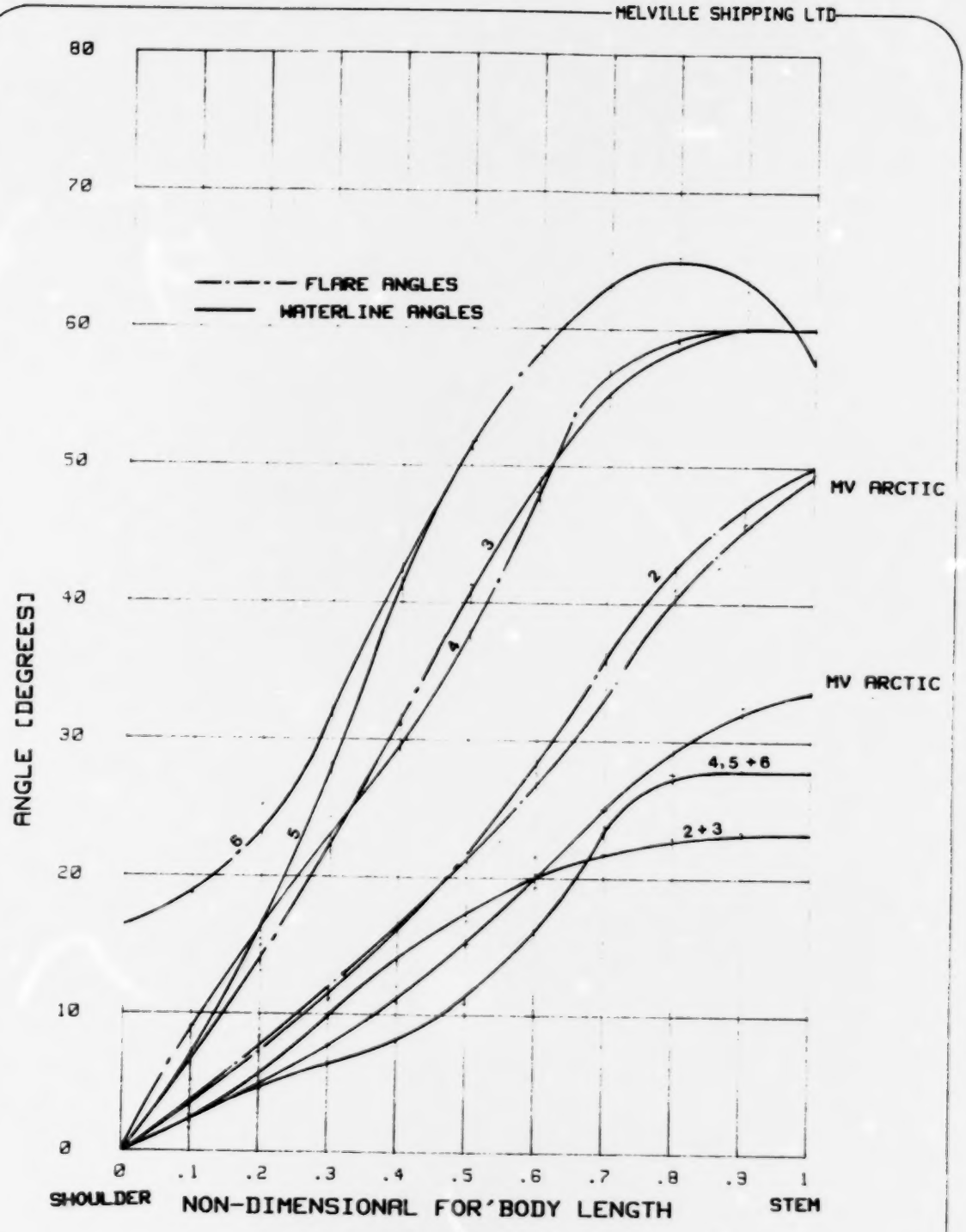

FLARE AND WATERLINE
ANGLES FOR THE EXISTING AND
MODIFIED BOWS OF THE MV ARCTIC
FIGURE 3.11

Bow 6 is an extreme case of Bow 5 where, by inserting a knuckle at the shoulder, the flare angle at the shoulder is above 16°. However, although this will allow ample flare angle for icebreaking near the shoulders, the knuckle may cause crushing, and reduced open water efficiency.

The lines plans of the 5 bow forms developed for analysis are attached as Appendix 2. From these figures, the variation in bow angle can be seen together with the existing frames showing how the new bow forms integrate into the existing hull.

Principal particulars of the modified bows are shown in Table 3.6. The length variation associated with each of the models was kept as small as possible. However, a number of different lengths have resulted and the effect of this has been discussed in the previous section and will be developed in the model tests analysis section.

3.3.2 Prediction of Performance

Throughout the design process, the predicted resistance of each bow form was monitored using the Melville equation developed in Section 3.3. The prediction of resistance for each new bow is presented in Figure 3.12.

Table 3.7 gives a comparison of the percent change in resistance for the 5 alternative bow forms in 0.8 m of ice.

It can be seen from Table 3.7 that Bows 3, 5 and 6 have the most significant reductions in resistance (approximately 37 - 38%).

In consultations with TDC, it was agreed that the two bow forms to be tested were Bows 2 and 5. Bow 2 was chosen to evaluate the effect of lengthening the effective ice breaking area of the bow without modifying the actual flare angles. With the exception of Bow 6, Bow 5 represented the best alternative design. It was decided not to test Bow 6 because of shoulder knuckle lines and the effect this may have on the open water performance.

	EXISTING M.V. ARCTIC	BOW 2	BOW 3	BOW 4	BOW 5	BOW 6
Length	196.6	205.4	204.41	206.07	206.16	212.71
Breadth	22.93	22.93	22.93	22.93	22.93	22.93
Draught	10.97	10.97	10.97	10.97	10.97	10.97
Forward Block Coefficient *	0.515	0.458	0.402	0.431	0.395	0.390
Stem Angle	30°	25°	15°	20°	20°	15°
Shimanski Coefficient	1.650	1.539	1.297	1.289	1.244	1.239
Kashteljan Coefficient	2.620	3.057	3.276	2.976	2.962	2.882

* The forward block coefficient here is defined as being the block coefficient forward of parallel mid-body at the load waterline.

TABLE 3.6
PRINCIPAL PARTICULARS OF THE MODIFIED BOWS

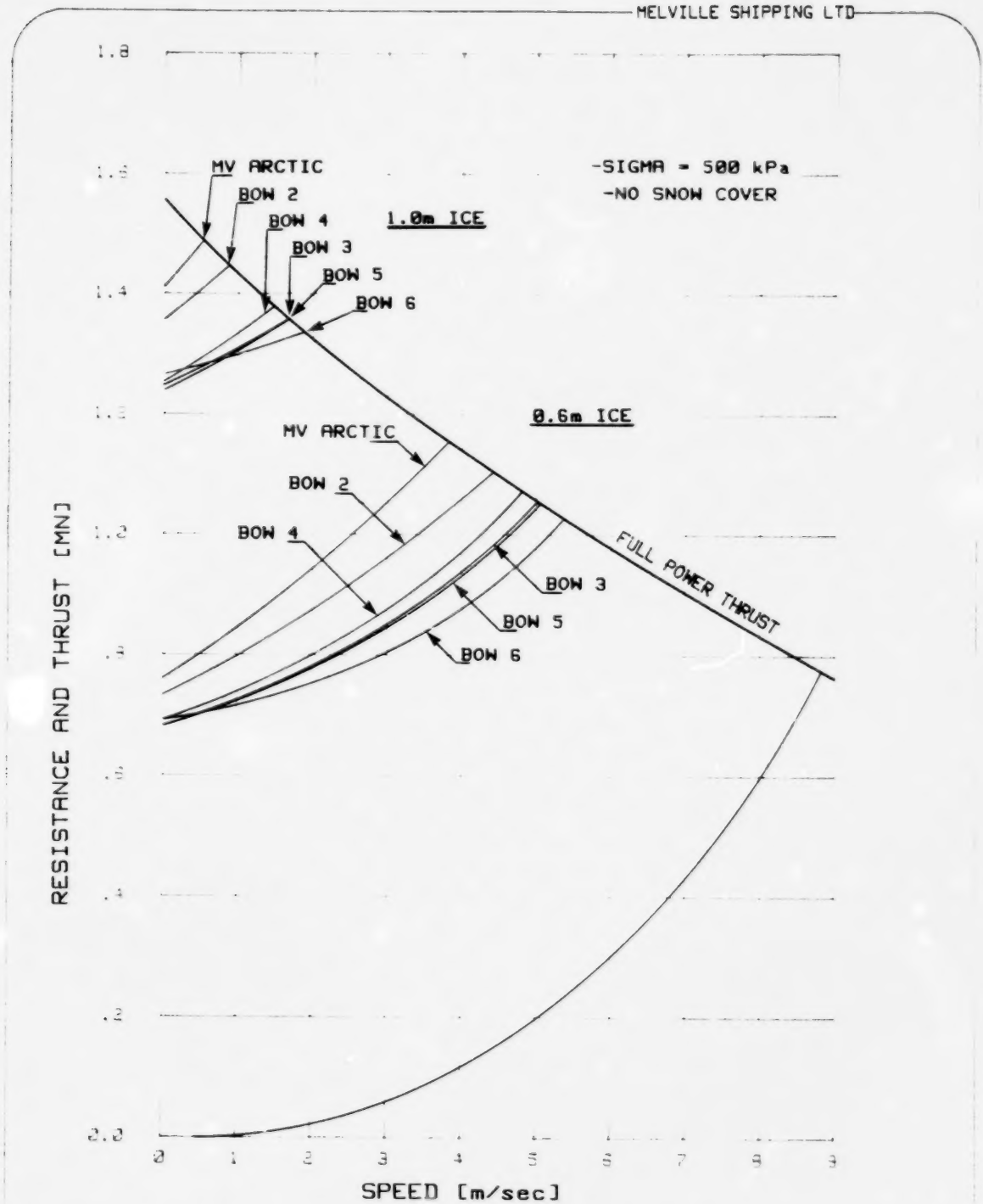

LEVEL ICE RESISTANCE
FOR THE MV ARCTIC AND
THE 5 MODIFIED BOW FORMS

FIGURE 3.12

EXISTING M.V. ARCTIC		BOW 2		BOW 3		BOW 4		BOW 5		BOW 6	
SPEED (m/sec)	RESISTANCE	RESISTANCE	% REDUCTION FROM EXIS. BOW	RESISTANCE	% REDUCTION FROM EXIS. BOW	RESISTANCE	% REDUCTION FROM EXIS. BOW	RESISTANCE	% REDUCTION FROM EXIS. BOW	RESISTANCE	% REDUCTION FROM EXIS. BOW
0	1.083	1.042	3.8	0.954	11.9	0.967	10.7	0.958	11.5	0.972	10.2
2	1.331	1.224	8.0	1.084	18.6	1.122	15.7	1.083	18.6	1.047	21.3
4	1.648	1.475	10.5	1.283	22.2	1.347	18.3	1.277	22.5	1.191	27.7
6	2.065	1.826	11.6	1.583	23.3	1.671	19.1	1.571	23.9	1.435	30.5
8	2.604	2.299	11.7	2.000	23.2	2.118	18.66	1.987	29.9	1.802	30.8

ICE THICKNESS = 0.8 m
ICE STRENGTH = 500 kPa

TABLE 3.7
COMPARISON OF EXISTING AND MODIFIED ICEBREAKING BOWS

4.0 MODEL TESTS

4.1 Open Water Tests

4.1.1 General

The development of the design of the five alternative bow forms for the M.V. ARCTIC has been described in Section 3. The emphasis was placed on methods to improve the ice breaking efficiency of the bow without unduly affecting its open water performance. In order to ascertain the actual open water resistance as a result of modifying the bow, tests were conducted at the National Research Council (NRC) Arctic Vessel Marine Research Institute (AVMRI) facility in Ottawa.

The resistance tests were conducted to examine the pure resistance of the hull at a range of speeds. The self-propulsion tests were run to examine propulsive efficiency and propeller performance.

From these tests it is possible to compare the effect of the modified bow form on resistance and on propeller performance.

4.1.2 Test Program

The test program is discussed in some detail in reference 4.1, and this document should be referred to for any detailed analysis. Resistance and self-propulsion tests were conducted on a 1/30 scale model of the existing M.V. ARCTIC and on two modifications. The modifications involved detaching the bow of the model at frame 163 (162.15m forward of the aft perpendicular full-scale), and successively replacing it with Bows 2 and 5.

IN THIS AND SUBSEQUENT SECTIONS OF THE REPORT, BOWS 2 AND 5 ARE REFERRED TO AS BOW C AND BOW B RESPECTIVELY AND THE EXISTING BOW IS REFERRED TO AS BOW A.

The models were tested over the speed range 4 to 19 knots (2 to 10m/sec.) using standard model test practices. The NRC model tank uses the 'English' method of self-propulsion model testing, which involves running the model at a specific speed, "connected" to a towing carriage. Differential positive and negative forces are recorded on the carriage during over and under propelled runs. These records were then analyzed and interpolated to give the self-propulsion point of the model, and hence the required thrust at the specific speed of the run.

Table 4.1 gives the propeller characteristics used during the tests. It can be seen from this table that two pitch settings are used during the tests, 22.50° and 20.44°. Two pitch settings are used on the model to simulate the controllable pitch propeller on the full-scale ship. A pitch angle of 22.5° was used for the high ship speed range, from 14 to 19 knots and 20.44° for the low ship speed range of 0 to 6 knots. Figure 4.1 shows the open water characteristics of the propellers at the two pitch settings.

PROPELLER 68

Diameter, m	5.273
Pitch Angle at 0.7R, deg	22.50 20.44
Pitch at 0.7R, m	4.800 4.329
Pitch Ratio at 0.7R	0.911 0.821
Blade Area Ratio	0.6407
Number of Blades	4
Direction of Rotation	Left Hand
Hub Diameter, m	1.600
Design	LIPS A1 10971, A1 10972

DUCT

Minimum Internal Diameter, m	5.33
Maximum External Diameter, m	6.42
Length of Nozzle, m	2.59
Design	N.S.M.B. 19-A
Height of Propeller Shaft above Baseline	4.50m
Position of Propeller Centre Forward of AP	2.90m

TABLE 4.1
PROPELLER 68 AND DUCT DESIGN PARTICULARS

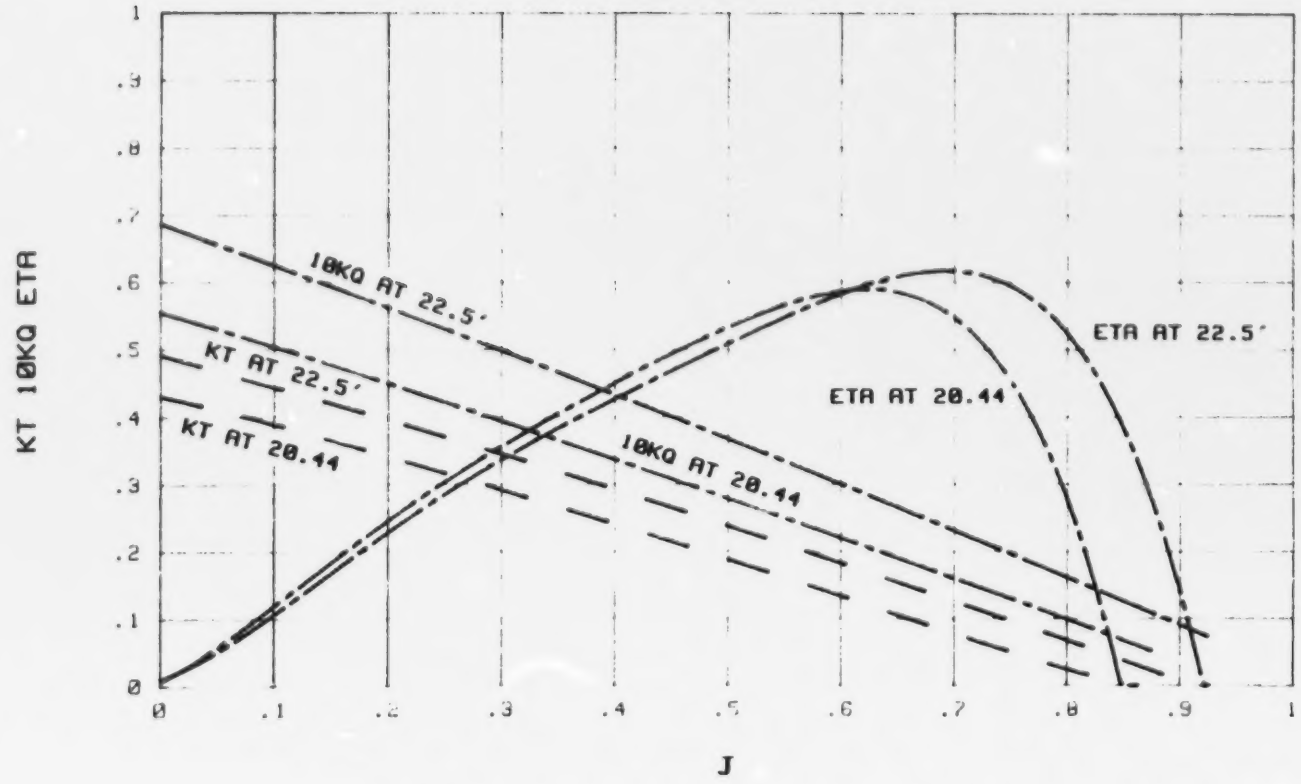

OPEN WATER TESTS
OF MV ARCTIC PROPELLER AT
22.5 AND 20.44 DEG PROP PITCH
FIGURE 4.1

Figure 4.2 shows the results of the resistance tests for each of the three bows. It can be seen in this figure that rather than compromising the open water resistance of the hull, the performance has been improved. However, in terms of model test accuracy, because the three curves are so close together, it is difficult to substantiate the improved resistance of the modified bows over the existing bow.

Figure 4.3 shows the full-scale delivered power prediction for the M.V. ARCTIC and the modified bows. It can be seen that the trend set in the resistance tests is maintained and although the modified bows appear to be slightly more efficient, they do not depart significantly from the existing ship.

It should also be noted that due to design constraints on the forward body of the existing hull, each of the bows has a different length. Model B is 4.8% longer than the existing hull and Model C is 4.5% longer. The corresponding displacements are affected by 0.1% and 2.1% respectively. The relative effects of this length variation are thought to be small and any analysis of this effect is not within this present scope of work.

The conclusions of these open water tests are:

- Within experimental error, there is no significant effect on open water resistance due to changing the bows.
- There is some indication that Bow C has a lower resistance than the existing bow above about 6 knots, and that below this they are identical.
- There is some indication that Bow B has a slightly higher resistance than the existing bow below about 14 knots, and that above this it is lower.
- There is some indication that Bow C has a lower resistance than Bow B.

4.2 Ice Tests

4.2.1 General

Model scale icebreaking tests were conducted at the Arctec Canada Ltd. facility in Kanata, Ontario. Any details regarding these ice tests not included in this section may be found in Ref. 4.2. The icebreaking tests were designed to demonstrate the icebreaking ability of the two modified bows. The model of the existing ship was incorporated into the tests to act as a base case for comparison. The model scaling was based on the Froude scaling laws and is discussed in Reference 1.1.

Three categories of tests were conducted at the Arctec Canada facility, with a model scale of 1/30:

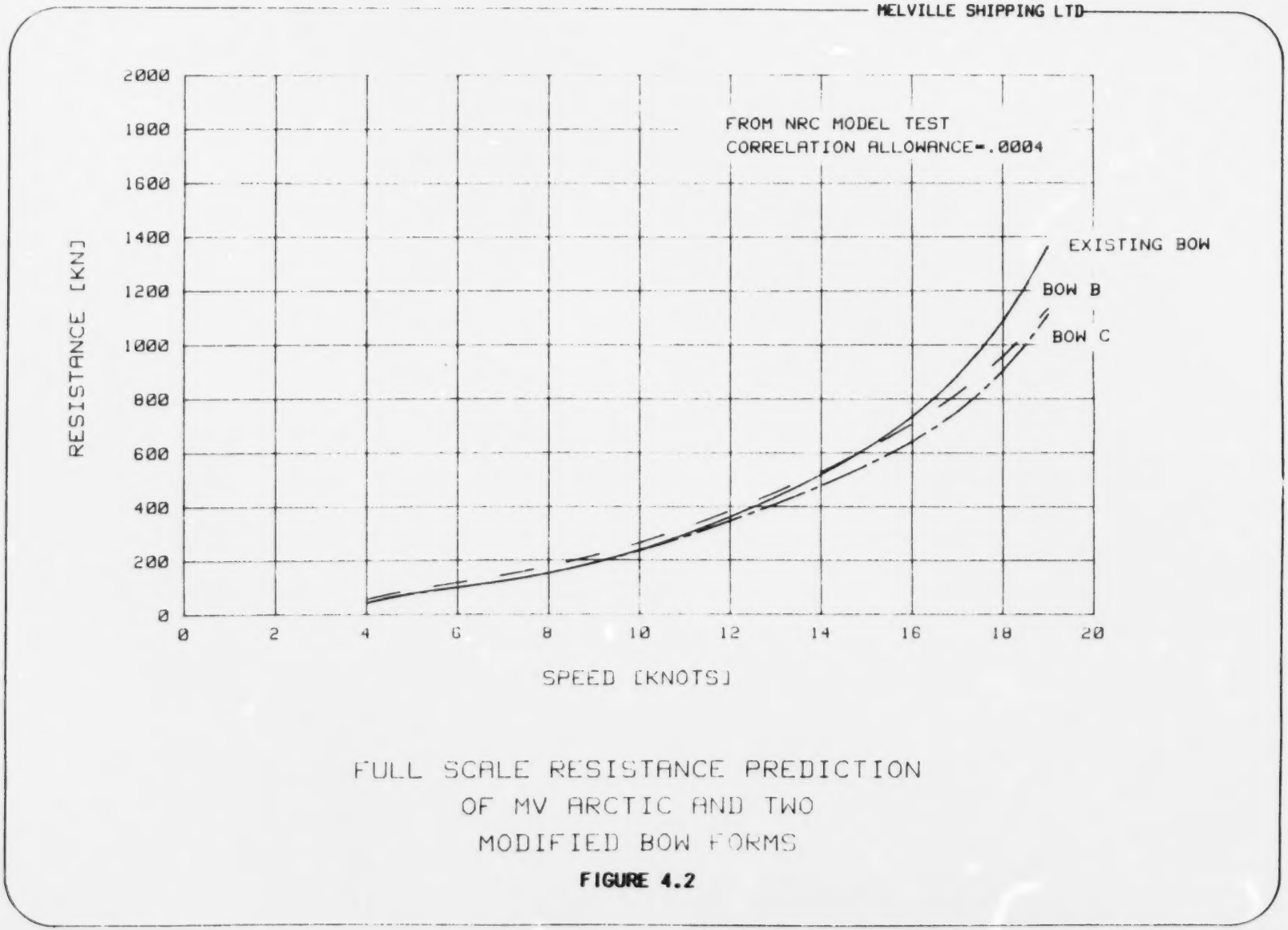

FULL SCALE RESISTANCE PREDICTION
OF MV ARCTIC AND TWO
MODIFIED BOW FORMS

FIGURE 4.2

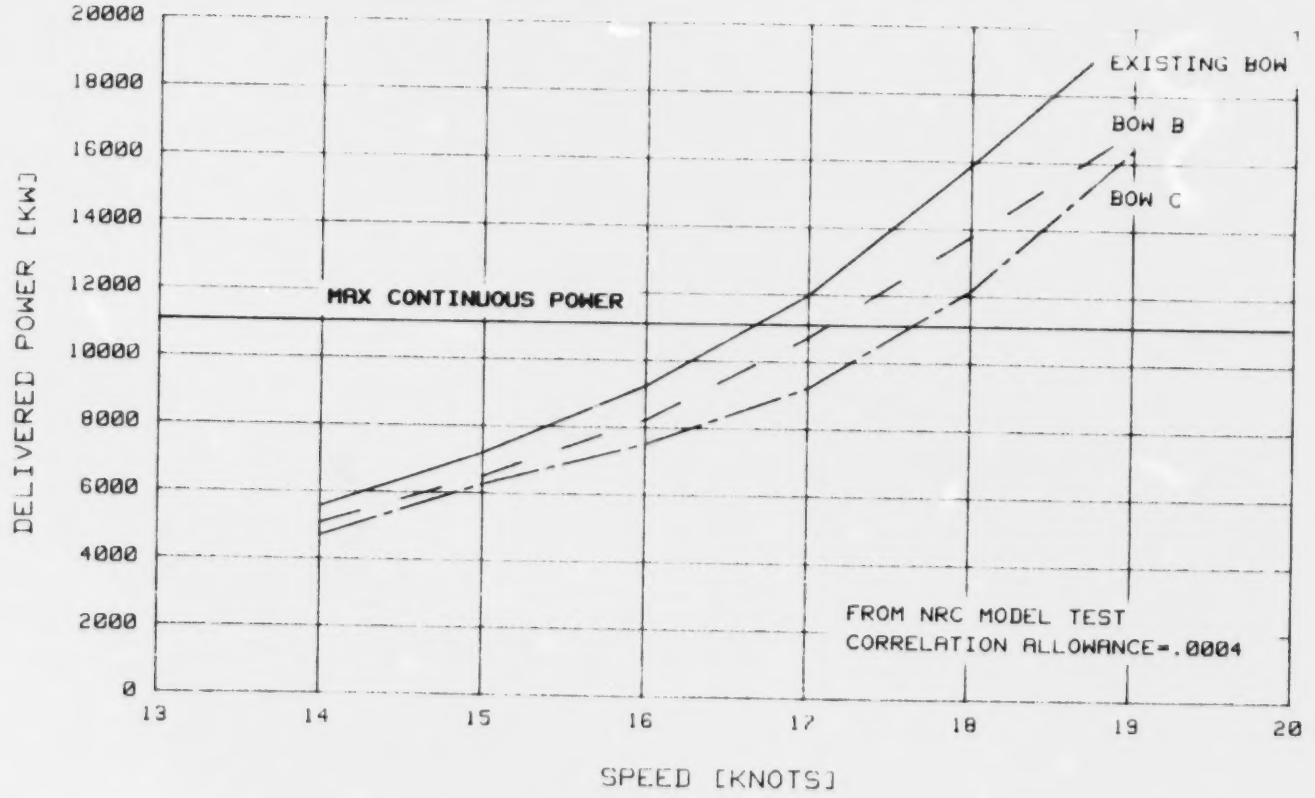

FULL SCALE POWER PREDICTION
OF MV ARCTIC AND TWO MODIFIED BOW FORMS

FIGURE 4.3

- level ice tests
- broken channel tests
- rubble field tests

The level ice tests were conducted in three ice thickness; 0.6, 0.8 and 1.2 m in both resistance and self-propelled modes. Following the level ice tests, the ice sheet was broken up and the model rerun in the simulated broken channel. Rubble field tests were conducted once for each model by compressing the broken ice of the 1.2 m sheet into a simulated rubble field. Table 4.2 shows the test program, giving the discrete speeds and ice thickness for each sheet. The "target" ice strength for every sheet was 500 kPa full-scale, or 16.7 kPa model scale. The test program was designed to allow an easy cross referencing of data points at equal ice thickness and speed. As a result, it was attempted to maintain similar speeds for the different bows and ice thicknesses.

In order to run both resistance and self-propulsion tests, the model basin was divided down the centre by a barrier. The divider consists of eight posts, positioned along the tank, supporting wooden beams approximately 3 m long. A schematic of the arrangement is shown in Figure 4.4.

This section of the report discusses the test series and presents the final results and conclusions.

4.2.2 Test Procedure

As with the open water tests, the "English" method of model testing was used throughout. The English method relies on the model being attached to the carriage by a "force block" and the force required to move the vessel through the ice is recorded. With the resistance this is always a unidirectional force. With the self-propulsion tests, the force can vary from positive to negative depending on the thrust from the model propeller. During the self-propulsion tests only propeller thrust was recorded so subsequent calculations of thrust and thrust deduction are based on propeller thrust and not total thrust (propeller and nozzle).

There are four variables that can be identified during the tests:

- model speed
- ice thickness
- ice strength
- ice elasticity

Tables 4.3 and 4.4 are reproduced from the ACL report (Ref. 4.2) and give the mean values of model speed, ice thickness, ice strength, elasticity, channel width (Bows B and C only), force block loading and propeller, thrust, torque and r.p.m. (self-propulsion test only).

		ICE THICKNESS		
		0.6 m	0.8 m	1.2 m
EXISTING M.V. ARCTIC BOW A	LEVEL ICE SPEED(kn)	1.5, 5, 8	1.5, 3, 5	1.5, 2, 3
	BROKEN CHANNEL SPEED(kn)	1.5, 5, 8	1.5, 3, 5	1.5, 2, 3
	RUBBLE FIELD SPEED(kn)	-	-	1.5
MODIFIED BOW B	LEVEL ICE SPEED(kn)	1.5, 5, 10	1.5, 5, 8	1.5, 2, 3
	BROKEN CHANNEL SPEED(kn)	1.5, 5, 10	1.5, 5, 8	1.5, 2, 3
	RUBBLE FIELD SPEED(kn)	-	-	1.5
MODIFIED BOW C	LEVEL ICE SPEED(kn)	1.5, 5, 8	1.5, 5, 8	1.5, 2, 3
	BROKEN CHANNEL SPEED(kn)	1.5, 5, 8	1.5, 5, 8	1.5, 2, 3
	RUBBLE FIELD SPEED(kn)	-	-	1.5

TABLE 4.2
ACL TEST SCHEDULE

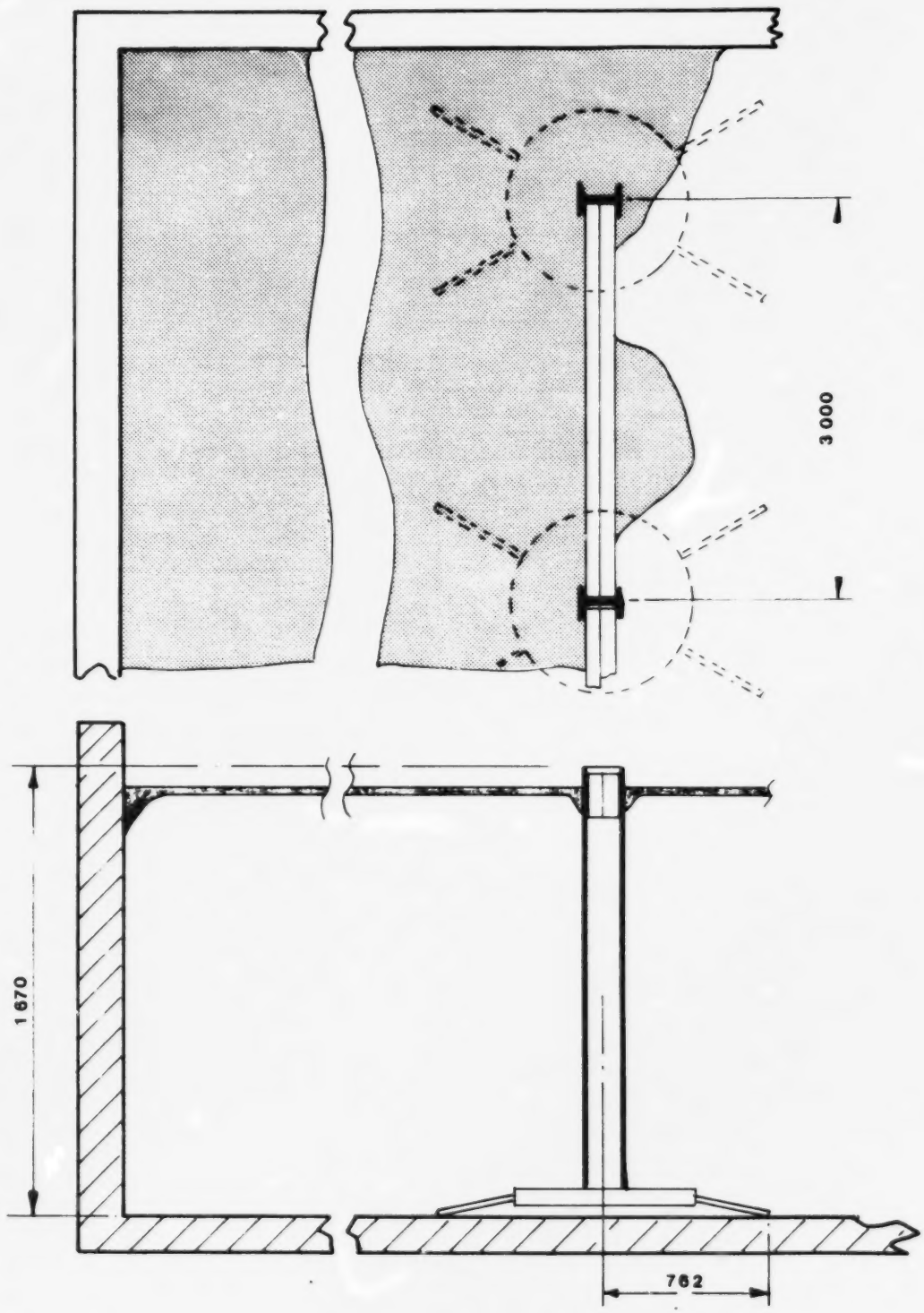

FIGURE 4.4 - DIAGRAMATIC OF ACL TANK BASIN DIVIDER

MELVILLE SHIPPING LTD

RESISTANCE FOR 326-A

Sheet/Run	v (m/s)	R (N)	h (mm)	f (kPa)	E/σ_f^*	Average Channel Width (m)
1/1	.46	41.3	19.5	32.5	692	-
1/2	.74	49.6	20.1	26.7	692	-
1/3	.14	25.4	19.4	22.7	692	-
1/4	.17	6.9	19.7	-	-	-
1/5	.46	5.8	19.7	-	-	-
1/6	.75	22.0	19.7	-	-	-
2/1	.29	32.9	27.6	11.3	199	-
2/2	.48	48.5	26.8	13.8	199	-
2/3	.15	11.3	18.7	13.6	199	-
2/4	.17	12.2	24.3	-	-	-
2/5	.28	16.0	24.3	-	-	-
2/6	.48	18.4	24.3	-	-	-
3/1-A	.21	73.1	40.5	18.7	611	-
3/1-B	.28	86.9	42.2	16.1	611	-
3/1-C	.16	73.3	43.4	19.9	611	-
3/2-A	.19	20.7	41.9	-	-	-
3/2-B	.28	25.9	41.9	-	-	-
3/2-C	.14	23.4	41.9	-	-	-

RESISTANCE FOR 326-B

Sheet/Run	v (m/s)	R (N)	h (mm)	f (kPa)	E/σ_f^*	Average Channel Width (m)
4/1	.47	38.4	27.6	16.8	248	.876
4/2	.74	51.7	28.6	22.7	248	.858
4/3	.15	22.5	26.1	21.2	248	.826
4/4	.16	8.7	27.8	-	-	-
4/5	.47	17.4	27.8	-	-	-
4/6	.74	21.7	27.8	-	-	-
5/1-A	.20	51.7	42.7	11.7	1567	.889
5/1-B	.27	56.1	43.1	16.5	1567	.909
5/1-C	.16	48.7	42.6	20.2	1567	.910
5/2-A	.19	27.1	42.9	-	-	-
5/2-B	.28	24.0	42.9	-	-	-
5/2-C	.15	25.7	42.9	-	-	-
6/1	.46	24.2	19.9	25.8	168	.840
6/2	.91	47.0	20.6	25.1	168	.849
6/3	.16	14.5	21.0	24.0	168	.850
6/4	.16	4.75	20.5	-	-	-
6/5	.46	10.3	20.5	-	-	-
6/6	.91	25.5	20.5	-	-	-

RESISTANCE FOR 326-C

Sheet/Run	v (m/s)	R (N)	h (mm)	f (kPa)	E/σ_f^*	Average Channel Width (m)
7/1	.46	53.9	29.8	10.4	1131	.864
7/2	.74	65.5	29.5	14.8	1131	.872
7/3	.15	28.7	28.0	10.0	1131	.890
7/4	.15	13.1	29.4	-	-	-
7/5	.47	26.9	29.4	-	-	-
7/6	.74	25.1	29.4	-	-	-
8/1	.46	22.4	18.7	17.9	178	.813
8/2	.74	38.6	19.2	23.8	178	.827
8/3	.15	11.7	17.5	12.7	178	.800
8/4	.15	4.8	18.9	-	-	-
8/5	.46	5.8	18.9	-	-	-
8/6	.74	18.3	18.9	-	-	-
9/1-A	.21	62.8	40.6	11.9	564	.883
9/1-B	.27	77.2	41.7	15.5	564	.920
9/1-C	.14	80.2	41.6	20.8	564	.918
9/2-A	.21	21.9	41.4	-	-	-
9/2-B	.28	28.1	41.4	-	-	-
9/2-C	.16	29.8	41.4	-	-	-

* represents one value for that sheet

TABLE 4.3
RESISTANCE TEST DATA (REPRODUCED FROM ACL REPORT)

SELF-PROPELLED FOR 326-A

SHEET RUN	v (m/s)	ΔR* (N)	h (mm)	σf (kPa)	E/σf**	Channel Width(m)	Q (N-m)	T (N)	RPM
1/7	.47	+20.7	20.9	18.2	979	-	+.75	+37.6	881
1/8	.76	+15.2	20.7	23.4	979	-	+1.22	+50.9	1020
1/9	.16	-20.3	25.3	26.1	979	-	-0.01	+ 6.0	252
1/10	.16	+ 4.5	21.3	-	-	-	-0.01	+ 6.6	343
1/11	.47	+41.0	21.3	-	-	-	+0.73	+39.4	892
1/12	.75	+45.9	21.3	-	-	-	1.22	46.5	971
2/7	.16	- 2.9	30.1	11.3	171	-	+ .39	+12.6	521
2/8	.47	- .4	28.3	14.1	171	-	+ .76	+33.7	858
2/9	.15	- 1.7	21.8	13.0	171	-	+ .10	10.3	438
2/10	.15	- 1.7	27.4	-	-	-	+ .05	9.2	436
2/11	.28	+ 8.1	27.4	-	-	-	+ .38	13.1	536
2/12	.47	+16.4	27.4	-	-	-	+ .62	24.3	726
3/3	.27	-17.3	40.3	11.7	725	-	1.12	48.0	943
3/4	.14	- 4.3	41.1	14.0	725	-	1.1	47.4	930
3/5	.16	- 4.3	40.2	11.1	725	-	1.13	39.2	851
3/6	.27	10.6	42.9	10.4	725	-	1.53	53.2	1052
3/7	.14	1.5	41.3	-	-	-	.36	12.9	498
3/8	.20	1.6	41.3	-	-	-	.36	16.9	563
3/9	.28	- 6.5	41.3	-	-	-	.42	21.4	635
3/10	.15	-83.7	240.	-	-	-	1.47	53.9	1061

SELF-PROPELLED FOR 326-B

SHEET RUN	v (m/s)	ΔR* (N)	h (mm)	σf (kPa)	E/σf**	Channel Width (m)	Q (N-m)	T (N)	RPM
4/7	0.71	25.7	29.1	17.1	371	.867	1.54	53.8	904
4/8	0.17	-5.6	29.1	16.5	371	.808	0.01	7.7	352
4/9	0.16	-16.0	30.6	7.3	371	.845	0.00	6.8	330
4/10	0.15	2.6	29.4	-	-	-	0.00	7.0	325
4/11	0.47	18.9	29.4	-	-	-	0.73	24.2	569
4/12	0.76	21.3	29.4	-	-	-	0.78	31.5	656
5/3	0.29	9.2	43.0	15.5	1682	.952	1.15	38.0	859
5/4	0.16	-35.3	43.0	19.5	1682	.904	0.78	24.0	678
5/5	0.16	10.4	40.5	13.6	1682	.933	0.73	30.3	752
5/6	0.29	1.2	42.4	12.0	1682	.867	0.80	31.0	784
5/7	0.15	8.3	42.5	-	-	-	0.36	14.6	522
5/8	0.19	5.5	42.5	-	-	-	0.33	17.4	566
5/9	0.28	11.2	42.5	-	-	-	0.39	18.9	605
5/10	0.15	-80	233	-	-	-	1.48	53.1	997
6/7	0.93	-17.6	22.9	19.4	303	.809	0.77	28.7	784
6/8	0.16	14.0	22.7	13.4	303	.860	0.35	15.5	540
6/9	0.16	-8.7	25.4	19.9	303	.800	0.36	13.1	500
6/10	0.15	0.5	23.4	-	-	-	-0.05	7.1	355
6/11	0.48	-7.7	23.4	-	-	-	0.35	11.4	473
6/12	0.91	-0.6	23.4	-	-	-	0.75	25.9	746

SELF-PROPELLED FOR 326-C

SHEET RUN	v (m/s)	ΔR* (N)	h (mm)	σf (kPa)	E/σf**	Channel Width (m)	Q (N-m)	T (N)	RPM
7/7	.75	1.3	31.7	10.1	1322	.873	1.29	44.3	949
7/8	.16	4.9	31.6	10.5	1322	.905	0.40	18.7	599
7/9	.16	-3.2	33.8	10.9	1322	.915	0.39	16.1	554
7/10	.15	-5.5	31.9	-	-	-	-0.04	7.6	359
7/11	.47	0.9	31.9	-	-	-	0.37	21.2	647
7/12	.73	1.8	31.9	-	-	-	0.71	26.5	739
8/7	.75	-3.1	21.0	17.8	309	.855	0.86	31.3	813
8/8	.16	4.1	21.6	9.1	309	.843	0.03	8.9	423
8/9	.15	-1.1	21.9	11.9	309	.805	0.00	8.3	390
8/10	.15	5.6	21.2	-	-	-	0.02	5.4	327
8/11	.46	0.2	21.2	-	-	-	-0.02	8.5	409
8/12	.73	4.9	21.2	-	-	-	0.32	22.0	663
9/3	.27	28.1	40.3	12.0	676	.882	1.20	50.1	967
9/4	.17	18.5	41.8	19.7	676	.907	1.37	51.5	907
9/5	.16	7.5	43.8	13.0	676	.893	1.03	36.3	825
9/6	.27	- 7.0	43.2	10.9	676	.900	1.08	42.1	891
9/7	.14	2.2	42.4	-	-	-	0.33	14.8	514
9/8	.19	- 1.4	42.4	-	-	-	0.37	15.5	532
9/9	.28	9.2	42.4	-	-	-	0.40	18.1	605
9/10	.14	-21.5	224	-	-	-	1.44	52.3	1002

* represents one value for that sheet

** (+)ve ΔR is over propelled

TABLE 4.4
SELF-PROPULSION TEST DATA (REPRODUCED FROM ACL REPORT)

During the model testing program a number of testing problems arose which may or may not have an effect on the model test results. These were related to incidences during the testing and the data analysis procedure. These are discussed in Appendix 3. Partially as a result of these problems, three additional resistance runs were conducted for Model C. These are discussed in Ref. 4.2 and the development of the resistance predictor equation for Bow C in Table 4.5 includes these additional tests.

4.2.3 Test Data Analysis

The data collected was analyzed by ACL and the resulting predictor equations are presented in Table 4.5.

It should be noted that each bow configuration is represented by a different equation for the two test procedures (i.e., resistance and self-propulsion) and then these tests combined to create another set of equations which forms ACL's final prediction. The broken channel data was combined and is represented by only one predictor.

The rubble field tests analysis was not conducted in the same way and the results from these tests are in the form of mean penetration energy and presented in Table 4.6. Details of this analysis are also presented in Appendix 3.

4.2.4 Additional Analysis

In addition to the ice testing, ACL also conducted an "independent relative check" of the bow designs, together with a computer simulation prediction.

The "independent relative check" involves a comparison of the bows based on the hull form coefficients discussed in Section 3 and detailed in Reference 3.11. The results of the analysis are shown in Table 4.7 and Figure 4.5. These results indicate that the resistance of Bows A and C are quite close together with a significantly lower resistance shown for Bow B. The actual procedure for calculating these relative resistances is not discussed in the ACL report, so they cannot be commented on further.

The computer model prediction performed by ACL is based on the work prepared for TDC by ACL entitled "A Semi-Empirical Ice Resistance Model". The computer program is essentially based on the Ph.d thesis of J.N. Neagle (Ref. 4.3) which in turn was heavily influenced by Enkvist (Ref. 3.2). The original model by Neagle was modified primarily by replacing empirical constants by variables, deduced from an analysis of five vessels. Reference 4.4 includes a discussion on the predictive ability of the computer model with reference to the M.V. ARCTIC.

Figure 4.6 is reproduced from the ACL report (Ref. 4.2) and presents the mathematical prediction. It can be seen in Figure 4.6 that as with the hull form analysis, the computer model predicted similar benefits for Bow B over the original Bow A and Bow C. The major difference being the benefit indicated by Bow C over the original bow. This is negligible in the hull

	LEVEL ICE RESISTANCE	SELF-PROPULSION	RESISTANCE AND SELF-PROPULSION
MODEL A	$R = 20.99\sigma_f h + 1897vh + 24300h^2$	$T = 517\sigma_f h^2 + 1982vh + 377.9h$	$R = 1166\sigma_f h^2 + 1779vh + 574.1h$
MODEL B	$R = 2.292\sigma_f h + 1802vh + 18670h^2$	$T = 16.46\sigma_f h + 1448vh + 2859h^2$	$R = 2.795\sigma_f h + 1804vh + 18390h^2$
MODEL C	$R = 1573\sigma_f h^2 + 1507vh + 395.7h$	$T = 938.6\sigma_f h^2 + 1493vh + 17.08h$	$R = 28.54\sigma_f h + 1328vh + 24030h^2$

BROKEN CHANNEL
COMBINED PREDICTOR FOR
MODELS A, B AND C

$$R = 1.965 + 628.9vh + 8896h^2$$

TABLE 4.5
PREDICTOR EQUATIONS FROM MODEL SCALE TESTS CONDUCTED AT ACL

MODEL	AVERAGE THICKNESS (m)	RIDGE LENGTH (m)	MODEL VELOCITY (m/sec)	RPM	PENETRATION ENERGY (N/m)
326-A	.2413	3.0	.155	1066	653.8
326-B	.2330	4.0	.144	996	597.0
326-C	.2440	4.3	.137	1002	528.1

TABLE 4.6
RUBBLE FIELD TEST DATA

BOW	ICEBREAKING COEFFICIENT μ_1	ICE MOVING COEFFICIENT μ_2	SPEED DEPENDENT COEFFICIENT $\mu_1 + 1.17\mu_2$
326-A	0.852	0.536	1.479
326-B	0.391	0.516	0.995
326-C	0.799	0.429	1.301

TABLE 4.7
GEOMETRY FRICTION COEFFICIENTS

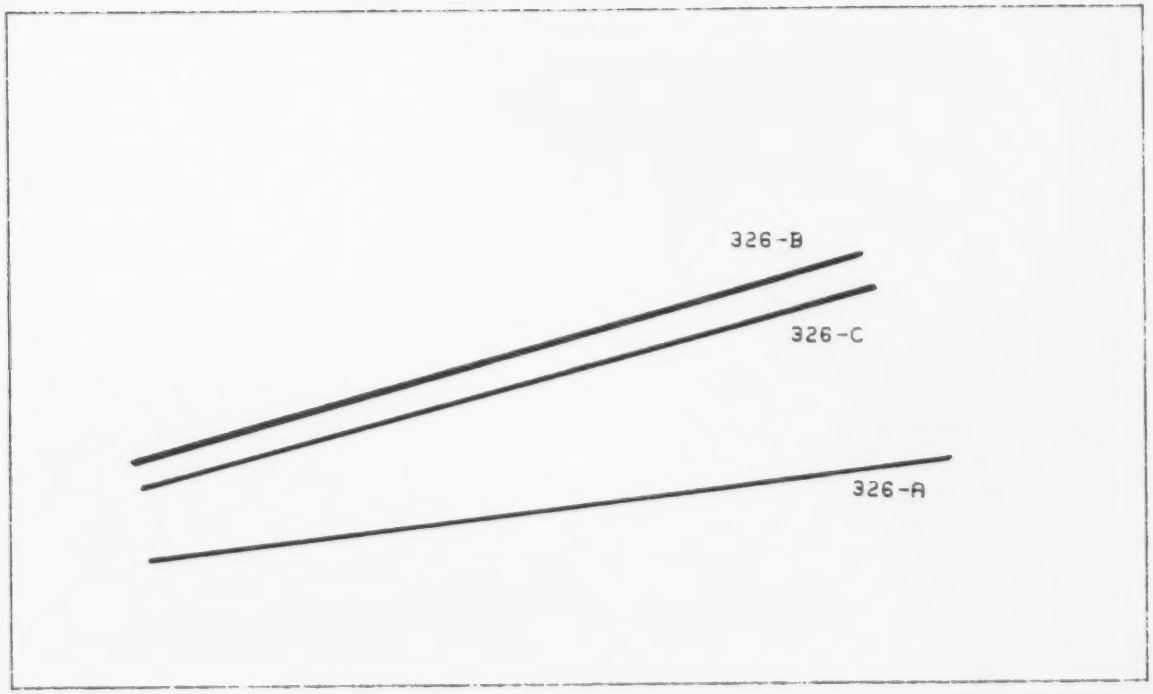

HULL FORM COEFICIENT REPRESENTATION
OF THE RELATIVE PERFORMANCE OF
THE THREE BOWS

FIGURE 4.5

FIGURE 4.6

MATHEMATICAL PREDICTION

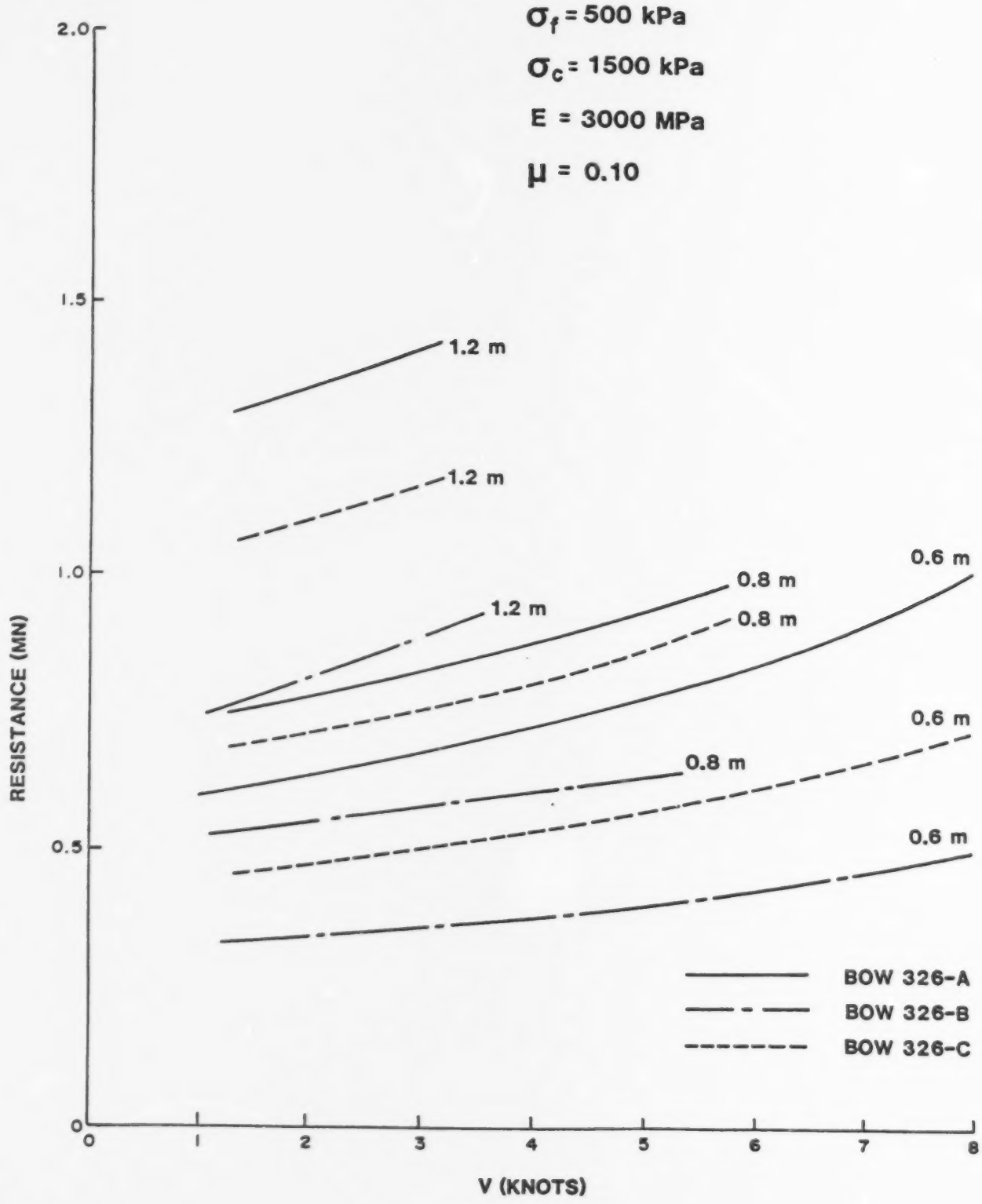

form analysis, but is significant with the computer model. It is thought that this difference indicates the relative effect of the hull form variables which are accounted for in the computer prediction but which do not affect the hull form coefficients.

4.2.5 Conclusions of Ice Testing

The ACL test analysis procedures resulted in the creation of a number of predictor equations. These are summarized in Table 4.5. The resistance and self-propulsion test predictor equations were combined and the resulting equations represent the ACL final model scale predictor equations.

The combined ACL resistance and self-propulsion predictor equations and the ACL thrust predictor equations were then transformed to a full-scale prediction by applying Froude's scale factors giving the final full-scale predictions:

MODEL A:

$$R = 0.001166\ \sigma_f h^2 + 0.1504\ vh + 0.5167\ h$$

$$T = 0.000517\ \sigma_f h^2 + 0.1675\ vh + 0.3401\ h$$

MODEL B:

$$R = 0.00008385\ \sigma_f h + 0.1525\ vh + 0.5517\ h^2$$

$$T = 0.0004938\ \sigma_f h + 0.1224\ vh + 0.08577\ h^2$$

MODEL C:

$$R = 0.0008562\ \sigma_f h + 0.1122\ vh + 0.7209\ h^2$$

$$T = 0.0009386\ \sigma_f h^2 + 9.1262\ vh + 0.01573\ h$$

where:

v = speed - knots (kn)
h = ice thickness - meters (m)
σ_f = ice flexural strength - kilo Pascals (kPa)
R = resistance - Mega Newtons (MN)
T = thrust - Mega Newtons (MN)

These full-scale resistance predictions are shown on Figure 4.7 together with the full power thrust line from the vessel. The thrust predictor lines are not reproduced, as they represent propeller thrust only and do not clarify the prediction any further. The final predictor for the broken channel tests is based on the data from all the model tests and as such does not represent a specific bow.

The predictor is:

$R = 1.965 + 628.9\ vh + 8896\ h^2$, and is reproduced in Figure 4.8.

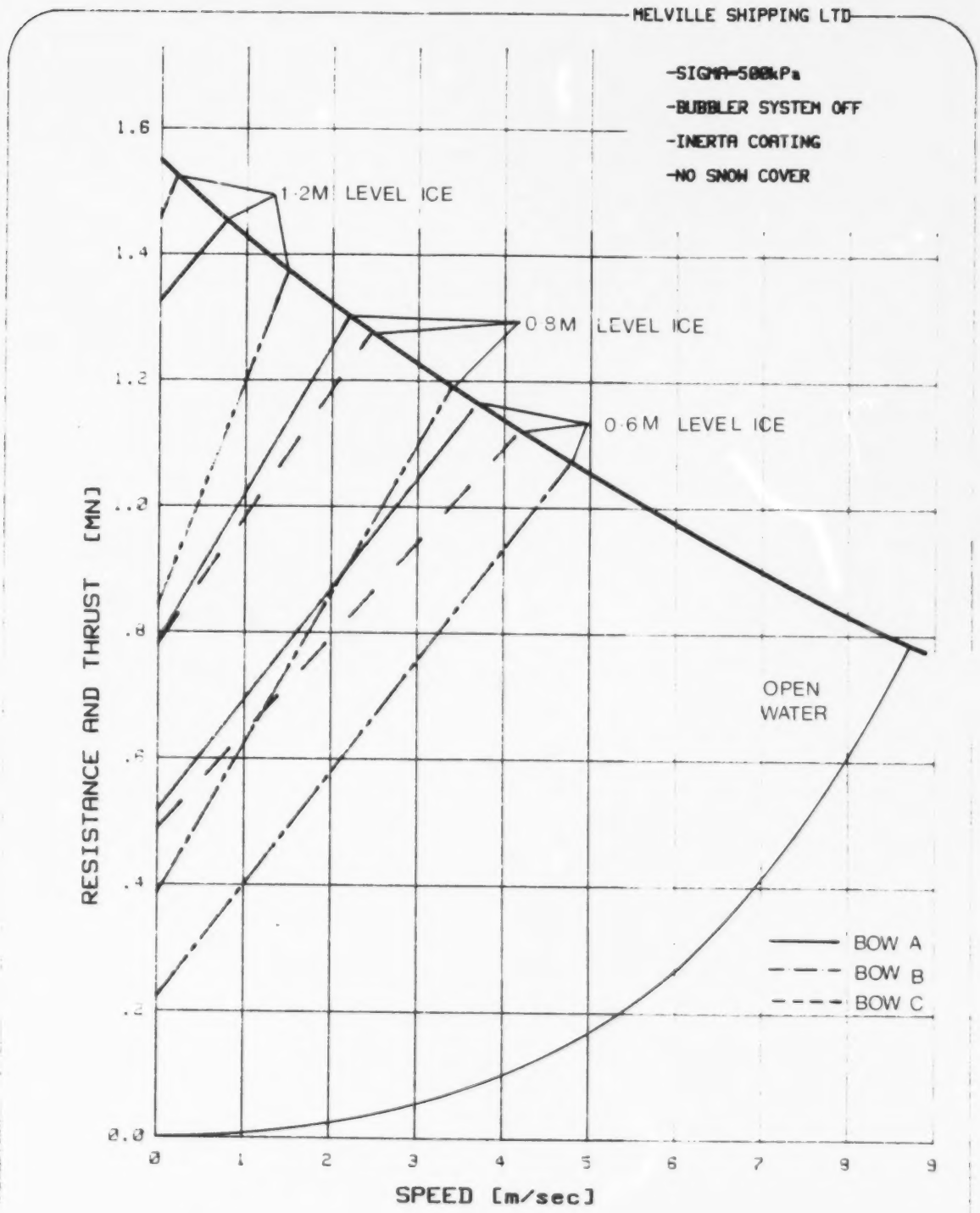

A.C.L. FINAL PREDICTION FOR MODELS A, B AND C

FIGURE 4.7

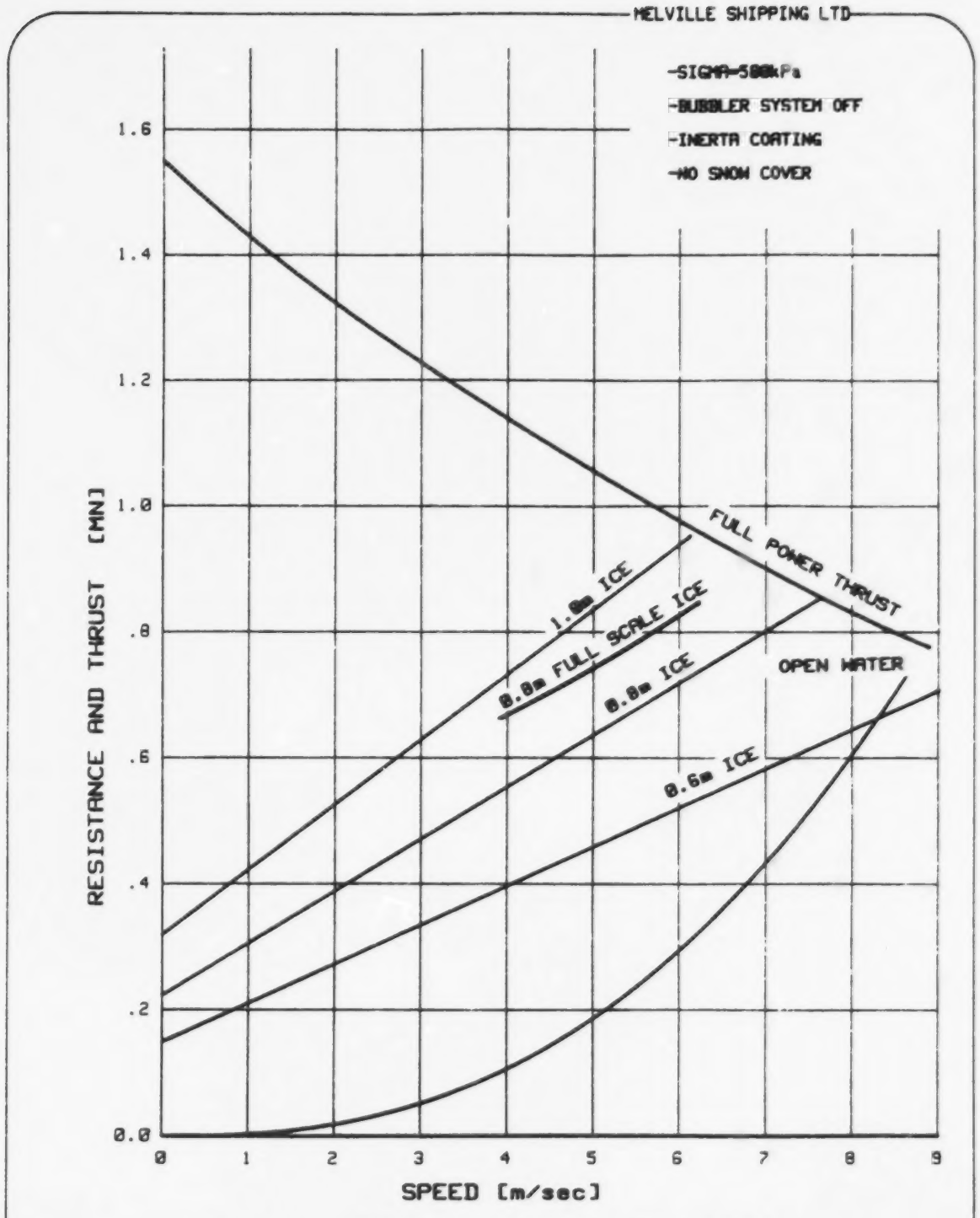

A.C.L. BROKEN CHANNEL PREDICTOR
AND FULL SCALE BROKEN CHANNEL DATA

FIGURE 4.8

5.0 ANALYSIS OF RESULTS

5.1 General

Following the model tests, the data collected by ACL was scanned and points that showed any peculiarity, or that were associated with a disturbance during the tests, were studied. These data points have been discussed in the last section. In this section, a comparison between the model scale results and the full-scale data collected during the Lake Melville trials is made, and the correlation between the two sets of data is discussed.

5.2 Level Ice

The full-scale data collected in Lake Melville is shown in Figure 5.1 together with the model scale prediction. The figure is based on a direct comparison between the full-scale data collected in Lake Melville normalized to 300 kPa using the Melville equation and the ACL final resistance prediction based on 300 kPa. There are a number of observations that can be made:

- the ACL prediction at full power for 0.8 m level ice appears to be representative of the full-scale data;
- the ACL predictor at lower and higher ice thicknesses than 0.8 m does not appear to represent the data so well;
- the speed dependancy of the ACL predictor does not coincide with that of the full-scale tests;
- the creeping resistance is much higher in the full-scale data than in the model scale predictor.

Similar observations can be made comparing the ACL predictor, plotted at 500 kPa (model testing target strength), and the full-scale data corrected to 500 kPa by the Melville equation. This is shown in Figure 5.2.

By increasing the strength of ice from 300 to 500 kPa the correlation between the model test predictor equation and the MSL equation, which is based on full-scale data, has changed. The best correlation at 500 kPa appears to be at 0.6 m whilst at 300 kPa it appears to be at 0.8 m. This ice thickness change is thought to be due to the dependance on strength in the predictor equations. The ACL predictor in 0.6 m ice at 4 knots has a strength component contributing approximately 11% to the total resistance. The Melville equation at the same ice thickness and speed has a strength component contributing approximately 32% to the total resistance.

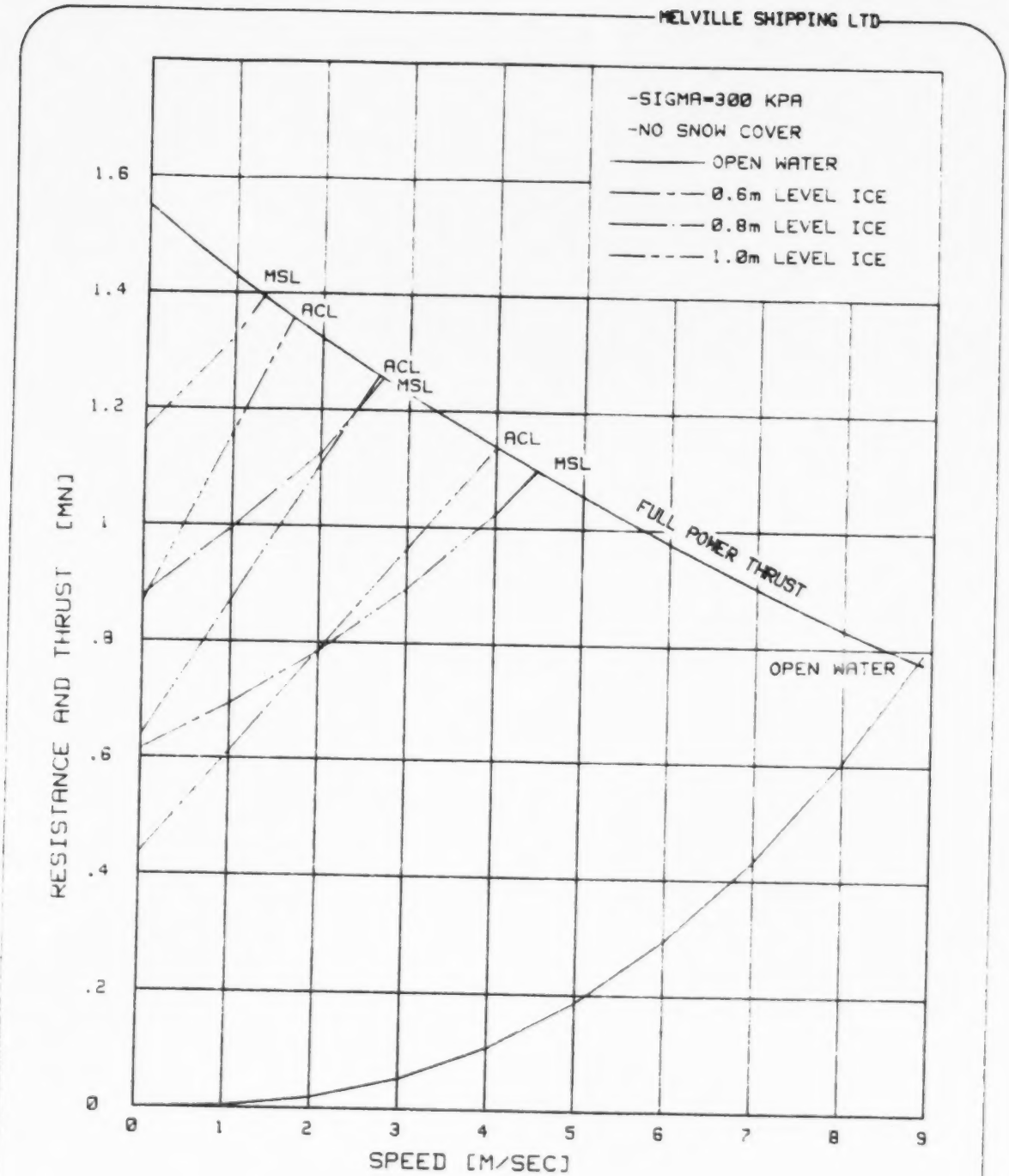

FULL SCALE RESISTANCE DATA AND
ACL MODEL SCALE PREDICTION
FOR THE EXISTING MV ARCTIC

FIGURE 5.1

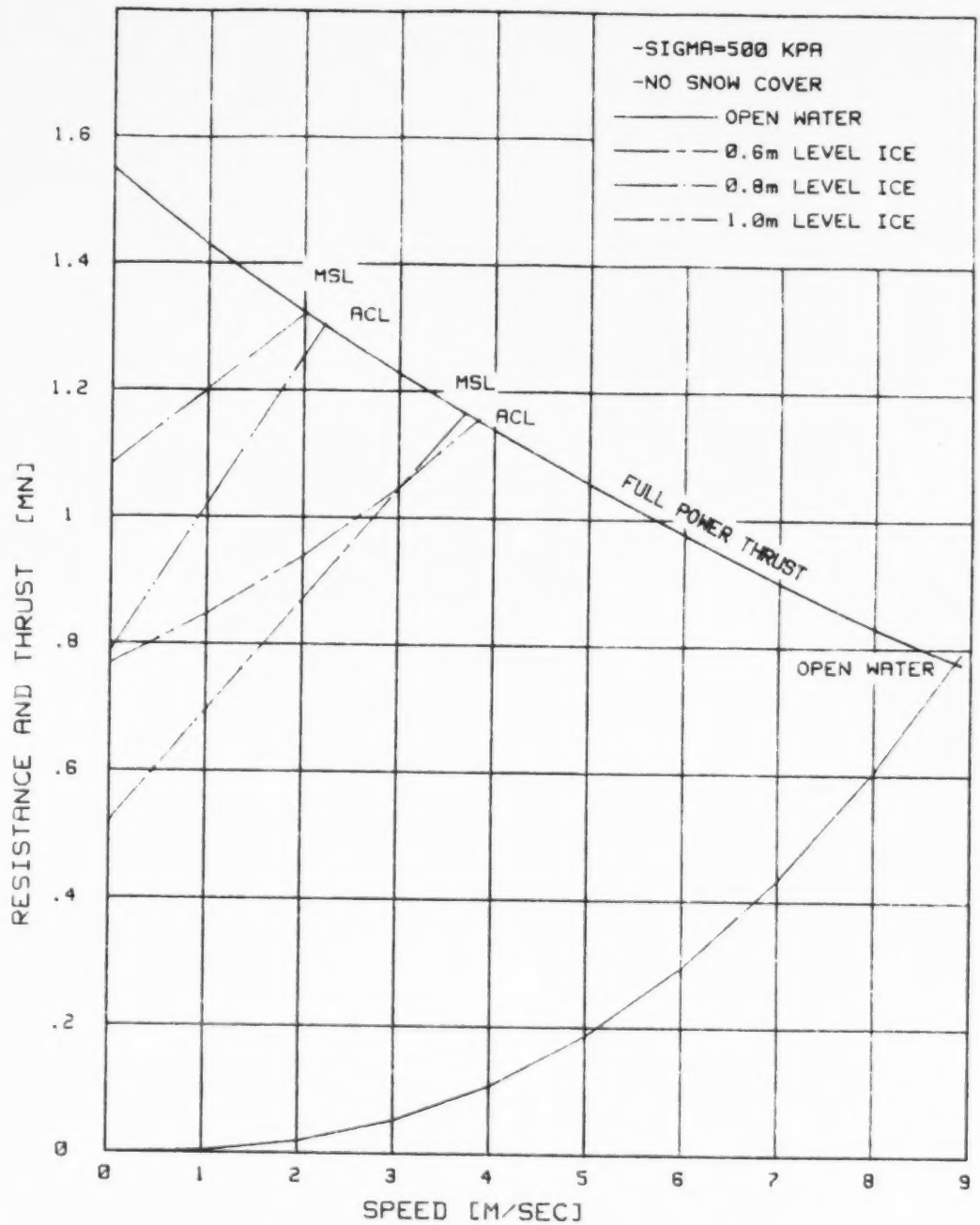

MSL PREDICTION BASED ON FULL SCALE DATA AND ACL PREDICTION FOR THE EXISTING MV ARCTIC

FIGURE 5.2

Since the model scale tests were conducted at 500 kPa and the Melville equation appears to model strength in a more representative way than the ACL predictor, the comparison between model scale data and full-scale data is based on 500 kPa. The results of the model tests can now be compared with the Melville equation for each of the bows. This is done in Figures 5.3 and 5.4 for Bows B and C respectively.

Similar observations can be made with regard to the comparison between the Melville equation and the ACL predictor as were made for the full-scale comparison above.

- the ACL full power prediction for all three bows for ice thicknesses of 0.6 and 0.8 m appears to agree well with the Melville equation;

- the speed dependancy of the ACL predictor does not appear to be representative of the actual ship performance;

- the low speed resistance of all three ACL predictors appears to be low.

The differences between the ACL model test data for the existing hull and the Melville equation which represents the full-scale performance of the vessel is thought to be partly due to the inaccurate modelling of friction during the model tests.

Enkvist (Ref. 3.2) conducted a number of experiments on the effect of friction in the total icebreaking resistance and arrived at a number of conclusions:

- the coefficient of friction is independant of velocity;

- the coefficient of friction rises with rising applied loads to a maximum value at an applied load of about 7,700 N/M^2, above which it is independent of load;

- no scale effects are apparent between the laboratory tests and the "on ice" tests;

- the coefficient of friction for snowless ice against steel is 0.041 to 0.109.

In another report by Calabrese (Ref. 5.1), a series of laboratory simulated tests were conducted which primarily examined the effects of different materials on friction with ice. However, the report also examines a number of other factors, and confirms the Enkvist result that, above critical low speeds, the friction is independent of velocity. In addition, the three friction modes are examined, Kinetic, Static and Breakaway. Figure 5.5 represents the effect of surface roughness on the coefficient of friction and is reproduced from Reference 5.1. As an indication, the

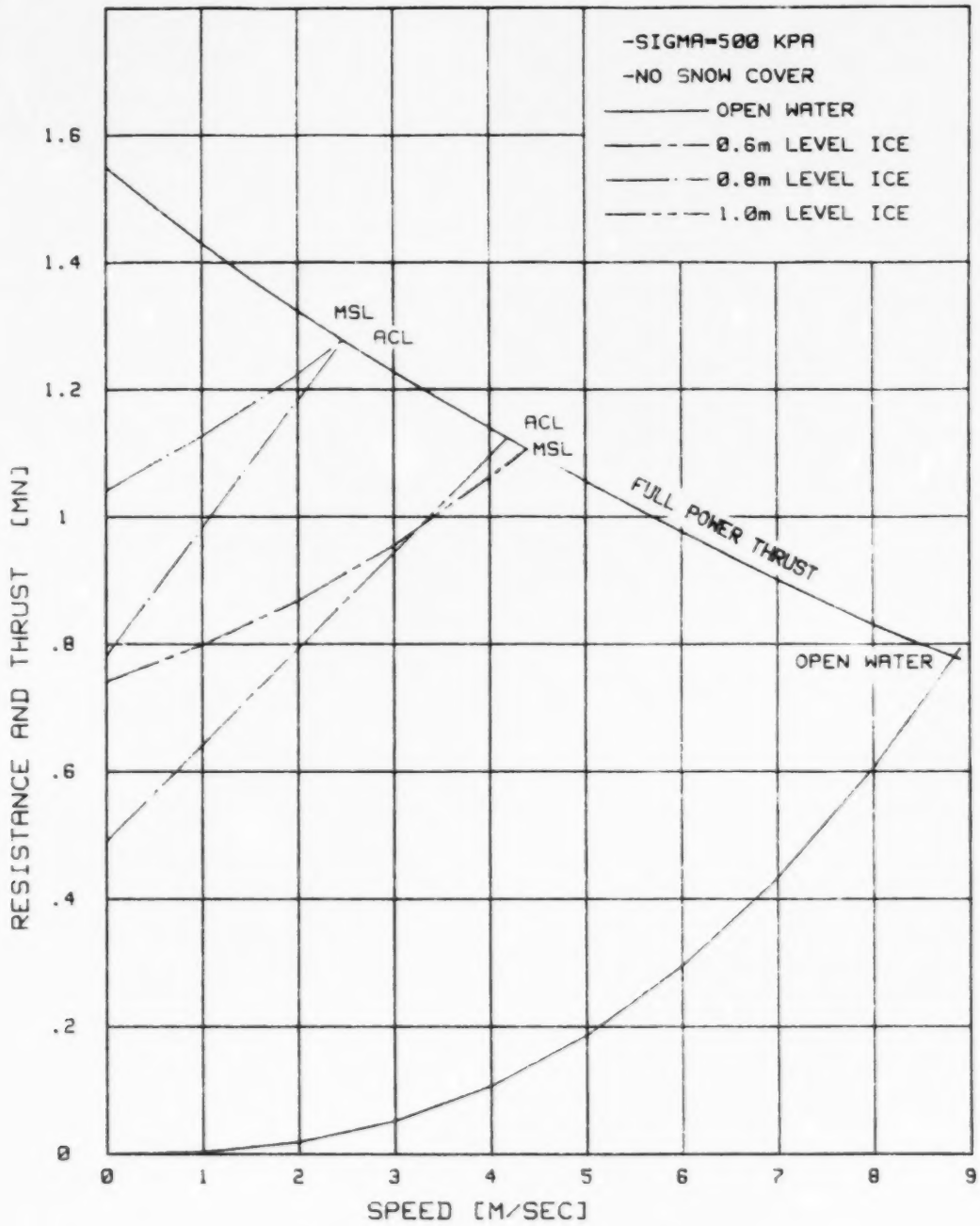

MSL PREDICTION AND ACL
PREDICTION FOR BOW 'B'

FIGURE 5.3

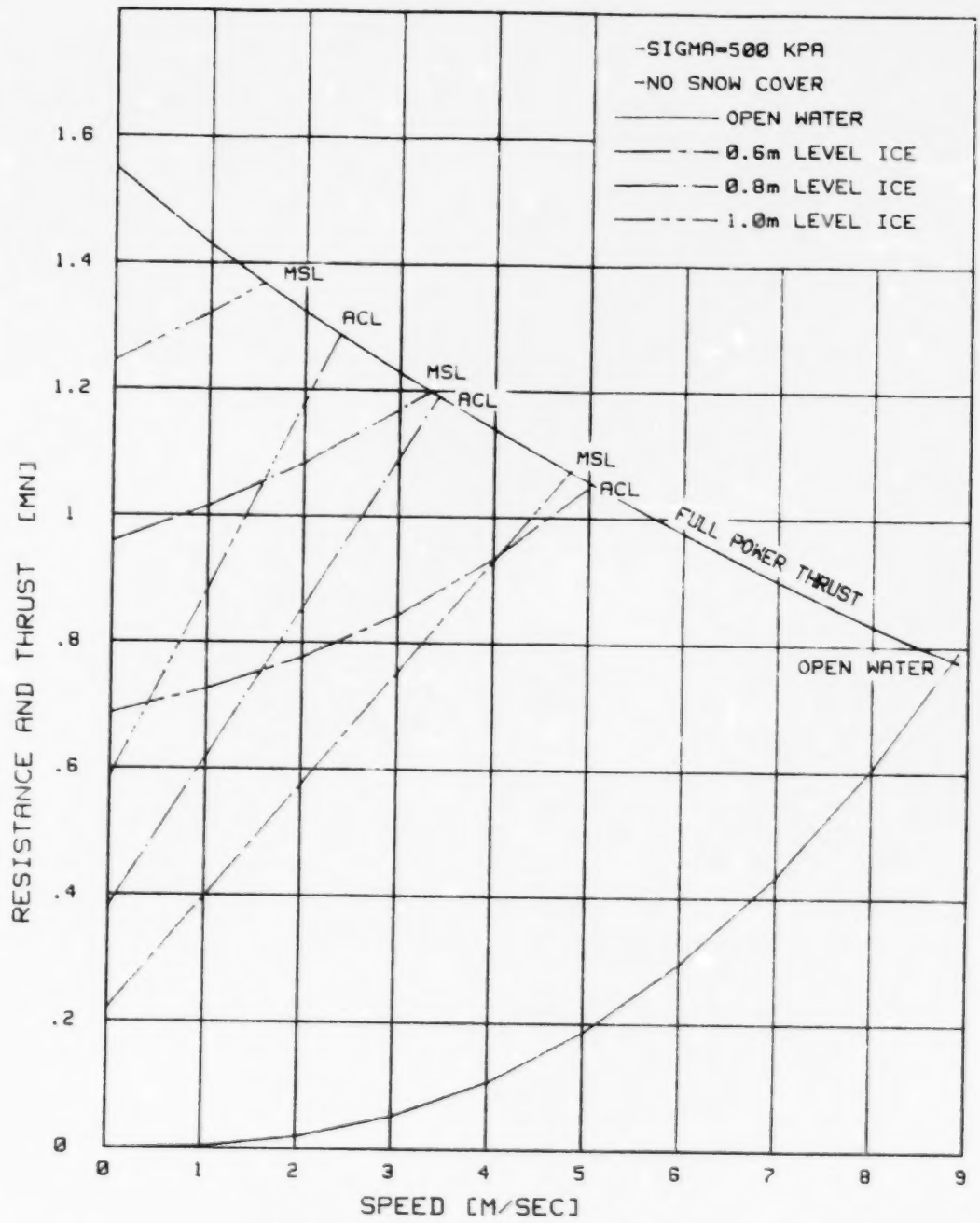

MSL PREDICTION AND ACL
PREDICTION FOR BOW 'C'

FIGURE 5.4

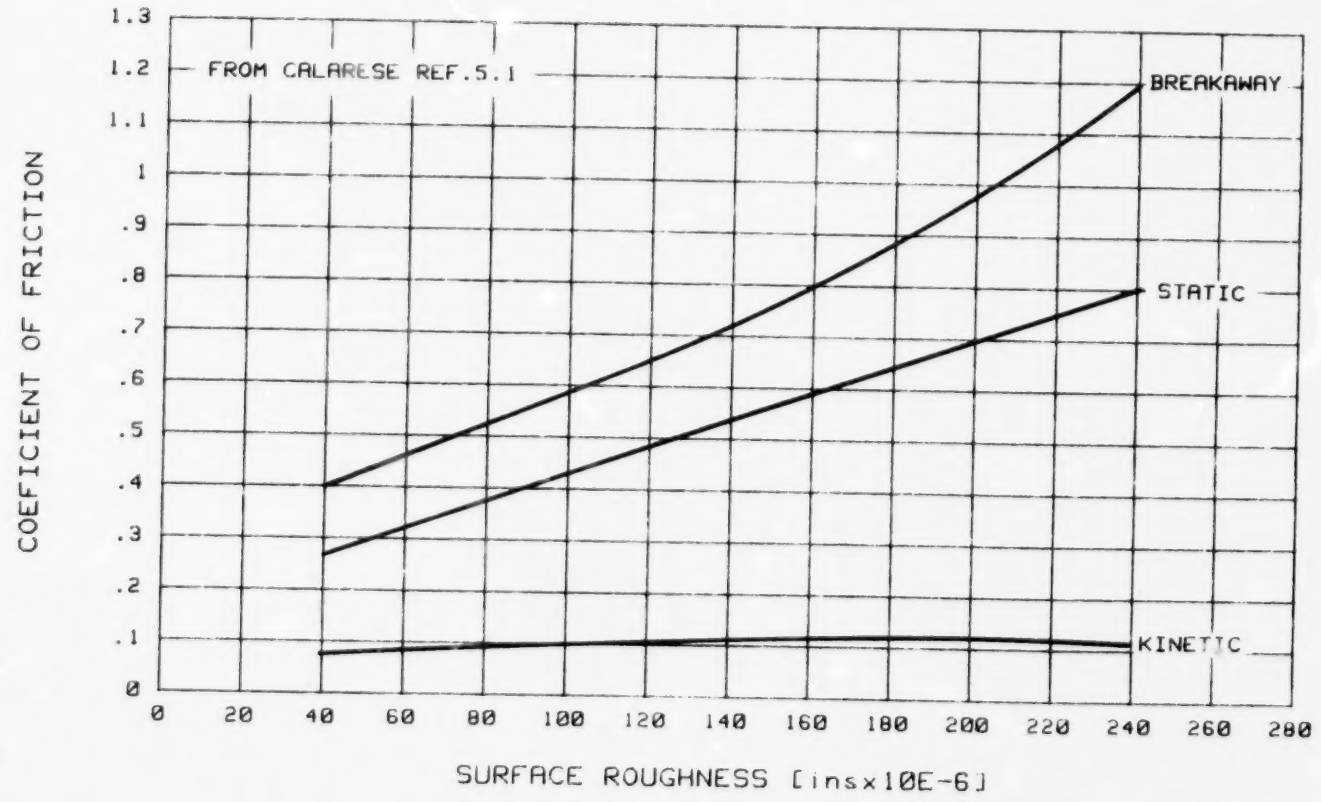

EFFECT OF SURFACE ROUGHNESS ON
THE COEFICIENT OF FRICTION BETWEEN
ICE AND STEEL

FIGURE 5.5

surface roughness of a new ship is approximately 120 - 140 x 10^{-6} in. and increases with age. It can be seen from Figure 5.5 that the coefficient of kinetic friction is hardly influenced by surface roughness and is approximately 0.1 The inerta coating, which is applied to the M.V. ARCTIC, will reduce the surface roughness and friction. This reduction is thought to be approximately 50% for dry ice.

From the above, it may be concluded that the hull kinetic friction for the ARCTIC, as tested in Lake Melville, was in the region of 0.05 to 0.1.

These conclusions indicate that there may be a failure in the modelling technique used to scale friction. As stated in Section 4, the model testing was based on the Froude similarity formulation which would require the same numerical value of friction to be used on model and full-scale ship. However, although the full-scale friction measured locally on icebreakers can be modelled, the "hungry horse" appearance of the hull in full scale has not been modelled and its effect remains an unknown.

The significance of this "hungry horse" appearance will, to a great extent, depend on the ship's length and the degree to which the ice sheet imposes itself on the ship's side.

Channel width measurements were recorded for Bows B and C but unfortunately not for Bow A. These are given in Tables 4.3 and 4.4. An analysis of the channel width data indicates that there is no channel width speed dependency within the limited speed ranges run. However, there does appear to be an ice thickness dependency with thicker ice sheets resulting in wider channels. Unfortunately, channel widths for the existing hull were not recorded and as a result they cannot be used as a comparison. However, from visual observation the model with Bow A tended to make a fairly narrow channel with the ice sheet being close up to the model's mid-body. Very little open space remained between the ice sheet and the model sides. The model width was 0.764 m (22.93/30) and the average channel width for Bows B and C were 0.859 m and 0.876 m respectively, or 9.5 cm and 11.2 cm wider than the model's beam. From visual observations and film record the channel width does appear wider with Bows B and C, although no conclusions can be reached, it is felt the friction effect present in model A, and demonstrated by comparing the model and full-scale data, is not present to such a degree in either model B or C. This is discussed in greater depth in Reference 1.1 when additional model tests were run.

It is not possible, within the scope of this analysis, to arrive at a conclusion with regard to the effect of ice friction during model testing. However, it is possible to conclude that the differences noted at low speed with the existing ship model is partly due to frictional effects.

In addition to the friction, there is thought to be another parameter which was not modelled correctly in the Melville equation. As discussed in Section 3, the hull form coefficient (which includes the friction coefficient) is an ACL coefficient developed in Reference 3.11. This coefficient is similar to the Shimanski and Kashteljan coefficients and does not take account of the relationship between the waterline and flare angles

which it is believed contribute significantly to the icebreaking performance. Because of the Melville equation was used primarily as a design tool to evaluate relative performance, the hull form coefficients were felt adequate for this application. It is not within the scope of this work to develop new hull form coefficients, but it would appear from this work that in order to correctly predict icebreaking performance with the semi-empirical type of predictor equation, a better hull form coefficient should be developed.

In order to arrive at a final predictor of the performance of the two new bow forms, a correlation factor was created. To assimilate frictional effects, the predicted resistance of each bow was increased by the value necessary to obtain exact correlation between the Melville prediction of full-scale resistance at 500 kPa, based on full-scale tests at 300 kPa, and the model scale tests at 500 kPa, for the existing bow.

The necessary modification to resistance as a function of thickness is shown in Figure 5.6. It should be noted that since both the model scale and full-scale data are associated with an "error margin" this figure should not be taken to represent the effect of friction or hull form, but only a correlation for this specific model test series.

Figures 5.8 and 5.9 show the resulting full-scale predictions for the two bows corrected for the friction factor. For convenience Figure 5.7 is included which represents the full-scale prediction for the existing M.V. ARCTIC. As expected, the friction correction largely influences the low speed values of resistance and, particularly with Bow B, brings the unrealistically low resistance values shown in Figure 5.3 to acceptable levels.

Figures 5.8 and 5.9 also show the Melville equation prediction for the two modified bow forms and it can be seen that the prediction compares well with the corrected model scale results. Bow C compares better than Bow B and this is felt to be due to the representation of the hull form in the equation.

5.3 Broken Channel

As noted in Section 4, all of the data generated by the broken channel tests for the three bows was combined and regressed to a single predictor equation. The reason for this is that the data collected during these test was erratic and did not conform to any trends for either ice thickness or bow form. There are a number of possible reasons for this lack of conformity:

- Inconsistent broken ice density in the model tank;
- successive runs through the same ice resulting in different floe sizes for each run;
- initially very weak or thin ice resulting in accelerated ice melting and ice disassociation.

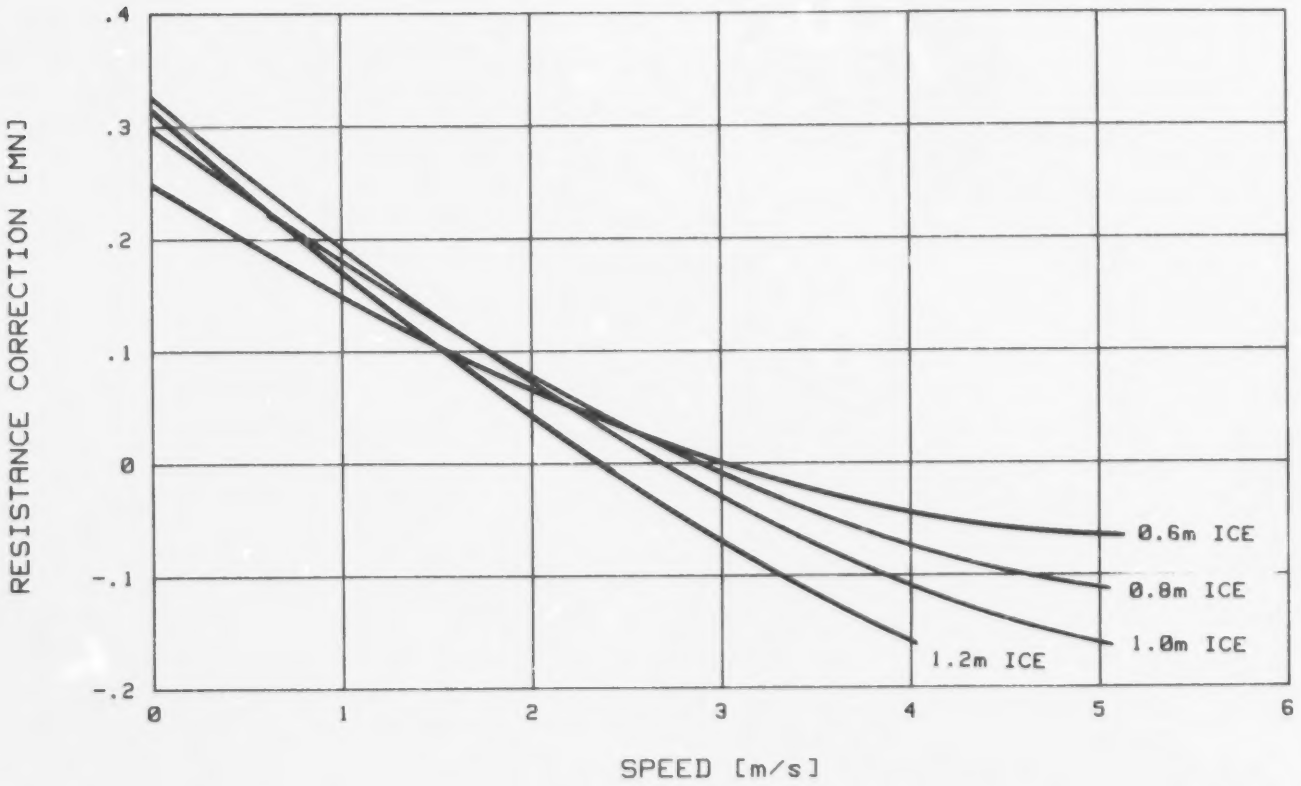

RESISTANCE CORRECTION FOR FULL SCALE
PREDICTION OF RESISTANCE
FOR BOWS 'C' AND 'B'

FIGURE 5.6

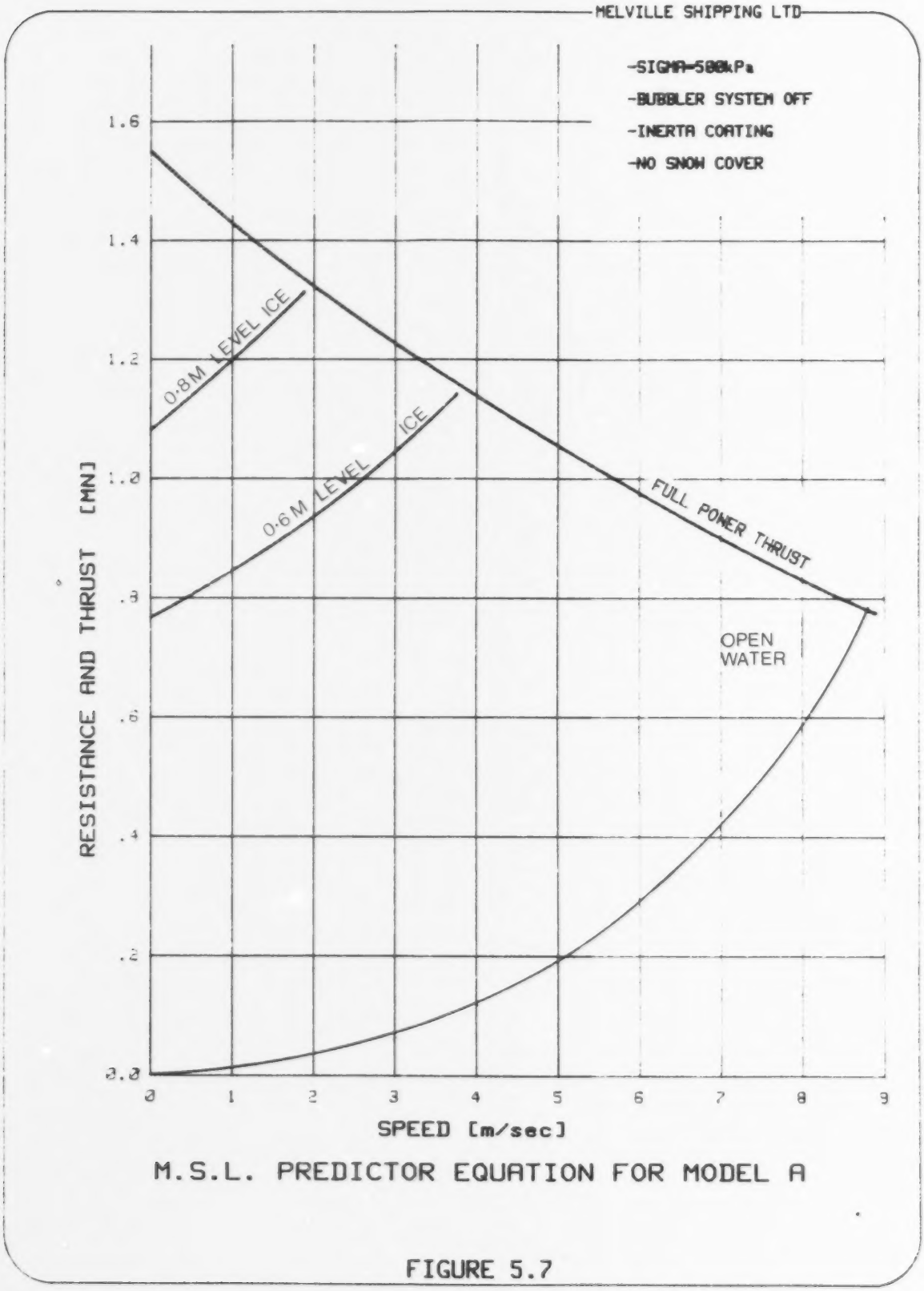
MELVILLE SHIPPING LTD
-SIGMA=500kPa
-BUBBLER SYSTEM OFF
-INERTA COATING
-NO SNOW COVER
1.6
1.4
1.2
1.0
.8
.6
.4
.2
0.0
0
1
2
3
4
5
6
7
8
9
0·8M LEVEL ICE
0·6M LEVEL ICE
FULL POWER THRUST
OPEN WATER
RESISTANCE AND THRUST [MN]
SPEED [m/sec]
M.S.L. PREDICTOR EQUATION FOR MODEL A

FIGURE 5.7

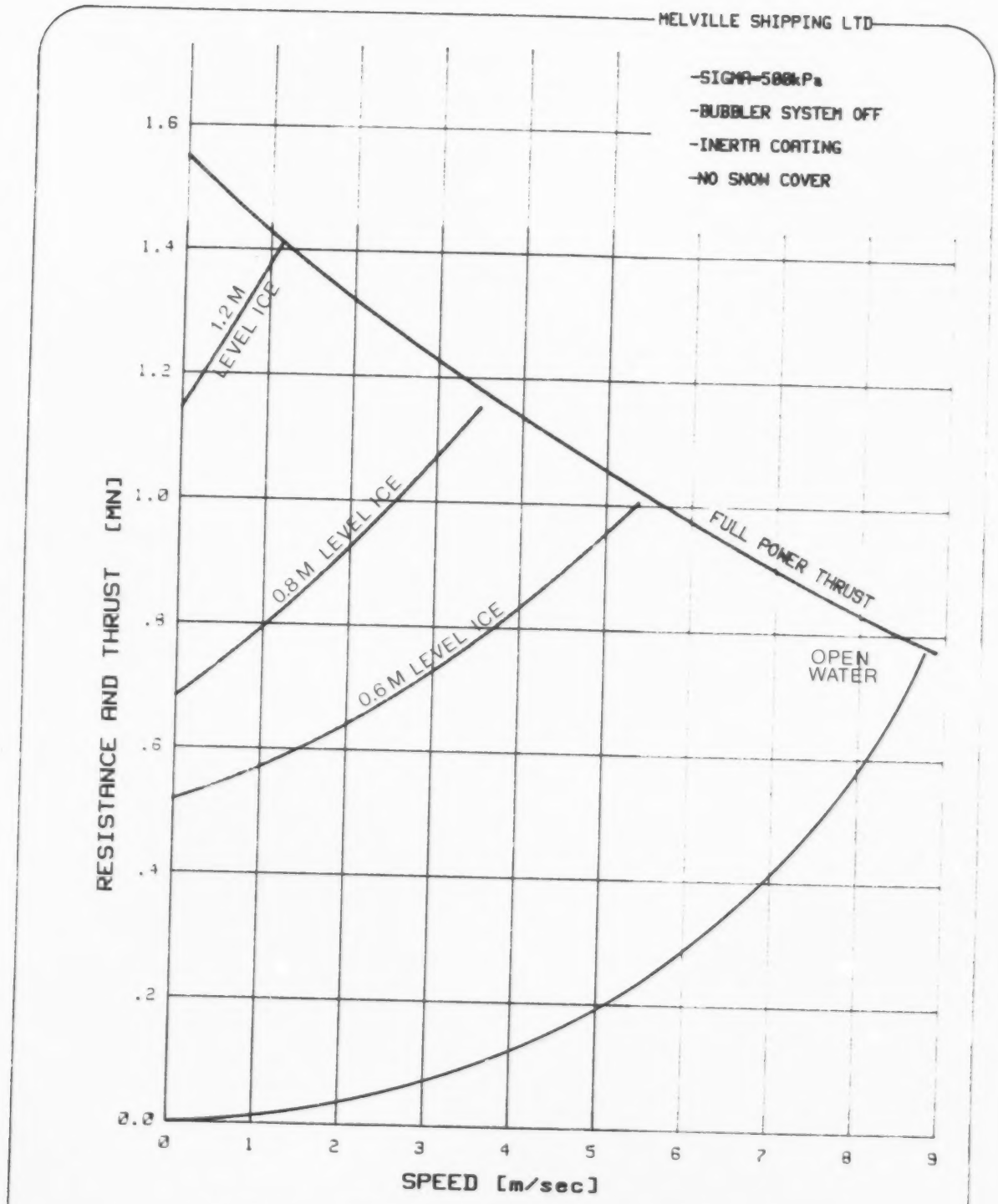

M.S.L. FINAL PREDICTION FOR BOW B

FIGURE 5.8

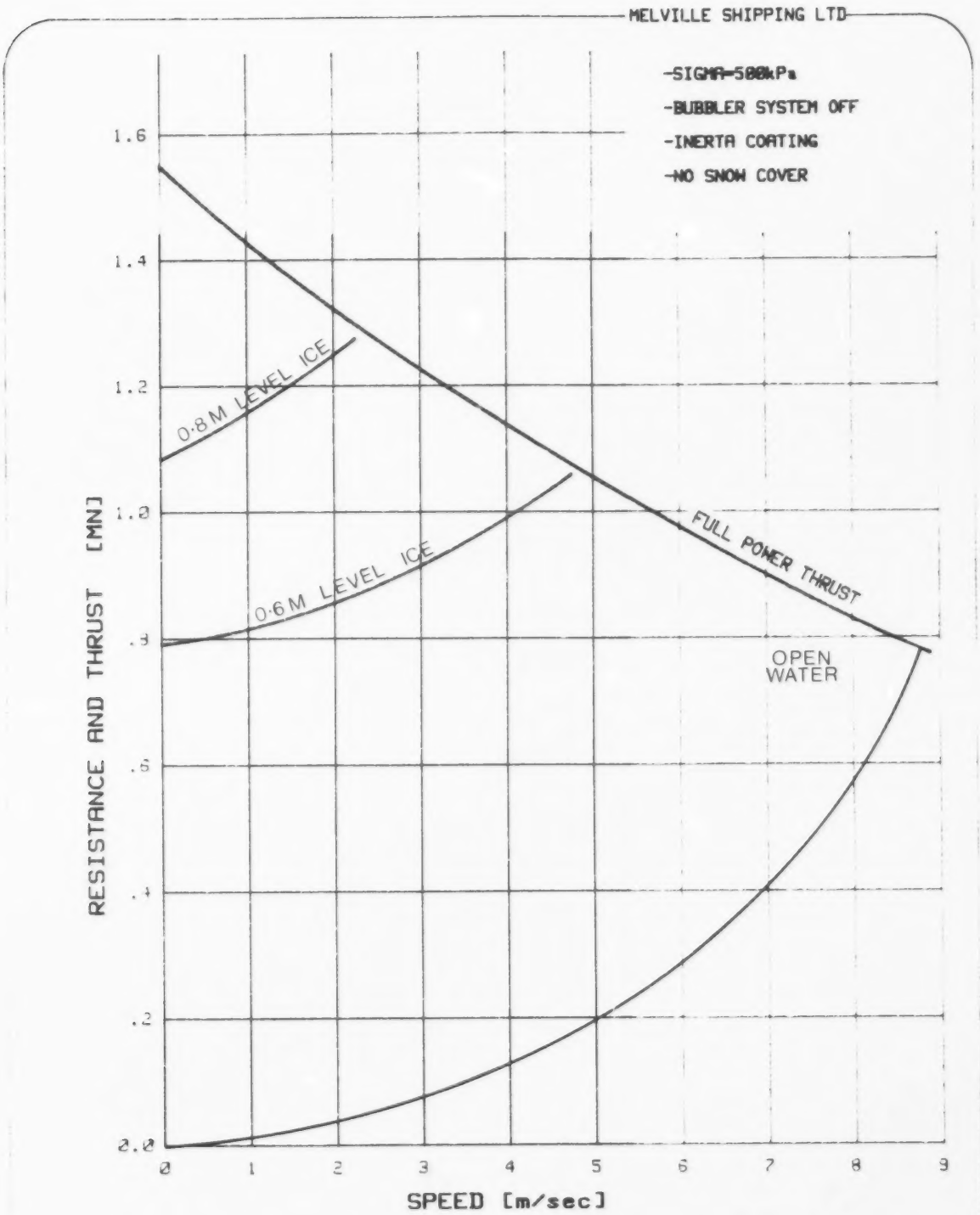

M.S.L. FINAL PREDICTION FOR BOW C

FIGURE 5.9

As a result of the above, very little can be concluded from the broken channel tests. Full-scale data in a broken channel was collected during the 1981 Lake Melville trials and is reported in Reference 3.6. Figure 5.7 presents the full-scale data, collected in a 90% full channel with 0.8 m thick ice, together with the ACL full-scale prediction. The correlation is surprisingly good and the slope of the full-scale and model scale lines are quite similar, particularly if the model test results are modified to reflect the correct open water performance. The existing vessel can achieve approximately 8.5 m/sec at full power in open water. Figure 5.10 shows that the vessel could achieve greater than 9 m/sec in 0.6 m ice. Thus, the ACL results should be adjusted up, bringing the predicted 0.8 m performance line even closer to full-scale for the existing M.V. ARCTIC.

If this broken channel testing can be said to represent the inertial and velocity components, then it may be postulated that the component due to breaking is the difference between this line and the level ice line for 0.8 m. The full-scale data shown in Figure 5.1 indicates a resistance of 0.878 MN at 0 m/sec and 1.274 MN at 3 m/sec. The broken channel tests at the same speeds indicated values of 0.43 MN and 0.78 MN or 49% and 39% respectively. This can be compared with the Melville equation breaking components which, for the same speeds, 0 and 3 m/sec, has 50% and 35% breaking component in the total resistance. This would indicate that the Melville equation represents strength well at 0.8 m.

5.4 Rubble Field

The rubble field data collected during the tests can only be indicative of the relative performance of the two new bow forms and, as such, indicated that Bow 'C' had the largest improvement over the existing bow, 19%, and Bow 'B' a smaller improvement of about 9%.

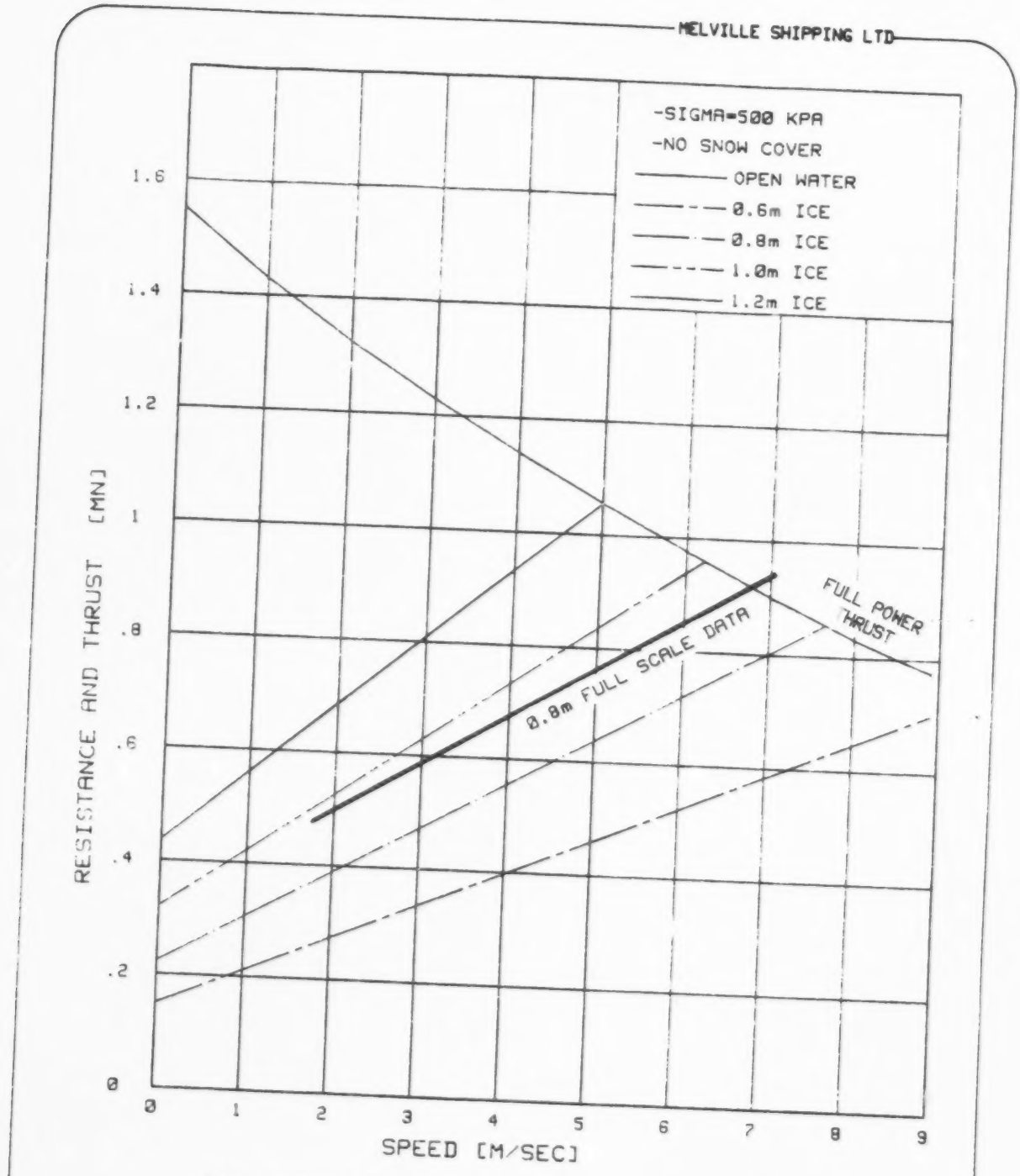

ACL PREDICTOR FOR BROKEN CHANNEL AND FULL SCALE DATA FOR THE EXISTING MV ARCTIC

FIGURE 5.10

6.0 BENEFIT ANALYSIS

6.1 General

The model test conducted at ACL was developed to allow a comparison between the existing hull form and modified hull forms developed by Melville. The previous sections of the report have described this model testing and identified a new bow which performs significantly better than the existing hull. This bow form, Bow B, is now compared on a "transit days" basis for a voyage from Europe to Nanisivik. The environmental conditions for this transit analysis are taken from Section 2 and Appendix 1. Considerable input from the M.V. ARCTIC's operator, Canarctic Shipping, and the ship's Master are included in the analysis.

6.2 Transit Analysis

The operating speed of the M.V. ARCTIC during its northern voyages depends on a great number of variables, including but not limited to

- ice thickness
- ice strength
- consolidation of ice
- prevailing winds
- sea state
- iceberg densities
- personnel comfort
- etc.

Clearly, within the scope of this work, it is not possible to develop a complex transit simulation which will account for all of these possible variables. The resistance prediction developed by ACL and as modified by Melville may be used to estimate the modified hull performance in different ice thicknesses and strengths. With regard to the other ice scenarios, input has been given by the ship's operator, Canarctic Shipping, and by members of the vessel's crew. Together, it is felt that this combination will allow a good comparitive indication of the transit capabilities of the new bow against the existing bow.

A number of assumptions have been made regarding the vessel's operation in this analysis.

- The open water performance of the new bow is the same as the old bow.

- The trans-Atlantic crossing from Europe to the southern tip of Greenland, Davis Strait and the return voyage is 5.62 days.

- The bubbler system is in operation for all ice work and has the same influence on resistance for the new bow as it does on the old.

- Open water transit speed in clear, moderate weather conditions is 16.5 knots.

- The effect of low visibility and inclement sea states for iceberg detection reduce the open water speed to 8 knots.

- Maximum power is available under all circumstances except in the event of low visibility or in areas of potential impact with multi-year floes.

Using these assumptions and input from the operators, transit days for the summer months, for the two bows, were developed. The months considered for the existing bow are June through to November, and for the new bow for the months of May to December.

The total transit days for each month were developed by considering transit through each of the five regions identified in Section 2.

- North Atlantic
- Davis Strait
- Baffin Bay
- Lancaster Sound
- Admiralty Inlet

Appendix 4 contains the tables used in this analysis and may be referenced for estimated speed through each of the five regions. The transit days represent the expected transit time for a one-way voyage between Europe and Nanisivik and do not include unloading or piloting time in Europe. Figure 6.1 summarizes the tables and compares the new and existing bow forms. Figure 6.1 also shows a number of data points from the vessel's log which represent the transit days of the vessel during the 1982 season. It can be seen that these compare well with the predicted performance based on the median ice conditions.

As would be expected from the model test results, the performance of the new bow is identical during the open water months of August and September.

Earlier and later in the year as ice becomes more prevalent the new bow performs better. However, because of the time spent in open water the benefit of the improved ice capability of the new bow is not fully realised until the existing vessel can no longer operate. This is usually the case before late June and after mid-November. The new bow is expected to be capable of operating during May and December as shown by Figure 6.1.

A summary of the transit days deduced are given in Table 6.1

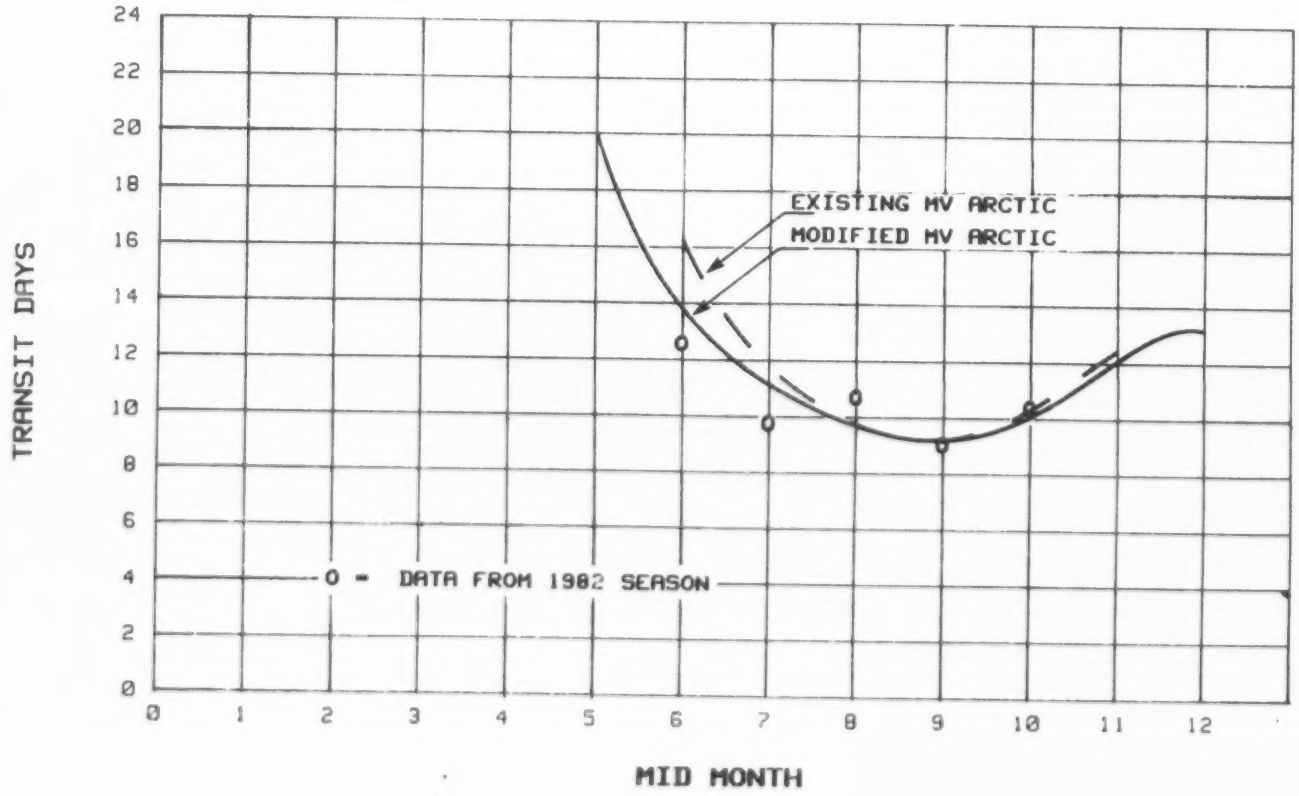

TRANSIT DAYS VS. MID MONTH
FOR THE EXISTING AND MODIFIED
ARCTIC AND DATA FROM 1982 SEASON

FIGURE 6.1

MONTH	EXISTING BOW	NEW BOW
May	-	19.98
June	16.24	13.88
July	11.78	11.03
August	9.74	9.74
September	9.20	9.20
October	10.29	9.96
November	12.42	12.10
December	-	13.17

TABLE 6.1
TRANSIT DAYS

7.0 CONCLUSIONS AND RECOMMENDATIONS

The objective of this study was to develop a modified ice breaking bow for the existing vessel M.V. ARCTIC. This has been completed in four stages:

- Environmental Analysis
- Bow Design
- Model Testing
- Transit Analysis

The conclusions of this work in each of these areas are presented below along with appropriate recommendations.

7.1 Conclusions

7.1.1 Environmental Analysis

a) The most onerous ice conditions through which the M.V. ARCTIC will operate are 1.8 to 2.2 m in thickness and 500 to 550 kPa in flexural strength. These conditions can exist in western Lancaster Sound and Barrow Strait and in Admiralty Inlet.

b) The data base for definition of ice thickness is good and is aided by the relationship between ice thickness and air temperature. Therefore, ice thickness can be reasonably well predicted by the input of cumulative freezing days to the Bilello equation.

c) The data base for ice strength is quite poor. The relationship between strength and air temperature is not nearly as well documented as that between ice thickness and temperature.

7.1.2 Bow Design

a) The analysis of bow forms based upon waterline and flare angles versus non dimensional forebody length allows a simplified understanding of the icebreaking action and assists icebreaking hull design.

b) The use of predictor equations is considered to be unreliable unless the equations are being used for a vessel of similar size and shape to that which is the basis for the equation.

c) The Arctec Canada Limited hull form coefficients and the treatment of friction in the predictor equation did not conform well to our current understanding of these variables.

d) The ACL predictor equation was adjusted to change some relationships and to ensure the predicted resistance was identical to existing full scale results for M.V. ARCTIC. This has been referred to throughout the report as the Melville equation.

e) The Melville equation was found to be useful as a design tool and was shown to predict quite well the model test results.

7.1.3 Model Testing

a) The open water model tests were carried out at the NRC, AVMRI facilities in Ottawa and incorporated tests of M.V. ARCTIC and two new bows. The open water test results indicated no detrimental effect due to changing the bow. For practical purposes the results were identical.

b) The ice tests were carried out at the Arctec Canada Ltd. facility in Ottawa. The test program consisted of level ice resistance and propulsion, broken ice resistance and propulsion and rubble field ramming for the M.V. ARCTIC and the two new bows.

c) The level ice testing indicated that the relative improvement in performance between the M.V. ARCTIC and the new bow "B" was approximately 30%.

d) The broken ice testing was inconclusive because of the inconsistent nature of the data collected. Clearly, based on the ACL tests, before meaningful broken ice tests can be conducted, more work must be done to simulate the ice regime.

e) The rubble field ramming tests indicated that the relative improvement over the existing bow for rubble field transit is 19% for Bow C and 9% for Bow B. It should be noted however, that these figures represent one test.

f) The ice test results generally produced fair correlation at full power with the full scale results obtained during the Lake Melville test program. This applies to both the level ice and broken ice tests.

g) Below the full power setting, the correlation between model test results and full scale performance was found to be very poor. This is thought to be as a result of the model representation of friction and is the subject of a recommendation later in this section.

h) The use of a middle divider in the Arctec Canada Ltd. model basin to allow two separate runs to be made with one ice sheet was shown to produce problems. These problems relate to the tendency for cracking of the ice to occur towards the middle barrier, and to the unevenness of ice thickness which occurs across the width of the tank, particularly close to one side.

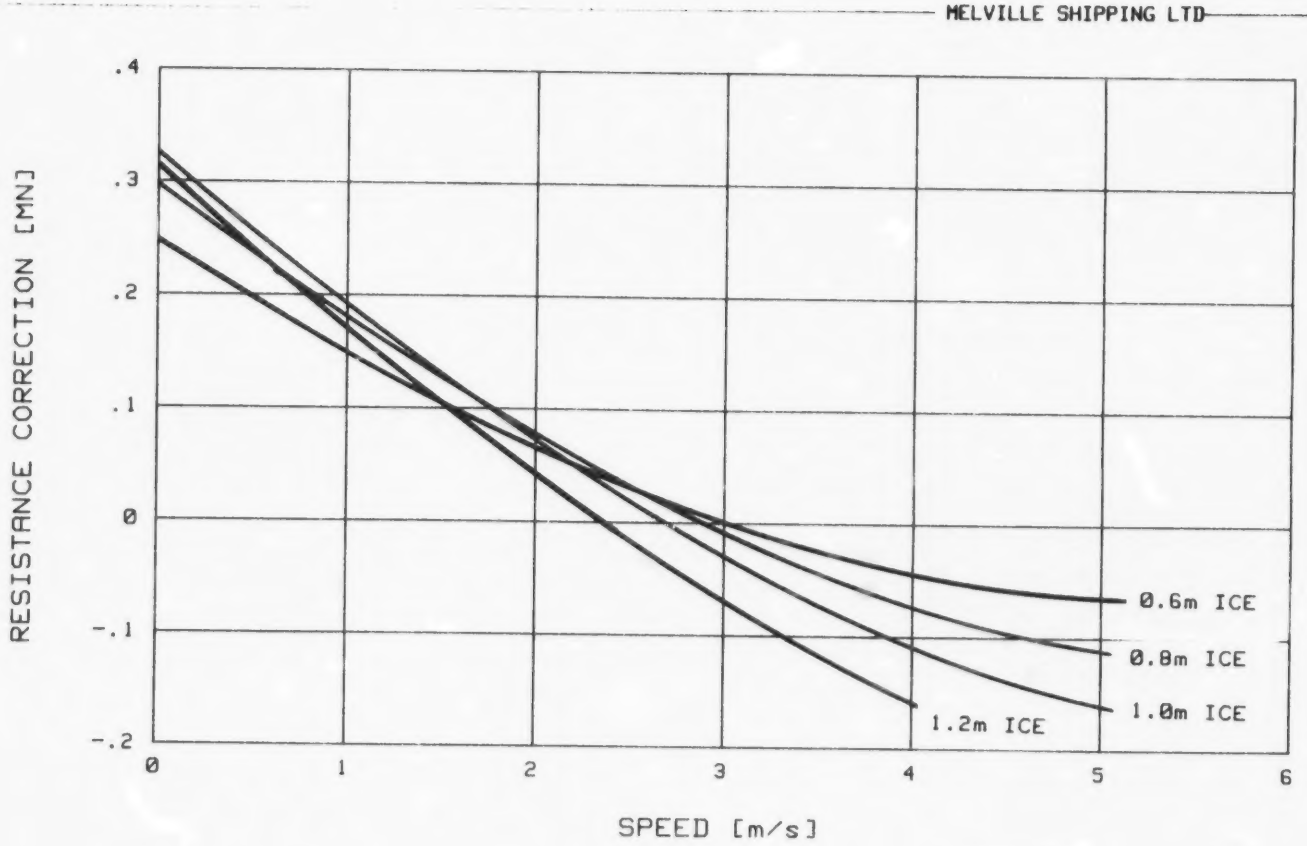

RESISTANCE CORRECTION FOR FULL SCALE
PREDICTION OF RESISTANCE
FOR BOWS 'C' AND 'B'

FIGURE 5.6

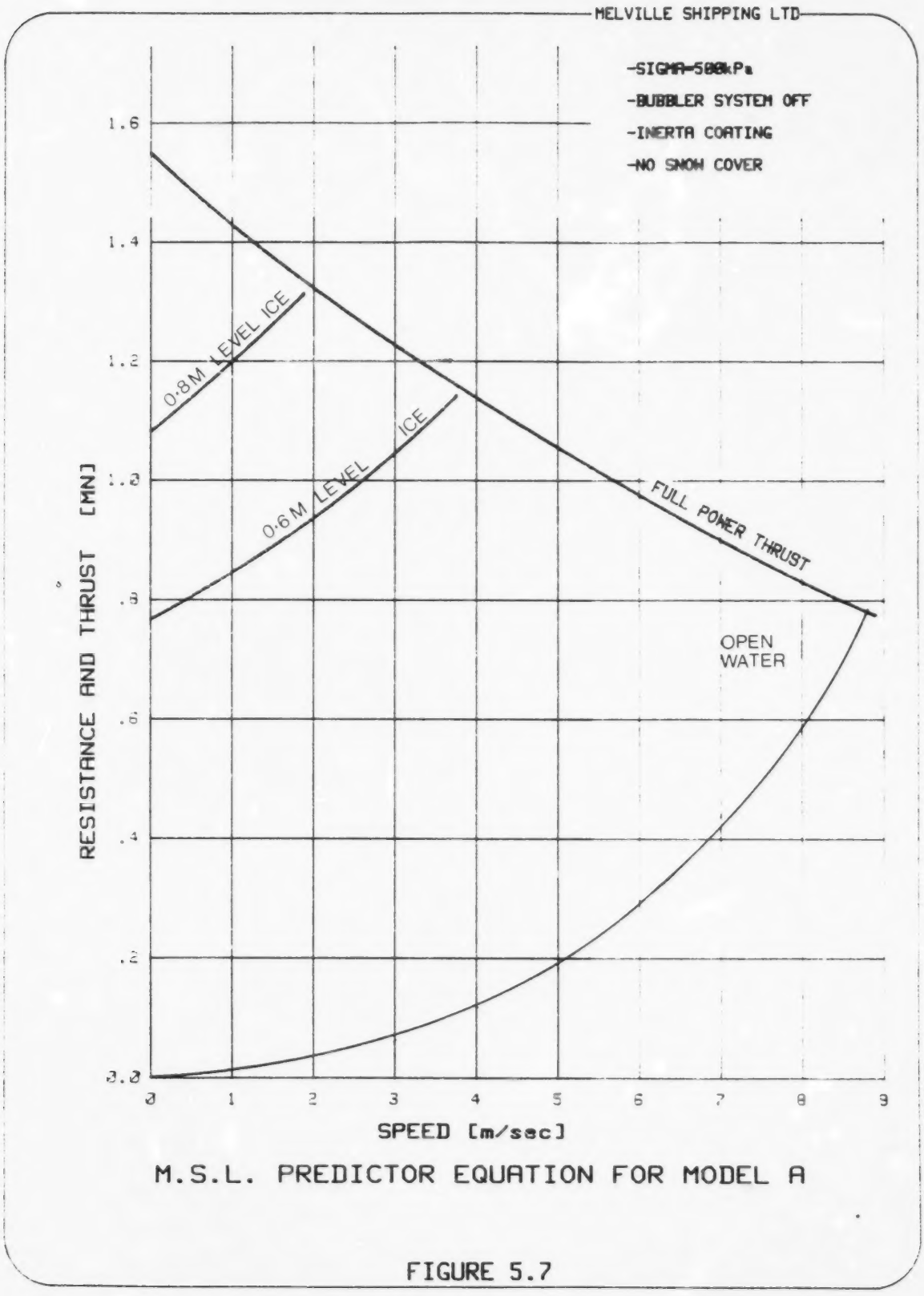

M.S.L. PREDICTOR EQUATION FOR MODEL A

FIGURE 5.7

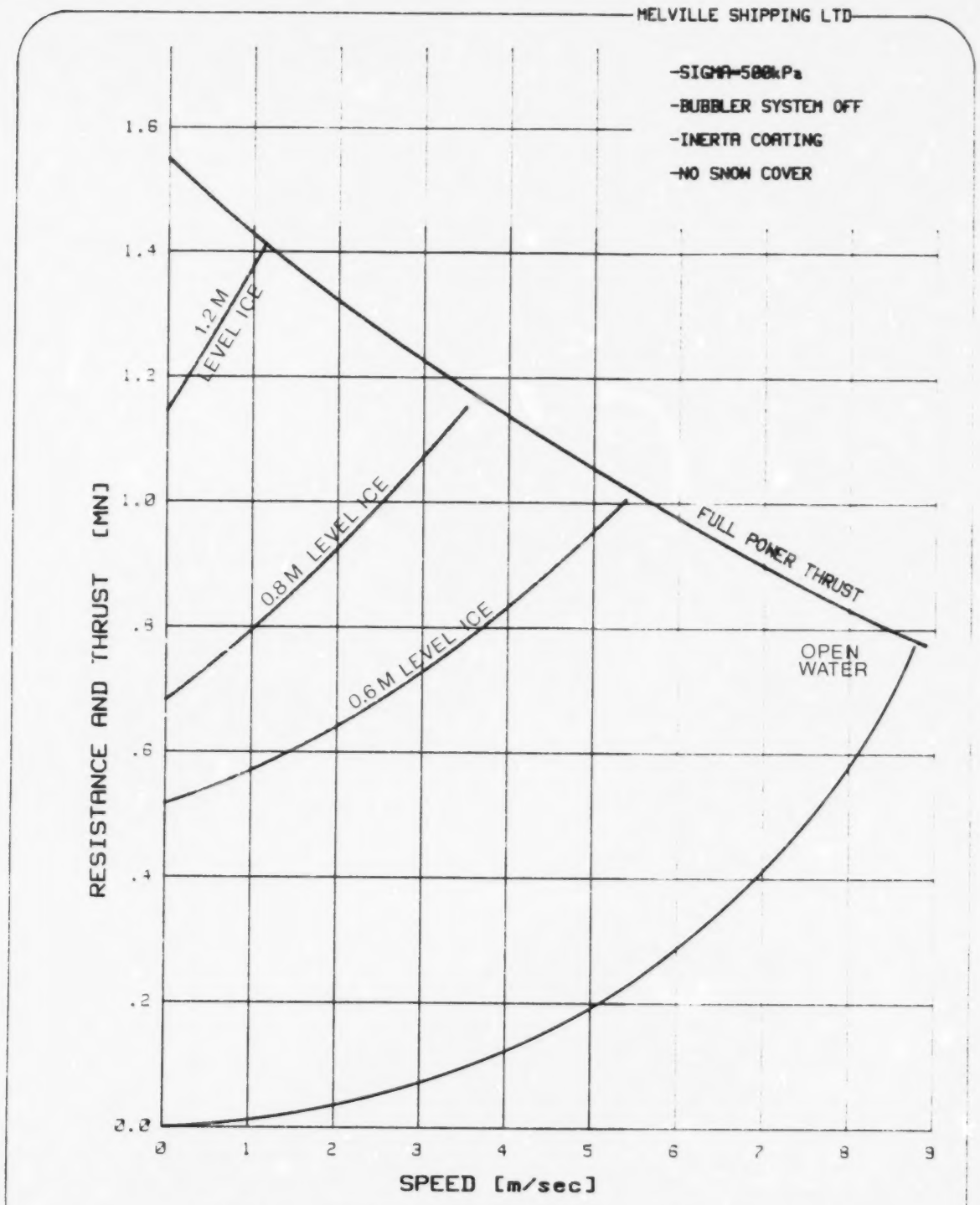

M.S.L. FINAL PREDICTION FOR BOW B

FIGURE 5.8

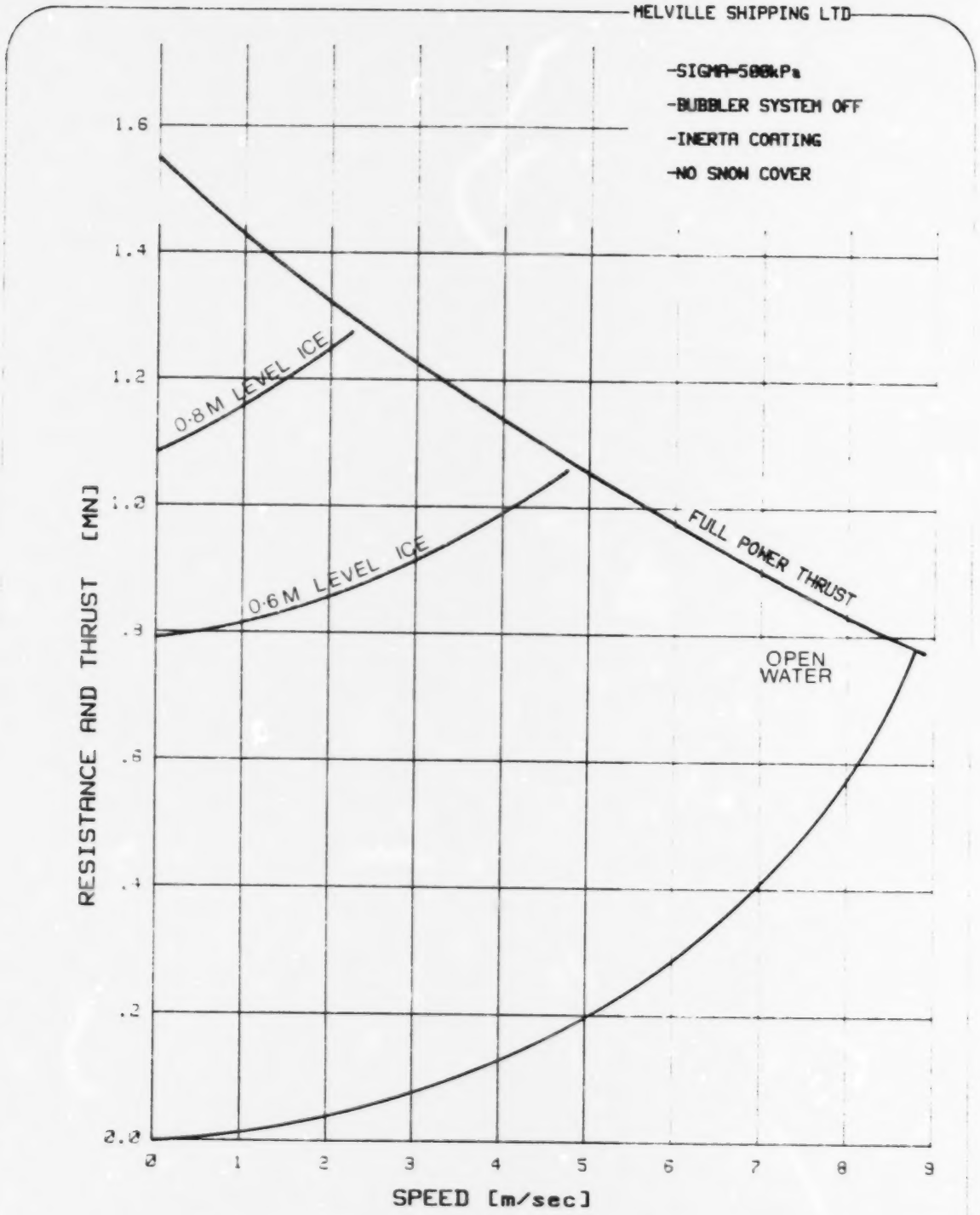

M.S.L. FINAL PREDICTION FOR BOW C

FIGURE 5.9

As a result of the above, very little can be concluded from the broken channel tests. Full-scale data in a broken channel was collected during the 1981 Lake Melville trials and is reported in Reference 3.6. Figure 5.7 presents the full-scale data, collected in a 90% full channel with 0.8 m thick ice, together with the ACL full-scale prediction. The correlation is surprisingly good and the slope of the full-scale and model scale lines are quite similar, particularly if the model test results are modified to reflect the correct open water performance. The existing vessel can achieve approximately 8.5 m/sec at full power in open water. Figure 5.10 shows that the vessel could achieve greater than 9 m/sec in 0.6 m ice. Thus, the ACL results should be adjusted up, bringing the predicted 0.8 m performance line even closer to full-scale for the existing M.V. ARCTIC.

If this broken channel testing can be said to represent the inertial and velocity components, then it may be postulated that the component due to breaking is the difference between this line and the level ice line for 0.8 m. The full-scale data shown in Figure 5.1 indicates a resistance of 0.878 MN at 0 m/sec and 1.274 MN at 3 m/sec. The broken channel tests at the same speeds indicated values of 0.43 MN and 0.78 MN or 49% and 39% respectively. This can be compared with the Melville equation breaking components which, for the same speeds, 0 and 3 m/sec, has 50% and 35% breaking component in the total resistance. This would indicate that the Melville equation represents strength well at 0.8 m.

5.4 Rubble Field

The rubble field data collected during the tests can only be indicative of the relative performance of the two new bow forms and, as such, indicated that Bow 'C' had the largest improvement over the existing bow, 19%, and Bow 'B' a smaller improvement of about 9%.

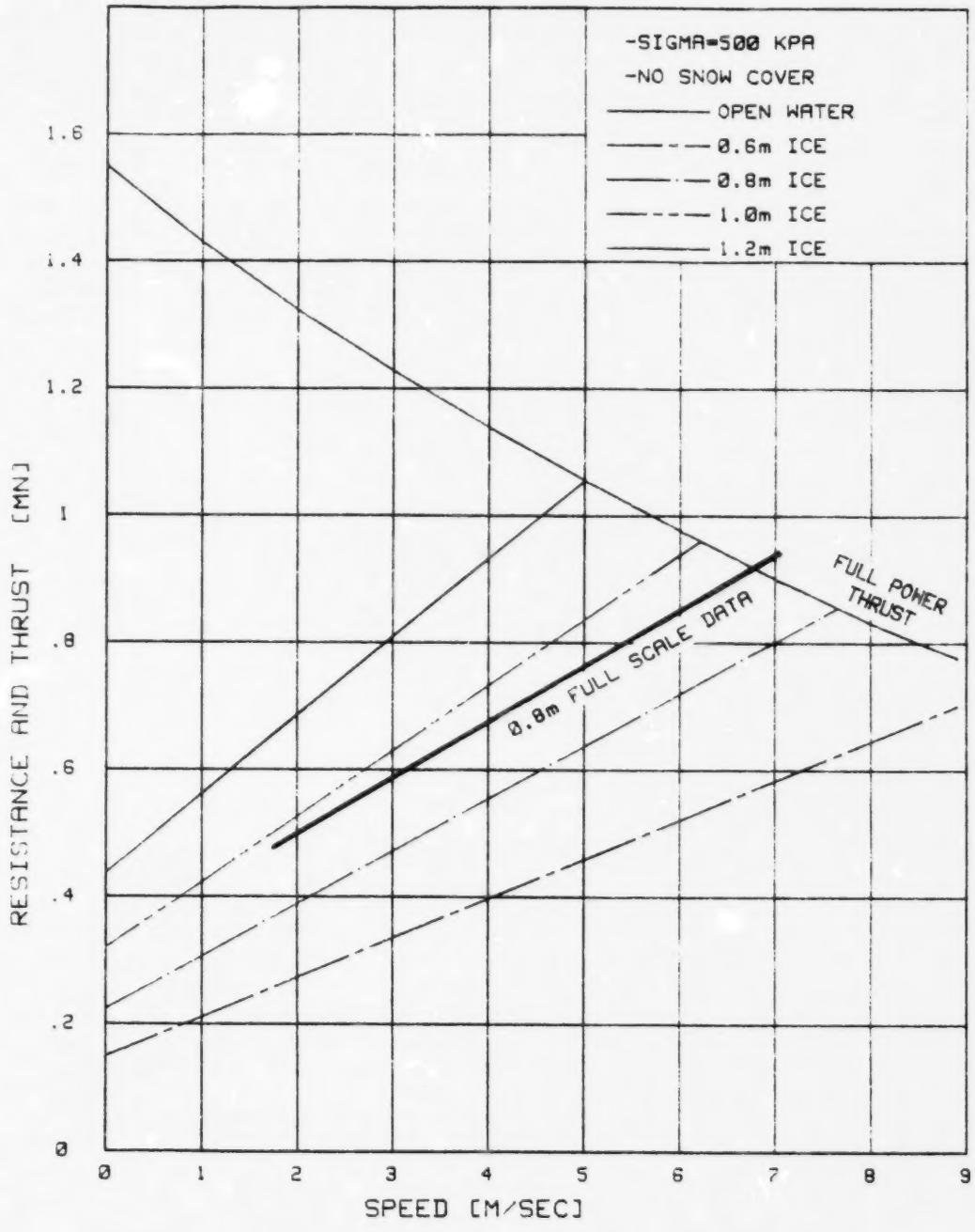

ACL PREDICTOR FOR BROKEN CHANNEL
AND FULL SCALE DATA FOR THE
EXISTING MV ARCTIC

FIGURE 5.10

6.0 BENEFIT ANALYSIS

6.1 General

The model test conducted at ACL was developed to allow a comparison between the existing hull form and modified hull forms developed by Melville. The previous sections of the report have described this model testing and identified a new bow which performs significantly better than the existing hull. This bow form, Bow B, is now compared on a "transit days" basis for a voyage from Europe to Nanisivik. The environmental conditions for this transit analysis are taken from Section 2 and Appendix 1. Considerable input from the M.V. ARCTIC's operator, Canarctic Shipping, and the ship's Master are included in the analysis.

6.2 Transit Analysis

The operating speed of the M.V. ARCTIC during its northern voyages depends on a great number of variables, including but not limited to

- Ice thickness
- Ice strength
- consolidation of ice
- prevailing winds
- sea state
- Iceberg densities
- personnel comfort
- etc.

Clearly, within the scope of this work, it is not possible to develop a complex transit simulation which will account for all of these possible variables. The resistance prediction developed by ACL and as modified by Melville may be used to estimate the modified hull performance in different ice thicknesses and strengths. With regard to the other ice scenarios, input has been given by the ship's operator, Canarctic Shipping, and by members of the vessel's crew. Together, it is felt that this combination will allow a good comparitive indication of the transit capabilities of the new bow against the existing bow.

A number of assumptions have been made regarding the vessel's operation in this analysis.

- The open water performance of the new bow is the same as the old bow.

- The trans-Atlantic crossing from Europe to the southern tip of Greenland, Davis Strait and the return voyage is 5.62 days.

- The bubbler system is in operation for all ice work and has the same influence on resistance for the new bow as it does on the old.

- Open water transit speed in clear, moderate weather conditions is 16.5 knots.

- The effect of low visibility and inclement sea states for iceberg detection reduce the open water speed to 8 knots.

- Maximum power is available under all circumstances except in the event of low visibility or in areas of potential impact with multi-year floes.

Using these assumptions and input from the operators, transit days for the summer months, for the two bows, were developed. The months considered for the existing bow are June through to November, and for the new bow for the months of May to December.

The total transit days for each month were developed by considering transit through each of the five regions identified in Section 2.

- North Atlantic
- Davis Strait
- Baffin Bay
- Lancaster Sound
- Admiralty Inlet

Appendix 4 contains the tables used in this analysis and may be referenced for estimated speed through each of the five regions. The transit days represent the expected transit time for a one-way voyage between Europe and Nanisivik and do not include unloading or piloting time in Europe. Figure 6.1 summarizes the tables and compares the new and existing bow forms. Figure 6.1 also shows a number of data points from the vessel's log which represent the transit days of the vessel during the 1982 season. It can be seen that these compare well with the predicted performance based on the median ice conditions.

As would be expected from the model test results, the performance of the new bow is identical during the open water months of August and September.

Earlier and later in the year as ice becomes more prevalent the new bow performs better. However, because of the time spent in open water the benefit of the improved ice capability of the new bow is not fully realised until the existing vessel can no longer operate. This is usually the case before late June and after mid-November. The new bow is expected to be capable of operating during May and December as shown by Figure 6.1.

A summary of the transit days deduced are given in Table 6.1

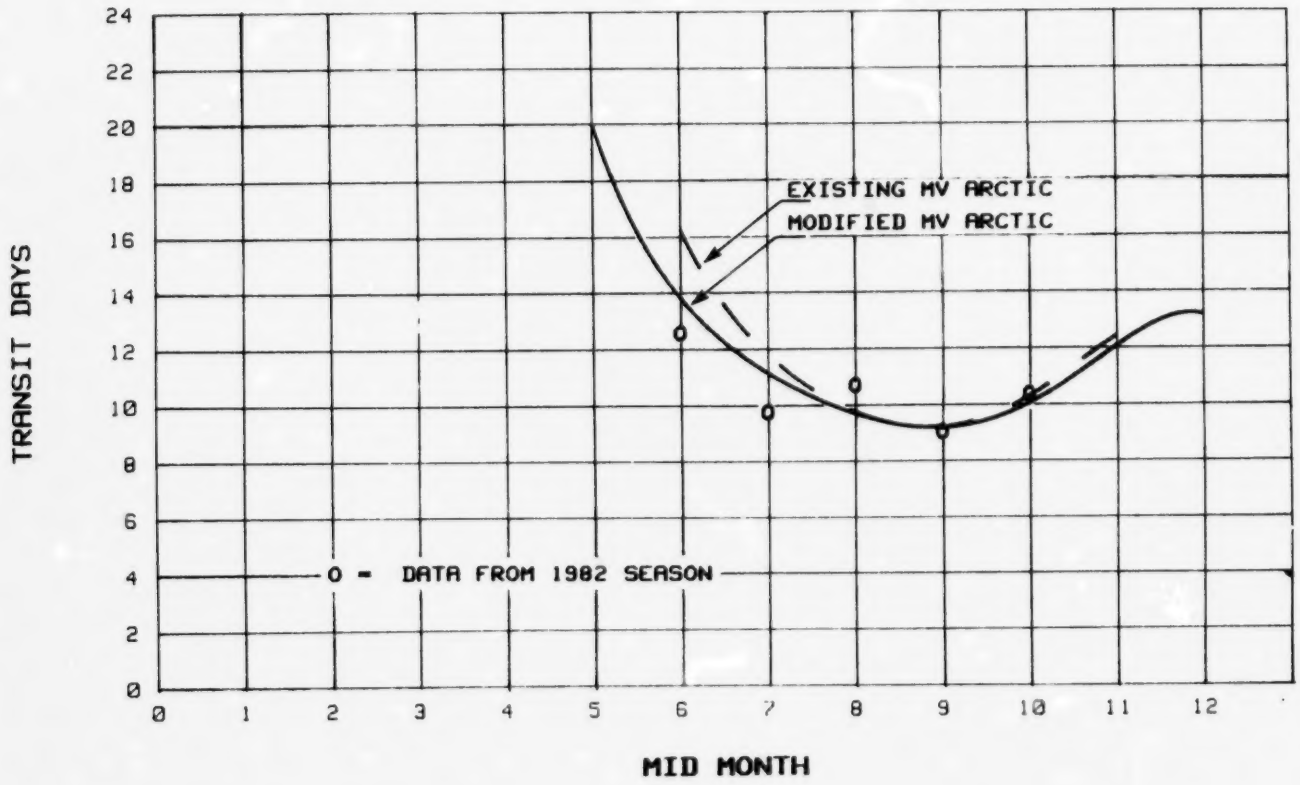

TRANSIT DAYS VS. MID MONTH
FOR THE EXISTING AND MODIFIED
ARCTIC AND DATA FROM 1982 SEASON

FIGURE 6.1

MONTH	EXISTING BOW	NEW BOW
May	-	19.98
June	16.24	13.88
July	11.78	11.03
August	9.74	9.74
September	9.20	9.20
October	10.29	9.96
November	12.42	12.10
December	-	13.17

TABLE 6.1
TRANSIT DAYS

7.0 CONCLUSIONS AND RECOMMENDATIONS

The objective of this study was to develop a modified ice breaking bow for the existing vessel M.V. ARCTIC. This has been completed in four stages:

- Environmental Analysis
- Bow Design
- Model Testing
- Transit Analysis

The conclusions of this work in each of these areas are presented below along with appropriate recommendations.

7.1 Conclusions

7.1.1 Environmental Analysis

a) The most onerous ice conditions through which the M.V. ARCTIC will operate are 1.8 to 2.2 m in thickness and 500 to 550 kPa in flexural strength. These conditions can exist in western Lancaster Sound and Barrow Strait and in Admiralty Inlet.

b) The data base for definition of ice thickness is good and is aided by the relationship between ice thickness and air temperature. Therefore, ice thickness can be reasonably well predicted by the input of cumulative freezing days to the Bilello equation.

c) The data base for ice strength is quite poor. The relationship between strength and air temperature is not nearly as well documented as that between ice thickness and temperature.

7.1.2 Bow Design

a) The analysis of bow forms based upon waterline and flare angles versus non dimensional forebody length allows a simplified understanding of the icebreaking action and assists icebreaking hull design.

b) The use of predictor equations is considered to be unreliable unless the equations are being used for a vessel of similar size and shape to that which is the basis for the equation.

c) The Arctec Canada Limited hull form coefficients and the treatment of friction in the predictor equation did not conform well to our current understanding of these variables.

d) The ACL predictor equation was adjusted to change some relationships and to ensure the predicted resistance was identical to existing full scale results for M.V. ARCTIC. This has been referred to throughout the report as the Melville equation.

e) The Melville equation was found to be useful as a design tool and was shown to predict quite well the model test results.

7.1.3 Model Testing

a) The open water model tests were carried out at the NRC, AVMRI facilities in Ottawa and incorporated tests of M.V. ARCTIC and two new bows. The open water test results indicated no detrimental effect due to changing the bow. For practical purposes the results were identical.

b) The ice tests were carried out at the Arctec Canada Ltd. facility in Ottawa. The test program consisted of level ice resistance and propulsion, broken ice resistance and propulsion and rubble field ramming for the M.V. ARCTIC and the two new bows.

c) The level ice testing indicated that the relative improvement in performance between the M.V. ARCTIC and the new bow "B" was approximately 30%.

d) The broken ice testing was inconclusive because of the inconsistent nature of the data collected. Clearly, based on the ACL tests, before meaningful broken ice tests can be conducted, more work must be done to simulate the ice regime.

e) The rubble field ramming tests indicated that the relative improvement over the existing bow for rubble field transit is 19% for Bow C and 9% for Bow B. It should be noted however, that these figures represent one test.

f) The ice test results generally produced fair correlation at full power with the full scale results obtained during the Lake Melville test program. This applies to both the level ice and broken ice tests.

g) Below the full power setting, the correlation between model test results and full scale performance was found to be very poor. This is thought to be as a result of the model representation of friction and is the subject of a recommendation later in this section.

h) The use of a middle divider in the Arctec Canada Ltd. model basin to allow two separate runs to be made with one ice sheet was shown to produce problems. These problems relate to the tendency for cracking of the ice to occur towards the middle barrier, and to the unevenness of ice thickness which occurs across the width of the tank, particularly close to one side.

i) The ununiformity of ice thickness and strength along and across the model tank and the subsequent "normalization" of this data gave reason for concern as to the accuracy of the final predictions. This concern is somewhat mitigated by the full scale predictions at full power resembling so closely the full scale results from Lake Melville.

j) Insufficient knowledge is available as to the effect of these inaccuracies upon full scale predicted resistance, particularly as a function of bow shape. It not known whether the major differences in bow shape between the new bows and the M.V. ARCTIC affects the reliability of full scale predictions made from the model test results. It is therefore impossible to speculate as to how the nonuniformity of ice strength and thickness exhibited during the test program, and the subsequent treatment ot these differences, has impacted upon the test results.

7.1.4 Transit Analysis

a) Compared to the M.V. ARCTIC, the best of the new bows showed a significant improvement in performance during the early and late parts of the existing shipping season. During the middle months of the season, due to the presence of extensive open water areas, very little difference is noted.

b) The new bow extends the existing season (June to November) to May to December.

Generally, the design and testing process can be considered to be a success. A substantial improvement in ship performance has been achieved by redesigning the existing bow to more effectively break level ice. This has been achieved with no detriment to the calm open water performance of the ship, resulting in a significant extension to the Arctic shipping season.

7.2 Recommendations

The performance of this program of work has resulted in the development of several recommendations. These are indicated below.

a) Although the use of prediction equations, sensitive to ship shape, has been found useful as a design tool, the reliability of these equations is suspect. A program of work is required to analyse the acceptability of existing prediction equations for a range of ship types. Sensitivity to all major hull form variables should be considered and full scale correlation determined where possible.

b) Although the 30% benefit achieved by the new bow over the existing ship is impressive, this is not considered to be optimum. The limited financial resources available to this project placed constraints upon the extent of design refinements. Similarly, the

need for this design to be suitable for application to M.V. ARCTIC placed a limitation upon the benefits which may be gained by appropriate design. A program should be mounted to determine the "optimum" shape for a commercial vessel which operates for prolonged periods both in ice and in open water.

c) The model test results from this program have been shown to be incorrect below the full power range. Very poor correlation exists between these lower power model test results and those obtained during full scale tests. The reasons for this poor correlation should be determined, most likely by use of model testing, and preferably in a manner which would benefit the whole model test community. This problem, to a greater or lesser extent, has been found to be common throughout the major ice model basins and is a subject of great interest. International support would probably be found for a program to improve the model test result correlation with full scale throughout the speed range.

REFERENCES

1.1 Melville Shipping Ltd., "Redesign of the M.V. ARCTIC Bow - Additional Model Tests at H.S.V.A. and W.A.R.C.", Report No. TP 5812E, Report for the Transportation Development Centre.

2.1 Melville Shipping Ltd., "M.V. ARCTIC Northern Routing Environment", Final Report to Canarctic Shipping Company Limited, 1982.

2.2 Ochi, M.K., "Prediction of Extreme Ship Responses in Rough Seas of the North Atlantic"

3.1 Kashteljan, V.I., "Methods of Estimating the Ice Navigating Capabilities of a Ship in Solid Ice", Draft translation 417 by U.S. Joint Publications Research Service for U.S. Cold Regions Research Laboratory, 1973 from Arktícheskii I, Antarktícheskii Navchno Issledovatel's Institut, Trudy 309, 1973.

3.2 Enkvist, E., "On the Ice Resistance Encountered by Ships Operating in the Continuous Mode of Ice Breaking", Swedish Academy of Engineering in Finland, Report No. 24, UDC 629.124.75:532.58, 1972.

3.3 White, R.M., Commander, "Prediction of Ice Breaker Capability", Royal Institute of Naval Architects, 1961.

3.4 Milano, V.R., "Ship Resistance to Continuous Motion in Ice", The Society of Naval Architects and Marine Engineers, Annual Meeting, New York, 1973.

3.5 Milano, V.R., "A Re-Analysis of Ship Resistance When in Continuous Motion Through Solid Ice"

3.6 Melville Shipping Ltd., "M.V. ARCTIC Experimental Voyage to Lake Melville, Labrador, in February/March, 1981", Report No. Tp 3646E, Report for Transportation Development Centre, 1981.

3.7 Poznyak, I.I., "The Division of Icebreaker Resistance into Components", Society of Naval Architects and Marine Engineers, Star Symposium, Ottawa, June, 1981.

3.8 Johansson, B.M., Makinen, "Icebreaking Model Tests: Systematic Variation of Bow Lines and Main Dimensions of Hull Forms Suitable for Great Lakes" Society of Naval Architects and Marine Engineers, Great Lakes and Rivers Section, 1973.

3.9 Vance, G.P., "The Analysis of Model Testing in Three Different Test Basins", U.S. Army Cold Regions Research and Engineering Laboratory, 1978.

3.10 Enkvist, E., "A Survey of the Submersion and Breaking Components of Level Ice Resistance to Ships", The Seventh International Conference in Port and Ocean Engineering Under Arctic Conditions, Volume I, Helsinki, 1983.

3.11 Edwards, R.Y., Nawwar, A.M., "Compilation and Analysis of Recent Icebreaking Model Test Data of a World Wide Variety of Hull Forms", Report No. TP 1294, Report to Transportation Development Centre,, 1978.

3.12 Vance, G.P., "A Scaling System for Vessels Modelled in Ice", The Society of Naval Architects and Marine Engineers, Ice Tech Symposium, Montreal, April, 1975.

3.13 Edwards, R.Y., "Comparative Model Tests of the Icebreaker Performance of Two Canadian Coast Guard Icebreakers", Second International Conference on Port and Ocean Engineering Under Arctic Conditions, 1974.

4.1 Molyneux, W.D., "M.V. ARCTIC and Two Alternative Bow Designs Results of Resistance Propulsion and Overload Experiments with Model Hulls 326-A, 326-B and 326-C and Model Propeller 68", Report for the Transportation Development Centre by the National Research Council, May 1983.

4.2 Howard, D., Steele, M., Glen, I.F., "M.V. ARCTIC Bow Study", Report By Arctec Canada Ltd., Report to Melville Shipping Ltd., 1983.

4.3 Neagle, J.N., "Ice Resistance Prediction and Motion Simulation for Ships Operating in the Continuous Mode of Icebreaking", Ph.d thesis, University of Michigan, 1980.

4.4 Lewis, J.W., et al, "A Semi-Empirical Ice Resistance Model", Report to the Transportation Development Centre, April, 1983.

5.1 Calabrese, S.J., et al, "Low Friction Coatings for Icebreakers", Report to the U.S. Coast Guard, Project No. CG-D-107-74, 1974.

PERIOD - MID JULY; NORTH OR SOUTH BOUND

	DAVIS STRAIT	BAFFIN BAY	LANCASTER SOUND TO NANISIVIK	LANCASTER SOUND TO POLARIS	ADMIRALTY INLET	BARROW STRAIT + McDOUGALL SOUND	TOTAL
LENGTH - km OPEN WATER	1300	750	140	300	-	-	2190-N 2350-P
VERY OPEN PACK	-	150	-	-	-	-	150
OPEN PACK	SOME STORIS	200	-	-	-	-	200
CLOSE PACK	-	-	-	130	-	-	130-P
VERY CLOSE PACK	-	-	-	-	-	45	45-P
CONSOLIDATED	-	-	-	-	100*	135	100-N 135-P
OLD ICE[1]	-	-	-	-	-	-	-
ICE THICKNESS m	-	-	-	1.2-1.5	1.2-1.5	1.5-1.75	**
FLEXURAL STRENGTH kPa[2]	-	-	-	200-300	200-300	300-400	**
COMPRESSIVE STRENGTH MPa[3]	-	-	-	10	6	15	**

1. LENGTH CALCULATED BY X MEDIAN AMOUNT OF OLD ICE BY ROUTE LENGTH IN THAT AREA - NO MANEOUVRING ACCOUNTED FOR.
2. MEAN FLEXURAL STRENGTH USING BEAM TEST (ESTIMATED).
3. MEAN MAXIMUM CONFINED COMPRESSIVE STRENGTH USING FENCO BORE JACK (ESTIMATED).

* ASSUMING NO PREVIOUS VOYAGE, BROKEN CHANNEL OTHERWISE.

N = NANISIVIK P = POLARIS

Median Ice Conditions
Table 3

PERIOD - MID AUGUST, NORTH OR SOUTH BOUND

	DAVIS STRAIT	BAFFIN BAY	LANCASTER SOUND TO NANISIVIK	LANCASTER SOUND TO POLARIS	ADMIRALTY INLET	BARROW STRAIT + McDOUGALL SOUND	TOTAL
LENGTH - km OPEN WATER	1200	1100	140	430	100	-	2540-N 2400-P
VERY OPEN PACK	-	-	-	-	-		-
OPEN PACK	-	-	-	-	-	-	-
CLOSE PACK	-	-	-	-	-	45	45-P
VERY CLOSE PACK	-	-	-	-	-	135	135-P
CONSOLIDATED	-	-	-	-	-	-	-
OLD ICE[1]	-	-	-	-	-	-	-
ICE THICKNESS m	-	-	-	-	-	1.0-1.2	**
FLEXURAL STRENGTH kPa[2]	-	-	-	-	-	200-300	**
COMPRESSIVE STRENGTH MPa[3]	-	-	-	-	-	6	**

1. LENGTH CALCULATED BY X MEDIAN AMOUNT OF OLD ICE BY ROUTE LENGTH IN THAT AREA - NO MANEOUVRING ACCOUNTED FOR.
2. MEAN FLEXURAL STRENGTH USING BEAM TEST (ESTIMATED).
3. MEAN MAXIMUM CONFINED COMPRESSIVE STRENGTH USING FENCO BORE JACK (ESTIMATED).

N - NANISIVIK P - POLARIS

Median Ice Conditions
Table 4

PERIOD - MID SEPTEMBER; NORTH BOUND

	DAVIS STRAIT	BAFFIN BAY	LANCASTER SOUND SOUND		ADMIRALTY INLET	BARROW STRAIT + McDOUGALL SOUND	TOTAL
			TO NANISIVIK	TO POLARIS			
LENGTH - km OPEN WATER	1200	920	140	420	100	160	2360-N 2700-P
VERY OPEN PACK	-	-	-	-	-	-	-
OPEN PACK	-	-	-	-	-	-	-
CLOSE PACK	-	-	-	-	-	-	-
VERY CLOSE PACK	-	-	-	-	-	-	-
CONSOLIDATED	-	-	-	-	-	-	-
OLD ICE[1]	-	-	-	-	-	12	-
ICE THICKNESS m	-	-	-	-	-	-	X
FLEXURAL STRENGTH kPa[2]	-	-	-	-	-	-	X
COMPRESSIVE STRENGTH MPa[3]	-	-	-	-	-	-	X

1. LENGTH CALCULATED BY X MEDIAN AMOUNT OF OLD ICE BY ROUTE LENGTH IN THAT AREA - NO MANEOUVRING ACCOUNTED FOR.
2. MEAN FLEXURAL STRENGTH USING BEAM TEST (ESTIMATED).
3. MEAN MAXIMUM CONFINED COMPRESSIVE STRENGTH USING FENCO BORE JACK (ESTIMATED).

N = NANISIVIK P = POLARIS

Median Ice Conditions
Table 5

PERIOD - MID SEPTEMBER; SOUTH BOUND

	DAVIS STRAIT	BAFFIN BAY	LANCASTER SOUND SOUND		ADMIRALTY INLET	BARROW STRAIT + McDOUGALL SOUND	TOTAL
			TO NANISIVIK	TO POLARIS			
LENGTH - km OPEN WATER	1350	670	140	420	100	160	2260-N 2600-P
VERY OPEN PACK	-	-	-	-	-	-	-
OPEN PACK	-	-	-	-	-	-	-
CLOSE PACK	-	-	-	-	-	-	-
VERY CLOSE PACK	-	-	-	-	-	-	-
CONSOLIDATED	-	-	-	-	-	-	-
OLD ICE[1]	-	-	-	-	-	12	-
ICE THICKNESS m	-	-	-	-	-	-	X
FLEXURAL STRENGTH kPa[2]	-	-	-	-	-	-	X
COMPRESSIVE STRENGTH MPa[3]	-	-	-	-	-	-	X

1. LENGTH CALCULATED BY X MEDIAN AMOUNT OF OLD ICE BY ROUTE LENGTH IN THAT AREA - NO MANEOUVRING ACCOUNTED FOR.
2. MEAN FLEXURAL STRENGTH USING BEAM TEST (ESTIMATED).
3. MEAN MAXIMUM CONFINED COMPRESSIVE STRENGTH USING FENCO BORE JACK (ESTIMATED).

N = NANISIVIK P = POLARIS

Median Ice Conditions
Table 6

APPENDIX 1

SUMMARY OF CANADIAN ARCTIC ENVIRONMENTAL CRITERIA

These tables give mid-month median environmental values for a typical voyage route of the M.V. ARCTIC transiting from Europe to Nanisivik or Polaris. The tables are self-explanatory. Additional information on the areas can be found in the report "M.V. ARCTIC Northern Routing Environment" (Ref. 1.1).

PERIOD - MID MAY; NORTH AND SOUTH BOUND

	DAVIS STRAIT	BAFFIN BAY	LANCASTER SOUND SOUND TO NANISIVIK	LANCASTER SOUND SOUND TO POLARIS	ADMIRALTY INLET	BARROW STRAIT + McDOUGALL SOUND	TOTAL
LENGTH - km OPEN WATER	1175	-	-	-	-	-	1175
VERY OPEN PACK	-	-	-	-	-	-	-
OPEN PACK	SOME STORIS	-	-	-	-	-	-
CLOSE PACK	-	-	-	-	-		-
VERY CLOSE PACK	-	1200	150	270	-	-	1350-N 1470-P
CONSOLIDATED	-	-	-	150	100	160	100-N 310-P
OLD ICE[1]	-	-	-	-	-	-	-
ICE THICKNESS m	-	1.3-1.6	1.8-2.0	1.8-2.0	1.75-2.0	2.0-2.2	••
FLEXURAL STRENGTH kPa[2]	-	450-500	500	500	500	550	••
COMPRESSIVE STRENGTH MPa[3]	-	10-15	17.5-20.0	17.5-20.0	17.5-20.0	20	••

1. LENGTH CALCULATED BY X MEDIAN AMOUNT OF OLD ICE BY ROUTE LENGTH IN THAT AREA - NO MANEOUVRING ACCOUNTED FOR.
2. MEAN FLEXURAL STRENGTH USING BEAM TEST (ESTIMATED).
3. MEAN MAXIMUM CONFINED COMPRESSIVE STRENGTH USING FENCO BORE JACK (ESTIMATED).

N = NANISIVIK P = POLARIS

Median Ice Conditions
Table 1

PERIOD - MID JUNE: NORTH AND SOUTH BOUND

	DAVIS STRAIT	BAFFIN BAY	LANCASTER SOUND SOUND TO NANISIVIK	LANCASTER SOUND SOUND TO POLARIS	ADMIRALTY INLET	BARROW STRAIT + McDOUGALL SOUND	TOTAL
LENGTH - km OPEN WATER	1200	500	70	X	-	X	1770
VERY OPEN PACK	-	-	70	X	-	X	70
OPEN PACK	SOME STORIS	60	-	X	-	X	60
CLOSE PACK	-	340	-	X	-	X	340
VERY CLOSE PACK	-	300	-	X	-	X	300
CONSOLIDATED	-	-	-	X	100	X	100
OLD ICE[1]	-	-	-	-	-	X	X
ICE THICKNESS m	-	0.7-1.0	0.75	X	1.75-2.0	X	••
FLEXURAL STRENGTH kPa[2]	-	350	-	X	450	X	••
COMPRESSIVE STRENGTH MPa[3]	-	6	-	X	13	X	••

1. LENGTH CALCULATED BY X MEDIAN AMOUNT OF OLD ICE BY ROUTE LENGTH IN THAT AREA - NO MANEOUVRING ACCOUNTED FOR.
2. MEAN FLEXURAL STRENGTH USING BEAM TEST (ESTIMATED).
3. MEAN MAXIMUM CONFINED COMPRESSIVE STRENGTH USING FENCO BORE JACK (ESTIMATED).

N - NANISIVIK P - POLARIS

Median Ice Conditions
Table 2

PERIOD - MID OCTOBER, NORTH BOUND

	DAVIS STRAIT	BAFFIN BAY	LANCASTER SOUND SOUND		ADMIRALTY INLET	BARROW STRAIT + McDOUGALL SOUND	TOTAL
			TO NANISIVIK	TO POLARIS			
LENGTH - km OPEN WATER	1200	700	-	-	-	-	1900
VERY OPEN PACK	-	45	-	-	-	-	45
OPEN PACK	-	45	-	-	-	-	45
CLOSE PACK	-	-	-	-	-	-	-
VERY CLOSE PACK	-	260	65	420	120	160	445-N 840-P
CONSOLIDATED	-	-	-	-	-	-	-
OLD ICE[1]	-	-	-	-	-	12	-
ICE THICKNESS m	-	.2	.2*	.2*	.1	.15	X
FLEXURAL STRENGTH kPa[2]	-	VERY WEAK	VERY WEAK	VERY WEAK	VERY WEAK	VERY WEAK	X
COMPRESSIVE STRENGTH MPa[3]	-	VERY WEAK	VERY WEAK	VERY WEAK	VERY WEAK	VERY WEAK	X

1. LENGTH CALCULATED BY X MEDIAN AMOUNT OF OLD ICE BY ROUTE LENGTH IN THAT AREA - NO MANEOUVRING ACCOUNTED FOR.
2. MEAN FLEXURAL STRENGTH USING BEAM TEST (ESTIMATED).
3. MEAN MAXIMUM CONFINED COMPRESSIVE STRENGTH USING FENCO BORE JACK (ESTIMATED).

* SOME OLD ICE, LOW STRENGTH.

N = NANISIVIK P = POLARIS

Median Ice Conditions
Table 7

PERIOD - MID OCTOBER, SOUTH BOUND

	DAVIS STRAIT	BAFFIN BAY	LANCASTER SOUND SOUND		ADMIRALTY INLET	BARROW STRAIT + McDOUGALL SOUND	TOTAL
			TO NANISIVIK	TO POLARIS			
LENGTH - km OPEN WATER	1350	450	-	-	-	-	1800
VERY OPEN PACK	-	45	-	-	-	-	45
OPEN PACK	-	45	-	-	-	-	45
CLOSE PACK	-	-	-	-	-	-	-
VERY CLOSE PACK	-	260	65	420	120	160	445-N 840-P
CONSOLIDATED	-	-	-	-	-	-	-
OLD ICE[1]	-	-	-	-	-	12	-
ICE THICKNESS m	-	.2	.2*	.2*	.1	.15	X
FLEXURAL STRENGTH kPa[2]	-	VERY WEAK	VERY WEAK	VERY WEAK	VERY WEAK	VERY WEAK	X
COMPRESSIVE STRENGTH MPa[3]	-	VERY WEAK	VERY WEAK	VERY WEAK	VERY WEAK	VERY WEAK	X

1. LENGTH CALCULATED BY X MEDIAN AMOUNT OF OLD ICE BY ROUTE LENGTH IN THAT AREA - NO MANEOUVRING ACCOUNTED FOR.
2. MEAN FLEXURAL STRENGTH USING BEAM TEST (ESTIMATED).
3. MEAN MAXIMUM CONFINED COMPRESSIVE STRENGTH USING FENCO BORE JACK (ESTIMATED).

* SOME OLD ICE, LOW STRENGTH.

N = NANISIVIK P = POLARIS

Median Ice Conditions
Table 8

PERIOD - MID NOVEMBER, NORTH BOUND

	DAVIS STRAIT	BAFFIN BAY	LANCASTER SOUND SOUND		ADMIRALTY INLET	BARROW STRAIT +	TOTAL
			TO NANISIVIK	TO POLARIS		McDOUGALL SOUND	
LENGTH - km OPEN WATER	1250	-	-	-	-	-	1250
VERY OPEN PACK	-	100	-	-	-	-	100
OPEN PACK	-	-	-	-	-	-	-
CLOSE PACK	-	850	-	-	-	-	850
VERY CLOSE PACK	-	-	160	420	-	100	160-N 520-P
CONSOLIDATED	-	-	-	-	100	60	100-N 60-P
OLD ICE[1]	-	26	-	-	-	-	-
ICE THICKNESS m	-	.2-.4	.5	.5	.3	.5-.6	X
FLEXURAL STRENGTH kPa[2]	-	WEAK	300-400	300-400	400	400	X
COMPRESSIVE STRENGTH MPa[3]	-	WEAK	18*	18*	5-10	10	X

1. LENGTH CALCULATED BY X MEDIAN AMOUNT OF OLD ICE BY ROUTE LENGTH IN THAT AREA - NO MANEOUVRING ACCOUNTED FOR.
2. MEAN FLEXURAL STRENGTH USING BEAM TEST (ESTIMATED).
3. MEAN MAXIMUM CONFINED COMPRESSIVE STRENGTH USING FENCO BORE JACK (ESTIMATED).

* OLD ICE PRESENT, PARTICULARLY AT ENTRANCE TO LANCASTER SOUND.

N = NANISIVIK P = POLARIS

Median Ice Conditions
Table 9

PERIOD - MID NOVEMBER; SOUTH BOUND

	DAVIS STRAIT	BAFFIN BAY	LANCASTER SOUND SOUND		ADMIRALTY INLET	BARROW STRAIT +	TOTAL
			TO NANISIVIK	TO POLARIS		McDOUGALL SOUND	
LENGTH - km OPEN WATER	1100	-	-	-	-	-	1100
VERY OPEN PACK	130	-	-	-	-	-	130
OPEN PACK	-	-	-	-	-	-	-
CLOSE PACK	130	800	-	-	-	-	930
VERY CLOSE PACK	-	-	160	420	-	100	160-N 520-P
CONSOLIDATED	-	-	-	-	100	60	100-N 60-P
OLD ICE[1]	-	26	-	-	-	-	-
ICE THICKNESS m	.1	.2-.4	.5	.5	.3	.5-.6	X
FLEXURAL STRENGTH kPa[2]	VERY WEAK	WEAK	300-400	300-400	400	400	X
COMPRESSIVE STRENGTH MPa[3]	VERY WEAK	WEAK	18*	18*	5-10	10	X

1. LENGTH CALCULATED BY X MEDIAN AMOUNT OF OLD ICE BY ROUTE LENGTH IN THAT AREA - NO MANEOUVRING ACCOUNTED FOR.
2. MEAN FLEXURAL STRENGTH USING BEAM TEST (ESTIMATED).
3. MEAN MAXIMUM CONFINED COMPRESSIVE STRENGTH USING FENCO BORE JACK (ESTIMATED).

* OLD ICE PRESENT, PARTICULARLY AT ENTRANCE TO LANCASTER SOUND.

N = NANISIVIK P = POLARIS

Median Ice Conditions
Table 10

PERIOD - MID DECEMBER; NORTH BOUND

	DAVIS STRAIT	BAFFIN BAY	LANCASTER SOUND SOUND		ADMIRALTY INLET	BARROW STRAIT +	TOTAL
			TO NANISIVIK	TO POLARIS		McDOUGALL SOUND	
LENGTH - km OPEN WATER	740	-	-	-	-	-	740
VERY OPEN PACK	150	-	-	-	-	-	150
OPEN PACK	280	500	-	-	-	-	780
CLOSE PACK	-	460	-	-	-	-	460
VERY CLOSE PACK	-	-	160	420	-	100	160-N 520-P
CONSOLIDATED	-	-	-	-	100**	60	100-N 60-P
OLD ICE[1]	-	-	-	-	-	-	-
ICE THICKNESS m	-	.75	0.8-0.9	0.8-0.9	0.65	0.9	X
FLEXURAL STRENGTH kPa[2]	-	300-400	450-550	450-550	450-550	550	X
COMPRESSIVE STRENGTH MPa[3]	-	12.5-15	15*	15*	15	15-17.5	X

1. LENGTH CALCULATED BY X MEDIAN AMOUNT OF OLD ICE BY ROUTE LENGTH IN THAT AREA - NO MANEOUVRING ACCOUNTED FOR.
2. MEAN FLEXURAL STRENGTH USING BEAM TEST (ESTIMATED).
3. MEAN MAXIMUM CONFINED COMPRESSIVE STRENGTH USING FENCO BORE JACK (ESTIMATED).

* OLD ICE PRESENT, PARTICULARLY AT ENTRANCE TO LANCASTER SOUND.

** REFROZEN CHANNEL IF USED IN MID NOVEMBER.

N = NANISIVIK P = POLARIS

Median Ice Conditions
Table 11

PERIOD - MID DECEMBER, SOUTH BOUND

	DAVIS STRAIT	BAFFIN BAY	LANCASTER SOUND SOUND		ADMIRALTY INLET	BARROW STRAIT +	TOTAL
			TO NANISIVIK	TO POLARIS		McDOUGALL SOUND	
LENGTH - km OPEN WATER	725	-	-	-	-	-	725
VERY OPEN PACK	130	-	-	-	-	-	130
OPEN PACK	-	-	-	-	-	-	-
CLOSE PACK	385	410	-	-	-	-	795
VERY CLOSE PACK	-	400	160	420	-	100	560-N 920-P
CONSOLIDATED	-	-	-	-	100**	60	100-N 60-P
OLD ICE[1]	-	-	-	-	-	-	-
ICE THICKNESS m	.5	.75	0.8-0.9	0.8-0.9	0.65	0.9	X
FLEXURAL STRENGTH kPa[2]	90-350	300-400	450-550	450-550	450-550	550	X
COMPRESSIVE STRENGTH MPa[3]	12.5	12.5-15	15*	15*	15	15-17.5	X

1. LENGTH CALCULATED BY X MEDIAN AMOUNT OF OLD ICE BY ROUTE LENGTH IN THAT AREA - NO MANEOUVRING ACCOUNTED FOR.
2. MEAN FLEXURAL STRENGTH USING BEAM TEST (ESTIMATED).
3. MEAN MAXIMUM CONFINED COMPRESSIVE STRENGTH USING FENCO BORE JACK (ESTIMATED).

* OLD ICE PRESENT, PARTICULARLY AT ENTRANCE TO LANCASTER SOUND.

** REFROZEN CHANNEL IF USED IN MID NOVEMBER.

N = NANISIVIK P = POLARIS

Median Ice Conditions
Table 12

APPENDIX 2

LINES PLANS AND BODY PLANS OF THE M.V. ARCTIC AND MODIFIED BOW FORMS

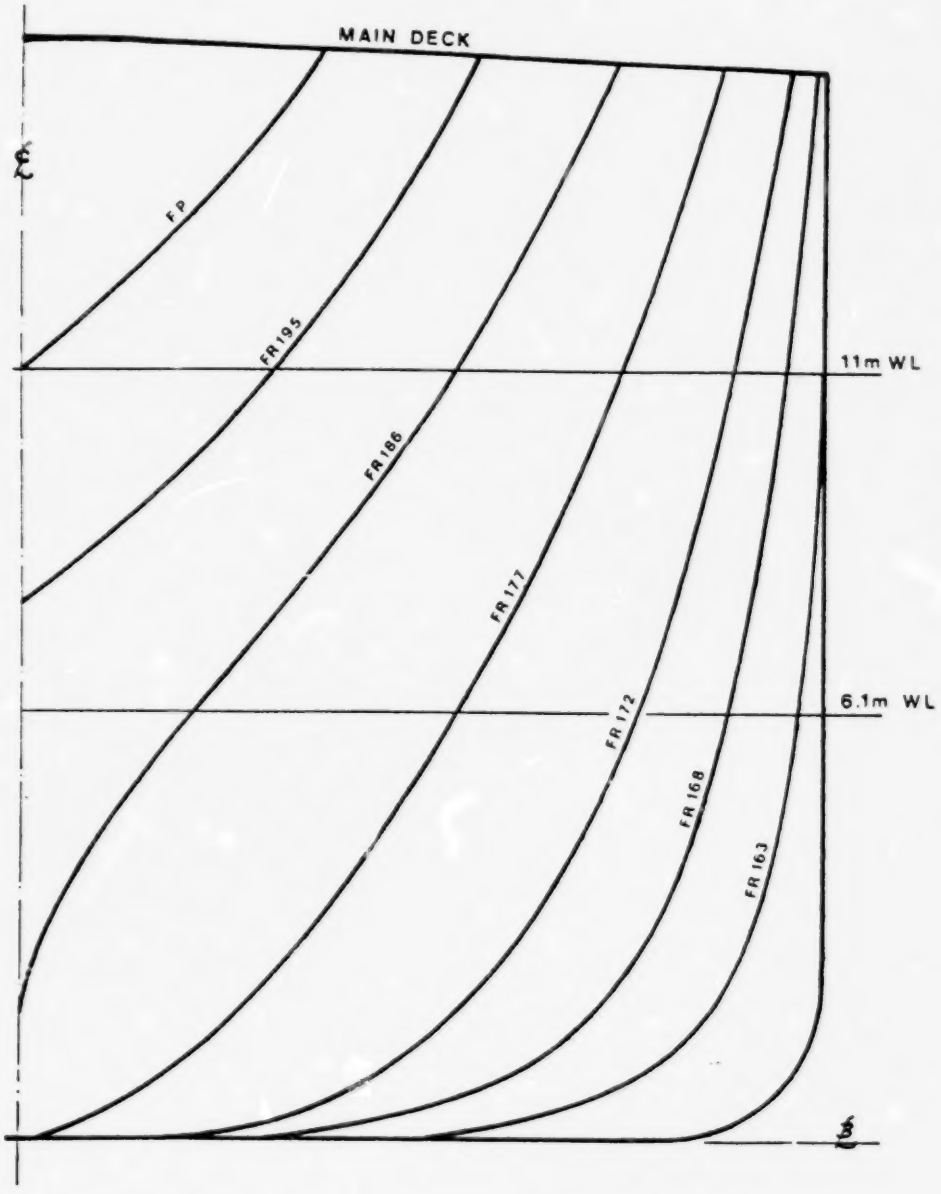

M.V. ARCTIC - EXISTING BOW
CASE 1 - BODY PLAN

FIGURE 1

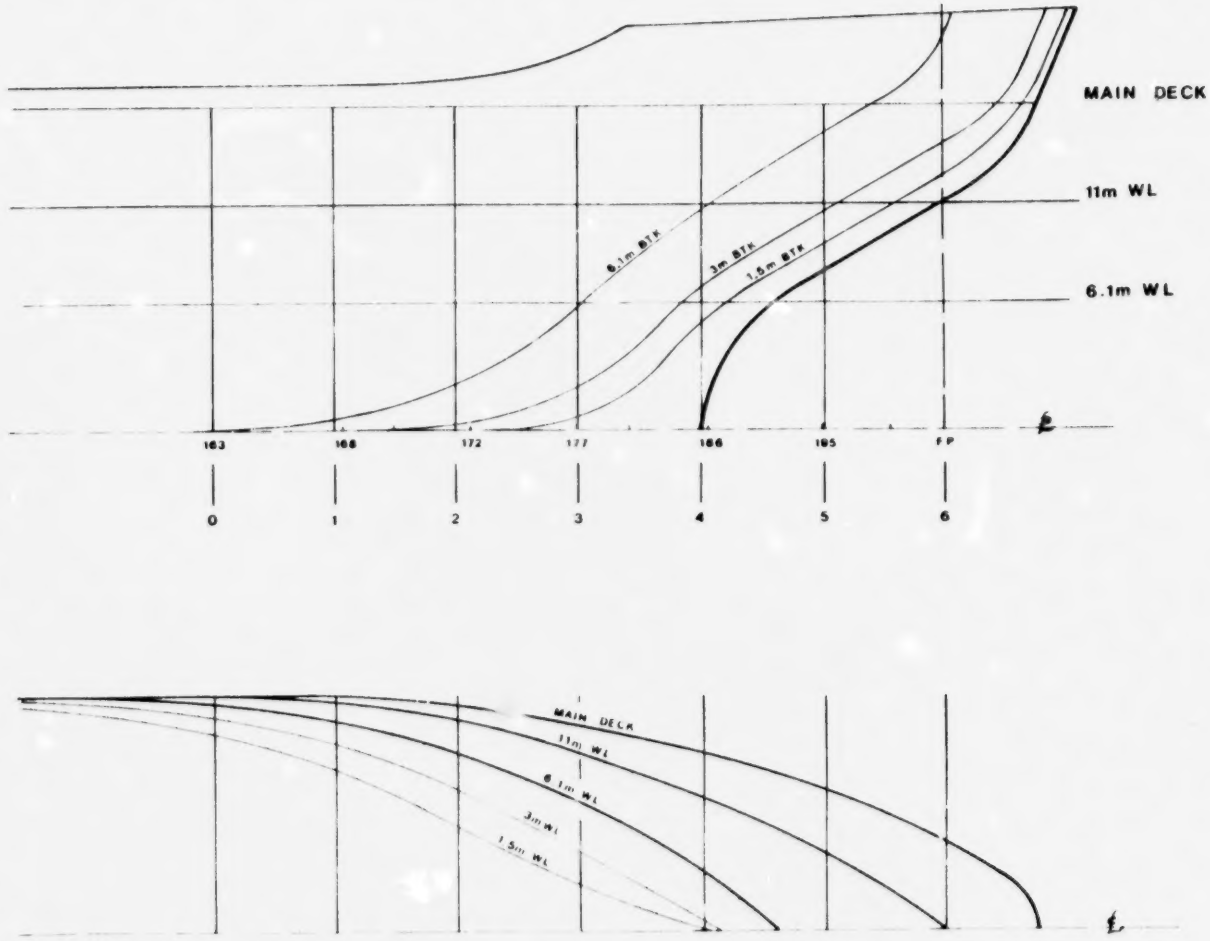

M.V. ARCTIC - EXISTING BOW - CASE 1 - LINES PLAN

FIGURE 2

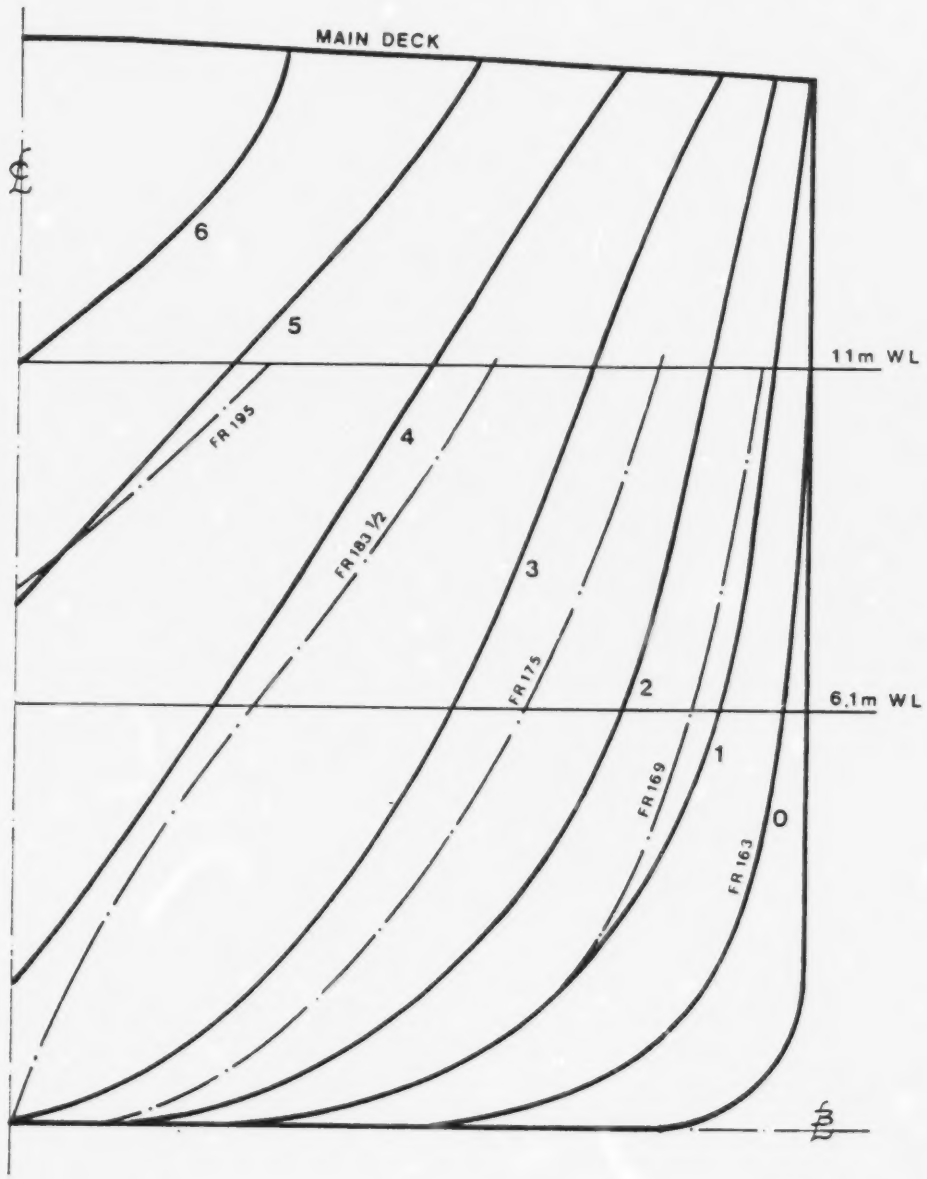

M.V. ARCTIC - MODIFIED BOW
CASE 2 - BODY PLAN

FIGURE 3

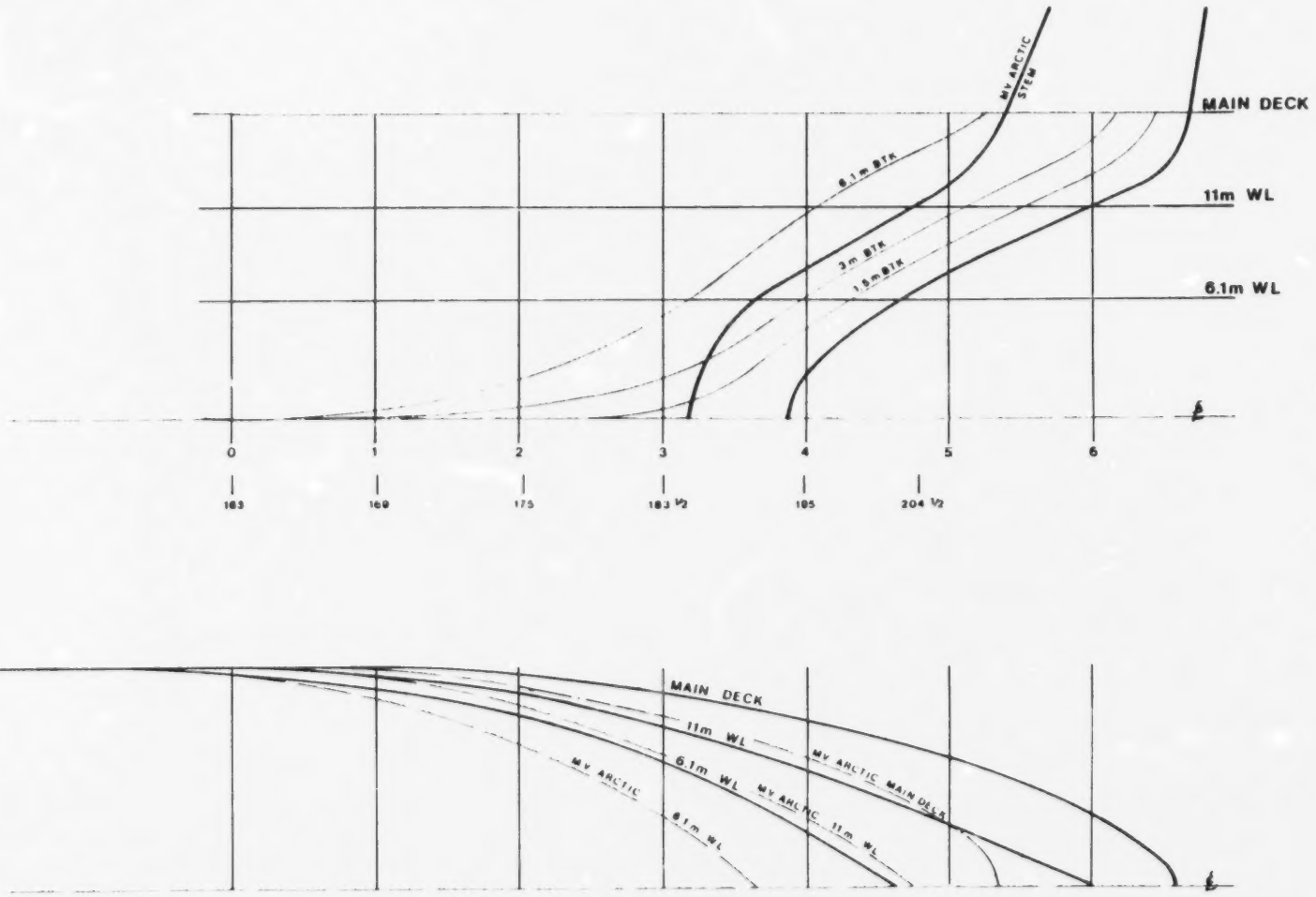

M.V. ARCTIC - MODIFIED BOW - CASE 2 - LINES PLAN

FIGURE 4

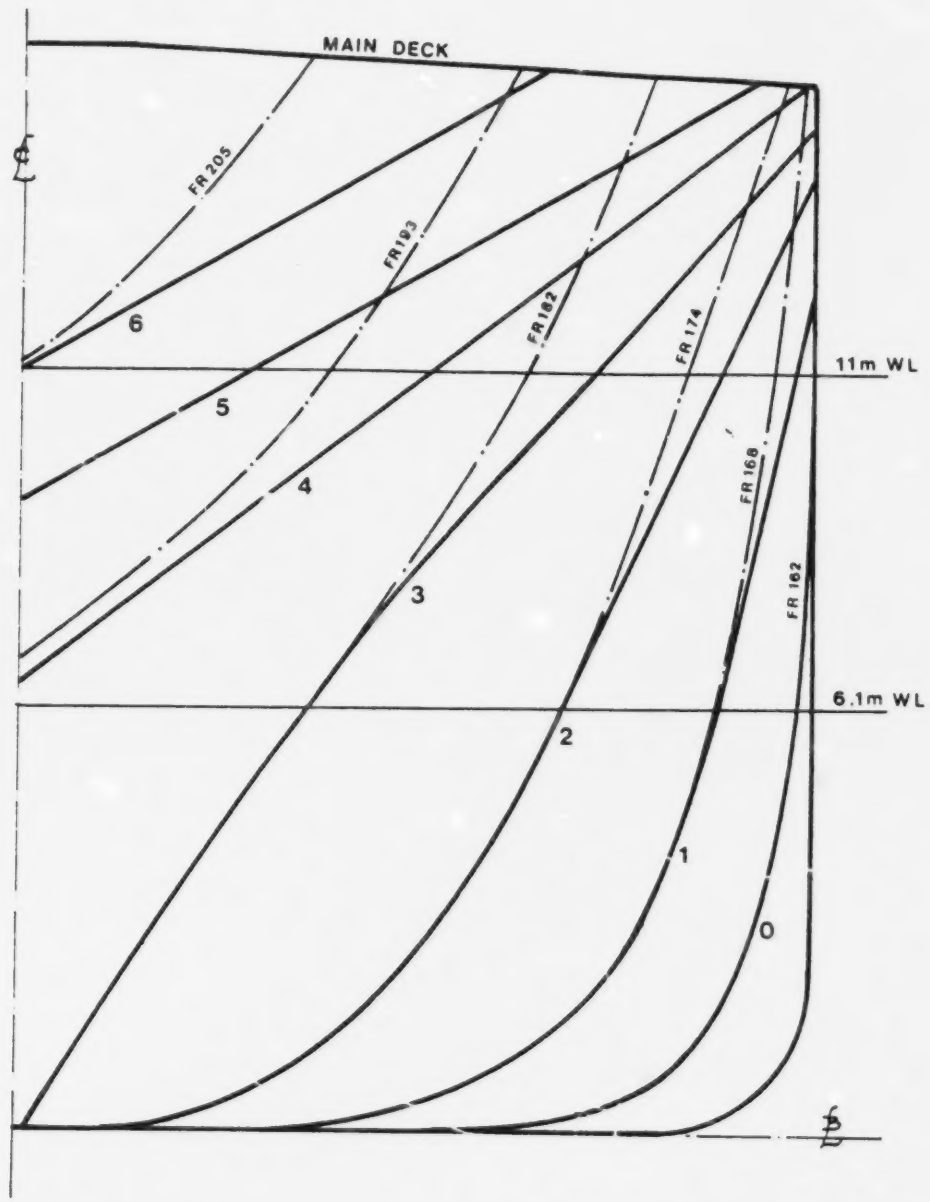

M.V. ARCTIC - MODIFIED BOW
CASE 3 - BODY PLAN

FIGURE 5

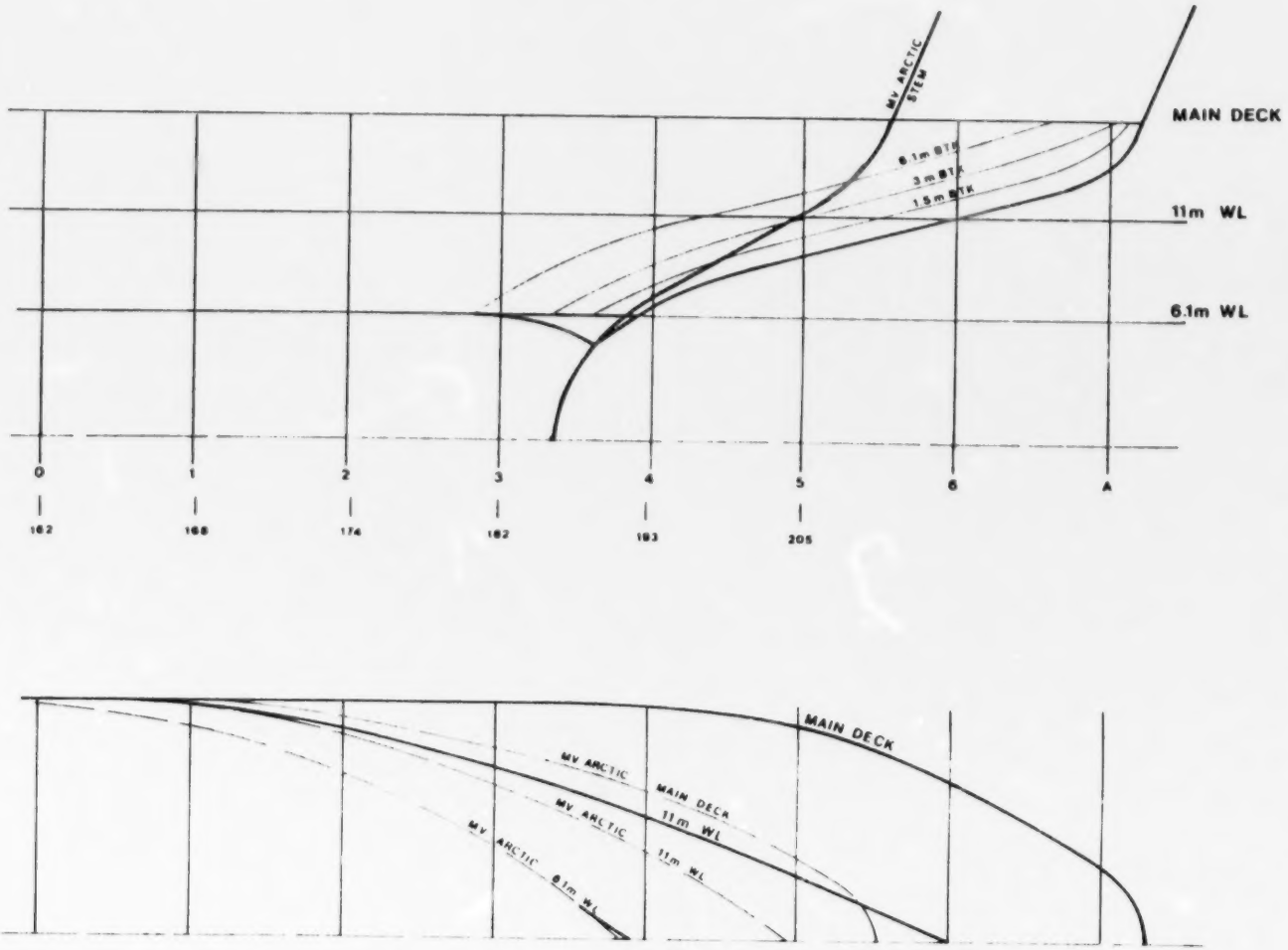

M.V. ARCTIC - MODIFIED BOW - CASE 3 - LINES PLAN

FIGURE 6

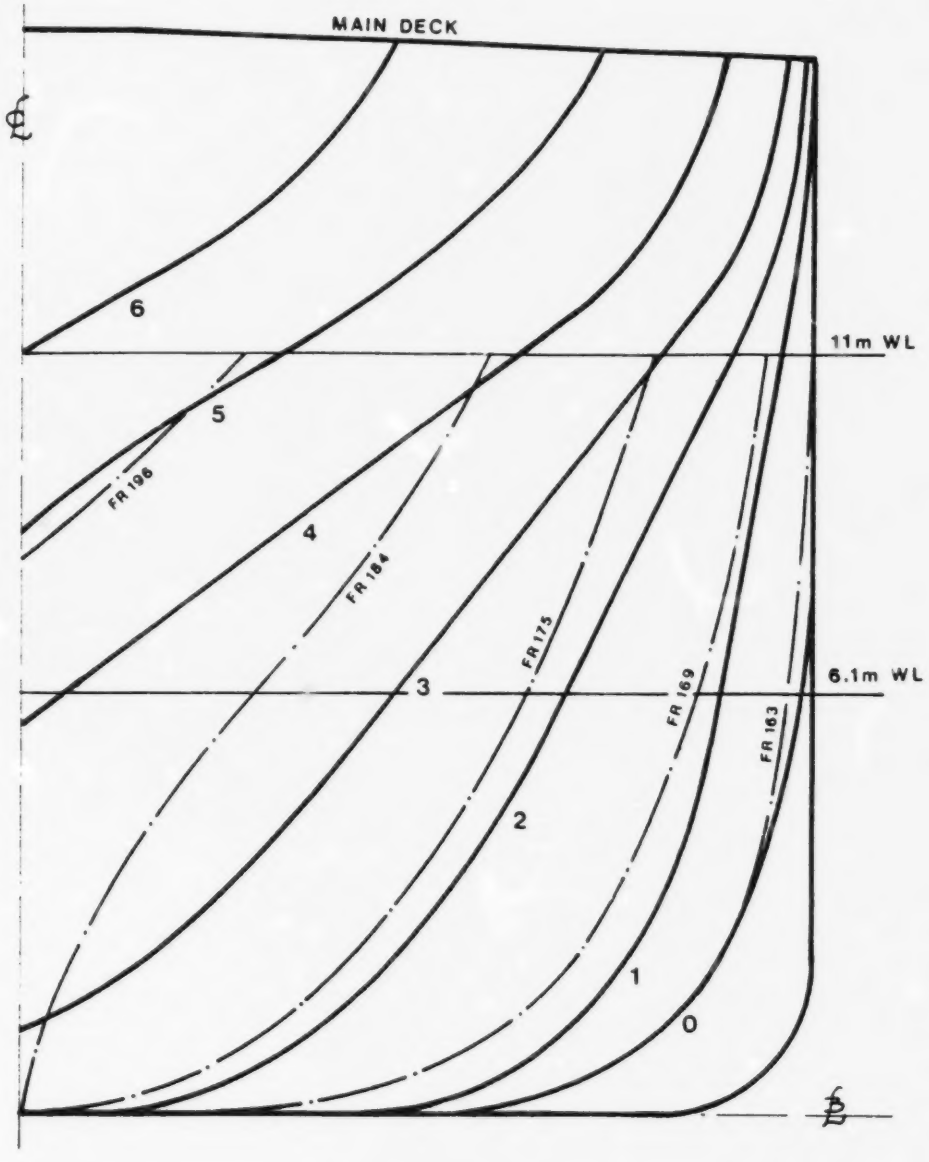

M.V. ARCTIC - MODIFIED BOW
CASE 4 - BODY PLAN

FIGURE 7

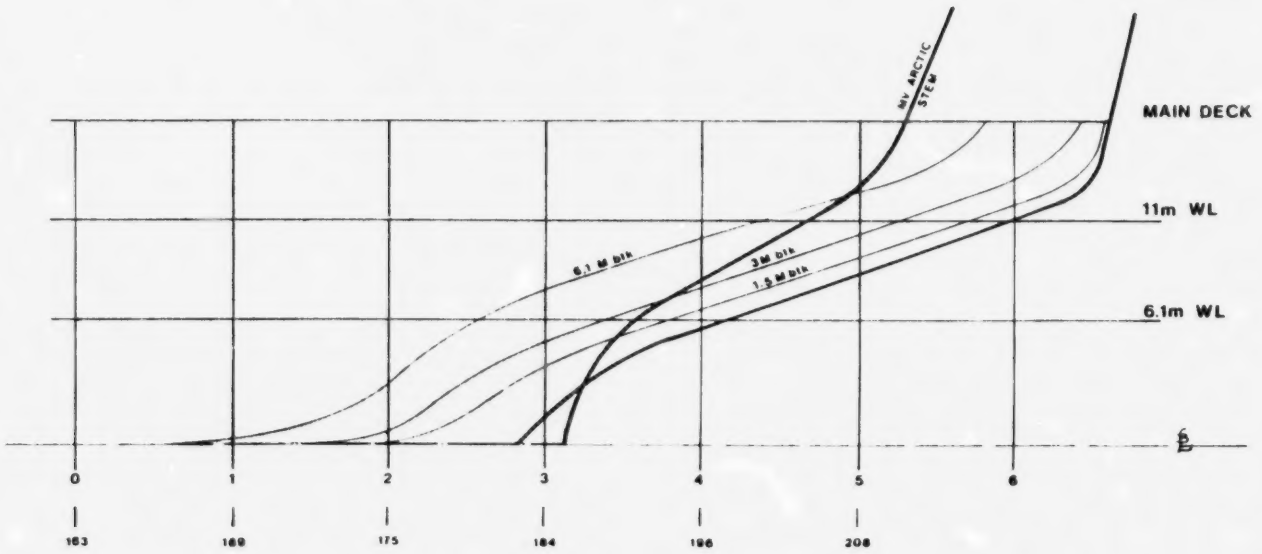

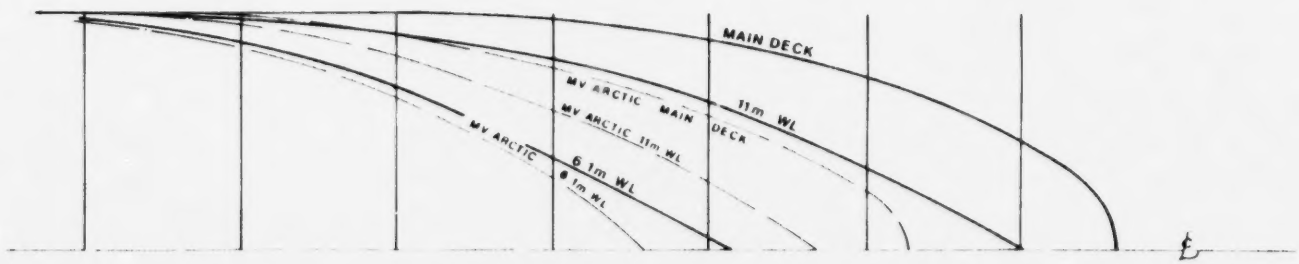

M.V. ARCTIC - MODIFIED BOW - CASE 4 - LINES PLAN

FIGURE 8

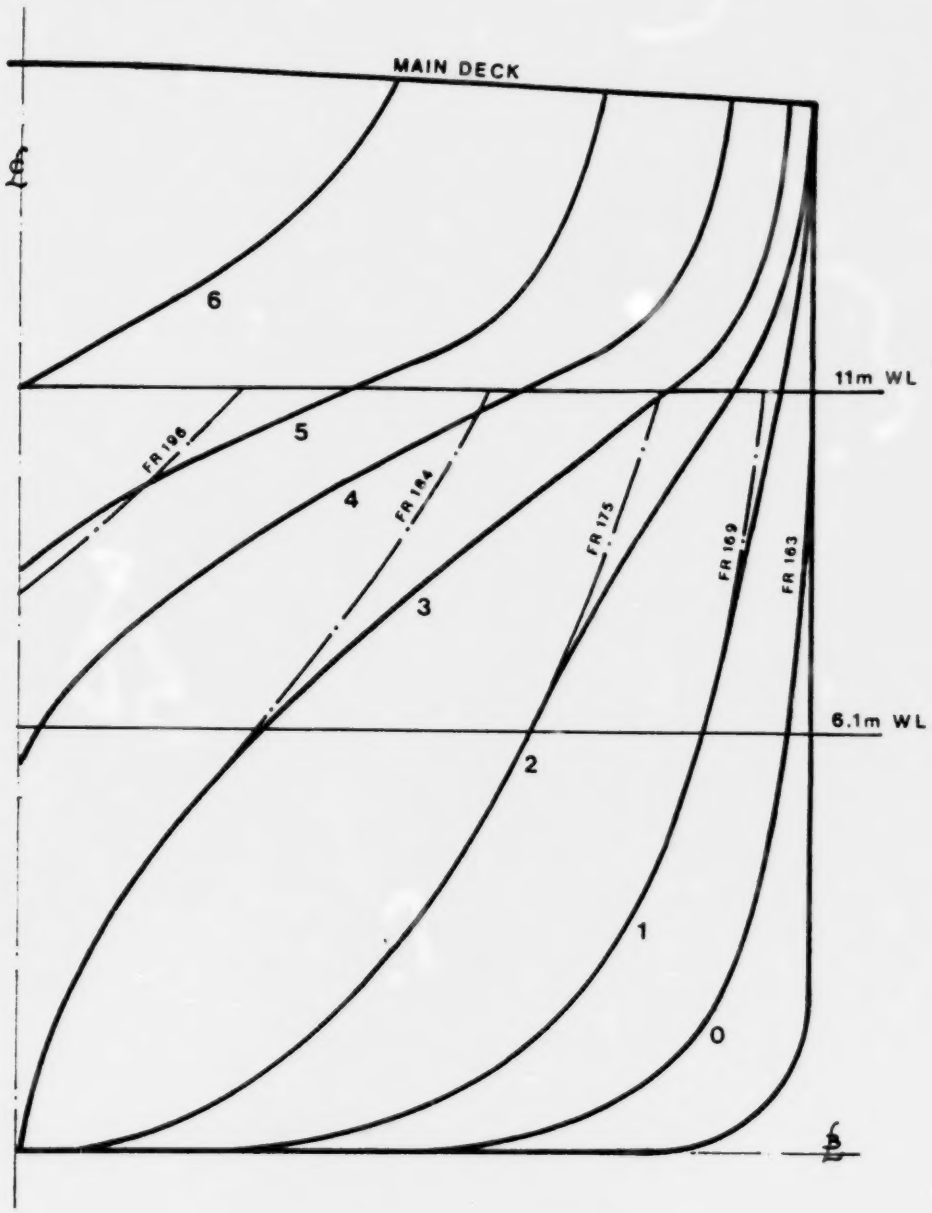

M.V. ARCTIC - MODIFIED BOW
CASE 5 - BODY PLAN

FIGURE 9

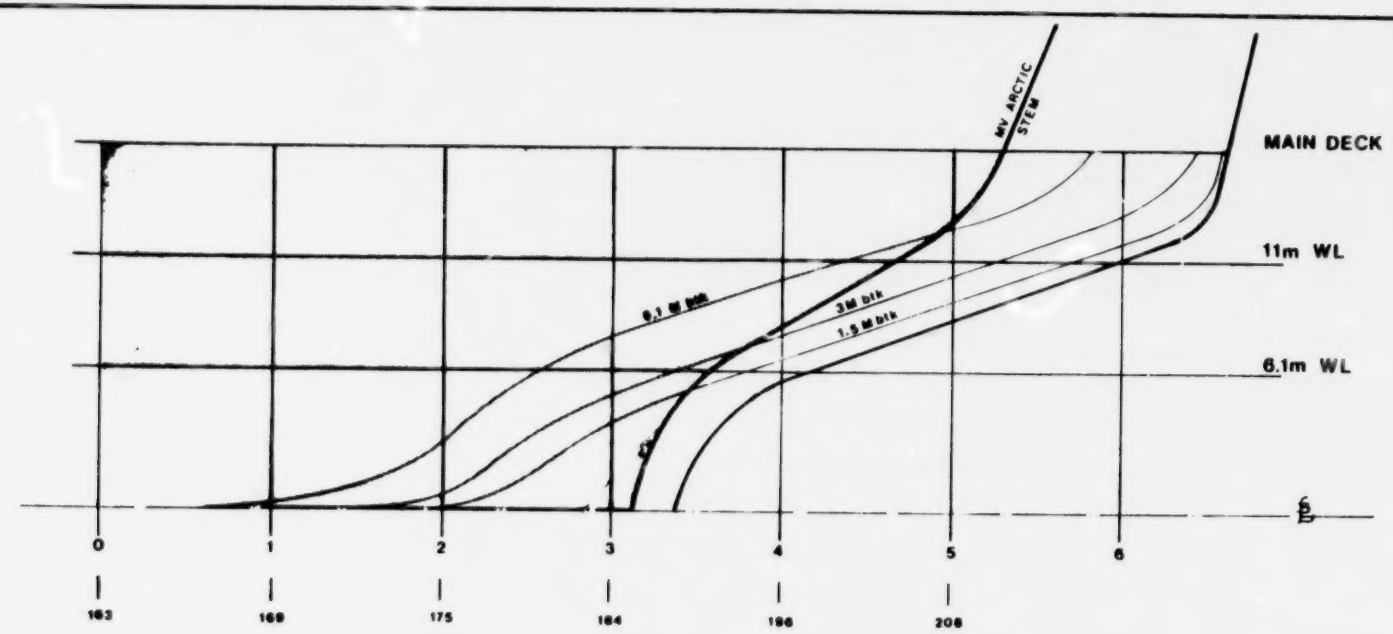

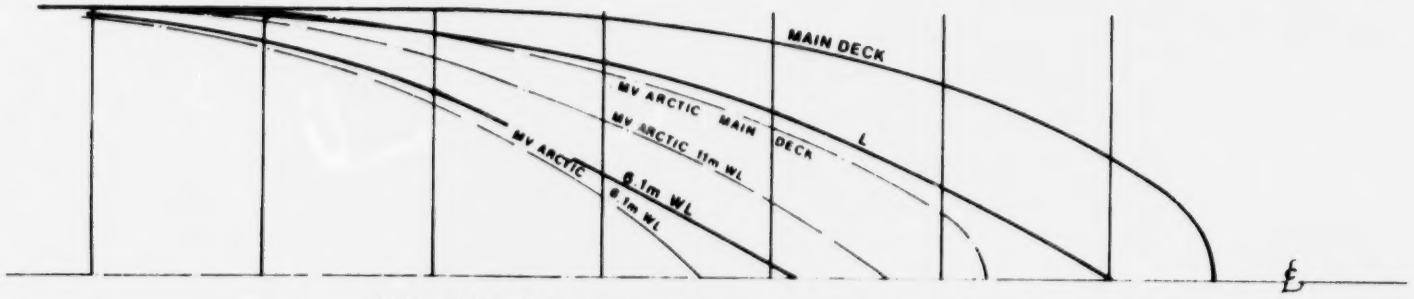

M.V. ARCTIC - MODIFIED BOW - CASE 5 - LINES PLAN

FIGURE 10

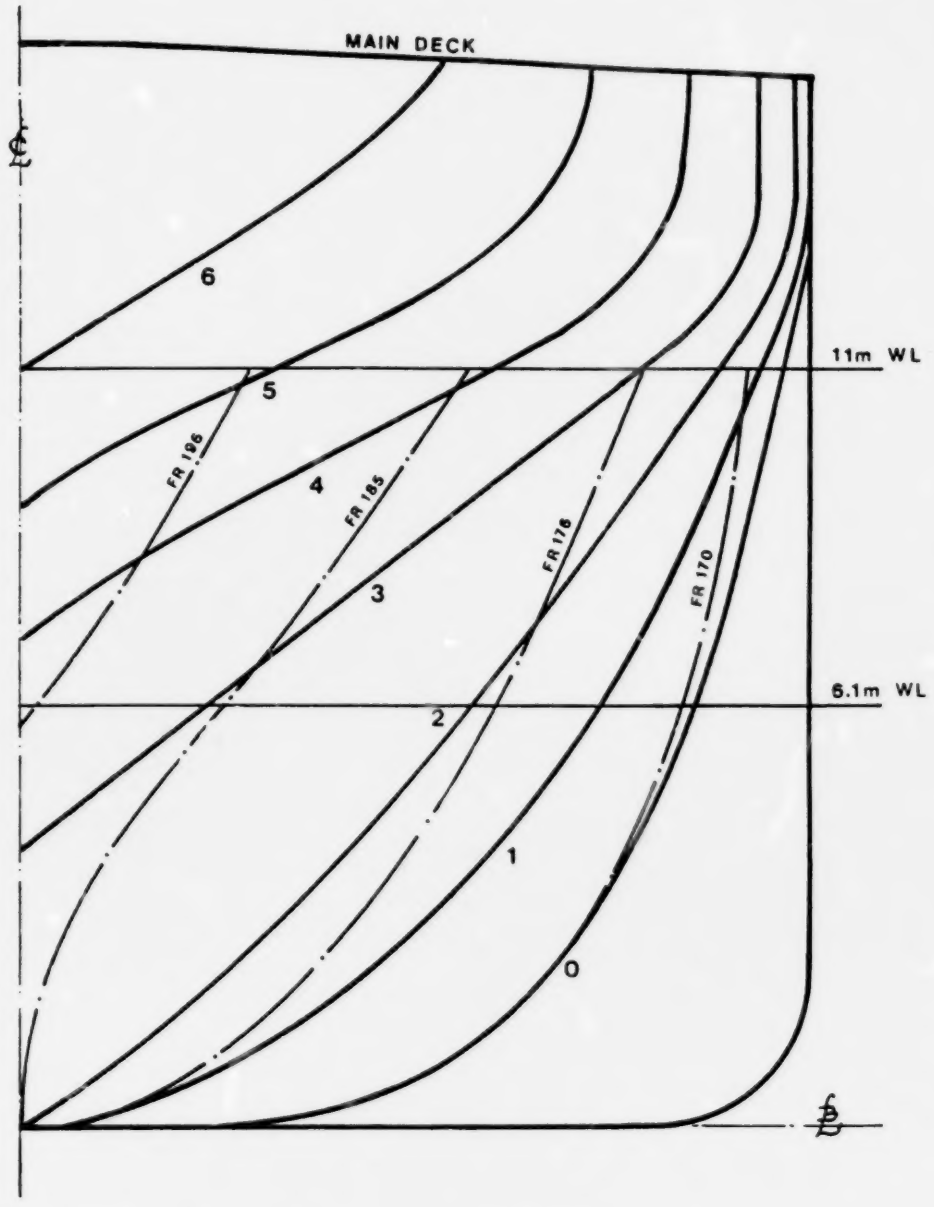

M.V. ARCTIC - MODIFIED BOW
CASE 6 - BODY PLAN

FIGURE 11

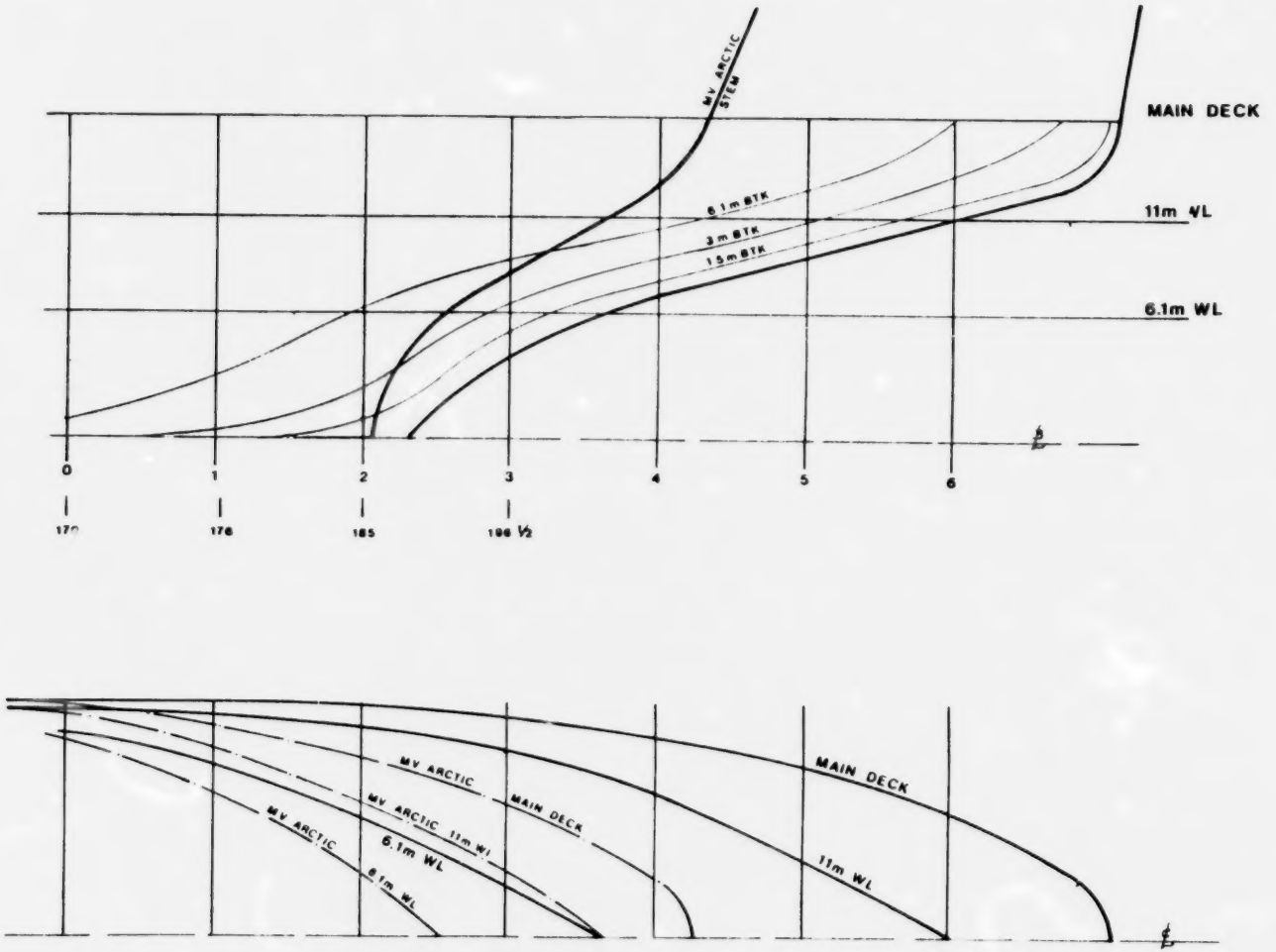

M.V. ARCTIC - MODIFIED BOW - CASE 6 - LINES PLAN

FIGURE 12

APPENDIX 3

NOTES ON ICE MODEL TESTS

An analysis of the ACL data collection, and data reduction procedures was conducted and is summarized here.

A) VARIANCES FROM MODEL TEST TARGET VALUES

The model speed was modelled accurately through all the tests and the average variance from the target values was low.

The ice thicknesses varied more, both as individual values and as means, from target values. The largest mean variation, from target values, was run 203, the 0.8 m ice sheet with model A. This was a variance of 8.3 mm, or 41.5% lower than the target value. Other thickness variances are smaller, ranging up to about 3 mm with only 3 runs above a 4 mm variance. The effect of discrete ice thickness variances within a single sheet on the model resistance is not known, and since there is no account for this variance in the ACL report, it is assumed that ACL considers this insignificant.

The ice strength also varied. The target value was 16.7 kPa for all the tests. The largest variance was 15.8 kPa, during the first resistance run. Later strength variances were around 4 to 5 kPa from target values. The mean of the strength variation was 4.55 and the standard deviation was 2.94. The effect of strength variation on the resistance data points does not appear to be significant with this test series. Run 101, 0.6 m full-scale, model A, has a strength nearly 95% higher than target, but as can be seen from Table 4.3 in this report, the effect on the model resistance appears negligible.

The Young's modulus was recorded throughout the test series, at one location, on either side of the tank barrier. The results are given in Table 4.3 and 4.4 as E/σ_f ratios. The centre value of the ice sheet is the only recorded value and this is assumed to be constant over the sheet. The E/σ_f values range from 168 to 1682, and there is no correction for this variance in the analysis. The effect of this variance of E is not clear, and is discussed in greater detail in Reference 4.2.

B) DATA COLLECTION

The data was recorded in real time onto a tape recorder and simultaneously the analogue signal was digitized and filtered. The digitizing frequency for the tests was 4 Hz per channel, with filtering at 0.5 Hz, except for test 1, which was digitized at 20 Hz and filtered at 4 Hz. The digitizing frequency, four samples per second, is reported by ACL to have been selected as a result of the size of the model and the system dynamics. The digitizing sample rate, it is reported, was changed to 4 samples per second to eliminate the "system originating inputs". A filtering frequency was then selected at 1/5th of this rate.

Digitizing rates are normally selected after an analysis of the analogue signal so that the predominant frequencies are represented in the output. Thus, if the predominant frequencies are around, for example, 5 Hz, a digitizing rate of 40 to 50 would be chosen so that each wave is represented by 8 to 10 points. This will ensure that the digitzing process does not vary the mean. The filtering frequency can then be selected to eliminate any system dynamics, since filtering has, effectively, no influence on the mean of the sample. The ACL approach has been to use the digitizing sample rate to filter the signal which may, in part, explain some of the questionable data points discussed later.

C) DATA ANALYSIS

C1) General

Figure A3.1 is reproduced from the ACL report and is an example of a resistance test output from the ACL testing. The positions of the model along the tank is shown in the upper plot. The second plot shows the speed of the model and shows three speed regimes. The third plots the force block response to the motion.

The data presented below the plots give mean values for the parameters during selected intervals along the basin. The intervals, referenced 1, 2, 3 and 4 are shown above the upper graph. By selecting the intervals, the mean resistance and speed are obtained. Reference to Table 4.3 shows that for this example, the values for intervals 1, 2 and 4 are selected, viz, -73.11, -86.87 and -73.32 newtons. The selection of these intervals is extremely important in deriving the model test data. The example shown in Figure 4.6 demonstrates this. Interval 3, shown as -115.88, is nearly 60% higher than the value selected for the data point even though the mean speed of the period is the same. Clearly, the selection of the left hand boundary of sample 4 could increase or decrease this value since the speed of the model is constant and shows no sign of any major disturbance. The reason for the high value of sample 3 is not clear unless it can be associated with the dymanics of the speed change.

Tables showing all the computer outputs for the data can be found in Ref. 4.1.

Following the acquisition of the raw data ACL conducted a regression analysis on the data based on the resistance being a function of variables in the form:

$$R = fn(v, h, h^2, \sigma_f, E/\sigma_f, vh, vh^2, \sigma_f h, \sigma_f h^2, v\sigma_f, v\sigma_f{}^2, v^2\sigma_f, v^2, v^3)$$

1300-C M.V.ARCTIC TESTS IN BASIN MEASURING RESISTANCE ONLY
TEST #3 RUN 01 MARCH 19 1983

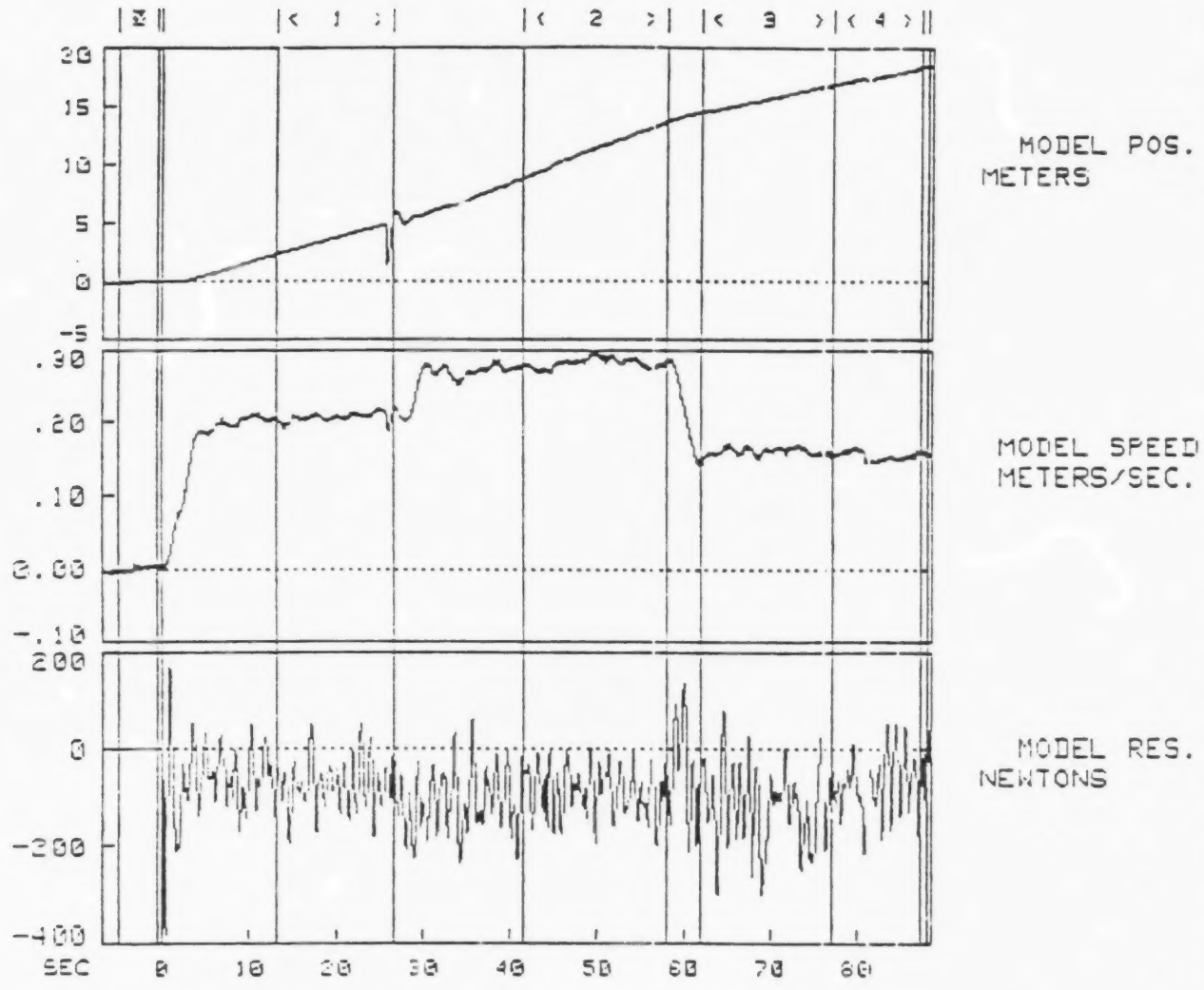

MEAN VALUES OVER THE ABOVE INTERVALS

TRANSDUCER	1	2	3	4	UNIT
MODEL POS.	3.62	11.31	15.72	17.62	METERS
MODEL SPEED	0.21	0.28	0.16	0.16	METERS/SEC.
MODEL RES.	-73.11	-86.87	-115.88	-73.32	NEWTONS

PEAK VALUES WITHIN THE ABOVE INTERVALS

MODEL POS.	5.19	13.65	17.03	19.42	METERS
MODEL RES.	-193.27	-199.00	-299.96	-212.01	NEWTONS

FIGURE A3.1
SAMPLE OUTPUT FROM ACL DATA ANALYSIS
(REPRODUCED FROM ACL REPORT)

The selection of these variables was based on ACL past experience. The results of this analysis are shown in Tables A3.1, A3.2 and A3.3, which also include the predictor equation derived. However, following the analysis it was decided by ACL to develop the prediction based on a semi-empirical approach due to the limited number of data points.

The two predictor equations used for the semi-empirical analysis are drawn from a previous report by ACL (Ref. 3.11).

$$R = C_1\sigma_f h + C_2 v h + C_3 h^3$$

$$R = C_1\sigma_f h^2 + C_2 v h + C_3 h$$

Using these two predictor equations forms a regression analysis was conducted on the data to determine the coefficient for each of the equations. Then the "best fit" equation was selected to represent that data set.

Predictor equations were generated in this way for each of the bows during the pure resistance runs, for each of the bows during the self-propulsion runs and then by combining the data sets, a final set of predictor equations was developed which represents the whole test series. The broken channel test data was massed together and only one resistance predictor was generated which represents all three bows.

The rubble field data was not analysed in the same way and is presented as a "mean penetration energy". The mean penetration energy is calculated for each of the bows and then used as a comparative measure of rubble field transit capability.

All the ACL predictor equations generated in their report are presented in Table A3.4. The rest of this section will discuss the details of the test data acquisition and particular data points which warrant further investigation.

C2) Resistance Tests

As discussed above the resistance data collected was used in a regression analysis to determine the coefficients of the ACL resistance predictor equations.

Following the selection of the predictor equations which best represented the respective data sets these prdictors where then used to normalise the data to target ice thicknesses (0.6, 0.8, 1.2 m full scale) and target ice strengths (500 kPa full scale). The normalisation of the raw data points was accomplished by multiplying the raw data point by a ratio of the resistance predicted by the resistance predictor at target values over the same predictor at actual test values, thus;

$$R_{NORMALISED} = R_{MEASURED} \times \frac{R \text{ FROM PREDICTOR AT TARGET VALUES}}{R \text{ FROM PREDICTOR AT ACTUAL VALUES}}$$

VARIABLE	CORRELATION	'F' TEST VARIABLE*
v	.0546	0.00
h	.8791	0.00
σ_f	.0350	0.00
E/σ_f	.4416	5.29
vh	.5384	38.48
vh^2	.9056	405.48
$\sigma_f h$	.8305	77.98
$\sigma_f h^2$	.8869	0.00
$v\sigma_f$	.0185	0.00
$v\sigma_f^2$	-.0247	0.00
$v^2\sigma_f$	-.0076	0.00
v^2	.0115	0.00
v^3	-.0035	0.08
h^2	.8803	0.00

$$R = -4.36 + .00811\ E/\sigma_f - 1242\ vh + 146650\ vh^2 + 42.41\ \sigma_f h$$

with a standard error of 2.6% of mean resistance

* For the variable combination in the above resistance equation

TABLE A3.1
STEPWISE REGRESSION OF RESISTANCE DATA
FOR MODEL 326-A

VARIABLE	CORRELATION	'F' TEST VARIABLE*
v	.3069	0.00
h	.7021	147.34
σ_f	-.5121	0.76
E/σ_f	.6384	0.00
vh	.6148	0.00
vh^2	.9987	11.99
$\sigma_f h$	.4821	0.89
$\sigma_f h^2$	.6401	0.49
$v\sigma_f$	.1972	0.00
$v\sigma_f^2$	.1295	0.00
$v^2\sigma_f$	.2666	0.00
v^2	.3020	60.35
v^3	.2977	0.00
h^2	.6928	0.00

$$R = -14.00 + 1317\ h + 21440\ vh^2 + 30.55\ v^2$$

with a standard error of 3.8% of mean resistance

* For the variable combination in the above resistance equation

TABLE A3.2
STEPWISE REGRESSION OF RESISTANCE DATA
FOR MODEL 326-B

VARIABLE	CORRELATION	'F' TEST VARIABLE*
v	.0160	0.16
h	.8926	2.21
σ_f	.1549	0.75
E/σ_f	.3575	2.34
vh	.4129	0.09
vh^2	.7276	64.43
$\sigma_f h$	.8274	0.00
$\sigma_f h^2$	.8682	128.56
$v\sigma_f$	-.0533	0.22
$v\sigma_f^2$	-.0967	0.12
$v^2\sigma_f$	-.0628	0.14
v^2	.0170	0.21
v^3	.0281	0.24
h^2	.8797	1.37

$$R = 5.54 + 65850\ vh^2 + 1619\ \sigma_f h^2$$

with a standard error of 8.4% of mean resistance

* For the variable combination in the above resistance equation

TABLE A3.3
STEPWISE REGRESSION OF RESISTANCE DATA
FOR MODEL 326-C

	LEVEL ICE RESISTANCE	SELF-PROPULSION	RESISTANCE AND SELF-PROPULSION
MODEL A	$R = 20.99\sigma_f h + 1897vh + 24300h^2$	$T = 517\sigma_f h^2 + 1982vh + 377.9h$	$R = 1166\sigma_f h^2 + 1779vh + 574.1h$
MODEL B	$R = 2.292\sigma_f h + 1802vh + 18670h^2$	$T = 16.46\sigma_f h + 1448vh + 2859h^2$	$R = 2.795\sigma_f h + 1804vh + 18390h^2$
MODEL C	$R = 1573\sigma_f h^2 + 1507vh + 395.7h$	$T = 938.6\sigma_f h^2 + 1493vh + 17.08h$	$R = 28.54\sigma_f h + 1328vh + 24030h^2$

BROKEN CHANNEL
COMBINED PREDICTOR FOR
MODELS A, B AND C

$$R = 1.965 + 628.9vh + 8896h^2$$

TABLE A3.4
PREDICTOR EQUATIONS FROM MODEL SCALE
TESTS CONDUCTED AT ACL

These normalised data points are presented in Figures A3.2, A3.3 and A3.4 together with their associated predictor equations.

Details of the procedure can be found in Ref. 4.2.

A number of these data points are now described in more detail.

a) Model A, 0.8 m ice, Test Day 2

The 1.5 kn and 3 kn resistance values appear to be low. The speeds were run in the order 3, 5 and 1.5 knots (full scale). The 3 knot run was conducted successfully, but towards the end of the 5 knot run, the carriage wires became tangled and the model came to an abrupt halt.

This can be seen in the data output shown in Figure A3.5. The carriage jamming can be seen around the 50 second mark on the resistance output. It was also discovered that one of the compressors, located over the south end of the basin, had not functioned during the freeze period and may have effected the thickness and strength growth.

It is not possible to evaluate the effect of the carriage jamming on the resistance output. Figure A3.5 shows the approximate boundaries for the sample taken for this test and it can be seen that towards the end of the sample the record has begun to rise. This may indicate that the data point representing this sample has been influenced by the cables becoming tangled prior to the actual jamming. Clearly, from the data this can not be confirmed either way.

In addition to the erratic nature of the output it should be noted that there would appear to be a very low frequency influence in the data with a period of about 15 - 20 seconds. This is not referred to in the ACL report.

An analysis of the slow speed, 1.5 kn run, confirms 11.3 N. This point was recorded after some delay whilst the underwater carriage and wires were released, and is associated with thinner ice. Although not apparent in Table 4.3, the strength of the ice associated with these data points, "appeared" weaker at the time of testing.

b) Model A, 0.6 m ice, Full-Scale, TEST DAY 1

During the first resistance run, 5 kn full-scale, the yaw restraint string, attached between the stern of the model and the carriage, broke and the model was seen to yaw, stern to port and sway starboard and ice was seen to be pushed up the side of the mid-body. The force block, attached to the centre of the model,

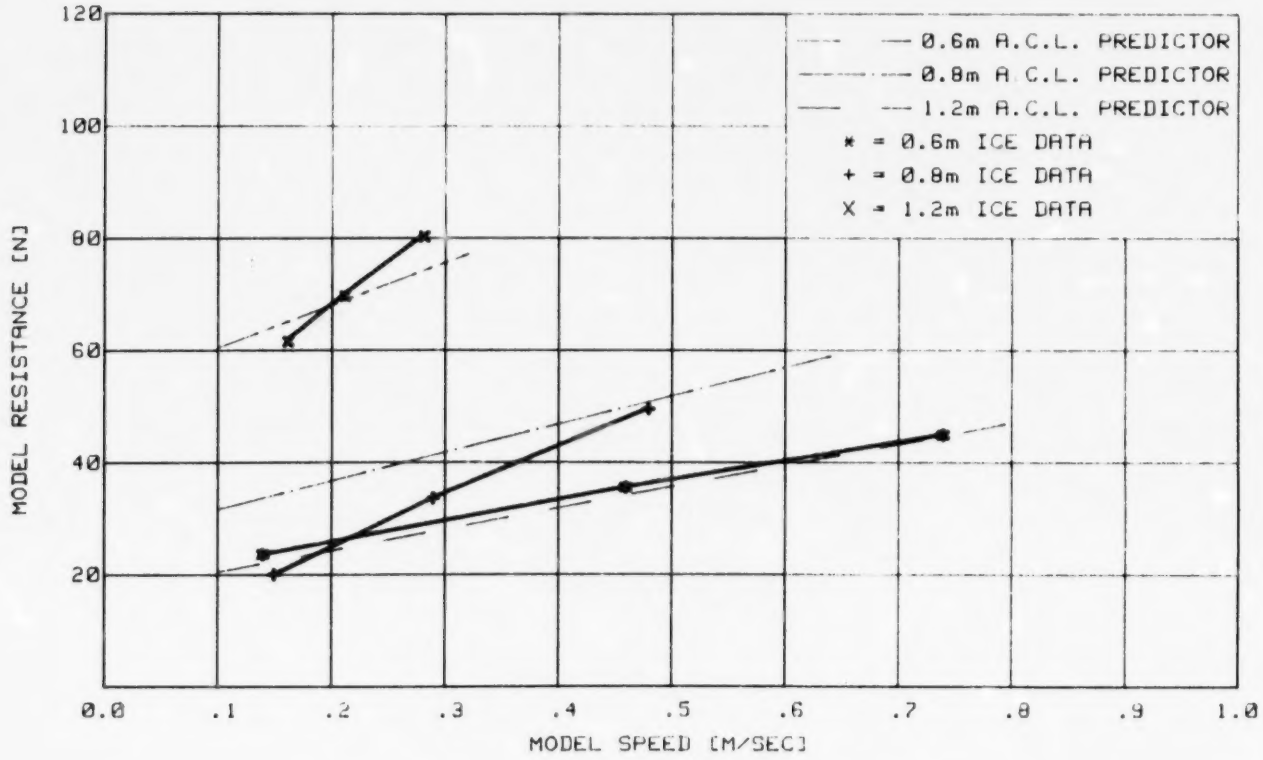

MODEL 'A' NORMALISED RESISTANCE DATA POINTS
WITH A.C.L. PREDICTOR EQUATION
FROM A.C.L. ICE MODEL TESTING

FIGURE A3.2

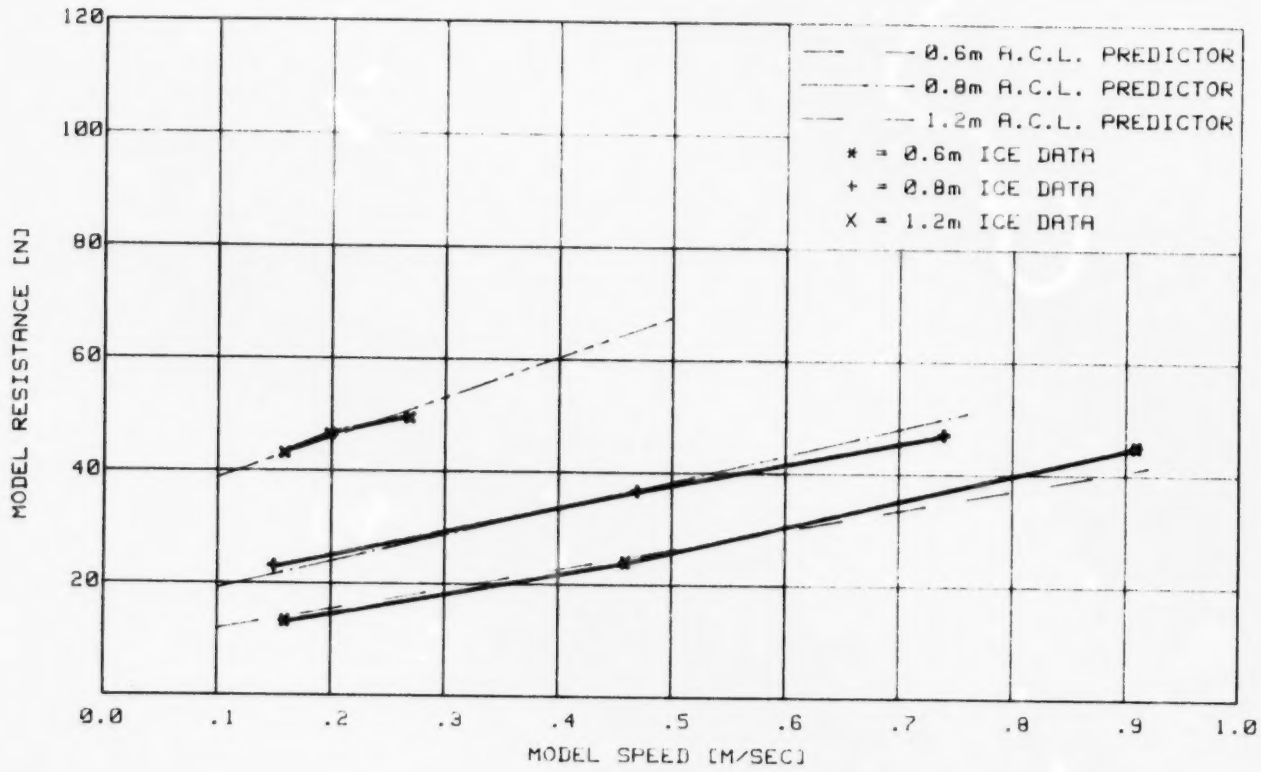

MODEL 'B' NORMALISED RESISTANCE DATA POINTS
WITH A.C.L. PREDICTOR EQUATION
FROM A.C.L. ICE MODEL TESTING

FIGURE A3.3

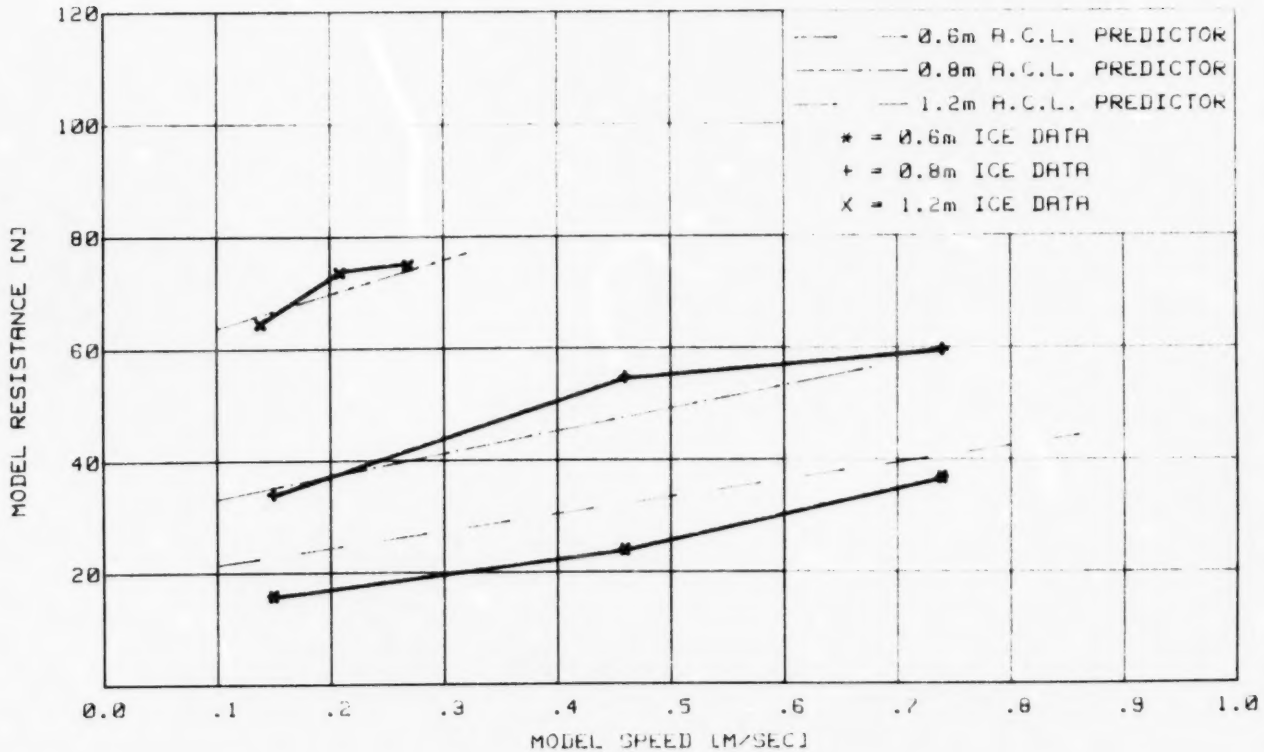

MODEL 'C' NORMALISED RESISTANCE DATA POINTS
WITH A.C.L. PREDICTOR EQUATION
FROM A.C.L. ICE MODEL TESTING

FIGURE A3.4

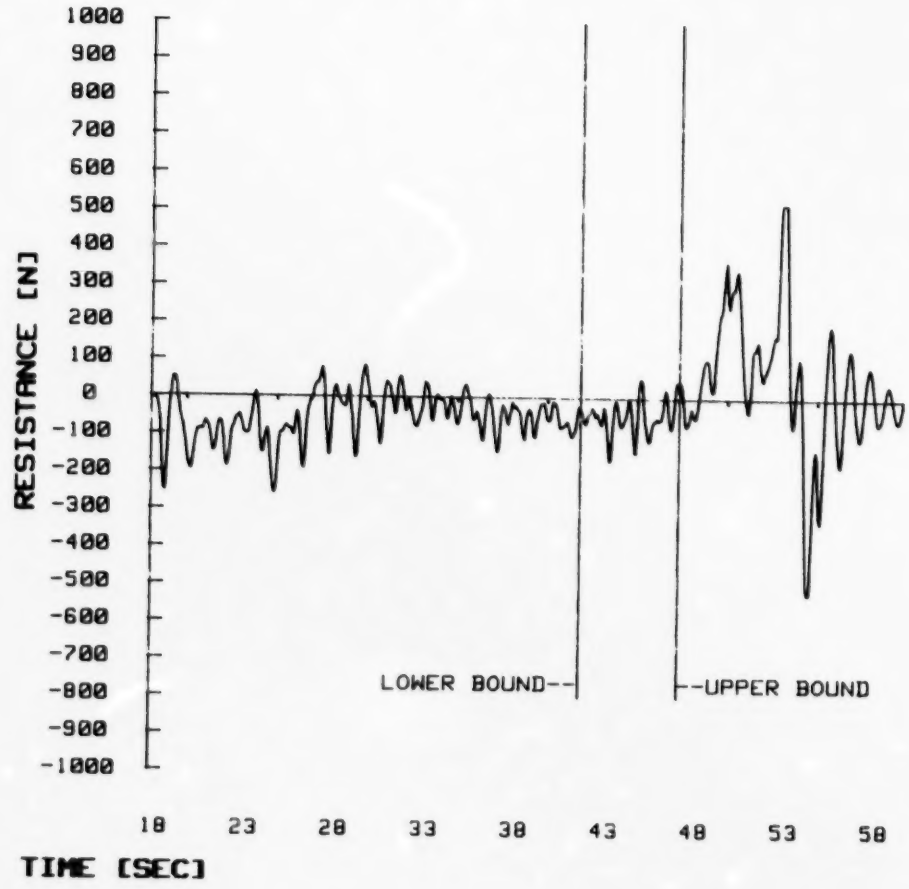

START OF SAMPLE = 41.8 SECS

END OF SAMPLE = 47.3 SECS

DURATION OF SAMPLE = 5.5 SECS

SIZE OF SAMPLE = 110

MAX.VALUE IN SAMPLE = 52.8442

MAX.NEG.VALUE IN SAMPLE = -167.843

MEAN OF SAMPLE = -47.91

STANDARD DEVIATION = 46.13

RESISTANCE OF MODEL RUN 202
M.V. ARCTIC MODEL TESTS
FIGURE A3.5

was unconstrained for this test and for all the other tests on Bow 1, with the exception of the last two self-propulsion tests on day 3. The string was replaced with wire for the subsequent tests. No identifiable affect could be seen on the force block output.

c) Model A, 1.2 m Ice, Full-Scale, TEST DAY 3

The three resistance test speeds, 1.5, 2 and 3 knots were run continuously without stopping between the speeds. After completion of the tests, the model was seen to have swayed to starboard approximately 27.5 cm.

Ice was seen being pushed up the port side of the model, aft of the bow, and the force block, which was free to move, translated to starboard. The yaw restraint held the stern of the model in its original transverse position.

As a result of this "crabbing" of the model, ACL elected to restrain the force block in all the subsequent tests. No effect of this could be identified on the force block output.

d) Model B, 0.6 m Ice, Full-Scale, TEST DAY 6

The underwater carriage cable snapped during the 10 kn resistance run. The reason for this was not reported and its effect on the results is unknown.

C3) Self-Propulsion Tests

As mentioned above the self-propulsion tests were conducted using the "English method". As a result propeller thrust and force block thrust were recorded during the tests. This procedure necessiates the calculation of the self-propulsion points by interpolating the propeller thrust between over and under propelled conditions. These are achieved by varying the propeller r.p.m.

Prior to the calculation of the self-propulsion points the over and under propelled data point pairs were normalised to a mean ice thickness and strength. This calcultion is described in detail in Ref. 4.2.

A typical output from the data collection (after digitizing) is shown in Figures A3.6 and A3.7. Figure A3.6 shows model position, speed and resistance; Figure A3.7 shows model propeller r.p.m. torque and thrust. The example shown is run Number 107, the 5 kn (0.47 m/sec) run, in 20 mm (0.6 m full-scale) ice. The digitizing rate for this run was 20 samples per second and as a result, the system dynamics can be seen in Figure A3.6 on the resistance output starting at the 15 second mark. This is discussed in more detail later in the main report.

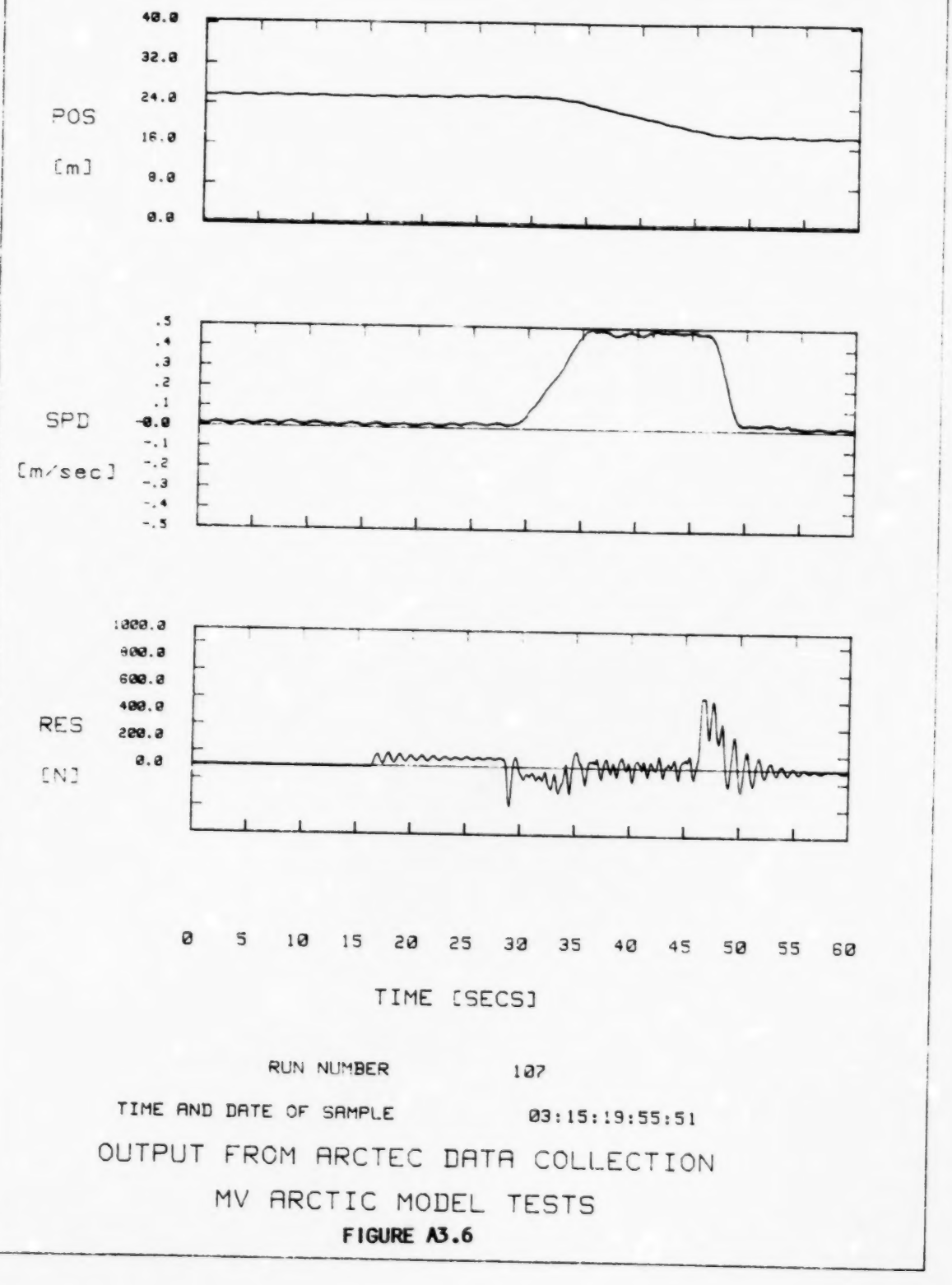
POS
[m]
40.0
32.0
24.0
16.0
8.0
0.0
SPD
[m/sec]
.5
.4
.3
.2
.1
-0.0
-.1
-.2
-.3
-.4
-.5
RES
[N]
1000.0
800.0
600.0
400.0
200.0
0.0
0 5 10 15 20 25 30 35 40 45 50 55 60
TIME [SECS]
RUN NUMBER 107
TIME AND DATE OF SAMPLE 03:15:19:55:51
OUTPUT FROM ARCTEC DATA COLLECTION
MV ARCTIC MODEL TESTS

FIGURE A3.6

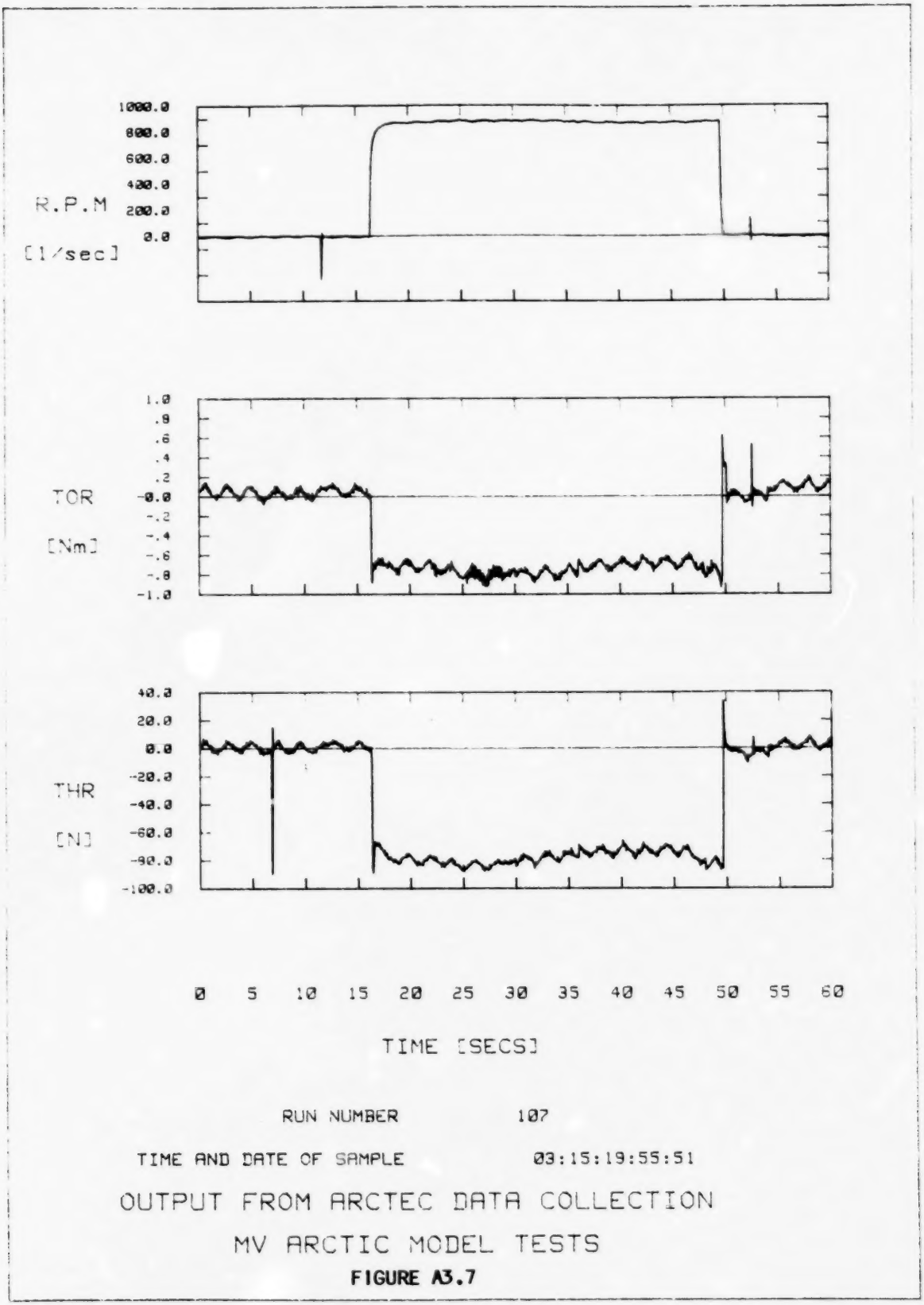
1000.0
800.0
600.0
400.0
R.P.M
200.0
0.0
[1/sec]
1.0
.8
.6
.4
.2
TOR
-0.0
-.2
-.4
[Nm]
-.6
-.8
-1.0
40.0
20.0
0.0
-20.0
THR
-40.0
-60.0
[N]
-80.0
-100.0
0 5 10 15 20 25 30 35 40 45 50 55 60
TIME [SECS]
RUN NUMBER 107
TIME AND DATE OF SAMPLE 03:15:19:55:51
OUTPUT FROM ARCTEC DATA COLLECTION
MV ARCTIC MODEL TESTS

FIGURE A3.7

The self-propulsion points were then calculated in the normal fashion and the resultant thrust data points are shown in Table A3.5.

A number of the self-propulsion runs were conducted at identical speeds but different propeller r.p.m. to deduce the self-propulsion point of the model. However, not all speeds were tested at two propeller r.p.m.'s due to ice sheet limitations. The self-propulsion point, for those that were not tested at two r.p.m.'s, was calculated by assuming the same thrust vs r.p.m. slope between the speed that was tested at two r.p.m.'s and the speed that was not. A full explanation of this calculation is given in Reference 4.2 and is discussed later in this report.

Following a regression analysis of this data, the ACL thrust predictor equations discussed earlier and presented in Table A3.4 were generated.

The data points listed in Table A3.4 are plotted with the thrust predictor equations in Figures A3.8, A3.9 and A3.10. The affect of normalizing the raw data points does not appear to have resulted in the data points being well represented by the predictor equations.

The predictor equations generated and discussed earlier are based on a regression analysis of the total thrust, or resistance data sets, for a particular bow. Therefore, although the predictor equations represent a regressed line through the data they do not necessarily pass through the recorded data points. This is discussed in more detail in Reference 4.2.

A number of non-consistant data points can be seen in the self-propulsion tests, which warrant additional discussion. No reference or explanation of these occurrences are given in the ACL report and as a result the comments given here are offered only as supposition, given the visual observations made during the tests by the author. It should be further noted that until the self-propulsion tests on day 3, Model A, 40 mm ice sheet, all tests had been conducted with an unconstrained force block. Following problems with the resistance test, the decision was made by ACL to clamp the block for all subsequent tests.

a) The 40 mm (1.2 m full-scale) tests for Bow A were run at 3, 1.5, 1.5 and 3 knots full-scale consecutively. The ice strength variation, over the runs, was 10.4 to 14 kPa, a range of 3.6 kPa, to 6.3 kPa below the target strengths. The ice thickness varied from 40.2 mm to 43.4 mm. In addition to fixing the force block, the model was also moved, transversely, closer to the centre divider in an attempt to reduce the discrete thickness variations associated with the ice near the tank wall. The first 3 kn run was conducted successfully without any unexpected occurrences. During the subsequent runs, the ice in front of the model, on a number of occasions, was seen to crack from the bow stem to the tank divider. In addition, the "anti-yaw" wire, attached to the stern of the model, became tight on the starboard side and loose on the port side, indicating a tendency of the model to yaw, with

MODEL #	VELOCITY (m/sec.)	h (m)	σ_f (KPa)	T (N)	RPM
326-A	.270	.04160	11.05	51.1	1008
	.150	.04065	12.55	54.3	996
	.155	.02595	12.15	11.8	491
	.470	.02830	14.10	33.8	861
	.470	.02090	18.20	34.0	753
	.760	.02070	23.40	48.3	926
	.160	.02530	26.10	9.5	378
326-B	.165	.02985	11.90	8.3	366
	.710	.02910	17.10	51.3	844
	.290	.04270	13.75	30.7	781
	.160	.04175	16.55	29.1	738
	.160	.02405	16.65	14.0	514
	.930	.02290	19.40	30.9	821
326-C	.160	.03270	10.70	16.8	565
	.750	.03170	10.10	43.4	933
	.155	.02175	10.50	8.3	390
	.750	.02100	17.80	31.9	847
	.165	.04280	16.35	36.3	825
	.270	.04175	11.45	43.4	904

TABLE A3.5
SELF-PROPULSION POINT DATA

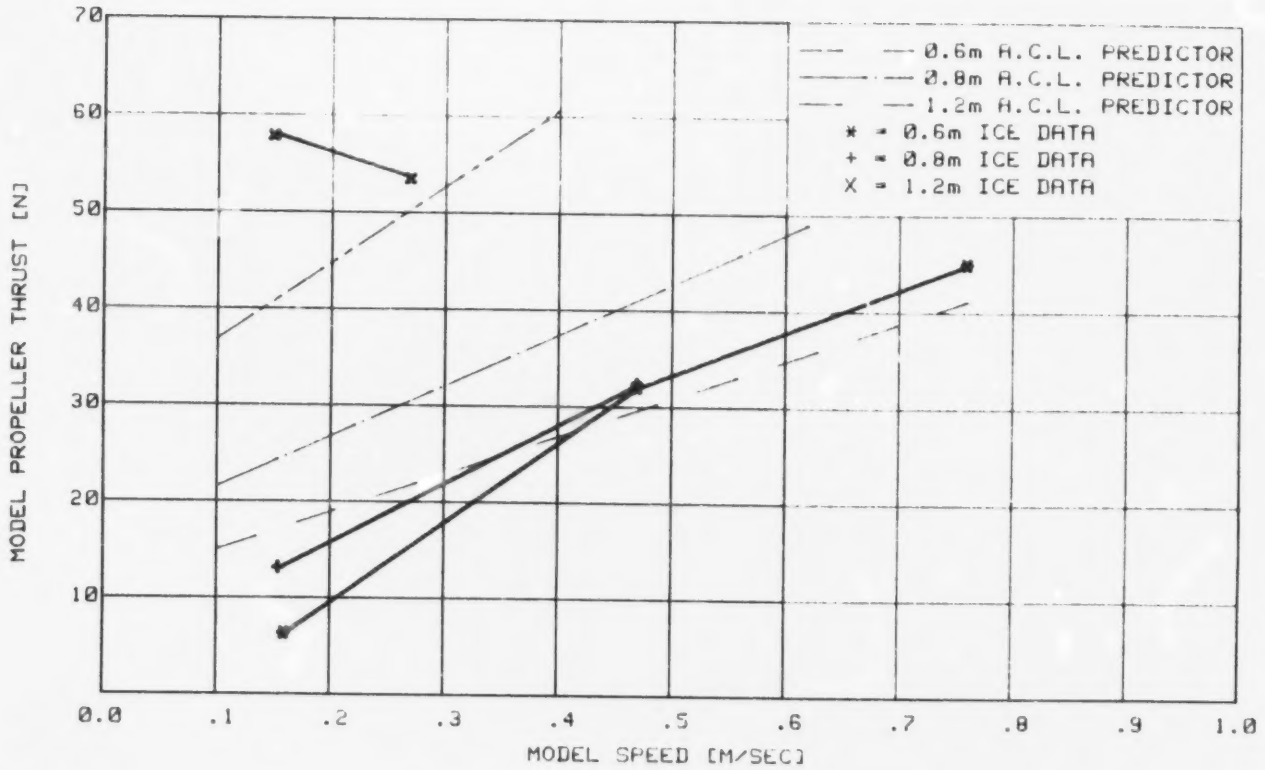

MODEL 'A' NORMALISED THRUST DATA POINTS
WITH A.C.L. PREDICTOR EQUATION
FROM A.C.L. ICE MODEL TESTING

FIGURE A3.8

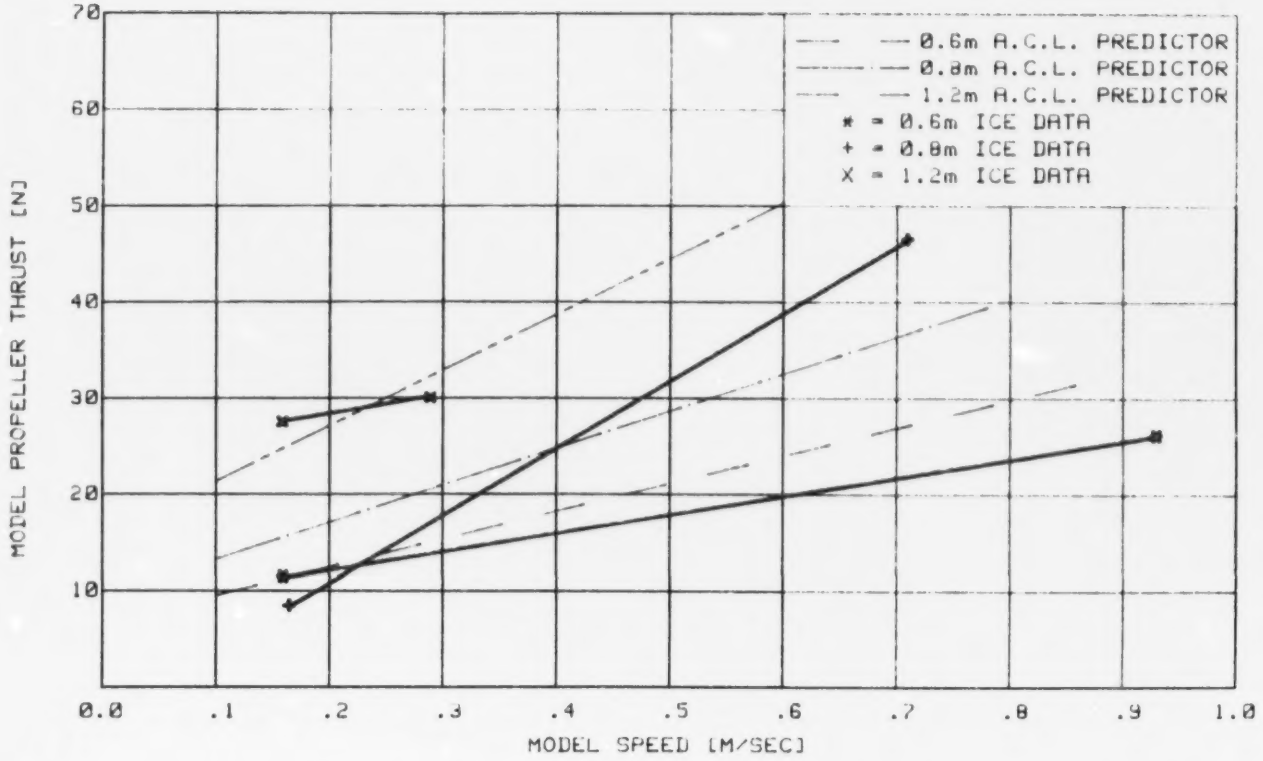

MODEL 'B' NORMALISED THRUST DATA POINTS
WITH A.C.L. PREDICTOR EQUATION
FROM A.C.L. ICE MODEL TESTING

FIGURE A3.9

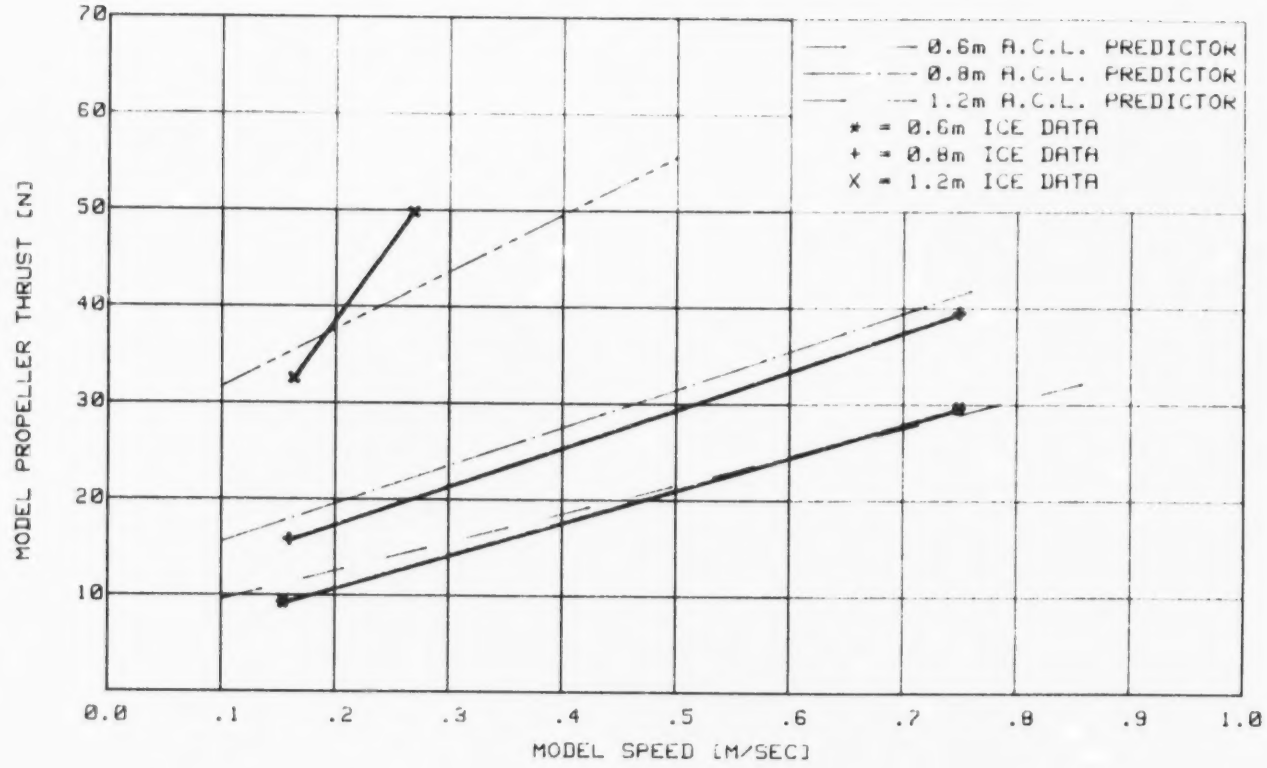

MODEL 'C' NORMALISED THRUST DATA POINTS
WITH A.C.L. PREDICTOR EQUATION
FROM A.C.L. ICE MODEL TESTING

FIGURE A3.10

the bow moving away from the tank divider. During the second 1.5 kn run and the last 3 kn run, the model was also seen to heel approximately 10 - 15° to starboard. The heeling of the model may be due to the icebreaking at the tank divider, rather than at the bow. The nature of the heeling and icebreaking would indicate that larger than expected data recordings would be obtained. This is confirmed by considering Figure A3.8 and Table A3.4. The two 1.5 kn runs are both higher than expected and the last 3 kn data point is higher than the first 3 kn data point. It is ACL's opinion that this does not influence the predictor equation and is within their range of experimental error.

A number of the remaining test data points on model A, B and C, as can be seen on the figures, also show a rather irregular representation of the predictor equations; however, there were no experimental incidences that can account for them although concern was expressed during the test program about the length of time between the resistance and self-propulsion tests.

b) Due to the characteristics of the tank and ambient weather conditions, ACL report that the strength reduction is not uniform over the tank and that the east side of the basin reduces in strength slower than the west side. This may affect the quality or control of the ice properties while testing, although this is not confirmed by analyzing the ice property data given in Tables 4.3 and 4.4. The mean differences and standard deviation between target and actual ice thickness is 1.64 mm and 1.66 mm during the resistance tests, and 2.61 mm and 1.74 mm for the self-propulsion tests. It would appear that the accuracy with which the target data was achieved is higher during the resistance tests than during the self-propulsion tests.

The ice strength properties are more comparable; the means of the difference between actual and target strength is 4.83 KPa for the resistance, and 4.3 KPa for the self-propulsion.

c) A possible source of error cited by ACL for the self-propulsion data points is the procedure for calculating the self-propulsion point. This procedure is described in detail in Reference 4.2.

The self-propulsion point for a vessel tested with the "English" method is ideally calculated with at least two fixed speeds, varying propeller r.p.m., self-propulsion runs. In the case of the testing at ACL, this was not possible due to ice sheet limitations. As a result, a number of speeds were run with only one r.p.m. value. The self-propulsion points for these runs were calculated by assuming that the thrust vs r.p.m. slope was constant over the range of r.p.m. and speed considered.

By using this assumption, it was possible to use the slope of the line obtained from data points associated with the two r.p.m. values and apply it to the data points associated with one r.p.m. value at the different speeds, and thus deduce the self-propulsion point. The accuracy of this method depends on the nature of the thrust vs r.p.m. curve.

Figure A3.11 is a plot of thrust vs propeller r.p.m. deduced from the ARCTIC's open water testing at NRC (Ref. 4.1). Two speeds, 2 and 4 knots, are compared over a range of propeller r.p.m. There is no indication that there was any propeller/ice interaction, so the same will be applicable to the ice tests. From Figure A3.11 it can be seen that any errors associated with assuming that the two curves do not have a similar slope at any specific thrust, will be small. This is due primarily to the nature of the K_T curve plotted against the advance coefficient (J). The straighter the K_T curve becomes, or the smaller the change of slope of the K_T curve, the straighter becomes the thrust vs propeller r.p.m. curve for a specific speed, and the smaller the effect of speed becomes on the slope of the thrust vs r.p.m. curve. Figure A3.11 shows how, in the case of the ARCTIC's propeller, the two curves are almost parallel and as a result only a nominal error is expected as a result of the assumption that they are parallel. As a result, although ACL consider this to be the major source of error in the self-propulsion data, this is not felt to be the case.

C4) Combined Resistance and Self-Propulsion Analysis

Following the completion of the resistance and self-propulsion data analysis the thrust data points were transformed to resistance and combined with the resistance data. Another regression analysis was then conducted using the two forms of predictor equation discussed earlier and a "final" resistance predictor for each of the three bows was generated. These are presented in Table A3.4.

The thrust/resistance transformation was accomplished by deducing the thrust deduction from the resistance and thrust predictor equations. Therefore:

$$\text{for Model A} \quad t = \frac{T-R}{T} = \frac{\sigma_f h\,(517h-20.99) + 85\ vh + h(377.9 - 24300h)}{517\sigma_f h^2 + 1982\ vh + 377.9\ h}$$

$$\text{for Model B} \quad t = \frac{T-R}{T} = \frac{14.17\sigma_f h - 354\ vh - 15811\ h^2}{16.46\sigma_f h + 1488\ vh + 2859\ h^2}$$

$$\text{for Model C} \quad t = \frac{T-R}{T} = \frac{-634.4\ \sigma_f h^2 - 14\ vh - 378.6\ h}{938.6\ \sigma_f h^2 + 1493\ vh + 17.08\ h}$$

These thrust deduction relationships are reproduced from the ACL report in Figure A3.12.

The reasons for the form and magnitude of the thrust deduction curves shown in Figure A3.12 are not known. Intuitively, since only the bows changed form and because of the ship's length, it was expected that the thrust deduction would be similar for each bow. The effect of ice interaction with either nozzle or propeller is not thought to be the reason since no ice was seen in this area.

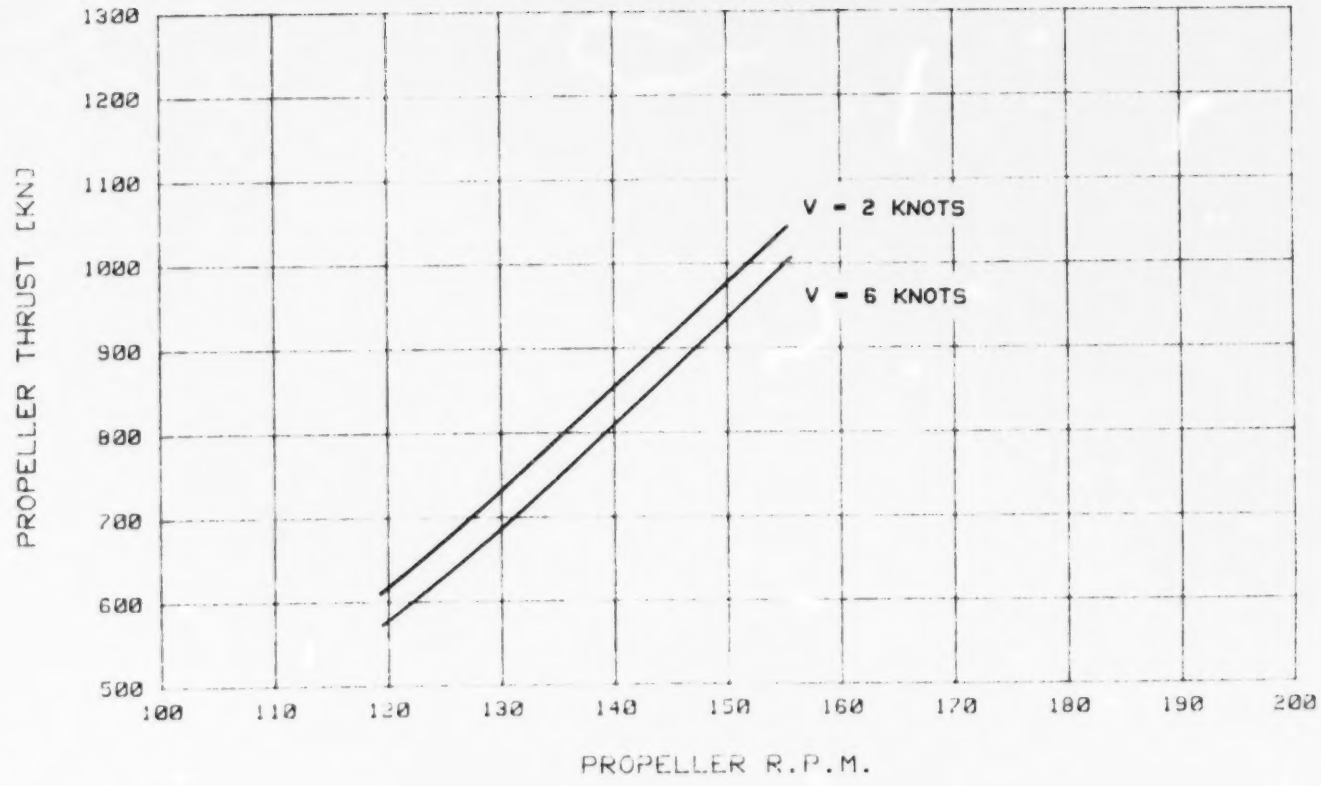

PROPELLER THRUST VS. RPM
AT CONSTANT SHIP SPEED
FROM OPEN WATER TESTS

FIGURE A3.11

FIGURE 6.8a
MODEL 326-A

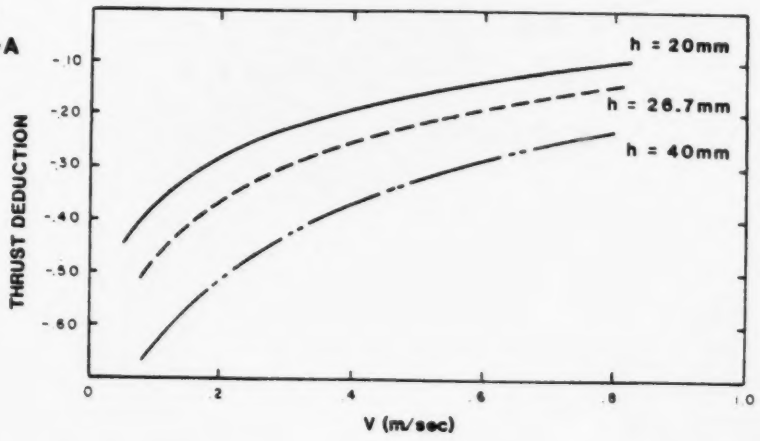

FIGURE 6.8b
MODEL 326-B

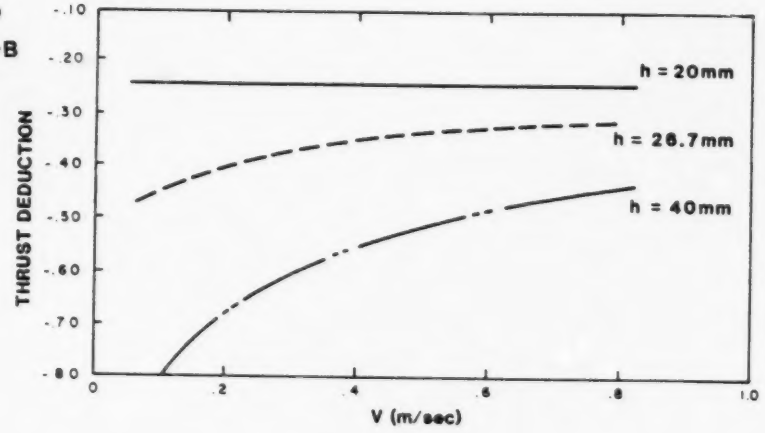

FIGURE 6.8c
MODEL 326-C

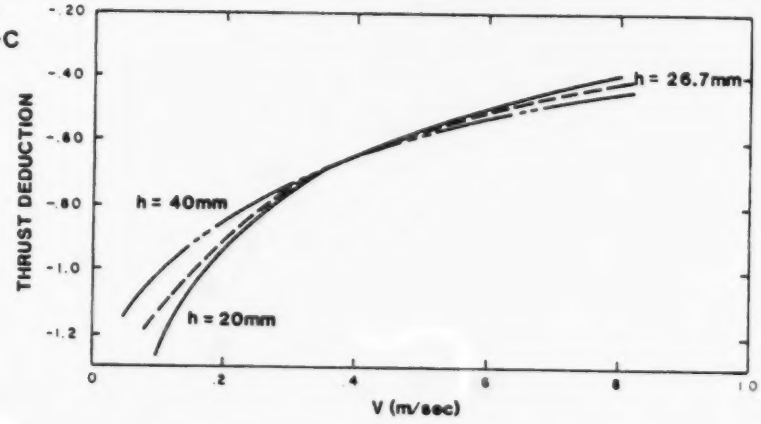

THRUST DEDUCTION CURVES
BASED ON THE SELF-PROPULSION AND
RESISTANCE TESTS AT A.C.L.

FIGURE A3.12

It should be noted that the thrust deduction for Bow A in 40 mm ice is -0.6 whilst for Bow C is -1.2, or 100% difference.

C5) Broken Channel Tests

Following the level ice tests in the east and west channels, self-propelled and resistance broken channel tests were conducted. These are described in detail in Reference 4.2. The results from these self-propulsion and resistance tests were combined, and regressed together, for all three bow designs. The self-propulsion data points were reduced to "resistance" values by using the open water thrust deduction factor. The resulting basic predictor equation is presented in Table A3.4.

ACL report that model A averages approximately 8.5% above, model B 11.7% below and model C 3.2% above this regression line.

The data also varies between self-propulsion and resistance tests, with the exception of model A. Model B self-propulsion data is approximately 27.4% below the predictor line, while the resistance data is 3.9% above the predictor line. For model C, the self-propulsion data is approximately 6.4% below the predictor line and the resistance data is 12.7% above the regression line.

Figures A3.13 and A3.14 show the broken channel resistance and self-propulsion test results for model A and the ACL predictor line. Figures A3.15, A3.16, A3.17 and A3.18 show similar curves and data points for Bows B and C.

C6) Rubble Field Tests

Following the 1.2 m full-scale level ice and broken channel testing, the broken ice was consolidated in the west side of the basin and re-frozen. The model was then run through this rubble field in the self-propulsion mode. A detailed description of the test and test analysis is given in Reference 4.2.

The propeller thrust recording was converted to a resistance using the open water thrust deduction. The data was analyzed by integrating the propeller thrust vs distance curve, subtracting the integral of the force block thrust vs distance curve and thus obtaining an energy value for each of the three bows. By normalizing each of these to a value of energy per unit area of the cross section of the rubble field, the energy per square meter for each bow can be deduced.

From the data, it would appear that model C required the least energy, followed by Bows B and A. Model C was approximately 19% lower than model A and model B was 9% lower than model A.

Table A3.6 shows the average thickness and width of the rubble field together with the integral of the resistance and thrust curves ($\int Rdx$, $\int Tdx$), the integral period (x), thrust deduction (t), total energy (P.E.) and the average energy per volume of the rubble field.

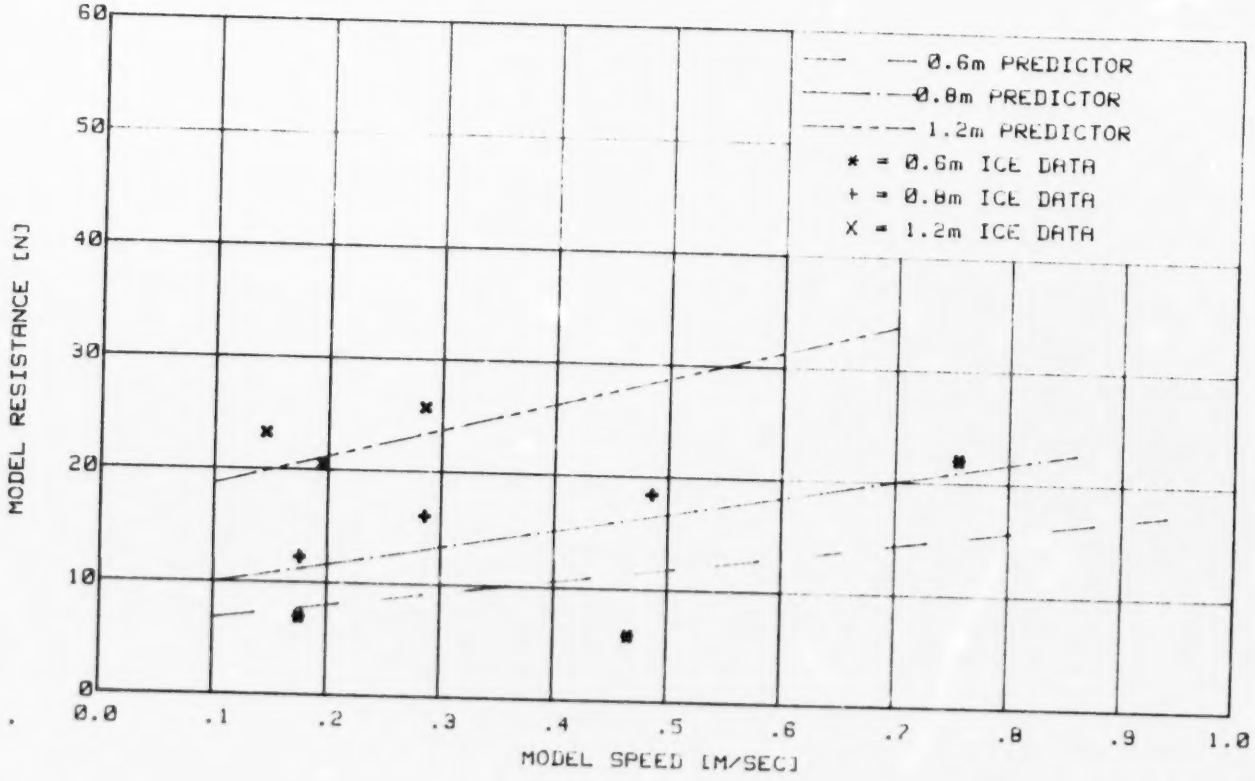

EXISTING MV ARCTIC BROKEN CHANNEL RESISTANCE DATA POINTS
WITH A.C.L. PREDICTOR EQUATION
FROM A.C.L. ICE MODEL TESTING

FIGURE A3.13

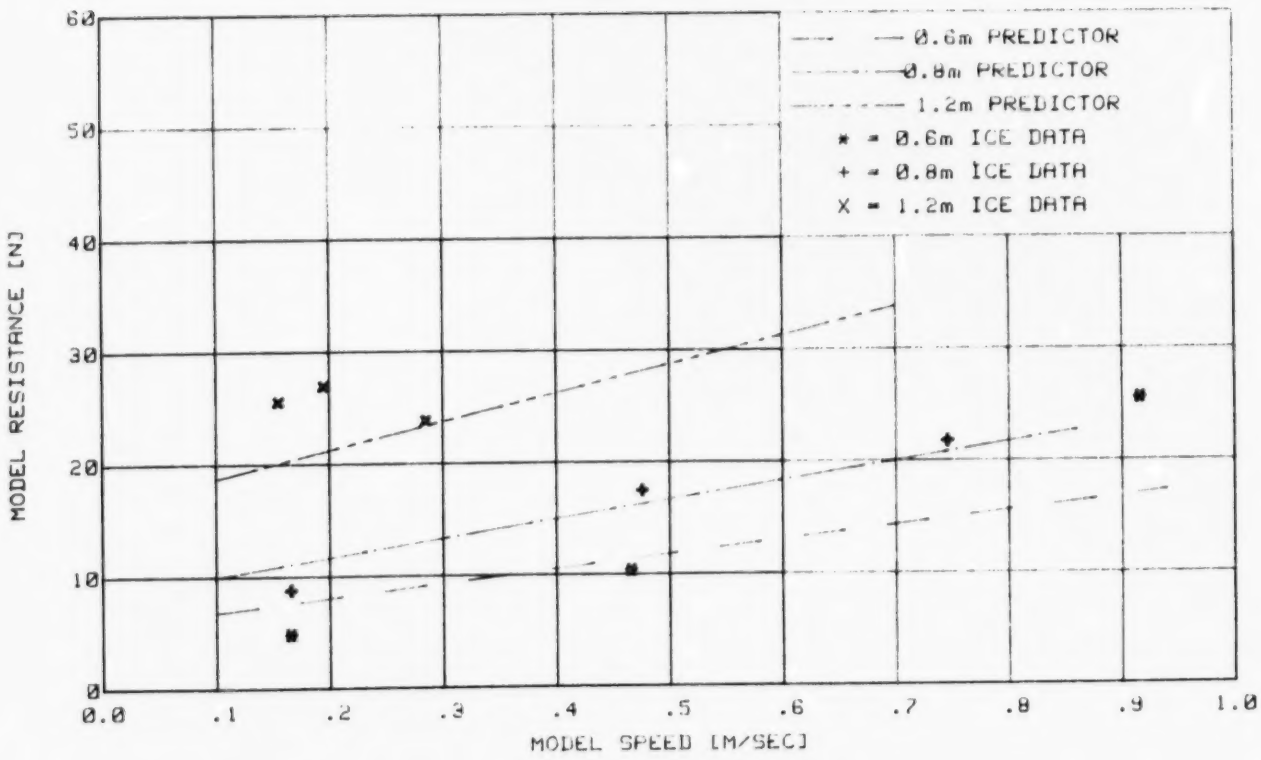

MODEL 'B' BROKEN CHANNEL RESISTANCE DATA POINTS
WITH A.C.L. PREDICTOR EQUATION
FROM A.C.L. ICE MODEL TESTING

FIGURE A3.14

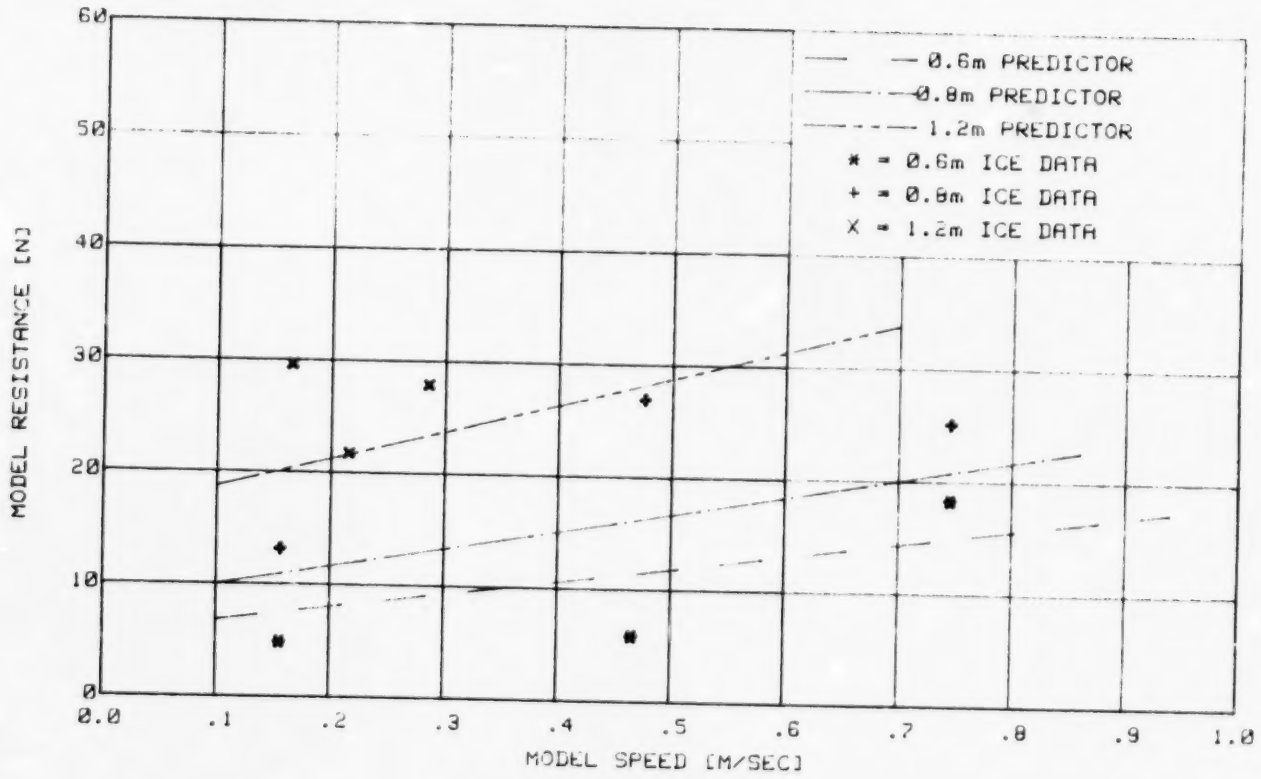

MODEL 'C' BROKEN CHANNEL RESISTANCE DATA POINTS
WITH A.C.L. PREDICTOR EQUATION
FROM A.C.L. ICE MODEL TESTING

FIGURE A3.15

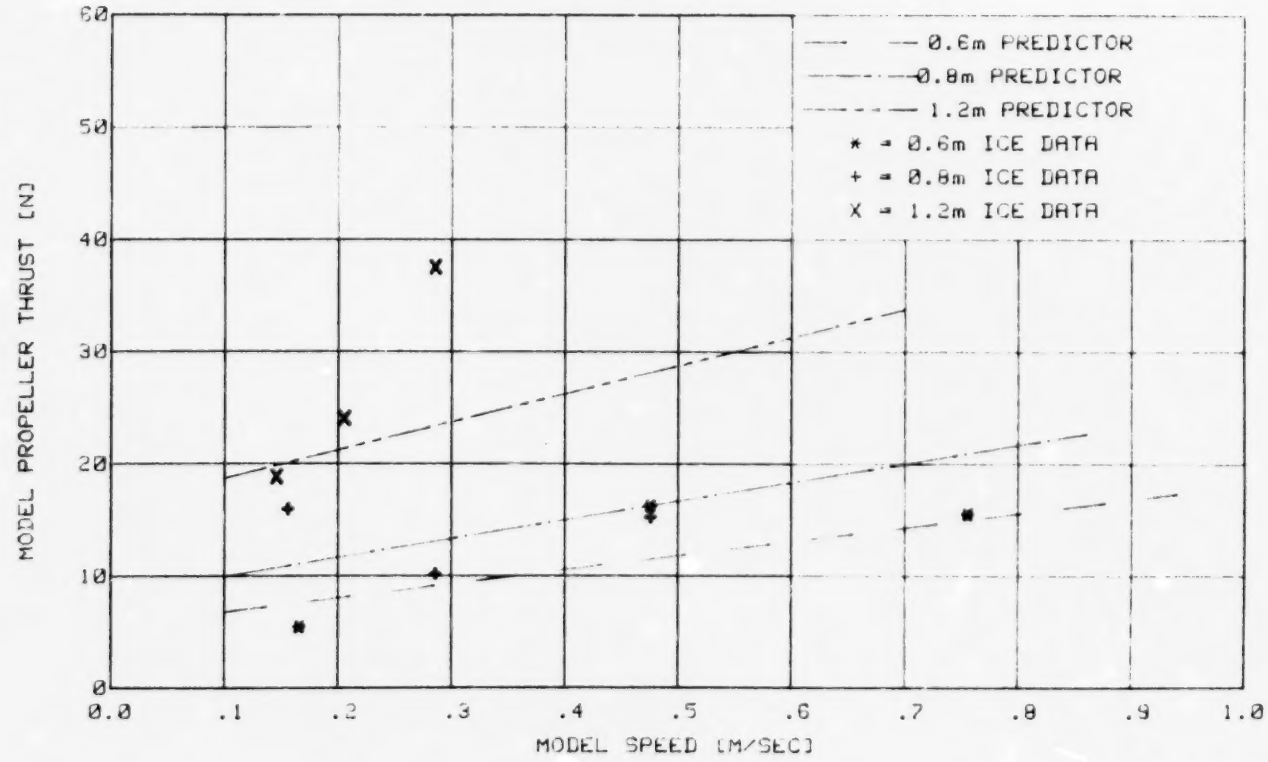

EXISTING MV ARCTIC BROKEN CHANNEL SELF-PROPULSION DATA POINTS
WITH A.C.L. PREDICTOR EQUATION
FROM A.C.L. ICE MODEL TESTING

FIGURE A3.16

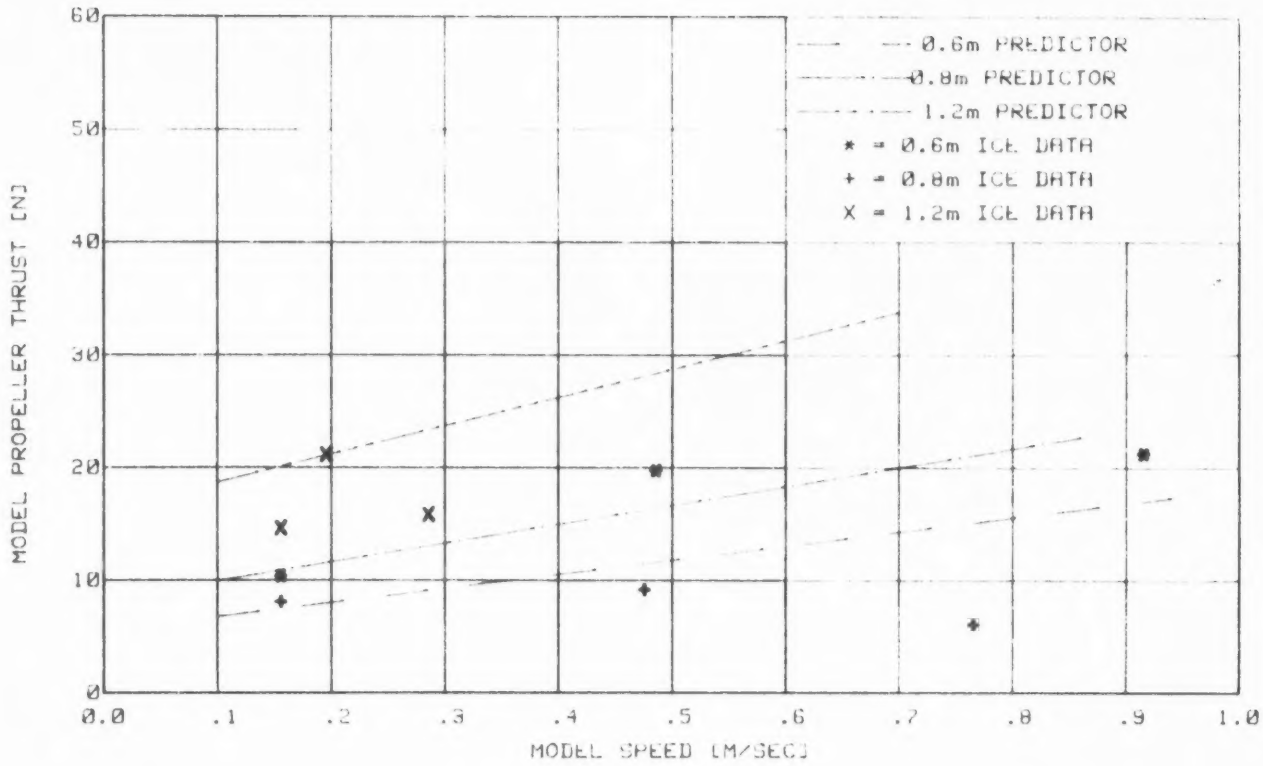

MODEL 'B' BROKEN CHANNEL SELF-PROPULSION DATA POINTS
WITH A.C.L. PREDICTOR EQUATION
FROM A.C.L. ICE MODEL TESTING

FIGURE A3.17

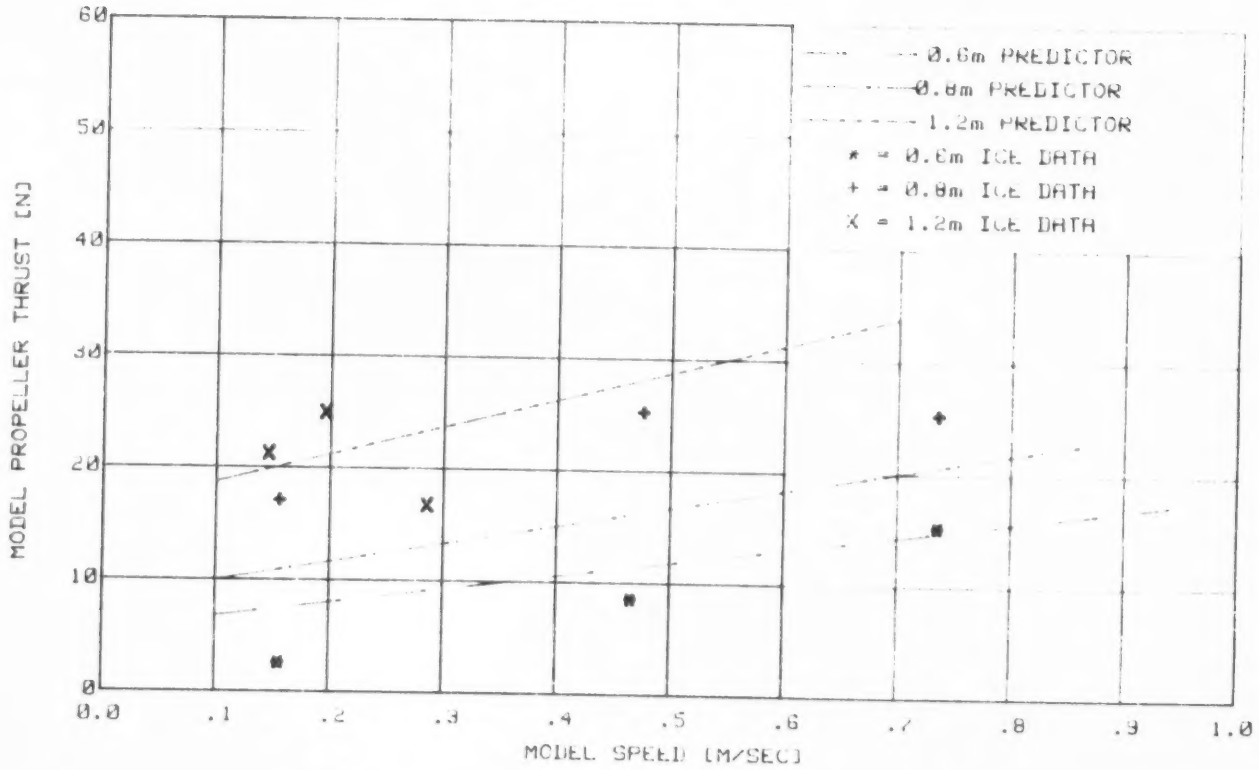

MODEL 'C' BROKEN CHANNEL SELF-PROPULSION DATA POINTS
WITH A.C.L. PREDICTOR EQUATION
FROM A.C.L. ICE MODEL TESTING

FIGURE H3.18

MODEL	AVERAGE THICKNESS (m)	RIDGE LENGTH (m)	MODEL VEL. (m/sec)	R dx (N-m)	RPM	T dx (N-m)	WIDTH OF RIDGE x (m)	THRUST DEDUCTION	TOTAL P.E. (N-m)	P.E. (N-m)
326-A	.2413	3.0	.155	-33.60	1066	259.6	4.76	-.694	473.3	653.8
326-B	.2330	4.0	.144	-75.60	996	285.5	5.27	-.684	556.4	597.0
326-C	.2440	4.3	.137	-18.56	1002	290.4	5.31	-.688	508.7	528.1

TABLE A3.6
RUBBLE FIELD TEST DATA

Figure A3.19 is reproduced from Reference 4.2 and shows graphically the analysis procedure.

During the actual tests it was noted that Bows B and C tended to ride up on the rubble field and depress the ice down along the entire length of the rubble field. However, Bow A tended to push through the rubble field rather than ride up on top of it.

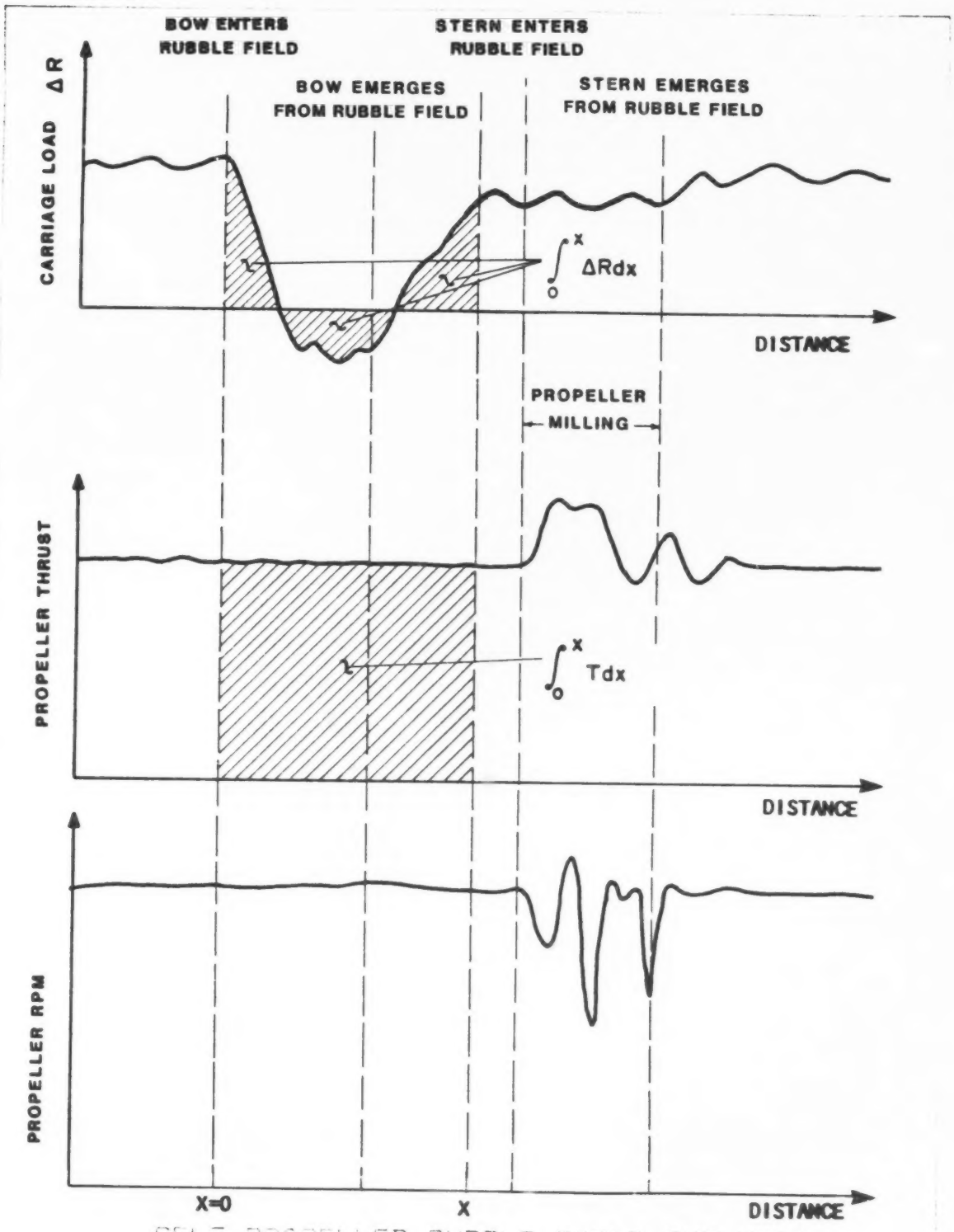

SELF PROPELLED RUBBLE FIELD ANALYSIS
FROM ACL TEST REPORT

FIGURE A3.19

APPENDIX 4

SUMMARY OF ICE CONDITIONS AND TRANSIT TIMES
FOR VOYAGE FROM EUROPE TO NANISIVIK

EXISTING BOW - JUNE

	ICE CONDITION	THICKNESS [m]	AVERAGE SPEED [kn]	LENGTH [nm]	TIME [days]	COMMENTS
North Atlantic	-	-	-		5.62	
Davis Strait	O.W.	-	16.5	462.8	1.169	Icebergs, significantly higher around Disko I., ice edge west of ship's passage.
	O.W. & fog	-	8.0	171.1	0.891	
Baffin Bay	O.W.	-	16.5	242.83	0.613	Decaying first-year ice 350 kPa. High concentration of bergs. Possible pressure ridges. Very little multi-year ice.
	O.W. & fog	-	8.0	80.94	0.422	
	O.P.	0.7-1	10.0	32.38	0.135	
	C.P.	0.7-1	8.0	183.47	0.956	
	V.C.P.	0.7-1	2.0	161.88	3.373	
Lancaster Sound	O.W.	-	16.5	30.22	0.076	Berg density highest at entrance to sound, decreasing towards interior. Very little multi-year ice.
	O.W. & fog	-	8.0	7.56	0.039	
	O.P.	0.75	12.0	37.78	0.131	
Admiralty Inlet	C. & R.	1.75-2.0	0.8	53.97	2.811	Land fast 450 kPa ice.

TOTAL - 16.236 days

NOMENCLATURE:

O.W. - Open Water
V.O.P. - Very Open Pack
O.P. - Open Pack
V.C.P. - Very Close Pack
C. - Consolidated
R. - Ridges
C.P. - Consolidated

TABLE A4.1
SUMMARY OF ICE CONDITIONS AND TRANSIT TIMES
FOR VOYAGE FROM EUROPE TO NANISIVIK

EXISTING BOW - JULY

	ICE CONDITION	THICKNESS [m]	AVERAGE SPEED [kn]	LENGTH [nm]	TIME [days]	COMMENTS
North Atlantic	-	-	-		5.62	
Davis Strait	O.W.	-	16.5	455.97	1.151	Decreasing berg densities generally but higher near Disko Island.
	O.W. & fog	-	8.0	245.5	1.279	
Baffin Bay	O.W.	-	16.5	263.1	0.664	Decaying first-year ice with large areas of open water. Very little multi-year ice.
	O.W. & fog	-	8.0	141.7	0.738	
	V.O.P.	-	14.0	80.95	0.241	
	O.P.	-	12.0	107.93	0.375	
Lancaster Sound	O.W.	-	16.5	68.00	0.170	Very low berg concentration reducing moving west.
	O.W. & fog	-	8.0	7.55	0.039	
Admiralty Inlet	C.	1.2-1.5	1.5	53.97	1.499	Weak decaying first-year ice.

TOTAL - 11.776 days

NOMENCLATURE:

O.W. - Open Water
V.O.P. - Very Open Pack
O.P. - Open Pack
V.C.P. - Very Close Pack
C. - Consolidated
R. - Ridges
C.P. - Consolidated

TABLE A4.2
SUMMARY OF ICE CONDITIONS AND TRANSIT TIMES
FOR VOYAGE FROM EUROPE TO NANISIVIK

EXISTING BOW - AUGUST

	ICE CONDITION	THICKNESS [m]	AVERAGE SPEED [kn]	LENGTH [nm]	TIME [days]	COMMENTS
North Atlantic	-	-	-		5.62	
Davis Strait	O.W.	-	16.5	453.32	1.145	Increasing berg densities
	O.W. & fog	-	8.0	194.30	1.012	approaching Disko Island.
Baffin Bay	O.W.	-	16.5	359.4	0.908	Seasonal maximum iceberg
	O.W. & fog	-	8.0	126.3	0.658	densities during summer months particularly across entrance to Lancaster Sd.
Lancaster Sound	O.W.	-	16.5	60.4	0.153	Highest berg concentrations
	O.W. & fog	-	8.0	15.1	0.079	at entrance to sound.
Admiralty Inlet	O.W.	-	16.5	43.2	0.109	-
	O.W. & fog		8.0	10.8	0.056	
				TOTAL -	9.740 days	

NOMENCLATURE:

O.W. - Open Water
V.O.P. - Very Open Pack
O.P. - Open Pack
V.C.P. - Very Close Pack
C. - Consolidated
R. - Ridges
C.P. - Consolidated

TABLE A4.3
SUMMARY OF ICE CONDITIONS AND TRANSIT TIMES
FOR VOYAGE FROM EUROPE TO NANISIVIK

EXISTING BOW - SEPTEMBER

	ICE CONDITION	THICKNESS [m]	AVERAGE SPEED [kn]	LENGTH [nm]	TIME [days]	COMMENTS
North Atlantic	-	-	-		5.62	
Davis Strait	O.W.	-	16.5	619.27	1.564	Increasing berg densities
	O.W. & fog	-	8.0	109.28	0.569	approaching Disko Island.
Baffin Bay	O.W.	-	16.5	307.34	0.776	Seasonal maximum iceberg
	O.W. & fog	-	8.0	54.24	0.283	densities during summer months particularly across entrance to Lancaster Sd.
Lancaster Sound	O.W.	-	16.5	64.22	0.162	Possible occurrence of old
	O.W. & fog	-	8.0	11.33	0.059	ice.
Admiralty Inlet	O.W.	-	16.5	43.17	0.109	-
	O.W. & fog	-	8.0	10.79	0.056	
				TOTAL -	9.198 days	

NOMENCLATURE:

O.W. - Open Water
V.O.P. - Very Open Pack
O.P. - Open Pack
V.C.P. - Very Close Pack
C. - Consolidated
R. - Ridges
C.P. - Consolidated

TABLE A4.4
SUMMARY OF ICE CONDITIONS AND TRANSIT TIMES
FOR VOYAGE FROM EUROPE TO NANISIVIK

EXISTING BOW - OCTOBER

	ICE CONDITION	THICKNESS [m]	AVERAGE SPEED [kn]	LENGTH [nm]	TIME [days]	COMMENTS
North Atlantic	-	-	-		5.62	
Davis Strait	O.W.	-	16.5	619.2	1.564	Increasing berg densities approaching Disko Island.
	O.W. & fog	-	8.0	68.8	0.358	
Baffin Bay	O.W.	-	16.5	264.4	0.67	Initial formation of first-year ice. Seasonal maximum iceberg densities during summer months particularly across entrance to Lancaster Sound.
	+ fog	-	8.0	113.3	0.590	
	V.O.P.	-	14.0	24.3	0.072	
	V.O.P.	-	12.0	24.3	0.084	
	V.C.P.	0.2	10.0	140.3	0.585	
Lancaster Sound	V.C.P.	0.2	8.0	35.08	0.337	Very weak new ice and possible occurrence of multi-year ice. Ridges are large rubble areas.
Admiralty Inlet	V.C.P.	0.1	8.0	64.76	0.338	Very weak new ice.

TOTAL - 10.286 days

NOMENCLATURE:

O.W. - Open Water
V.O.P. - Very Open Pack
O.P. - Open Pack
V.C.P. - Very Close Pack
C. - Consolidated
R. - Ridges
C.P. - Consolidated

TABLE A4.5
SUMMARY OF ICE CONDITIONS AND TRANSIT TIMES
FOR VOYAGE FROM EUROPE TO NANISIVIK

EXISTING BOW - NOVEMBER

	ICE CONDITION	THICKNESS [m]	AVERAGE SPEED [kn]	LENGTH [nm]	TIME [days]	COMMENTS
North Atlantic	-	-	-		5.62	
Davis Strait	O.W.	-	14.0	507.3	1.51	Iceberg densities higher near Disko Island. Very weak new ice with some stories.
	O.W. & fog	-	7.0	126.8	0.755	
	V.O.P.	-	14.0	35.0	0.104	
	C.P.	-	10.0	35.0	0.146	
Baffin Bay	V.O.P.	0.2-0.4	8.0	53.97	0.141	Growth of weak first-year ice. Highest berg densities near Disko Island. Rubble fields and occurrence of multi-year ice.
	C.P.	0.2-0.4	6.0	458.71	3.092	
Lancaster Sound	V.C.P.	0.2	6.0	86.35	0.600	First-year ice 300-400 kPa. Old ice predominantly across entrance to Sound. Pressure ridges and rubble fields.
Admiralty Inlet	C.	0.3	5.0	53.97	0.45	Land fast cover 400 kPa.

TOTAL - 12.418 days

NOMENCLATURE:

O.W. - Open Water
V.O.P. - Very Open Pack
O.P. - Open Pack
V.C.P. - Very Close Pack
C. - Consolidated
R. - Ridges
C.P. - Consolidated

TABLE A4.6
SUMMARY OF ICE CONDITIONS AND TRANSIT TIMES
FOR VOYAGE FROM EUROPE TO NANISIVIK

MODIFIED BOW - MAY

	ICE CONDITION	THICKNESS [m]	AVERAGE SPEED [kn]	LENGTH [nm]	TIME [days]	COMMENTS
North Atlantic	-	-	-	-	5.62	
Davis Strait	O.W.	-	16.5	539.0	1.361	First year ice with decayed stories in western side of strait. No multi-year. Bergs present, with highest concentration near Disko Island.
	O.W. & fog	-	8.0	95.12	0.495	
Baffin Bay	V.C.P.	1.3-1.6	3.5	701.6	8.352	First year ice 450-500 kPa. Very little multi-year ice. Ridging possible between fast and mobile ice.
Lancaster Sound	V.C.P. & R.	1.8-2	2.5	80.95	1.349	First year ice, 500 kPa with occurrences of multi-year ice.
Admiralty Inlet	C.	1.75-2.0	0.8	53.97	2.811	Land fast 500 kPa ice.

TOTAL - 19.98 days

NOMENCLATURE:

O.W. - Open Water
V.O.P. - Very Open Pack
O.P. - Open Pack
V.C.P. - Very Close Pack
C. - Consolidated
R. - Ridges
C.P. - Consolidated

TABLE A4.7
SUMMARY OF ICE CONDITIONS AND TRANSIT TIMES
FOR VOYAGE FROM EUROPE TO NANISIVIK

MODIFIED BOW - JUNE

	ICE CONDITION	THICKNESS [m]	AVERAGE SPEED [kn]	LENGTH [nm]	TIME [days]	COMMENTS
North Atlantic	-	-	-		5.62	
Davis Strait	O.W.	-	16.5	462.8	1.169	Icebergs, significantly higher around Disko I., ice edge west of ship's passage.
	O.W. & fog	-	8.0	171.1	0.891	
Baffin Bay	O.W.	-	16.5	242.83	0.613	Decaying first-year ice 350 kPa. High concentration of bergs. Possible pressure ridges. Very little multi-year ice.
	O.W. & fog	-	8.0	80.94	0.422	
	O.P.	0.7-1	10.0	32.38	0.135	
	C.P.	0.7-1	8.0	183.47	0.956	
	V.C.P.	0.7-1	3.5	161.88	1.927	
Lancaster Sound	O.W.	-	16.5	30.22	0.076	Berg density highest at entrance to sound, decreasing towards interior. Very little multi-year ice.
	O.W. & fog	-	8.0	7.56	0.039	
	O.P.	0.75	10.0	37.78	0.157	
Admiralty Inlet	C. & R.	1.75-2.0	1.2	53.97	1.87	Land fast 450 kPa ice.

TOTAL - 13.875 days

NOMENCLATURE:

O.W. - Open Water
V.O.P. - Very Open Pack
O.P. - Open Pack
V.C.P. - Very Close Pack
C. - Consolidated
R. - Ridges
C.P. - Consolidated

TABLE A4.8
SUMMARY OF ICE CONDITIONS AND TRANSIT TIMES
FOR VOYAGE FROM EUROPE TO NANISIVIK

MODIFIED BOW - JULY

	ICE CONDITION	THICKNESS [m]	AVERAGE SPEED [kn]	LENGTH [nm]	TIME [days]	COMMENTS
North Atlantic	-	-	-		5.62	
Davis Strait	O.W.	-	16.5	455.97	1.151	Decreasing berg densities generally but higher near Disko Island.
	O.W. & fog	-	8.0	245.5	1.279	
Baffin Bay	O.W.	-	16.5	263.1	0.664	Decaying first-year ice with large areas of open water. Very little multi-year ice.
	O.W. & fog	-	8.0	141.7	0.738	
	V.O.P.	-	14.0	80.95	0.241	
	O.P.	-	12.0	107.93	0.375	
Lancaster Sound	O.W.	-	16.5	68.00	0.170	Very low berg concentration reducing moving west.
	O.W. & fog	-	8.0	7.55	0.039	
Admiralty Inlet	C.	1.2-1.5	3.0	53.97	0.749	Weak decaying first-year ice.

TOTAL - 11.026 days

NOMENCLATURE:

O.W. - Open Water
V.O.P. - Very Open Pack
O.P. - Open Pack
V.C.P. - Very Close Pack
C. - Consolidated
R. - Ridges
C.P. - Consolidated

TABLE A4.9
SUMMARY OF ICE CONDITIONS AND TRANSIT TIMES
FOR VOYAGE FROM EUROPE TO NANISIVIK

MODIFIED BOW - AUGUST

	ICE CONDITION	THICKNESS [m]	AVERAGE SPEED [kn]	LENGTH [nm]	TIME [days]	COMMENTS
North Atlantic	-	-	-		5.62	
Davis Strait	O.W.	-	16.5	453.32	1.145	Increasing berg densities approaching Disko Island.
	O.W. & fog	-	8.0	194.30	1.012	
Baffin Bay	O.W.	-	16.5	359.4	0.908	Seasonal maximum iceberg densities during summer months particularly across entrance to Lancaster Sd.
	O.W. & fog	-	8.0	126.3	0.658	
Lancaster Sound	O.W.	-	16.5	60.4	0.153	Highest berg concentrations at entrance to sound.
	O.W. & fog	-	8.0	15.1	0.079	
Admiralty Inlet	O.W.	-	16.5	43.2	0.109	-
	O.W. & fog		8.0	10.8	0.056	
				TOTAL -	9.740 days	

NOMENCLATURE:

O.W. - Open Water
V.O.P. - Very Open Pack
O.P. - Open Pack
V.C.P. - Very Close Pack
C. - Consolidated
R. - Ridges
C.P. - Consolidated

TABLE A4.10
SUMMARY OF ICE CONDITIONS AND TRANSIT TIMES
FOR VOYAGE FROM EUROPE TO NANISIVIK

MODIFIED BOW - SEPTEMBER

	ICE CONDITION	THICKNESS [m]	AVERAGE SPEED [kn]	LENGTH [nm]	TIME [days]	COMMENTS
North Atlantic	-	-	-		5.62	
Davis Strait	O.W.	-	16.5	619.27	1.564	Increasing berg densities approaching Disko Island.
	O.W. & fog	-	8.0	109.28	0.569	
Baffin Bay	O.W.	-	16.5	307.34	0.776	Seasonal maximum iceberg densities during summer months particularly across entrance to Lancaster Sd.
	O.W. & fog	-	8.0	54.24	0.283	
Lancaster Sound	O.W.	-	16.5	64.22	0.162	Possible occurrence of old ice.
	O.W. & fog	-	8.0	11.33	0.059	
Admiralty Inlet	O.W.	-	16.5	43.17	0.109	-
	O.W. & fog	-	8.0	10.79	0.056	
				TOTAL -	9.198 days	

NOMENCLATURE:

O.W. - Open Water
V.O.P. - Very Open Pack
O.P. - Open Pack
V.C.P. - Very Close Pack
C. - Consolidated
R. - Ridges
C.P. - Consolidated

TABLE A4.11
SUMMARY OF ICE CONDITIONS AND TRANSIT TIMES
FOR VOYAGE FROM EUROPE TO NANISIVIK

MODIFIED BOW - OCTOBER

	ICE CONDITION	THICKNESS [m]	AVERAGE SPEED [kn]	LENGTH [nm]	TIME [days]	COMMENTS
North Atlantic	-	-	-		5.62	
Davis Strait	O.W.	-	16.5	619.2	1.564	Increasing berg densities approaching Disko Island.
	O.W. & fog	-	8.0	68.8	0.358	
Baffin Bay	O.W.	-	16.5	264.4	0.67	Initial formation of first-year ice. Seasonal maximum iceberg densities during summer months particularly across entrance to Lancaster Sound.
	+ fog	-	8.0	113.3	0.590	
	V.O.P.	-	14.0	24.3	0.072	
	V.O.P.	-	12.0	24.3	0.084	
	V.C.P.	0.2	10.0	140.3	0.585	
Lancaster Sound	V.C.P.	0.2	10.0	35.08	0.146	Very weak new ice and possible occurrence of multi-year ice. Ridges are large rubble areas.
Admiralty Inlet	V.C.P.	0.1	10.0	64.76	0.270	Very weak new ice.
				TOTAL -	9.959 days	

NOMENCLATURE:

O.W. - Open Water
V.O.P. - Very Open Pack
O.P. - Open Pack
V.C.P. - Very Close Pack
C. - Consolidated
R. - Ridges
C.P. - Consolidated

TABLE A4.12
SUMMARY OF ICE CONDITIONS AND TRANSIT TIMES
FOR VOYAGE FROM EUROPE TO NANISIVIK

MODIFIED BOW - NOVEMBER

	ICE CONDITION	THICKNESS [m]	AVERAGE SPEED [kn]	LENGTH [nm]	TIME [days]	COMMENTS
North Atlantic	-	-	-		5.62	
Davis Strait	O.W.	-	14.0	507.3	1.51	Iceberg densities higher near Disko Island. Very weak new ice with some stories.
	O.W. & fog	-	7.0	126.8	0.755	
	V.O.P.	-	14.0	35.0	0.104	
	C.P.	-	10.0	35.0	0.146	
Baffin Bay	V.O.P.	0.2-0.4	8.0	26.98	0.141	Growth of weak first-year ice. Highest berg densities near Disko Island. Rubble fields and occurrence of multi-year ice.
	C.P.	0.2-0.4	6.0	445.22	3.092	
Lancaster Sound	V.C.P.	0.2	8.0	86.35	0.450	First-year ice 300-400 kPa. Old ice predominantly across entrance to Sound. Pressure ridges and rubble fields.
Admiralty Inlet	C.	0.3	8.0	53.97	0.281	Land fast cover 400 kPa.
				TOTAL - 12.099 days		

NOMENCLATURE:

O.W. - Open Water
V.O.P. - Very Open Pack
O.P. - Open Pack
V.C.P. - Very Close Pack
C. - Consolidated
R. - Ridges
C.P. - Consolidated

TABLE A4.13
SUMMARY OF ICE CONDITIONS AND TRANSIT TIMES
FOR VOYAGE FROM EUROPE TO NANISIVIK

MODIFIED BOW - DECEMBER

	ICE CONDITION	THICKNESS [m]	AVERAGE SPEED [kn]	LENGTH [nm]	TIME [days]	COMMENTS
North Atlantic	-	-	-		5.62	
Davis Strait	O.W. 70%	-	14.0	276.7	0.824	Iceberg densities higher
	fog 30%	-	7.0	118.6	0.706	near Disko Island. Very weak
	V.O.P.	-	14.0	75.55	0.225	new ice with some stories.
	O.P.	-	12.0	75.55	0.262	
	C.P.	-	10.0	103.88	0.433	
Baffin Bay	O.P.	0.75	8.0	134.9	0.703	First-year ice 300-400 kPa.
	C.P.	-	6.0	234.7	1.630	Iceberg densities nearest
	V.C.P.	-	3.5	107.9	1.285	Disko Island.
Lancaster Sound	V.C.P.	0.8-0.9	3.5	86.35	1.028	Ridging highest at entrance to Sound. First-year ice 300-400 kPa.
Admiralty Inlet	C.	0.65	5.0	53.97	0.450	Fast ice 450-500 kPa.

TOTAL - 13.166 days

NOMENCLATURE:

O.W. - Open Water
V.O.P. - Very Open Pack
O.P. - Open Pack
V.C.P. - Very Close Pack
C. - Consolidated
R. - Ridges
C.P. - Consolidated

TABLE A4.14
SUMMARY OF ICE CONDITIONS AND TRANSIT TIMES
FOR VOYAGE FROM EUROPE TO NANISIVIK

POOR
QUALITY
ORIGINAL